

*Development of Ruthenium and Iron Complexes for  
Catalytic Applications in Sustainable Oxidations and  
Reductions*

**By**

**Rahul Ghosh**

**CHEM11201804019**

**NISER, Bhubaneswar**

**Odisha- 752050**

A thesis submitted to the Board of Studies in Chemical Sciences In partial  
fulfilment of requirements for the Degree of

**DOCTOR OF PHILOSOPHY**

Of

**HOMI BHABHA NATIONAL INSTITUTE**

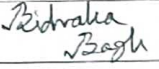
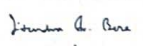
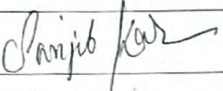
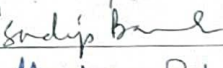


**May, 2023**

# Homi Bhabha National Institute<sup>1</sup>

## Recommendations of the Viva Voce Committee

1. As members of the Viva Voce Committee, we certify that we have read the dissertation prepared by **Rahul Ghosh** entitled "**Development of Ruthenium and Iron Complexes for Catalytic Applications in Sustainable Oxidations and Reductions**" and recommend that it may be accepted as fulfilling the thesis requirement for the award of Degree of Doctor of Philosophy.

Chairman - Dr. Prasenjit Mal		Date: 11/10/23
Guide / Convener - Dr. Bidraha Bagh		Date: 11/10/23
Examiner - Dr. Jitendra K. Bera		Date: 11/10/2023
Member 1- Dr. Sanjib Kar		Date: 11/10/23
Member 2- Dr. Sudip Barman		Date: 11/10/23
Member 3- Dr. Shantanu Pal		Date: 11/10/23

Final approval and acceptance of this thesis is contingent upon the candidate's submission of the final copies of the thesis to HBNI.

I/We hereby certify that I/we have read this thesis prepared under my/our direction and recommend that it may be accepted as fulfilling the thesis requirement.

Date: 11/10/23

Place: NISER



(Dr. Bidraha Bagh)

Guide

<sup>1</sup> This page is to be included only for final submission after successful completion of viva voce.

## STATEMENT BY AUTHOR

This dissertation has been submitted in partial fulfilment of requirements for an advanced degree at Homi Bhabha National Institute (HBNI) and is deposited in the Library to be made available to borrowers under rules of the HBNI. Brief quotations from this dissertation are allowable without special permission, provided that accurate acknowledgement of source is made. Requests for permission for extended quotation from or reproduction of this manuscript in whole or in part may be granted by the competent authority of HBNI when in his or her judgement the proposed use of the material is in the interest of scholarship. In all other instances, however, permission must be obtained from the author.

*Rahul Ghosh*  
Rahul Ghosh

## DECLARATION

I, hereby declare that the investigation presented in the thesis has been carried out by me.  
The work is original and has not been submitted earlier as a whole or in part for a degree /  
diploma at this or any other Institution / University.

*Rahul Ghosh*  
Rahul Ghosh

## List of Publications arising from the thesis

### Journal

1. Ghosh, R.; Jana, N. C.; Panda, S.; Bagh, B. Transfer Hydrogenation of Aldehydes and Ketones in Air with Methanol and Ethanol by an Air-Stable Ruthenium–Triazole Complex. *ACS Sustain*, **2021**, *9*, 4903-4914.
2. Ghosh, R.; Behera, R. R.; Panda, S.; Behera, S. K.; Jana, N. C.; Bagh, B. Catalytic Transfer Hydrogenation of Lignocellulosic Biomass Model Compounds Furfural and Vanillin with Ethanol by an Air-stable Iron (II) Complex. *ChemCatChem*, **2023**, *15*, e202201062.
3. Ghosh, R.; Panda, S.; Mahakhuda, A.; Saha, R.; Bagh, B. Base Metal Iron Catalyzed Sustainable Oxidation of Vanillyl Alcohol to Vanillic Acid in Deep Eutectic Solvent and Implementation of Vanillic Acid for Fine-Chemical Synthesis. *RSC Sustain.*, **2023**, Accepted Manuscript. (DOI: 10.1039/D3SU00114H)

### Conference

- 1) Oral presentation: International Conference on “Main-group Molecules to Materials-II (MMM-II), 2022” at dept. of chemistry, NISER Bhubaneswar.
- 2) Poster Presentation: International conference on “Modern Trends in inorganic Chemistry 2022 (MTIC- XIX)” at dept. of chemistry, BHU.

Rahul Ghosh

Rahul Ghosh

**DEDICATED TO....**

**TO MY PARENTS**

**&**

**DR. BIDRAHA BAGH**

## ACKNOWLEDGEMENTS

First and foremost, I appreciate God for gifting me this wonderful life. I have been able to succeed from the beginning of my academic career to this doctoral level due to His grace and blessings. This thesis appears in its current form due to the constant support and assistance of several people. I would like to extend my sincere gratitude to all of them. I am deeply grateful to my thesis supervisor Dr. Bidraha Bagh for his invaluable guidance and wisdom throughout my tenure. I appreciate all his contributions of valuable time, stimulating ideas and funding for the smooth sailing of my work. His discipline, work-ethics has been an inspiration for me and will be for generations to come. I hope I will be able to stand up to his expectations and excel in my upcoming endeavours. My sincere gratitude goes to Prof. Sudhakar Panda, Former Director (NISER), Prof. T. K. Chandrashekar, founder-Director (NISER) and Prof. V. Chandrashekar, former-Director (NISER). I would like to thank my doctoral committee members, for their support and suggestions. I would also like to thank other faculties members of School of Chemical Sciences for refining concepts of chemistry. I heartily thank Dr. Subhayan Chakraborty for teaching me NMR operation and for his help in NMR studies. I would like to recognize Mr. Sanjaya Mishra for his kind help in recording NMR data, Mr. Deepak Kumar Behera for his kind help in X-ray analysis and Mr. Amit Sankar Sahu and Mr. Prakash Kumar Sahoo for their kind help in ESIMS analysis. I am also thankful to all the staff members of School of Chemical Sciences for their cooperation. My former and current labmates have a special place in my heart for their constant and unconditional support throughout this process. I cherish all the moments spent with Dr. N.C. Jana, Surajit, Rakesh, Subrat, Ratnakar, Souvik, Prasanna, Sandip, Subrat Khamari, Ashutosh, Amreshwar and Ashish. I thank them all for their valuable inputs, constructive criticisms about my research. I would also like to thank my NISER friends for all the wonderful memories. Financial assistance (fellowship) by DAE is gratefully acknowledged. I

would also like to acknowledge DST-SERB, New Delhi, Govt. of India for research funding. I would like to thank my parents and my beloved family for providing love and confidence in many ups and down throughout this process. Finally, again I would express my gratitude to the almighty for His grace, blessings and wish without which this entire process would not have been possible. Thank you all so much for your unconditional support and encouragement.

*Rahul Ghosh*  
Rahul ghosh

# SYNOPSIS

1. **Name of the Student:** Mr. Rahul Ghosh
2. **Name of the Constituent Institution:** National Institute of Science Education and Research (NISER)
3. **Enrolment No:** CHEM11201804019
4. **Title of the Thesis:** Development of Ruthenium and Iron Complexes for Catalytic Applications in Sustainable Oxidations and Reductions
5. **Board of Studies:** Chemical Sciences

## **INTRODUCTION (Chapter 1.1 and 1.2)**

Reduction of different functional groups is one of the key transformations in organic synthesis. Commonly used metal-hydride reducing agents such as  $\text{LiBH}_4$ ,  $\text{NaBH}_4$ ,  $\text{LiAlH}_4$  and DIBAL-H are toxic and produce a huge amount of inorganic waste. Thus, Hydrogenation reaction is one of the alternatives for the reduction of different functionalities. However, the conventional direct hydrogenation method tolerates several drawbacks due to its hazardous pressurized hydrogen gas, elaborated experimental setup, and expensiveness.<sup>1-3</sup> Catalytic Transfer hydrogenation reaction is one of the most attractive alternatives to direct hydrogenation as it not only deals with the easy and readily available hydrogen donors but also easy-to-handle protocol, inexpensive nature and recyclability of the side products makes this process more sustainable. Even though transfer hydrogenation using isopropanol and formic acid is well explored in literature but using comparatively challenging primary alcohol like ethanol and methanol is now in focus. Transition metal elements, especially ruthenium and iron have been used potentially in transfer hydrogenation reactions. In my thesis I will discuss about the utilization of a half sandwich ruthenium complex for TH of ketone and aldehyde in air using ecological benign ethanol and methanol. Later a tridentate Iron NNO

complex has been developed which has been utilised for the transfer hydrogenation of lignocellulosic biomass model compounds vanillin and furfural using ethanol as sacrificial hydrogen donor.

On the other hand, the oxidation of different functional groups has become an important and ideal transformations and one of the key interesting research topics for chemists for academic and industrial purposes. Several methods and reagents like dimethyl sulfoxide, Dess-Martine periodinane,  $\text{KMnO}_4$ ,  $\text{CrO}_3$ , etc were used extensively for oxidation of alcohols. The traditional oxidation reagents are toxic, harmful, explosive and produce a huge amount of hazardous chemical waste when carried out on an industrial scale.<sup>4-5</sup> A significant research interest has been devoted on oxidation to explore sustainable approach, which includes aerobic and peroxidative oxidation. In the last part of my thesis, I will discuss on the synthesis and characterizations of a series of iron complexes with pincer ligands and their effective use in peroxidative oxidation of lignocellulosic biomass model compounds and other substrates too. Finally, the green credentials of the above-mentioned transformations were evaluated with the help of CHEM 21 Green Metrics Toolkit.

## **Scope and organisation of present thesis**

A half sandwich ruthenium complex is synthesised with N, O chelating arm of 1,2,3 triazole ligand and utilised the ruthenium complex for selective TH of aldehyde and ketones to their corresponding alcohols using both ethanol and isopropanol as sacrificial hydrogen donor. Later, a pincer ligand designed and synthesised with NNO chelating arm and the facial coordination of that ligand and  $\text{FeCl}_2 \cdot 4\text{H}_2\text{O}$  furnishes an Iron complex which is successfully utilised for efficient TH of lignocellulosic based model compounds Furfural and Vanillyl. In recent time, it is very crucial to evaluate the drawbacks and sustainability of any catalytic transformations. In this view I have evaluate the green credentials of the above mention

catalytic transformations using CHEM21 green tool matrix, which is the quantitative extension of “12 principle of green chemistry”.

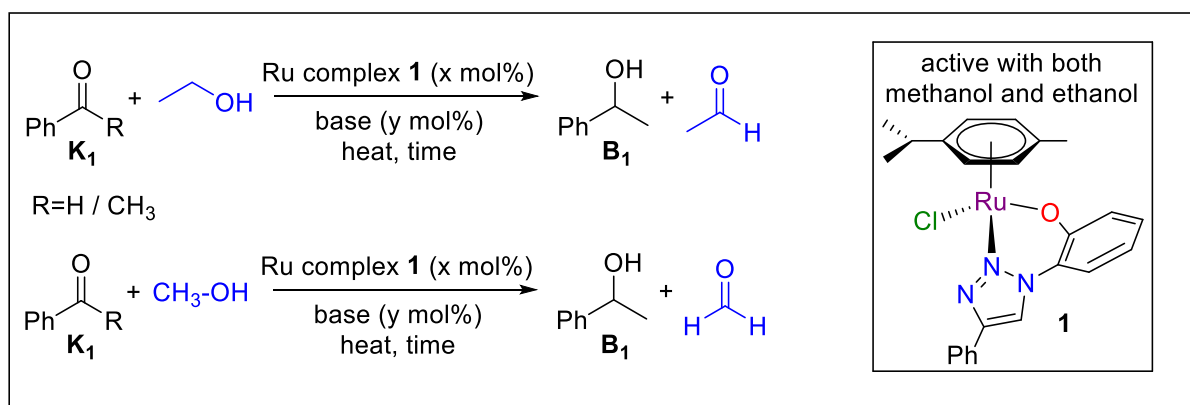
Oxidation reactions are one of the most important transformations, not only in terms of academia but also industrial purpose. There are many organic and inorganic reagents that used in stoichiometric amount for the oxidations of alcohols. But those transformations produce a huge chemical waste. To avoid this, it is necessary to developed sustainable catalytic protocol for the selective oxidation alcohols. There are two heavily used sustainable catalytic protocols, one is aerobic oxidation and another is peroxidative oxidation. So, in the last part of my thesis, I will discuss about the selective peroxidative oxidation of primary alcohols to theirs corresponding aldehydes and acids. For this purpose, I have synthesised and characterised a series of Iron complexes that successfully utilised for the selective peroxidative oxidation of biomass model compound Vanillin and other substrates too.

## **Chapter 2**

Coordination of 1,4-disubstituted 1,2,3-triazoles L1 and L2 with [(p-cymene)RuCl<sub>2</sub>]<sub>2</sub> followed by dehydrochlorination in the presence of a base resulted in the formation of complexes 1 and 2, respectively. Both were tested for the transfer hydrogenation of aldehydes and ketones in the air using ecologically benign and cheap ethanol as the hydrogen source in the presence of a catalytic amount of a base. Air-stable complex 1 was proved to be an active catalyst for the transfer hydrogenation of a wide variety of aromatic and aliphatic aldehydes and ketones bearing various functionalities. Catalyst 1 was also effective for the transfer hydrogenation of carbonyls using the simplest primary alcohol, methanol, under aerobic conditions. Under the present catalytic protocol, labile or reducible functionalities such as nitro, cyano, and ester groups were tolerated. Good selectivity was also observed for acyclic  $\alpha,\beta$ -unsaturated carbonyls. However, this catalytic protocol was not selective for 2-

cyclohexen-1-one as both alkene and keto moieties were reduced. The transfer hydrogenations are believed to proceed via a ruthenium-hydride intermediate. Finally, transfer hydrogenation of acetophenone using isopropanol as a commonly used hydrogen source was also performed and the sustainable and green credentials of these catalytic protocols utilizing methanol, ethanol, and isopropanol were compared with the help of the CHEM21 green metrics toolkit.

### SCHEME 1: Ruthenium catalysed TH of ketone and aldehydes using both Ethanol and Methanol

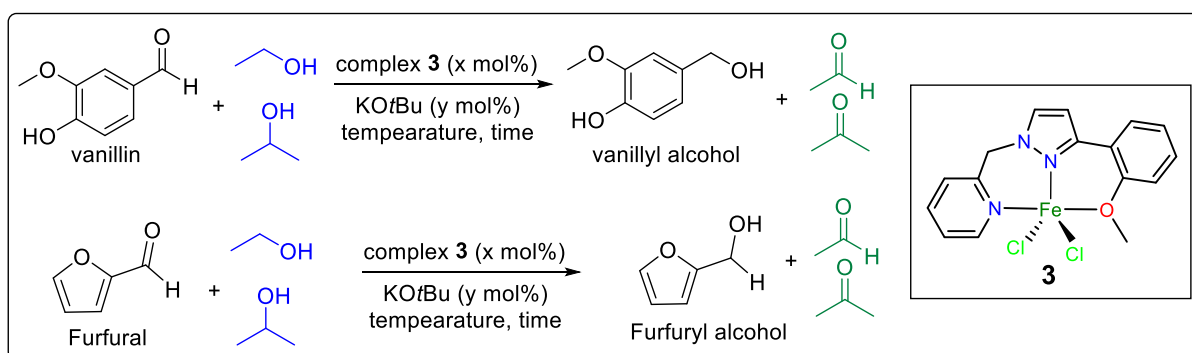


## Chapter 3

The chemical transformation of biomass for the synthesis of various fine chemicals is the necessity for the sustainable developments in the present age. Various components of lignocellulosic biomass can be chemically reduced to numerous value-added products and this field of research has attracted enormous attentions. The scientific community has devoted a significant research interest to develop catalysts for the reduction of cellulose and lignin model compounds furfural and vanillin, respectively. In this context, an iron (II) catalyst (**1**) was readily synthesized by the facile coordination of NNO pincer ligand with  $\text{FeCl}_2 \cdot 4\text{H}_2\text{O}$  salt as precursor. The air-stable complex **1** was utilized for the catalytic transfer

hydrogenation of cellulose and lignin model compounds furfural and vanillin, respectively, using ecologically benign but challenging primary alcohol ethanol as the hydrogen source in presence of catalytic amount of base. Secondary alcohol isopropanol was also utilized as the sacrificial hydrogen donor. Complex **3** as a sustainable iron compound was proved to be a very efficient catalyst for the transfer hydrogenation of furfural and vanillin under ambient conditions with both primary and secondary alcohols as hydrogen donors. Under the present catalytic protocol, various other biomass model carbonyl compounds and structurally related aldehydes were effectively reduced to the corresponding alcohols. Kinetic studies for transfer hydrogenation of vanillin with ethanol suggested first order kinetics in catalyst (complex **3**) and zeroth order in substrate vanillin. Based on the experimental evidences (isolation of intermediate by stoichiometric reactions and kinetic studies) and published reports, a catalytic cycle for the transfer hydrogenations is proposed which proceed via iron (II)-dialkoxides and alkoxide-hydride intermediates. Finally, CHEM21 green metrics toolkit was utilized to evaluate the sustainable and green credentials of the catalytic protocols.

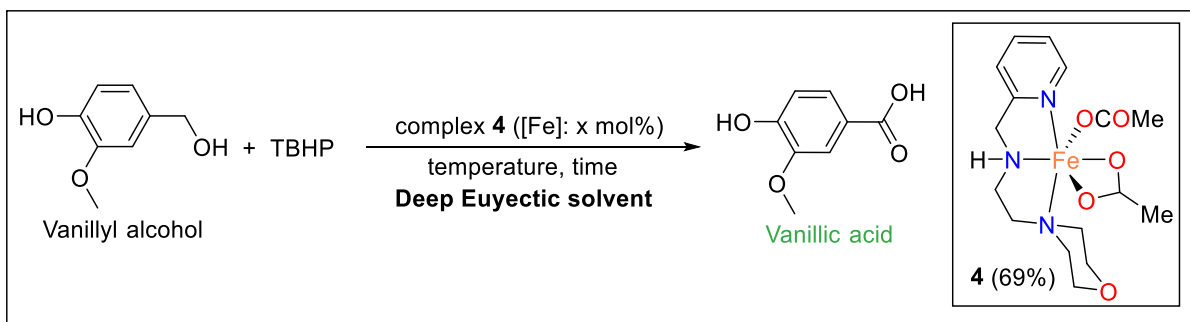
**SCHEME 2: Iron catalysed TH of vanillyl and Furfural using both Ethanol and isopropanol**



**Chapter 4**

In the modern era, sustainable developments for the productions of fine chemicals from abundant biomass by utilizing various chemical transformations have become a strong trend of research in the research community. This may provide a sustainable alternative to petrochemicals as the major source of fine chemicals. Lignin is an alternative major source of monomeric phenolic compounds and the syntheses of fine chemicals by oxidising lignin-based monomeric phenolics are gaining serious attention. For instance, biomass derived vanillin or vanillyl alcohol can be oxidized to vanillic acid which has been employed as a new building block for the syntheses of various value-added products. In this context, an air-stable iron (II) complex has been synthesized and utilized as an excellent base-metal catalyst for the selective oxidation of vanillyl alcohol to vanillin. We used tert-butyl hydroperoxide as a green oxidant. This peroxidative oxidation of vanillyl alcohol to vanillic acid was performed in metal-free type-III deep eutectic solvents as green and sustainable reaction media. After the first set of oxidations, the catalyst and the reaction medium were recycled four times without any noticeable change in catalytic performance. CHEM21 green metrics toolkit was also used to examine the sustainable and green features of the optimized oxidation protocol for the conversion of vanillyl alcohol to vanillic acid. Finally, vanillic acid was used as a starting material for the syntheses of several fine chemicals with various (potential) applications such as flavorant, odorant, surfactant and bio-based plasticizer.

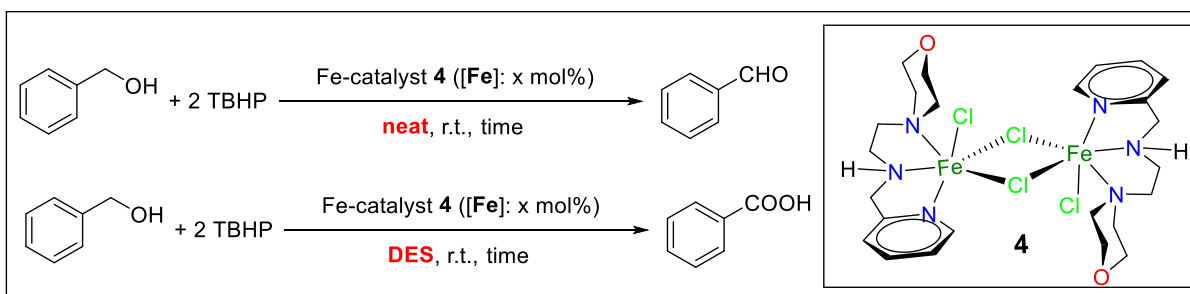
**SCHEME 3: Iron catalysed selective peroxidative oxidation of vanillyl alcohol to vanillic acid in DES**



## Chapter 5

Chemodivergent transformations are important class of reactions in recent time. The most studied solutions for switching the chemoselectivity rely on the catalyst, ligand, additive, solvent, temperature, time, pressure, pH, and even small modifications in the substrate. Herein, in this chapter a NNN Iron (II) pincer complex has been introduced for the chemodivergent oxidation of primary alcohol by switching only solvent condition. In the neat condition the above-mentioned iron catalyst selectively furnishes aldehydes. Whereas, in deep eutevctic solvent the catalyst selectively oxidise alcohol to their corresponding acids. The catalyst shows a fantastic catalytic activity as TOF goes up to  $1000000 \text{ h}^{-1}$ .

**SCHEME 4: Iron catalysed chemodivergent transformation of primary alcohol to corresponding aldehydes and acids.**



**References:**

- (1) de Vries, J. G., Elsevier, C. J., Eds. *The Handbook of Homogeneous Hydrogenation*; Wiley-VCH: Weinheim, 2007.
- (2) Andersson, P. G., Munslow, I. J., Eds. *Modern Reduction Methods*; Wiley-VCH Verlag GmbH & Co. KGaA: Weinheim, 2008.
- (3) Magano, J.; Dunetz, J. R. Large-Scale Carbonyl Reductions in the Pharmaceutical Industry. *Org. Process Dev.* **2012**, *16*, 1156–1184.
- (4) Nutting, J. E., Mao, K., & Stahl, S. S. Iron (III) nitrate/TEMPO-catalyzed aerobic alcohol oxidation: distinguishing between serial versus integrated redox cooperativity. *Journal of the American Chemical Society*, **2021**, *143*, 10565-10570.
- (5) Joshi, S. R., Kataria, K. L., Sawant, S. B., Joshi, J. B. Kinetics of oxidation of benzyl alcohol with dilute nitric acid. *Industrial & engineering chemistry research*, **2005**, *44*, 325-333.

	<b>List of schemes</b>	<b>Page no</b>
1	<b>Scheme 1.1.1:</b> Ruthenium catalysed hydrogenation of Esters	27
2	<b>Scheme 1.1.2:</b> Rh catalyzed TH of ketone utilizing ethanol as hydrogen donor	31
3	<b>Scheme 1.1.3:</b> Ruthenium catalysed ATH using chiral ligand in ethanol	32
4	<b>Scheme 1.1.4:</b> Nickel catalysed TH of ketones utilising bidentate phosphene ligand in ethanol	33
5	<b>Scheme 1.1.5:</b> Rhodium catalysed TH of aldehydes in methanol and proposed mechanistic cycle	34
6	<b>Scheme 1.1.6:</b> Tridentate Ruthenium complex catalysed TH using ethanol as hydrogen source in inert condition	35
7	<b>Scheme 1.1.7:</b> iridium catalysed TH utilising methanol as hydrogen source	36
8	<b>Scheme 1.1.8:</b> Half sandwich iridium complex catalysed TH utilising methanol and proposed mechanistic cycle	37
9	<b>Scheme 1.1.9:</b> Ru-MACHO catalysed TH of $\alpha$ , $\beta$ unsaturated carbonyl and proposed reaction pathway	38
10	<b>Scheme 1.1.10:</b> Rhodium complex catalysed TH of $\alpha$ , $\beta$ unsaturated carbonyls	39
11	<b>Scheme 1.2.1:</b> Iron catalysed aerobic oxidation of both primary and secondary alcohols	42
12	<b>Scheme 1.2.2:</b> Iron catalysed peroxidative oxidation of both primary and secondary alcohols	43
13	<b>Scheme 2.3.1.</b> Synthesis of ruthenium-triazole complexes 1 and 2 with the molecular structure of 2 showing 50% ellipsoids <sup>a</sup>	61
14	<b>Scheme 2.3.2.</b> Transfer hydrogenation of ketones using ethanol catalyzed by complex 1	64
15	<b>Scheme 2.3.3.</b> Transfer hydrogenation of aldehydes using ethanol catalyzed by 1	66
16	<b>Scheme 2.3.4.</b> Transfer hydrogenation of ketones and aldehydes with methanol catalyzed by 1	70
17	<b>Scheme 2.3.5.A.</b> Transfer hydrogenation of Acetophenone using	71

	different optimized condition	
19	<b>Scheme 2.3.5</b> Proposed catalytic cycle for the transfer hydrogenation of carbonyls with methanol/ethanol catalyzed by complex 1	73
20	<b>Scheme 3.3.1.</b> Synthesis of complex 3 with the molecular structure showing 50% ellipsoids	124
21	<b>Scheme 3.3.2.</b> Gram-scale transfer hydrogenation of vanillin to vanillyl alcohol using different optimized reaction conditions	131
22	<b>Scheme 3.3.3.</b> Transfer hydrogenation of structurally related aldehydes and biomass model aldehyde compounds using ethanol catalyzed by 3 <sup>a</sup>	134
23	<b>Scheme 3.3.4.</b> Proposed catalytic cycle for the transfer hydrogenation of carbonyls with methanol/ethanol catalyzed by complex 3	136
24	<b>Scheme 3.3.5</b> a) Stoichiometric reactivity study with complex 3; b) and c) formation of byproducts from alcohols as hydrogen source.	137
25	<b>Scheme 4.2.1.</b> Catalytic oxidation of vanillyl alcohol	176
26	<b>Scheme 4.3.1:</b> Synthesis of complex 7 (the molecular structure of complex 7 showing 70% ellipsoids and all hydrogen atoms except N-H are omitted for clarity).	180
27	<b>Scheme 4.3.2</b> Application of vanillic acid in the syntheses of vanillic esters and diesters with (potential) applications.	189
28	<b>Scheme 5.2.1.</b> Iron catalyzed peroxidative oxidation of primary alcohol	220
29	<b>Scheme 5.3.1.</b> Synthesis of iron complex 8 with the molecular structures, using 50% probability ellipsoids (Hydrogen atoms are omitted for clarity)	223
30	<b>Scheme 5.3.2.</b> Substrate scope for the selective oxidation of primary alcohols to aldehydes	227
31	<b>Scheme 5.3.3.</b> Substrate scope for the selective oxidation of primary alcohols to carboxylic acids	232
32	<b>Scheme 5.3.4.</b> Plausible reaction path for complex 8 catalyzed alcohol oxidation	234

### List of Figures

1	<b>Figure 1.1.1.</b> Chronic development transition metal catalyzed TH of unsaturated double bond	29
2	<b>Figure 2.2.1.</b> Transition metal catalysts for the transfer hydrogenation of carbonyls using methanol and ethanol as hydrogen source.	59
3	<b>Figure 2.5.1.</b> <sup>1</sup> H NMR (400 MHz) spectrum of L <sub>1</sub> in CDCl <sub>3</sub> at r.t.	94

4	<b>Figure 2.5.2.</b> $^1\text{H}$ NMR (400 MHz) spectrum of $\text{L}_2$ in $\text{CDCl}_3$ at r.t.	95
5	<b>Figure 2.5.3.</b> $^1\text{H}$ NMR (400 MHz) spectrum of complex 1 in $\text{CDCl}_3$ at r.t. (* indicates $\text{H}_2\text{O}$ ).	95
6	<b>Figure 2.5.4.</b> $^1\text{H}$ NMR (400 MHz) spectrum of complex 2 in $\text{CDCl}_3$ at r.t. (* indicates $\text{H}_2\text{O}$ ).	96
7	<b>Figure 2.5.5.</b> $^1\text{H}$ NMR (400 MHz) spectrum of 1-Phenylethan-1-ol ( $\text{B}_1$ ) in $\text{CDCl}_3$ at r.t. (* indicates H-grease).	96
8	<b>Figure 2.5.6.</b> $^{13}\text{C}\{^1\text{H}\}$ NMR (101 MHz) spectrum of 1-Phenylethan-1-ol ( $\text{B}_1$ ) in $\text{CDCl}_3$ at r.t.	97
9	<b>Figure 2.5.6.</b> $^1\text{H}$ NMR (400 MHz) spectrum of Phenylmethanol ( $\text{C}_1$ ) in $\text{CDCl}_3$ at r.t.	97
10	<b>Figure 2.5.7.</b> $^{13}\text{C}\{^1\text{H}\}$ NMR (101 MHz) spectrum of Phenylmethanol ( $\text{C}_1$ ) in $\text{CDCl}_3$ at r.t.	98
11	<b>Figure 3.2.1.</b> Furfural, furfuryl alcohol, vanillin, vanillyl alcohol and important downstream fine chemicals by biomass valorization.	117
12	<b>Figure 3.2.2.</b> Transition metal catalysts for the transfer hydrogenation of carbonyls using ethanol as hydrogen source.	121
13	<b>Figure 3.3.3</b> Reduction of vanillin to vanillyl alcohol in ethanol and isopropanol at various temperatures in 3 h using 1 mol% of complex 3 and 3 mol% $\text{KO}t\text{Bu}$ .	128
14	<b>Figure 3.3.4.</b> Kinetic analyses for the conversion of vanillin to vanillyl alcohol.	139
15	<b>Figure 3.5.1.</b> Molecular Structure of complex 3 showing 50% Ellipsoids	153
16	<b>Figure 3.5.2.</b> $^1\text{H}$ NMR (400 MHz) spectrum of $\text{L}_4$ in $\text{CDCl}_3$ at r.t.	153
17	<b>Figure 3.5.3.</b> $^{13}\text{C}$ NMR (400 MHz) spectrum of $\text{L}_2$ in $\text{CDCl}_3$ at r.t.	154
18	<b>Figure 3.5.4.</b> $^1\text{H}$ NMR (400 MHz) spectrum of vanillyl alcohol in $\text{CDCl}_3$ at r.t.	154
19	<b>Figure 3.5.5.</b> $^{13}\text{C}\{^1\text{H}\}$ NMR (101 MHz) spectrum of vanillyl alcohol in $\text{CDCl}_3$ at r.t.	155
20	<b>Figure 3.5.6.</b> $^1\text{H}$ NMR (400 MHz) spectrum of furfuryl alcohol in $\text{CDCl}_3$ at r.t.	155

21	<b>Figure 3.5.7.</b> $^{13}\text{C}$ { $^1\text{H}$ } NMR (100 MHz) spectrum of furfuryl alcohol in $\text{CDCl}_3$ at r.t.	156
22	<b>Figure 4.5.1.</b> $^1\text{H}$ NMR (400 MHz) spectrum of $\text{L}_4$ in $\text{CDCl}_3$ at r.t.	192
23	<b>Figure 4.5.2.</b> $^{13}\text{C}$ { $^1\text{H}$ } NMR (400 MHz) spectrum of $\text{L}_4$ in $\text{CDCl}_3$ at r.t.	193
24	<b>Figure 4.5.3.</b> Mass spectrum of 7.	194
25	<b>Figure 4.5.4.</b> IR spectrum of $\text{L}_4$ .	195
26	<b>Figure 4.5.5.</b> IR spectrum of 7.	195
28	<b>Figure 4.5.6.</b> $^1\text{H}$ NMR (400 MHz) spectrum of vanillic acid in $\text{DMSO-d}_6$ at r.t. (* marks as water peak)	203
29	<b>Figure 4.5.6.</b> $^{13}\text{C}$ { $^1\text{H}$ } NMR (101 MHz) spectrum of vanillic acid in $\text{DMSO-d}_6$ at r.t.	204
30	<b>Figure 4.5.7.</b> $^1\text{H}$ NMR (400 MHz) spectrum of methyl 4-hydroxy-3-methoxybenzoate in $\text{CDCl}_3$ at r.t.	204
31	<b>Figure 4.5.8.</b> $^{13}\text{C}$ { $^1\text{H}$ } NMR (101MHz) spectrum of methyl 4-hydroxy-3-methoxybenzoate in $\text{CDCl}_3$ at r.t.	205
32	<b>Figure 4.5.8.</b> $^1\text{H}$ NMR (400 MHz) spectrum of butyl 4-acetoxy-3-methoxybenzoate in $\text{CDCl}_3$ at r.t.	206
33	<b>Figure 4.5.9.</b> $^{13}\text{C}$ { $^1\text{H}$ } NMR (101 MHz) spectrum of butyl 4-acetoxy-3-methoxybenzoate in $\text{CDCl}_3$ at r.t.	206
34	<b>Figure 5.5.1.</b> $^{13}\text{C}$ { $^1\text{H}$ } NMR (101 MHz) spectrum of Benzaldehyde in $\text{CDCl}_3$ at r.t.	241
35	<b>Figure 5.5.2.</b> $^{13}\text{C}$ { $^1\text{H}$ } NMR (101 MHz) spectrum of Benzaldehyde in $\text{CDCl}_3$ at r.t.	241
36	<b>Figure 5.5.3.</b> $^{13}\text{C}$ { $^1\text{H}$ } NMR (101 MHz) spectrum of Benzoic Acid in $\text{CDCl}_3$ at r.t.	242
37	<b>Figure 5.5.4.</b> $^{13}\text{C}$ { $^1\text{H}$ } NMR (101 MHz) spectrum of Benzoic Acid in $\text{CDCl}_3$ at r.t.	242

#### List of Tables

1	<b>Table 2.3.1.</b> Catalytic performance of ruthenium-triazole complexes 1 and 2 for transfer hydrogenation of acetophenone with ethanol	62
2	<b>Table 2.3.2.</b> Catalytic performance of complexes 1 for the transfer	68

hydrogenation of acetophenone with methanol<sup>a</sup>

3	<b>Table 3.3.1.</b> Catalytic performance of 3 for transfer hydrogenation of vanillin with ethanol	125
4	<b>Table 3.3.2.</b> Catalytic performance of 3 for transfer hydrogenation of vanillin with isopropanol	126
5	<b>Table 3.3.3.</b> Catalytic performance of 3 for transfer hydrogenation of vanillin with isopropanol	128
6	<b>Table 3.3.4.</b> Catalytic performance of 3 for transfer hydrogenation of furfural with ethanol and isopropanol	129
7	<b>Table 3.3.5.</b> Comparison of the five different methods of transfer hydrogenations from the CHEM21 Green Metrics Toolkit Calculation	133
8	<b>Table 3.5.1.</b> Crystallographic Data and Refinement Parameters for complex 3	152
9	<b>Table 4.3.1</b> Catalytic performance of complex 7 for the peroxidative oxidation of vanillyl alcohol to vanillic acid in a mixture of choline chloride and glycerol (1:2 molar ratio).	184
10	<b>Table 4.3.2.</b> Catalytic performance of complex 7 for the peroxidative oxidation of vanillyl alcohol in various DESs.	185
11	<b>Table 4.3.3</b> Calculation of different metrics of vanillyl alcohol oxidation under optimized condition.	186
12	<b>Table 4.5.1.</b> Crystallographic Data and Refinement Parameters for complex 7	206
13	<b>Table 5.3.1.</b> Catalytic performance of 8 for the peroxidative oxidation of benzyl alcohol to benzaldehyde.	225
14	<b>Table 5.3.2.</b> Catalytic performance of 8 for the peroxidative oxidation of benzyl alcohol in different solvents.	230
15	<b>Table 5.5.1.</b> Crystallographic Data and Refinement Parameters for complex 7	243

## List of Abbreviations Used

Å	Angstrom
Anal.	Analytically
Anhyd	Anhydrous
aq	Aqueous
bp	Boiling Point
br	Broad
°C	Degree Celcius
Calcd	Calculated
cm	Centimeter
Conc	Concentrated
conv	Conversion
d	Doublet
DCM	Dichloromethane
dd	Doublet of a Doublet
DMF	N,N-Dimethyl Formamide
eq	Equation
equiv	Equivalent

Et	Ethyl
g	Grams
h	Hours
HRMS	High-resolution Mass Spectrometry
IR	Infrared
K	Kelvin
kcal	Kilo calories
lit	Liter
m	Multiplet
M	Molar
MeCN	Acetonitrile
mp	Melting point
Me	Methyl
MHz	Mega Hertz
Min	Minutes
mL	Milliliter
mM	Millimolar
mmol	Millimole
mol	Mole
MS	Mass Spectra

N	Normal
NMR	Nuclear Magnetic Resonance
ppm	Parts per Million
rt	Room Temperature
s	Singlet, Seconds
TLC	Thin Layer Chromatography
TOF	Turn Over Frequency
TON	Turn Over Number
XRD	X-Ray Diffraction
NaOMe	Sodium methoxide
TH	Transfer Hydrogenation

<b>Table of contents</b>		<b>Page no</b>
Synopsis	Development of Ruthenium and Iron Complexes for Catalytic Applications in Sustainable Oxidations and Reductions	9
List of Schemes		17
List of Figures		18
List of Tables		20
List of Abbreviation used		22
Chapter 1.1	General introduction of TH	27
Chapter 1.2	General introduction of Oxidation	41
Chapter 2	Transfer Hydrogenation of Aldehydes and Ketones in Air with Methanol and Ethanol by an Air-stable Ruthenium-triazole Complex	56
	2.1 Abstract	56
	2.2 Introduction	56
	2.3 Result and Discussion	61
	2.4 Conclusion	75
	2.5 Experimental section	75
	2.6 Reference	75
		99
Chapter 3	Catalytic Transfer Hydrogenation of Lignocellulosic Biomass Model Compounds Furfural and Vanillin with Ethanol by an Air-stable Iron (II) Complex	116
	3.1 Abstract	116
	3.2 Introduction	117
	3.3 Result and discussion	122
	3.4 Conclusion	140
	3.5 Experimental section	141
	3.6 Reference	157
Chapter 4	Base Metal Iron Catalyzed Sustainable Oxidation of Vanillyl Alcohol to Vanillic Acid in Deep Eutectic Solvent and Implementation of Vanillic Acid for Fine-Chemical Synthesis	174
	4.1 Abstract	174
	4.2 Introduction	177
	4.3 Result and discussion	180
	4.4 Conclusion	189
	4.5 Experimental section	191

	4.6 Reference	207
Chapter 5	Iron Catalyzed Oxidation of Primary Alcohols: Reaction Media Induced Chemodivergent Aldehyde and Acid Selectivity	216
	5.1 Abstract	216
	5.2 Introduction	217
	5.3 Result and discussion	221
	5.4 Conclusion	235
	5.5 Experimental section	236
	5.6 Reference	244
Chapter 6	Summary of the thesis	251

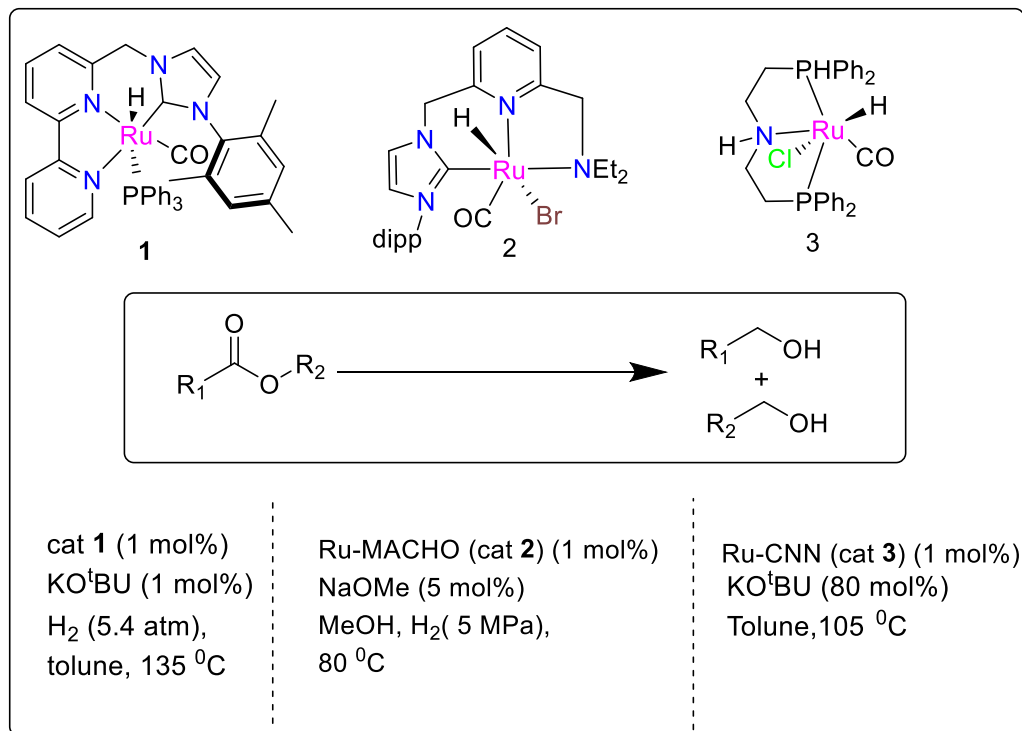
## Chapter 1.1

### **General introduction of TH of carbonyls with transition metal catalyst utilising both ethanol and methanol as sacrificial hydrogen donor**

Reduction of different functionalities is one of the most fundamental and important reaction in academia, as well as industrial point of view. Historically several hydrides donating reagents like  $\text{LiBH}_4$ ,  $\text{NaBH}_4$ , DIBAL-H etc., are used to meet the fulfilment of above requirement. However, the above synthetic procedures have the drawback as they are produced a large amount of by products which is not suitable for the industrial purpose. To overcome the above-mentioned drawback catalytic hydrogenation is most acceptable one. Till now a number of reports published over catalytic hydrogenation using different transition metal catalyst for the selective reduction of different functional groups like,  $-\text{C}=\text{O}$ ,  $-\text{C}\equiv\text{C}$ ,  $-\text{C}\equiv\text{N}$ ,  $-\text{NO}_2$ ,  $-\text{COOR}$  etc. The selective hydrogenation is most precious jewel in the crown of hydrogenation transformations.<sup>1-6</sup> In 1823, French chemist Paul Sabatier, Father of hydrogenation process, developed a device named Döbereiner's lamp where he successfully did the addition of hydrogen to oxygen molecule in the presence of palladium catalyst. With time to time more development had done in hydrogenation specially with heterogeneous catalyst. In recent time scientist are also interested to explore the efficiency of hydrogenation with homogenous catalytic systems. In 2006 Milstein's group had reported ruthenium mediated pincer type complex for the selective hydrogenation of ester to alcohol.<sup>7</sup> Later in 2011 Song and co-workers published a pyridine-based ruthenium CNN pincer type complex for the selective hydrogenation of esters.<sup>8</sup> Further development was archived by Kuriyama's research group in the same year. They reported ruthenium based PNP pincer type complex for the selective hydrogenation esters and other functionalities.<sup>9</sup> Though catalytic hydrogenations are the important class of reactions in academia as well as industry, it suffers some the major limitations. Firstly, the use of hazardous Hydrogen gas at high temperature

and high pressure, secondly use of elaborated experimental set up and lastly possibility formation side products due to over reduction or limitation in showing selectivity.

### Scheme 1.1.1: Ruthenium catalysed hydrogenation of Esters



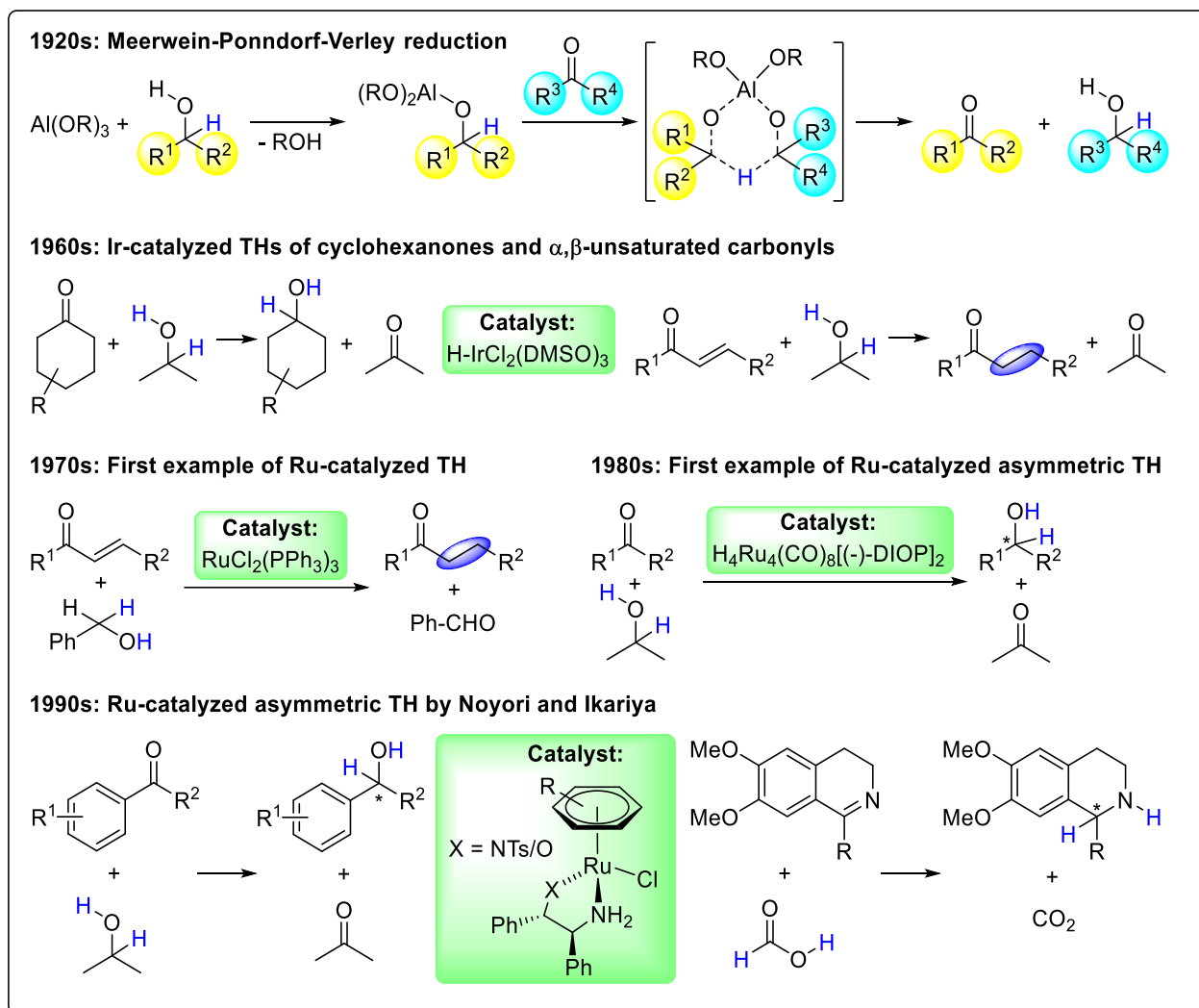
Transfer hydrogenation (TH) is one of the easy alternatives of hydrogenation as it avoids all the difficulties on hydrogenation. Most of the cases the catalysts used for TH are easily accessible and air-stable and the major side products can be recycled.<sup>6</sup> In 1903 Knoevenagel reported TH of dimethyl 1,4-dihydroterephthalate effectively to cis-hexahydroterephthalate and dimethyl terephthalate using palladium back as catalyst.<sup>10</sup> Later on, Braude and Linstead explained different types of hydrogen transfer reactions. Among them TH-dehydrogenation which occurs between unlike donor and acceptor units, widely known as TH. The first TH reaction of carbonyls was performed by Meerwein-Ponndorf-Verley (MPV) in 1925, using aluminium alkoxide as a catalyst.<sup>11</sup> In the MPV process the reaction proceeds via a six-membered cyclic transition state where both the carbonyl and reducing secondary alcohol are attached to the same metal centre. In recent times MPV reduction of carbonyls has been reported with different

metal zirconium, lanthanum, cerium, samarium etc. The mechanistic pathway of MPV reduction is well established.<sup>12-13</sup>

In last few decades, a significant number of reports had published in MPV reduction with heterogeneous Lewis acidic or basic catalyst which includes magnesium oxides, aluminium oxides, hydrotalcites, supported ZrO<sub>2</sub> etc.<sup>14</sup> The MPV reduction extensively applied in both industry and academia due to use of cheap, abundant, regenerable, and easy to separate catalytic systems and its chemoselectivity toward keto functionalities makes this process more applicable in chemical manufacture of flavour agents and pharmaceutical industry. However, the above process suffers with undesired side reactions, large amount of reagents and moistures sensitivity specially aluminium catalyst. In 1960 the breakthrough of TH occurs with the discovery of transition metal specially d<sup>6</sup>, d<sup>7</sup>, d<sup>8</sup> and d<sup>9</sup> catalysed TH using isopropanol as sacrificial hydrogen donor.<sup>15-17</sup> Iridium hydride complex catalysed TH was reported by Mitchell and co-workers for reduction of ketone using isopropanol as hydrogen donor. Later, in 1970 Sasson and Blum showed that, [RuCl<sub>2</sub>(PPh<sub>3</sub>)<sub>3</sub>] can be utilise as a catalyst for the TH of acetophenone using isopropanol at a very high temperature.<sup>18-20</sup> Another milestone of TH archive around 1990, when Choudhury and Bäckvall observed that the rate of TH increases many folds when catalytic amount of NaOH added along with [RuCl<sub>2</sub>(PPh<sub>3</sub>)<sub>3</sub>].<sup>21-22</sup> From the beginning of 1980 people showed a significant interest ruthenium catalysed asymmetric TH (ATH) of different functionalities. Since then, ATH had become the important part of TH as it is an important process in pharmaceutical and fragrance industry.<sup>23-24</sup> In 2001 Nyori and Knowles awarded Nobel Prize for their contribution in field of ATH. ATH with late transition metal is an excellent method for the asymmetric reduction of various functionalities to generate chirality in final products. Till now, a great advancement had done in the development of late transition metal catalyst for the both TH and ATH. A vast variation of transition metal, ligand, bases, hydrogen source,

unsaturated compounds are involved in this process, which makes the TH a talking point in scientific world.<sup>25-28</sup>

**Figure 1.1.1: Chronic development transition metal catalyzed TH of unsaturated double bond**

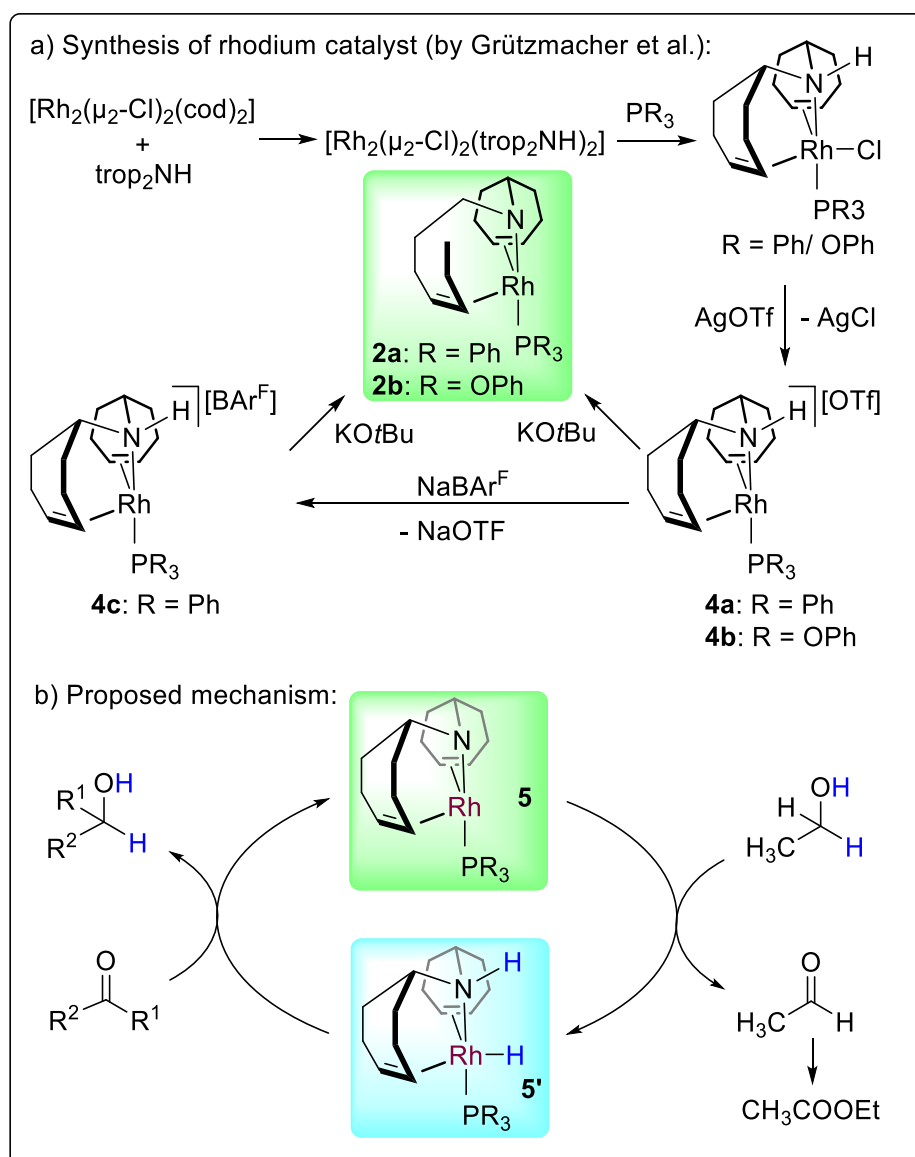


Later, the golden era of TH began with a large variety of homogeneous catalyst containing different transition metal (ruthenium, iron, osmium, cobalt, rhodium, iridium, nickel, palladium and gold) using isopropanol and formic acid as sacrificial hydrogen donor. TH with formic acid and isopropanol is extensively studied in last few years. However, TH with primary alcohols methanol and ethanol is challenging due to their unfavorable redox potentials and the number of reports is significantly very low. In 2018, Thiel et al. reported DFT calculation on the TH of acetophenone with isopropanol at 40 °C, where the  $\Delta G$  value

of + 4.4 kJ/mol was observed.<sup>29</sup> In contrast, a significantly higher  $\Delta G$  value (+ 24.2 kJ/mol) was obtained if ethanol is used instead of isopropanol. With methanol as hydrogen source, the equilibrium situation is even more unfavorable ( $\Delta G = + 40$  kJ/mol). In addition, methanol and ethanol produce aldehydes as reactive byproducts which may undergo unwanted side reactions in basic medium. However, isopropanol is mostly obtained from fossil fuels (hydration of propene).<sup>30-31</sup> Majority of important organic chemicals comes from fossil fuels which have limited reserves. Additionally, the extensive use of fossil fuels has other serious consequences. In contrast, methanol and ethanol are cheap, ecologically benign, bio-abundant and renewable and the use of methanol and ethanol in THs is very significant in the context of sustainable chemistry. Both methanol and ethanol are excellent hydrogen carriers with high 12.5%(w/w) of hydrogen and they are accessible from natural gas, carbon dioxide and renewable biomass. In THs, the replacement of isopropanol with ethanol and methanol is significant with the increasing demand for sustainable developments. In 2008, Grützmacher et al. made a breakthrough in the field of TH; the first example of TH using ethanol was published.<sup>32</sup> The syntheses of pre-catalysts were reported previously by the same group. The coordination of the bis(olefin)amine ligand trop<sub>2</sub>NH (**L**<sub>1</sub>) with [Rh<sub>2</sub>( $\mu$ -Cl)<sub>2</sub>(cod)<sub>2</sub>] followed by the reaction with phosphine/phosphite yielded neutral species [Rh (Cl)(trop<sub>2</sub>NH)(PR<sub>3</sub>)]. Replacement of coordinated chloride with non-coordinating anions such as resulted in the formation of cationic Rh(I) bis(olefin)amine complexes [Rh(trop<sub>2</sub>NH)(PR<sub>3</sub>)]<sup>+</sup>[X]<sup>-</sup> (**4a-c**). Pre-catalysts **4a-c** were activated in presence of base (KO<sup>t</sup>Bu). The resulted active species Rh(I) diolefin amide [Rh(trop<sub>2</sub>N)(PR<sub>3</sub>)] (**4a,c**) proved to be an outstanding catalyst (with maximum TON of 100000 and TOF of 500000 h<sup>-1</sup>) for the TH of various aliphatic and aromatic ketones at r.t. under inert atmosphere using ethanol as hydrogen donor as well as solvent (Scheme 1.1.1). Ethanol is converted to acetaldehyde which is further transformed into ethyl acetate as a more stable byproduct. Mechanistic path of the above THs involves the

activation of O-H and C-H bonds of ethanol by metal-ligand cooperation (Scheme 1.1.2). Hydrogen transfer from the ethanol to the Rh(I)-amide species (**5**) resulted in the formation of Rh(I)-hydride with coordinated amine (**5'**) with the formation of acetaldehyde as byproduct. Thereafter, hydrogens from N-H and Rh-H are transferred to the C=O bond in ketone substrate which yielded the alcohol product and regenerate the active catalyst **5**.

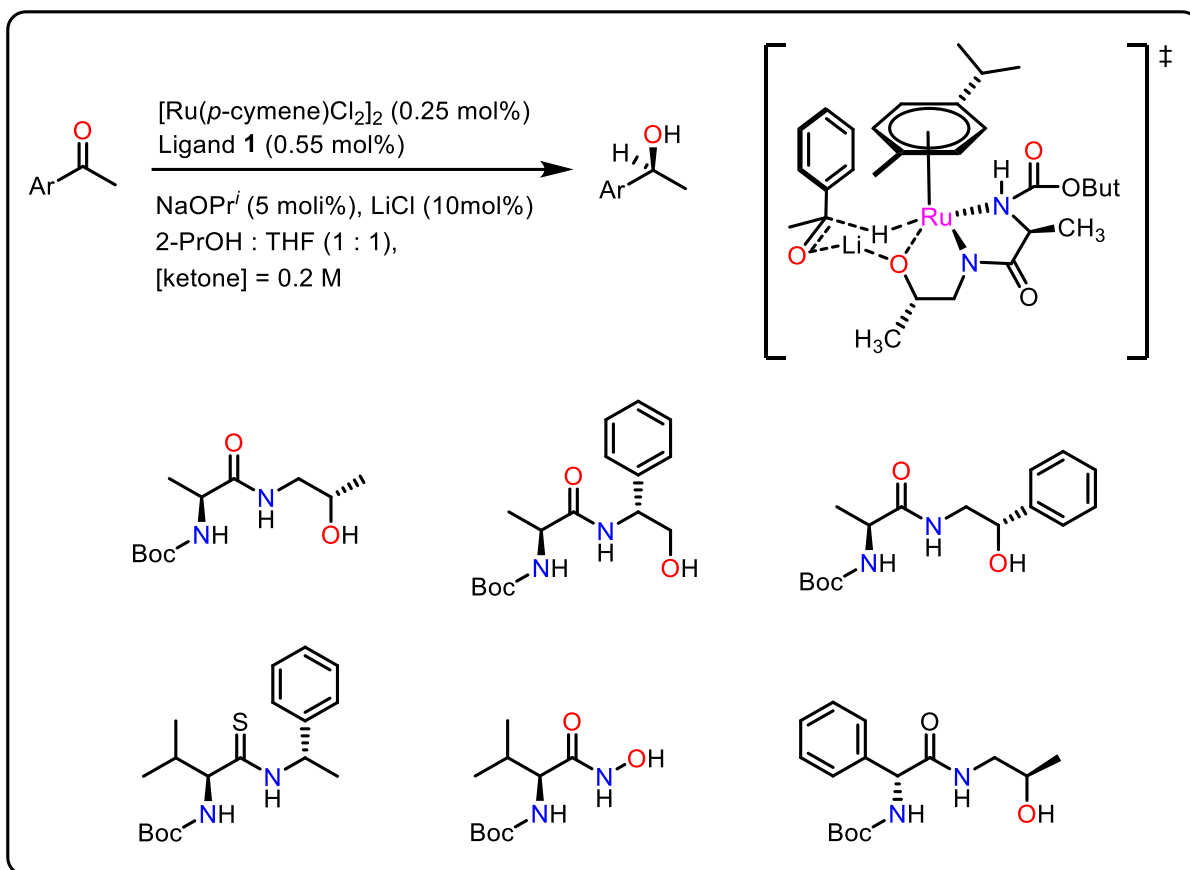
**Scheme 1.1.2. Rh catalyzed TH of ketone utilizing ethanol as hydrogen donor.**



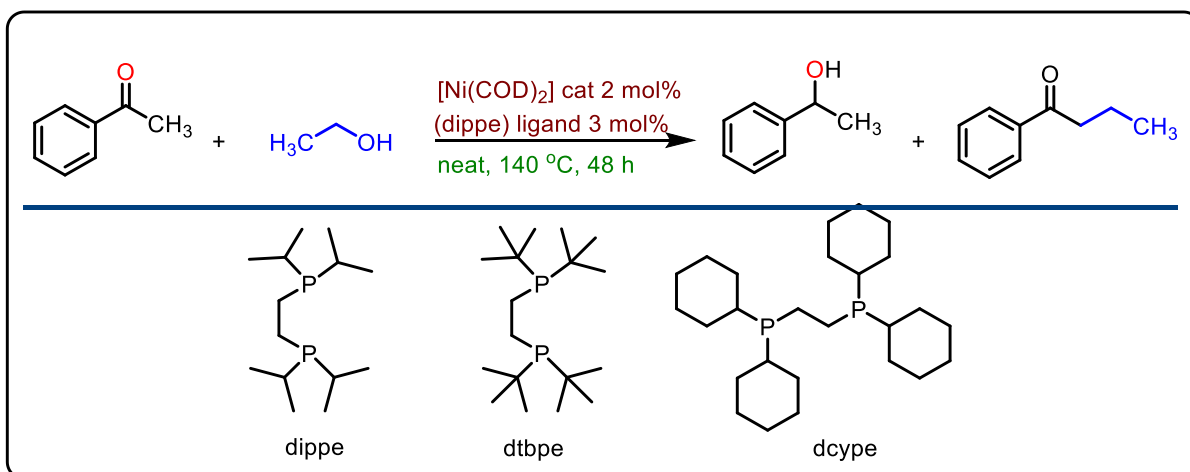
In the following year, same group reported various chiral bis(olefin)amine ligands and the corresponding cationic Rh(I) complexes with general formula  $[\text{Rh}(\text{trop}_2\text{NH}^*)(\text{CO})][\text{OTf}]$

were synthesized and utilized for asymmetric transfer hydrogenation of acetophenone with ethanol in presence of KO<sup>t</sup>Bu under argon atmosphere.<sup>33</sup> However, impressive enantioselectivity was not observed in ethanol. The following report on asymmetric TH of ketone in ethanol was published by Adolfsson et al. in 2011.<sup>34</sup> Under inert (N<sub>2</sub>) condition, ruthenium catalyzed asymmetric THs acetophenone were performed in 1:1 mixture of ethanol/THF at 40 °C in presence of LiCl as additive. [Ru(*p*-cymene)Cl<sub>2</sub>]<sub>2</sub> was used as the catalyst precursor and various chiral amino acid based ligands were screened. Amino acid hydroxyl-amide was tested as the most promising. Various aromatic ketones were reduced to the corresponding secondary alcohols in moderate to good yields and good to excellent enantioselectivity (*ee* 89-97%). Ruthenium is a heavily used metal for the homogeneous THs of carbonyls using isopropanol or formic acid as hydrogen sources.<sup>35</sup> This is also true if ethanol is used as a source of hydrogen. In last five years, three groups utilized ruthenium catalysts for the same purpose. In 2016, Garcia et al. published nickel (0) catalyzed TH of ketones using ethanol in absence of base (Scheme 1.1.4). This catalytic system reduced a variety of alkyl-aryl, diaryl, and aliphatic ketones to their corresponding alcohols.<sup>36</sup> Among all alcohols they have used as a hydrogen donor, interestingly ethanol showed an encouraging result. Ni(COD)<sub>2</sub> and dppe ligands in situ combinations give complete conversion of acetophenone to 1 phenylethanol at very high temperature and long time. Several phosphine ligands have been utilized for this catalytic system, and among them, dppe showed an attractive result. The use of electron-donating phosphine ligand helps to improve the catalytic performance towards a satisfactory result.

### **Scheme 1.1.3: Ruthenium catalysed ATH using chiral ligand in ethanol**



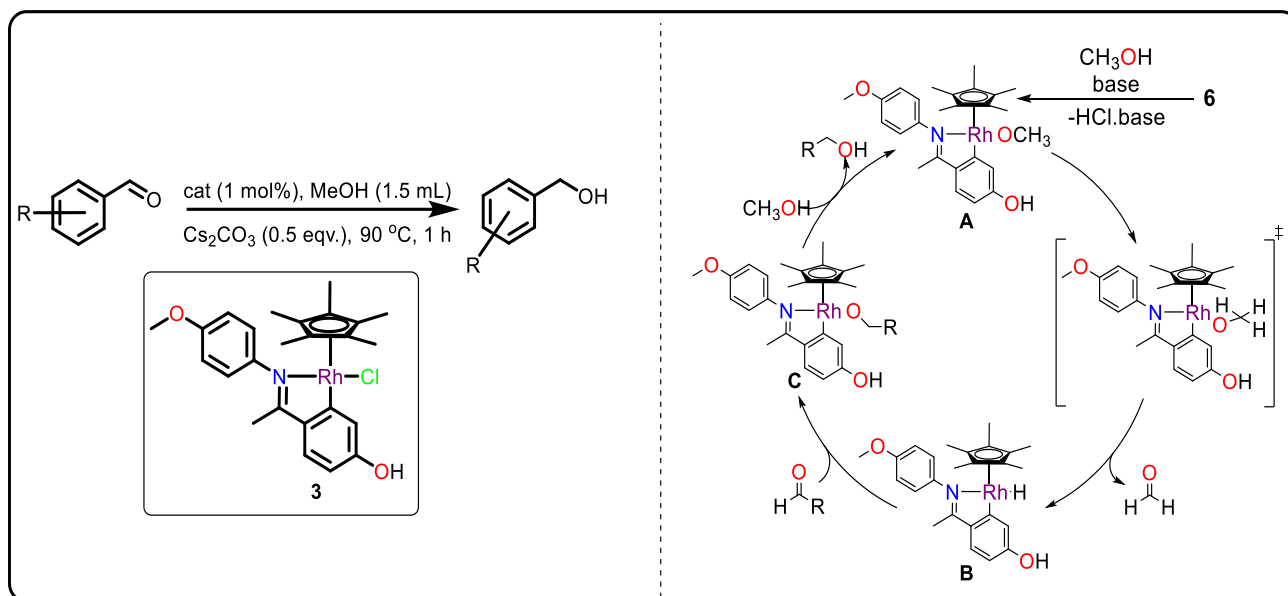
**Scheme 1.1.4: Nickel catalysed TH of ketones utilising bidentate phosphene ligand in ethanol**



A cyclometalated rhodium complex (6) which performed as an efficient catalyst for the reduction of aldehydes using methanol in an open atmosphere was reported by xiao et al. in 2018.<sup>37</sup> This catalyst incorporated high chemoselectivity towards a vast range of aromatic aldehydes<sup>22</sup> and was efficient enough to give a complete conversion of 4-nitro benzaldehyde

to corresponding alcohol within 1 hour (Scheme 1.1.5). To investigate the proper mechanistic cycle, they identified that the formation of rhodium hydride is the crucial step of the catalytic process. (Fig 1.1.1) In the presence of CD<sub>3</sub>OD, 90% deuterium incorporation in the benzylic position of benzyl alcohol proves that the methanol act as a hydrogen donor.

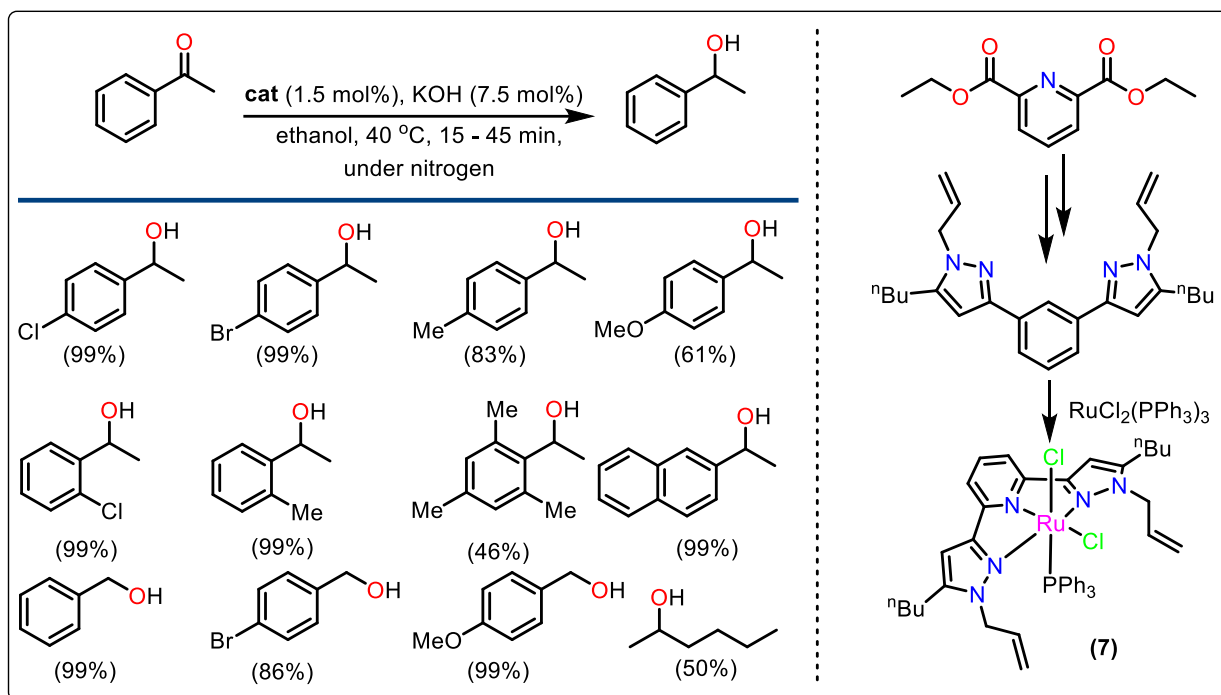
**Scheme 1.1.5: Rhodium catalysed TH of aldehydes in methanol and proposed mechanistic cycle**



In 2018, Thiel et al. reported a competent air and moisture-stable ruthenium (II) (7) catalyst for the TH in ethanol and this catalyst has avoided any undesired side products.<sup>29</sup> They have synthesized 2,6-bis(1H-pyrazol-3-yl)-pyridine ligand from cheap pyridine 2,6-dicarboxylic acid diethyl ether in just three steps to get around 60% yield. Later on, the simple addition of ligand and RuCl<sub>2</sub>(PPh<sub>3</sub>)<sub>3</sub> gave their desired ruthenium complex (Scheme 1.1.6). The author observed the formation of acetic aldehyde as a side product instead of ethyl acetate. In the presence of N<sub>2</sub> flow, they have achieved the complete conversion of acetophenone to its corresponding alcohol at 40 °C whereas in absence of nitrogen the conversion dropped to 33%. At 40 °C acetic aldehyde was removed from the reaction mixture due to its low boiling point and this helps the reaction to shift right side according to La chatelier's principle. This

indicates that acetic aldehyde removal during the reaction is much needed. The author has been able to get an excellent conversion with a wide variety of aromatic ketones.

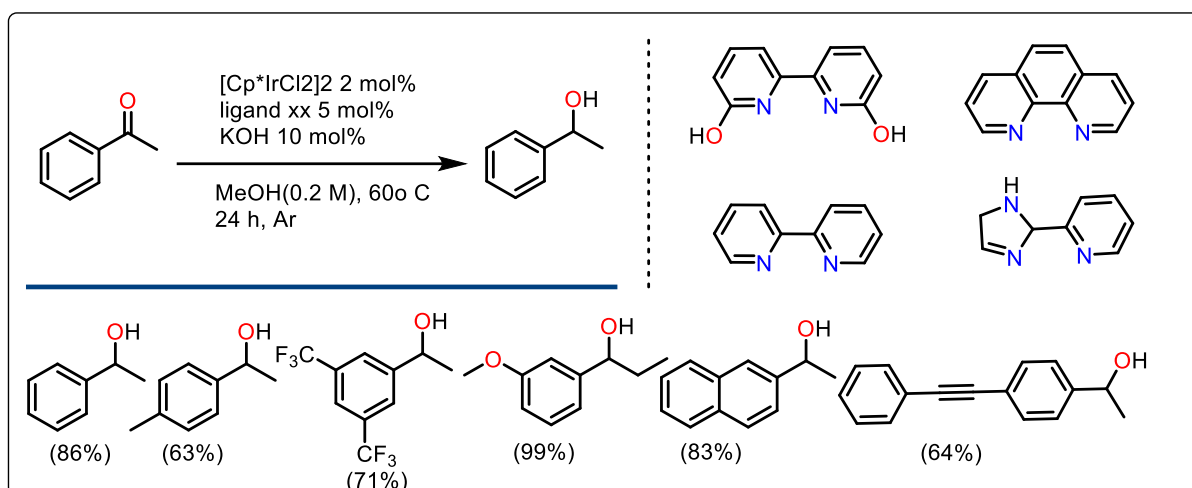
**Scheme 1.1.6: Tridentate Ruthenium complex catalysed TH using ethanol as hydrogen source under inert condition**



In 2020 Sundararaju and co-workers demonstrated an efficient catalytic protocol for the catalytic TH using Ir(III) as the catalyst and methanol as a liquid hydrogen carrier.<sup>38</sup> The in-situ combination of late transition metal precursor and commercially available ligand gave a fine conversion from ketone to a secondary alcohol. The transformation was promising for both electron donation and election withdrawing substrates. (Scheme 1.1.7) In the presence of different functional groups, this catalytic system can selectively reduce only the keto group with moderately to high yield. Reduction of challenging bioactive natural products such as stanolone, pentoxifylline, carvone, 16-dehydropregnenolone have been successfully done. To investigate the mechanistic pathway deuterated experiment was performed in the presence of acetophenone and CD<sub>3</sub>OD which resulted 56% incorporation of deuterium in alcohol. To Get further information about the mechanism, a reaction was carried out in the absence of

methanol using  $\text{HCO}_2\text{Na}$  as a hydrogen source, and 75% conversion to the expected product was observed. This suggests that in the reaction medium, methanol oxidized to an aldehyde and immediately converted to formate in the presence of a base that also acts as a hydrogen donor.

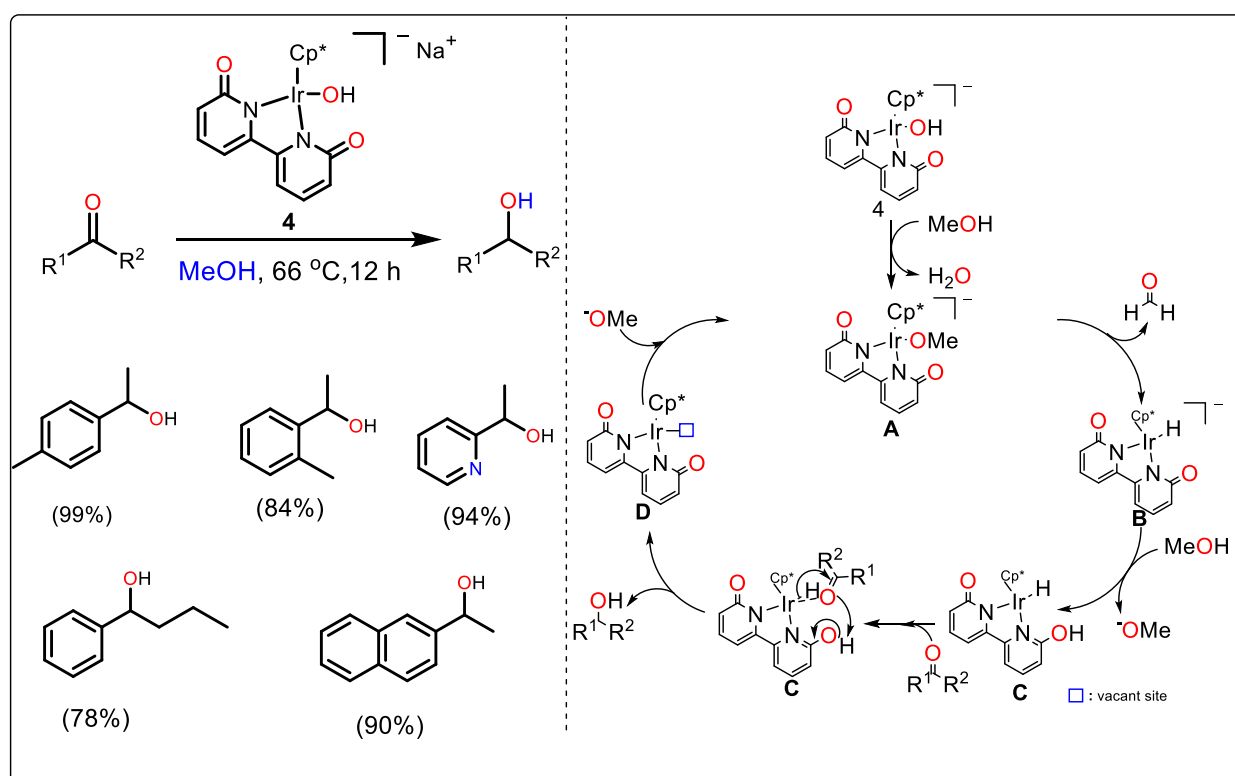
**Scheme 1.1.7: iridium catalysed TH utilising methanol as hydrogen source**



In the same year, Feng Li et al. published an anionic iridium complex that can be utilized for the TH of ketones in base-free conditions using methanol as the hydrogen source. The author has described a series of bidentate half sandwich iridium complexes involving metal-ligand cooperation.<sup>39</sup> Under nitrogen atmosphere  $[\text{Cp}^*\text{Ir}(2,2'\text{-bpyO})(\text{OH})][\text{Na}]$  (**8**) gives complete transformation from ketone to secondary alcohol in 12 h at 66 °C. The catalyst mentioned above efficiently reduces many substrates with electron-donating as well as electron-withdrawing groups, and in both cases, the result was satisfactory. (Scheme 1.1.8) Despite the fact that this catalyst was efficient but it failed to impart chemoselectivity when both  $\text{C}=\text{O}$  and  $\text{C}=\text{C}$  were present and reduced both under the same condition. In the proposed mechanistic cycle, the author depicted that initially, anionic methoxy species were generated via the iridium complex and methanol with the elimination of water. In the next step,  $\beta$ -hydride elimination takes place to form the iridium hydride complex, which is the important

step in the reported catalytic cycle following the proton transfer from the metal hydride complex to the keto group to give desired alcohol. A deuterium study was done to get further information on the catalytic cycle. Two parallel reactions were done in CH<sub>3</sub>OH and CD<sub>3</sub>OD and the kinetic isotope effect was found,  $K_H/K_D = 1.65$  which suggests that the cleavage of C-H is rate-determining step of the whole catalytic system.

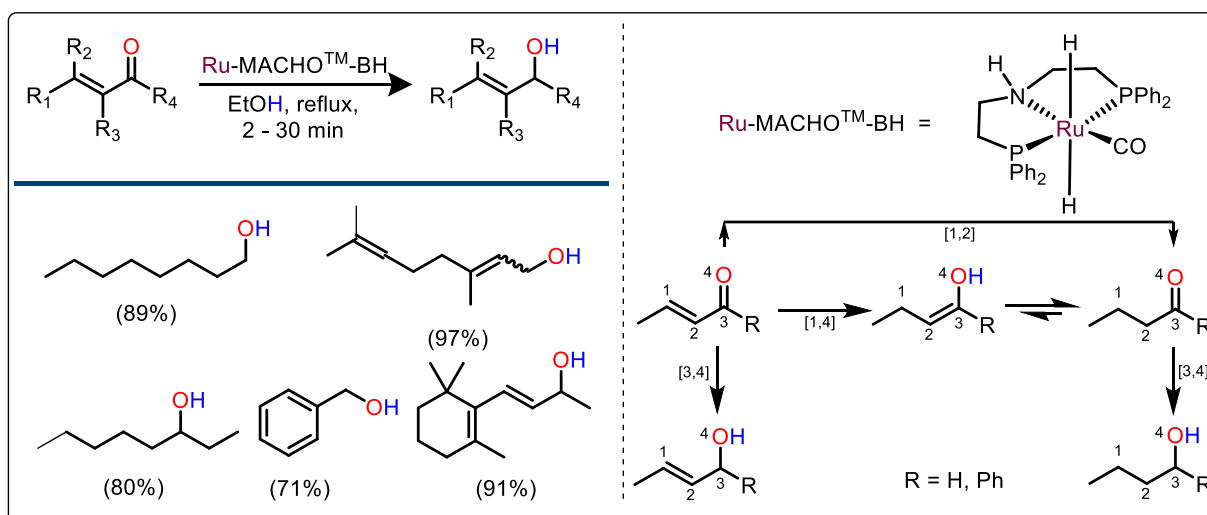
**Scheme 1.1.8: Half sandwich iridium complex catalysed TH utilising methanol and proposed mechanistic cycle**



Chemo selective reduction of  $\alpha, \beta$  unsaturated carbonyl compounds is one of the most exciting topics for the chemist. Amidst the World War 2, butadiene was produced from ethanol using a  $SiO_2-MgO-Ta_2O_5$  at 450 °C. A significant drawback of this process lies in its poor selectivity and maximum selectivity can be achieved up to 60%. In the last few years, several heterogeneous catalysts have been reported to improve selectivity but example of homogeneous catalysts for the selective reduction of  $\alpha, \beta$  unsaturated carbonyl is limited. In 2018 Jonathan G. de Vries reported a commercially available Ru-MACHOTM-BH catalyst

for the selective TH of  $\alpha$ ,  $\beta$  unsaturated carbonyl compounds using ethanol as a hydrogen source in base-free conditions.<sup>40</sup> (Scheme 1.1.9) With a very low catalyst loading, they achieved an excellent yield of allylic alcohol in a short period of time. The author had studied TH on a wide range of substrates and in most of the cases, the result was promising. They had proposed an outer sphere mechanism, and the rate-determining step proceeded via ruthenium hydride complex. B3PW91 Density fractional Theory calculation also supported the above fact. Methanol is a promising source of hydrogen, and our future economy has a high hydrogen capacity.

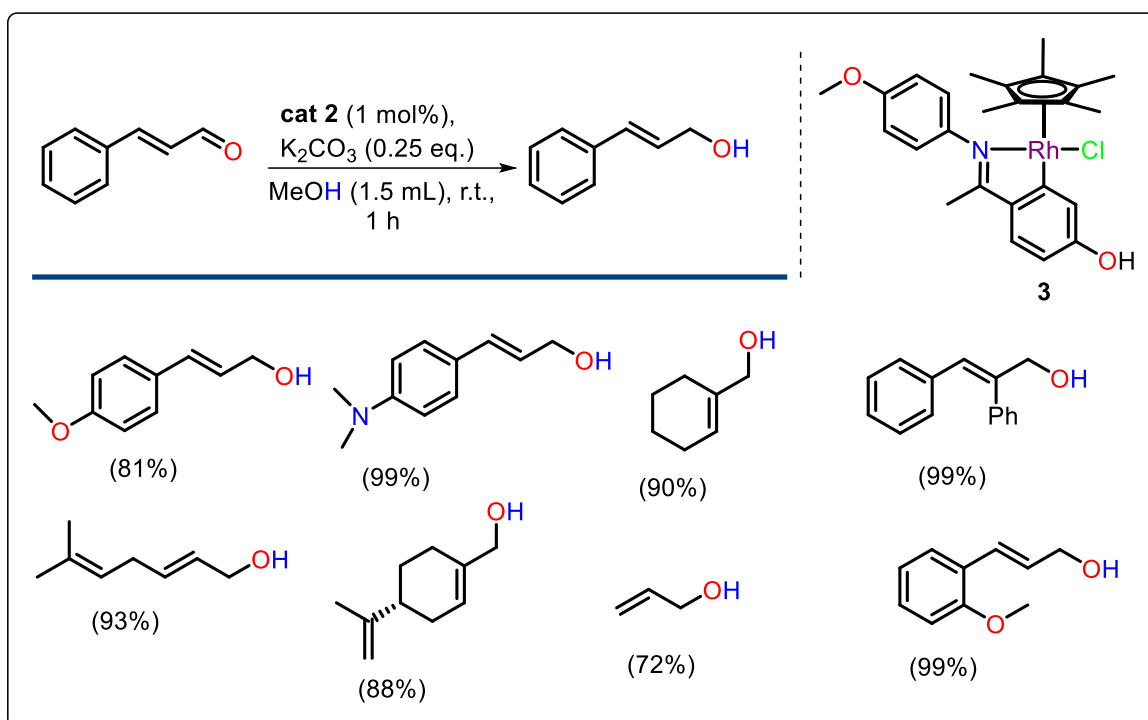
**Scheme 1.1.9: Ru-MACHO catalysed TH of  $\alpha$ ,  $\beta$  unsaturated carbonyl and proposed reaction pathway**



Xiao and co-workers published a cyclometalated rhodium complex (**7**) that has an excellent activity in TH of  $\alpha$ ,  $\beta$  unsaturated carbonyl compounds with methanol under mild conditions.<sup>41</sup> The author has shown that both groups, C=O and C=C, are reduced simultaneously. In the presence of 1 mol% rhodium catalyst, complete conversion was observed in just one hour at r.t. in broad range of substrate scopes of aromatic and aliphatic (Scheme 1.1.10). Even some steroids like deoxycholic acid lithocholic delivered excellent results towards TH. To enlighten the mechanistic pathway author claimed that the formation of rhodium hydride is a crucial step of the cycle. In presence of base metal, halides were

removed, and a rhodium alkoxy bond took place and subsequently  $\beta$ -hydrogen elimination took place to form rhodium hydride, which was confirmed by NMR spectroscopy. The rhodium hydride then transferred to an aldehyde to give the corresponding alcohol. To verify that methanol was the only hydrogen source a deuterated study was performed in  $\text{CD}_3\text{OD}$  and expectedly, 90% deuterated incorporation took place.

**Scheme 1.1.10: Rhodium complex catalysed TH of  $\alpha, \beta$  unsaturated carbonyls**



## Chapter 1.2

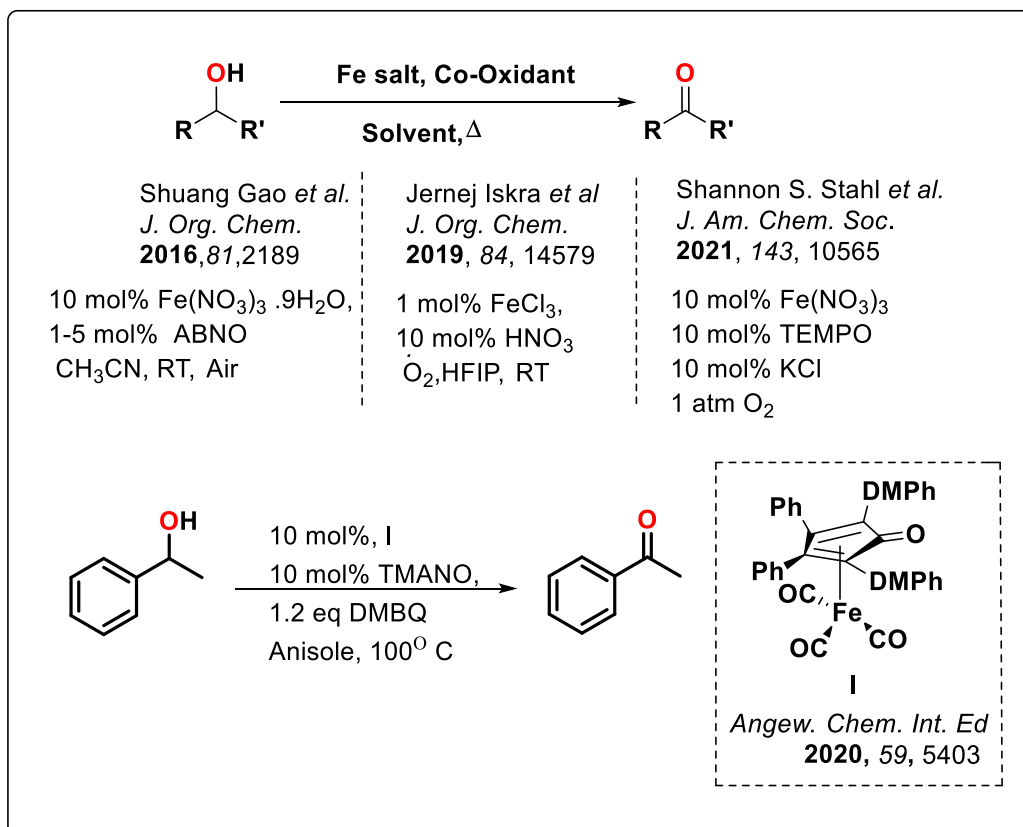
### General introduction of transition metal catalysed peroxidative oxidation of alcohols

Growing global economy and environmental safety concerns have pushed the synthetic chemist towards developing an efficient, selective, and atom economical organic transformation, which can be done under very safe and mild conditions.<sup>42-43</sup> In this point of view, alcohol is one of the most critical prospective substrates. Alcohol can produce from biomass and its high solubility in water and wide use as green solvents that attract the chemists. Having all the attractive features, alcohol's limitation lies in its poor reactivity in organic transformations. One of the main ways to overcome this issue is to oxidize alcohol to carbonyls which are far more reactive than alcohol.<sup>44-46</sup> The oxidation reaction of alcohol to carbonyl has become an important and ideal transformation and one of the key interesting research topics for chemists for academic and industrial purposes.<sup>47-49</sup> In recent years the utility and demand of carbonyl compounds have grown due to their use in pharmaceutical industries, fragrance, fine chemicals, and other industries.<sup>50-52</sup> Primary and secondary alcohol can both be oxidized to aldehyde and ketone.<sup>53</sup> Several methods were used extensively to transform alcohol to Carbonyl, which include activated dimethyl sulfoxide<sup>54</sup>, Dess-Martine periodinane<sup>55-56</sup>,  $\text{KMnO}_4$ <sup>57</sup>,  $\text{CrO}_3$ <sup>58</sup>, etc... The traditional oxidation systems are toxic, harmful, and explosive and produce a huge amount of hazardous chemical waste when carried out on an industrial scale.<sup>59-61</sup> There is a severe need to devolve atom economy, a cheap and sustainable catalytic methodology to overcome the problem.<sup>61-64</sup> Recently, many catalytic systems have been identified that can avoid the disadvantage of the traditional oxidation route. But the field is still growing, and this allows us to develop a system that can perform efficiently and effectively for the oxidation of secondary and primary alcohols to ketones and aldehydes respectively. In general, heterogeneous catalysts have shown a great dominance in the field of

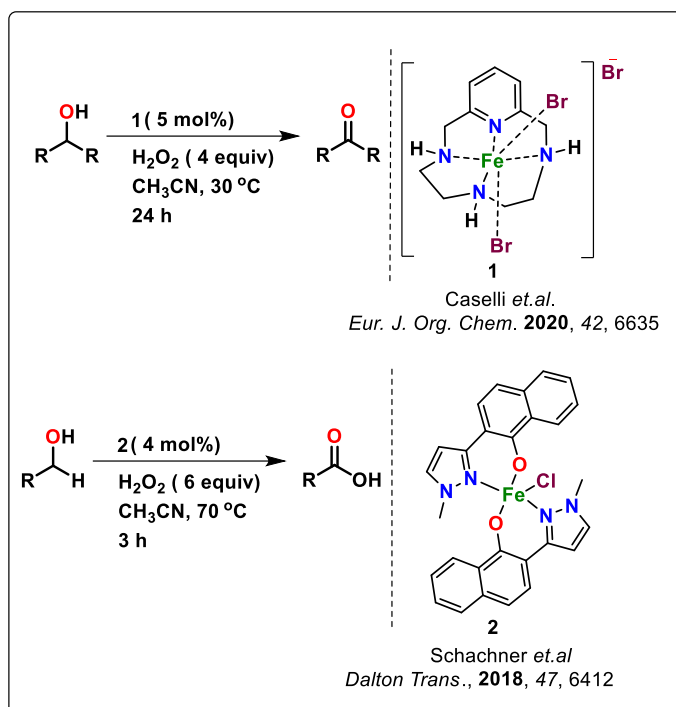
oxidation.<sup>65-66</sup> However, it has some drawbacks due to its very harsh conditions and long-time taken process.<sup>67</sup> Direct aerobic oxidation of alcohols in homogeneous transition metal catalysts is challenging. In past only some handful heavy metals Ru<sup>68-70</sup>, Pd<sup>71-73</sup>, Pt<sup>74-75</sup>, Rh<sup>76</sup>, and Au<sup>77-78</sup> are reported. But after completion of the reactions, heavy metals can contaminate the desired products, and that causes serious downsides in industrial applications.<sup>47</sup> To overcome this problem, chemists are always keen to design a new catalytic protocol that considers green and sustainable chemistry principles with care. So therefore, in recent time earth-abundant first row transition metal catalysts like Cu<sup>79-83</sup>, Co<sup>84-85</sup>, V<sup>86</sup>, Mo<sup>87</sup> and Ni<sup>88</sup> have grown significant attraction in terms of aerobic oxidation. Among all the transition metals, iron is the second most earth-abundant metal.<sup>89</sup> Iron is not only cheap, non-toxic, and economically attractive metal but also its unique electronic features help to improve the overall catalytic system.<sup>90</sup> In 2016 Shuang Gao and co-workers reported iron (III) nitrate catalysed oxidation of secondary alcohol in the presence of ABNO oxidant in the air using DCE as solvent.<sup>91</sup> Molecular oxygen in air helps to reactivate ABNO. In general, TEMPO is also a good candidate which is widely used as a co-oxidant. Molecular oxygen has an essential role in activating the TEMPO as a co-oxidant. Recently, Bagh *et al.* developed recyclable copper catalysts to oxidize vanillyl alcohol to vanillin under air using TEMPO as co-oxidant.<sup>92</sup> In 2020 Caselli *et al.* developed iron (III) complex with pyridine containing macro cycle ligand which shows good to excellent conversion of alcohol to carbonyl with H<sub>2</sub>O<sub>2</sub> co-oxidant.<sup>49</sup> Nitric acid also can be utilized as a co-oxidant.<sup>52</sup> In 2109 Ernež Iskra's research group published the selective oxidation of secondary alcohol using iron(III) chloride and nitric acid as a co oxidant where they had shown the formation of by-product as N<sub>2</sub>O and utilization of it in the reaction mechanism.<sup>93</sup> In 2021 Shannon S. Stahl's group oxidized secondary alcohol using iron(III) nitrate and tempo as co-oxidant. They successfully investigated Fe/aminoxyl catalytic process and distinguished between intrigated and serial redox co-operatively.<sup>94</sup> Most of the reports that are published in

recent time mostly on trivalent iron salts or complexes. But the use of divalent iron in oxidation protocol is infrequent. In 2020 Jan-E. Bäckvall and co-workers were the first to report Fe (II) catalysed Biomimetic alcohol oxidation along with electron-rich quinone and Co-(salen) type complex as electron transfer agents.<sup>95</sup> Since then, to our knowledge, no reports have been published yet. The need for developed green and sustainable catalytic systems has grown due to high carbonyl demand.<sup>96</sup> In 2018 schachaner et.al. reported a series of bidentate *N, O*-ligands containing phenol-pyrazole, naphthol-pyrazole, and the commercially available ligand 5-methylphenol-benzotriazole were utilised for the synthesis of iron(III) complexes <sup>97</sup> (scheme 1.2.1). The air and moisture sensitive mononuclear iron complexes are tested for the oxidation of primary alcohol with 30% aq. hydrogen peroxide (H<sub>2</sub>O<sub>2</sub>) as the oxidation agent. The reaction is straight forward and only biproduct is water.

**Scheme 1.2.1: Iron catalysed aerobic oxidation of both primary and secondary alcohols**



### Scheme 1.2.2: Iron catalysed peroxidative oxidation of both primary and secondary alcohols



The field of iron catalysed oxidation of alcohol has changed dramatically in last 15 years. Comparing with other transition metals iron is most attractive than others due to its low toxicity, abundant and cheap in price. From industrial point of view, switching to iron catalyst from precious heavy metal is a smart move and rapid research activity also help to find further potential application in this field. In recent time aerobic oxidation shown its utility to scientific world. Ma *et al.* published  $\text{Fe}(\text{NO}_3)_3$  catalysed aerobic oxidation of primary alcohols to their corresponding acids selectively using TEMPO and KCl as co catalyst. A moderate to high yield were obtained by the above-mentioned catalytic protocol.<sup>98</sup> Later on sato and co-workers utilise a mixture of  $\text{Fe}(\text{OAc})_2$  and picolinic acid for the selective oxidation of secondary alcohol to ketones with peroxides as oxidant.<sup>99</sup> The same group had also reported selective oxidation of  $\alpha,\beta$  unsaturated alcohol to acids with a comprehensive yield, utilising iron nitrate salt as catalyst. Iron nitrate is a fantastic candidate for the oxidation of alcohol.<sup>100</sup> Repo's group has reported selective oxidation of primary

alcohol to aldehyde using a mixture of  $\text{Fe}(\text{NO}_3)_3$  and 2,2'-bipyridine with TEMPO as co-catalyst.<sup>101</sup> They also showed that with increase the time upto 24 h a full conversion to acid has also observed. Further study showed that the cation  $\text{TEMPO}^+$  is predominantly oxidise alcohol to their corresponding aldehydes by the generation of TEMPOH. An aerobic oxidation of sulphides to sulfoxides, which have a great medicinal importance, was shown by Paine, utilising pyrazolyborate mediated iron complex. Martin groups also observed selective oxidation of cyclohexanol to cyclohexanone and 1 phenylethanol to acetophenone with similar type of pyrazolyl complex. Even though a significant result was observed in both solvent free and microwave assist condition. *N*-heterocyclic carbene complexes are very promising in showing catalytic oxidation of alcohols. Royo et. al. published a series of bis-*N*-heterocyclic carbene containing bipyridyl complexes with Fe(II) which showed a significant catalytic activity in solvent free condition of both primary and secondary alcohol utilising THHP as oxidant.<sup>102</sup> The catalytic protocol can be recycled and reused. Kim and co-workers also reported iron bipyridyl amide complex for the selective oxidation of both the alcohols to their corresponding carbonyls, utilising THHP as co-catalyst.<sup>103</sup> The secondary alcohol gives a significant yield of above 80%. But in case of primary alcohols both the oxidised products aldehyde and acids are obtained. That showed a poor selectivity of the mentioned catalytic protocol. A series of iron 2,2' - bipyridine complexes were reported by Farnetti and co-workers that successfully oxidise secondary alcohol to ketone.<sup>104</sup> They have shown a moderate to good selectivity in both primary and secondary alcohols. Later, Shul'pin et. al. demonstrate that silsesquioxanes formed by Fe, Na heterometallic system capable of oxidizing both cyclohexanol and 2 phenyl ethanol to their corresponding ketones up to 92% yields, utilising TBHP as oxidant.<sup>105</sup> Soon Mahamudov and pombebeiro published an iron formazan complex which show a catalytic activity in both solvent free and microwave assist conditions.<sup>106</sup> Oxidation of Methylene CH is also very important in chemistry point of view.

Di Stefano reported that imine pyridyl complexes can show oxidation methylene to keto with an excellent yield. However, the catalytic process also useful for the selective oxidation of both primary and secondary alcohols. They also demonstrated that utilisation of  $\text{H}_2\text{O}_2$  reduce the yield significantly due to competition with aryl hydroxylation reactions. Duan demonstrates chemo selective oxidation of primary alcohol to aldehyde with Fe (II) catalytic system which is both water soluble and re-useable.<sup>107</sup> The catalytic system was generated in situ from  $\text{FeCl}_3$ , assist with 8-amino quinoline. Some recent development in iron complexes also give us the broad aspect in oxidation of alcohols. Starting from simple iron salt to complicated and sophisticated iron complexes are tested for the successful alcohol oxidation. However, there is no clear trend observed which can predicts, which iron catalyst can be most promising one. For the methylene oxidation it supposed to be that two open coordination sites cis to each other can be beneficiary for the selective oxidation. In this view, tetradentate nitrogen donor ligand performed well. However, some reports in tridentate as well as bidentate ligand that have also showed promising result. Though both the oxidant TBHP and  $\text{H}_2\text{O}_2$  have crucial role in oxidation, the role of air is not negligible. Some catalytic protocols are reported in high temperature and some are in room temperature and room temperature reactions are reported with slightly longer reaction time. Most of reports demonstrate that acetonitrile is a good choice for solvent, but many reports suggest solvent free pathway. Baurer et.al. recently published an iron bis(picoly)amine complex for the selective oxidation of secondary alcohol to corresponding ketone, even in the presence of primary alcohol. Some recent development shown the challenging oxidation of glycerol which is the by product of industrial biodiesel production and its conversion to dihydroxyacetone have an economic interest. Farnetti use the same  $[\text{Fe}(\text{BPA})_2] (\text{OTf})_2$  for the oxidation of glycerol.<sup>108</sup> She observed that *in situ* generated complex from  $\text{Fe}(\text{OTf})_2$  and three equivalents of BPA give high selectivity in alcohol oxidation. Using the same catalyst with  $\text{H}_2\text{O}_2$  in aqueous medium

author found select oxidation from glycerol to formic acid. Mendelli and Shul'pin reported the oxidation hydroxyacetone with  $\text{FeCl}_3$  and  $\text{H}_2\text{O}_2$ .<sup>109</sup> Thus the iron catalysed oxidation of readily available glycerol to its derivative can be a game changer in industrial relevance. To develop a the green and sustainable organic process, the key factor is to use green solvents or go along with solvent-free.<sup>110</sup> In the present era, chemical industries are much concerned about selecting the solvents for the organic synthesis as solvents are one of the major sources to produce huge amounts of chemical waste. Water, ethanol, isopropanol, polarclean etc., are excellent candidates for utilizing green solvents for industrial purposes.<sup>64</sup> For the development of a green and sustainable reaction medium, we focus towards other potential alternatives. Deep eutectic solvents (DES) are the new class of green solvents which are recently come to light. DES is a good replacement of ionic liquids that can avoid the disadvantages of ionic liquids such as high cost, toxicity, complex synthetic procedure, and purification.<sup>111-114</sup> In recent times the utilization of DES in different fields such as solvent of electrochemical conducting polymers, production of carbon electrodes for capacitors,<sup>71</sup> recognizing of analytes (e.g.,  $\text{Na}^+$ ,  $\text{Li}^+$ ) in analytical devices etc. have grown significantly. Most interestingly, the use of DES as a solvent is still limited. This gives us the opportunity to explore the potential of DES as solvent in organic transformations.

### References:

- (1) Cervený, L., Ed.; Catalytic Hydrogenation; Elsevier: Amsterdam, 1986.
- (2) de Vries, J. G., Elsevier, C. J., Eds. The Handbook of Homogeneous Hydrogenation; Wiley-VCH: Weinheim, 2007.
- (3) Andersson, P. G., Munslow, I. J., Eds. Modern Reduction Methods; Wiley-VCH Verlag GmbH & Co. KGaA: Weinheim, 2008.
- (4) Magano, J.; Dunetz, J. R. Large-Scale Carbonyl Reductions in the Pharmaceutical Industry. *Org. Process Res. Dev.* **2012**, *16*, 1156–1184.

- (5) Robertson, A.; Matsumoto, T.; Ogo, S. The development of aqueous transfer hydrogenation catalysts. *Dalton Trans.* **2011**, *40*, 10304–10310.
- (6) Wang, D.; Astruc, D. *Chem. Rev.* **2015**, *115*, 6621–6686.
- (7) Zhang, J.; Leitun, G.; Ben-David, Y.; Milstein, D. *Angew. Chem., Int. Ed.* **2006**, *45*, 1113.
- (8) Sun, Y.; Koehler, C.; Tan, R.; Annibale, V. T.; Song, D. *Chem. Commun.* **2011**, *47*, 8349.
- (9) Kuriyama, W.; Matsumoto, T.; Ogata, O.; Ino, Y.; Aoki, K.; Tanaka, S.; Ishida, K.; Kobayashi, T.; Sayo, N.; Saito, T. *Org. Process Res. Dev.* **2012**, *16*, 166.
- (10) Wieland, H. Über Hydrierung und Dehydrierung. *Chem. Ber.* **1912**, *45*, 484–493.
- (11) Braude, E. A.; Linstead, R. P. Hydrogen Transfer. Part I. Introductory Survey. *J. Chem. Soc.* **1954**, 3544–3547.
- (12) Verley, A. *Bull. Soc. Chim. Fr.* **1925**, *37*, 537–542.
- (13) Meerwein, H.; Schmidt, R. *Liebigs Ann. Chem.* **1925**, *444*, 221–238.
- (14) Chuah, G. K.; Jaenicke, S.; Zhu, Y. Z.; Liu, S. H. Meerwein-Ponndorf-Verley Reduction over Heterogeneous Catalysts. *Curr. Org. Chem.* **2006**, *10*, 1639–1654.
- (15) Haddad, Y. M. Y.; Henbest, H. B.; Husbands, J.; Mitchell, T. R. B. *Proc. Chem. Soc. London* **1964**, 361–365.
- (16) Trochagr, J.; Henbest, H. B. *Chem. Commun.* **1967**, 544–544.
- (17) McPartli, M.; Mason, R. *Chem. Commun.* **1967**, 545–546.
- (18) Sasson, Y.; Blum, J. *Tetrahedron Lett.* **1971**, *12*, 2167–2170.
- (19) Blum, J.; Sasson, Y.; Iflah, S. *Tetrahedron Lett.* **1972**, *13*, 1015–1018.
- (20) Sasson, Y.; Blum, J. *J. Org. Chem.* **1975**, *40*, 1887–1896.
- (21) Bianchi, M.; Matteol, U.; Menchi, G.; Frediani, P.; Pratesi, U.; Piacenti, F.; Botteghi, C. *J. Organomet. Chem.* **1980**, *198*, 73–80.

- (22) Matteoli, U.; Frediani, P.; Bianchi, M.; Botteghi, C.; Gladiali, S. *J. Mol. Catal.* **1981**, *12*, 265–319.
- (23) Pugin, B.; Blaser, H.-U. *Top. Catal.* **2010**, *53*, 953–962.
- (24) Vaclavík, J.; Šot, P.; Vilhanova, B.; Pechaček, J.; Kuzma, M.; Kacer, P. *Molecules* **2013**, *18*, 6804–6828.
- (25) Kitamura, M.; Tokunaga, M.; Noyori, R. *J. Am. Chem. Soc.* **1995**, *117*, 2931–2932.
- (26) Fujii, A.; Hashiguchi, S.; Uematsu, N.; Ikariya, T.; Noyori, R. *J. Am. Chem. Soc.* **1996**, *118*, 2521–2522.
- (27) Uematsu, N.; Fujii, A.; Hashiguchi, S.; Ikariya, T.; Noyori, R. *J. Am. Chem. Soc.* **1996**, *118*, 4916–4917.
- (28) Noyori, R. Asymmetric Catalysis: Science and Opportunities (Nobel Lecture). *Angew. Chem., Int. Ed.* **2002**, *41*, 2008–2022.
- (29) Weingart, P.; Thiel, W. R.. *ChemCatChem.* **2018**, *10*, 4844–4848.
- (30) Xiao, H.; Wang, G.; Krische, M. J. Regioselective *Angew. Chem., Int. Ed.* **2016**, *128*, 16353–16356.
- (31) Castellanos-Blanco, N.; Flores-Alamo, M.; García, J. J. *Organometallics* **2012**, *31*, 680–686.
- (32) Zweifel, T.; Naubron, J.-V.; Büttner, T.; Ott, T.; Grützmacher, H. *Angew. Chem., Int. Ed.* **2008**, *47*, 3245–3249.
- (33) Zweifel, T.; Scheschke, D.; Ott, T.; Vogt, M.; Grützmacher, H. *Eur. J. Inorg. Chem.* **2009**, *2009*, 5561–5576.
- (34) Lundberg, H.; Adolfsson, H. *Tetrahedron Lett.* **2011**, *52*, 2754–2758.
- (35) Zielinski, G. K.; Samojłowicz, C.; Wdowik, T.; Grela, K. *Org. Biomol. Chem.* **2015**, *13*, 2684–2688.

- (36) Castellanos-Blanco, N.; Flores-Alamo, M.; García, J. J. *Organometallics*. **2012**, *31*, 680–686.
- (37) Aboo, A. H.; Bennett, E. L.; Deeprose, M.; Robertson, C. M.; Iggo, J. A.; Xiao, J. *Chem. Commun.* **2018**, *54*, 11805–11808.
- (38) Garg, N.; Paira, S.; Sundararaju, B. *ChemCatChem*. **2020**, *12*, 3472–3476.
- (39) Wang, R.; Han, X.; Xu, J.; Liu, P.; Li, F. *J. Org. Chem.* **2020**, *85*, 2242–2249.
- (40) Puylaert, P.; Dell’Acqua, A.; Ouahabi, F. E.; Spannenberg, A.; Roisnel, T.; Lefort, L.; Hinze, S.; Tin, S.; de Vries, J. G. *Catal. Sci. Technol.* **2019**, *9*, 61–64.
- (41) Aboo, A. H.; Bennett, E. L.; Deeprose, M.; Robertson, C. M.; Iggo, J. A.; Xiao, J. *Chem. Commun.* **2018**, *54*, 11805–11808.
- (42) Kamm, B.; Gruber, P. R.; Kamm, M. *Wiley-VCH*: **2006**; p 964.
- (43) Clark, J. H.; Luque, R.; Matharu, A. S. *Green Chemistry, Annu. Rev. Chem. Biomol. Eng.* **2012**, *3*, 183–204.
- (44) Frija, L. M.; Alegria, E. C.; Sutradhar, M.; Cristiano, M. L. S.; Ismael, A.; Kopylovich, M. N.; Pombeiro, A. J. *Journal of Molecular Catalysis A: Chemical*, **2016**, *425*, 283-290.
- (45) Gunanathan, C.; Milstein, D.; *Science*, **2013**, *341*, 12297121.
- (46) Marais, L.; Swarts, A. J. *Catalysts*, **2019**, *9*, 395.
- (47) Parmeggiani, C.; Matassini, C.; Cardona, F. *Green Chemistry*, **2017**, *19*, 2030-2050.
- (48) Chan-Thaw, C. E.; Savara, A.; Villa, A. *Catalysts*, **2018**, *8*, 431-343.
- (49) Meng, S. S.; Lin, L. R.; Luo, X.; Lv, H. J.; Zhao, J. L.; Chan, A. S. *Green Chemistry*, **2019**, *21*, 6187-619.
- (50) Panza, N.; di Biase, A.; Rizzato, S.; Gallo, E.; Tseberlidis, G.; Caselli, A. *European Journal of Organic Chemistry*, **2020**, 6635-6644.
- (51) Hudlicky, M. *ACS*, **1990**, Washington, DC

- (52) Rochat, S.; Minardi, C.; de Saint Laumer, J. Y.; Herrmann, A. *Helvetica Chimica Acta*, **2000**, *83*, 1645-1671.
- (53) Možina, S.; Iskra, J. *The Journal of Organic Chemistry*, **2019**, *84*, 14579-14586.
- (54) Smith III, A. B.; Leenay, T. L.; Liu, H. J.; Nelson, L. A.; Ball, R. G. *Tetrahedron letters*, **1988**, *29*, 49-52.
- (55) Dess, D. B.; Martin, J. C. *The Journal of Organic Chemistry*, **1983**, *48*, 4155-4156.
- (56) Dess, D. B.; Martin, J. C. *Journal of the American Chemical Society*, **1991**, *113*(19), 7277-7287.
- (57) Mahmood, A.; Robinson, G. E. Powell, L. *Organic Process Research & Development*, **1999**, *3*, 363-364.
- (58) Zhang, S.; Xu, L.; Trudell, M. L. *Synthesis*, **2005**, 1757-1760.
- (59) Sheldon, R. A.; Arends, I. W.; Ten Brink, G. J.; Dijksman, A. *Accounts of Chemical Research*, **2002**, *35*, 774-781.
- (60) Sheldon, R. A. *Catalysis Today*, **2015**, *247*, 4-13.
- (61) Sheldon, R. A. *Green Chemistry*, **2007**, *9*, 1273-1283.
- (62) Shi, F.; Tse, M. K.; Beller, M. *Chemistry—An Asian Journal*, **2007**, *232*, 411-415.
- (63) Davis, S. E.; Ide, M. S.; Davis, R. J. *Green Chemistry*, **2013**, *15*, 17-45.
- (64) Zhang, P.; Gong, Y.; Li, H., Chen, Z.; Wang, Y. *Nature communications*, **2013**, *4*, 1593.
- (65) Villa, A.; Dimitratos, N.; Chan-Thaw, C. E.; Hammond, C.; Prati, L.; Hutchings, G. J. *Accounts of chemical research*, **2015**, *48*, 1403-1412.
- (66) Yamaguchi, K.; Mori, K.; Mizugaki, T.; Ebitani, K.; Kaneda, K. *Journal of the American Chemical Society*, **2000**, *122*, 7144-7145.
- (67) Dhakshinamoorthy, A.; Asiri, A. M.; Garcia, H. *Chemical Communications*, **2017**, *53*, 10851-10869.

- (68) Sarmah, B.; Srivastava, R.; Manjunathan, P.; Shanbhag, G. V. *ACS Sustainable Chemistry & Engineering*, **2015**, *3*, 2933-2943.
- (69) Markó, I. E.; Giles, P. R.; Tsukazaki, M.; Chellé-Regnaut, I.; Urch, C. J.; Brown, S. M. *Journal of the American Chemical Society*, **1997**, *119*, 12661-12662.
- (70) Kotani, M.; Koike, T.; Yamaguchi, K.; Mizuno, N. *Green Chemistry*, **2006**, *8*, 735-741.
- (71) Murahashi, S.; Naota, T.; Ito, K.; Maeda, Y.; Taki, H. *The Journal of organic chemistry*, **1987**, *52*, 4319-4327.
- (72) Nishimura, T.; Maeda, Y.; Kakiuchi, N.; Uemura, S. *J. Chem. Soc., Perkin Trans. 1*, **2000**, Perkin Trans. 1.
- (73) Sato, K.; Tsuii, J. *Tetrahedron*, **1985**, *41*, 5645-5651.
- (74) Stuchinskaya, T. L.; Kozhevnikov, I. V. *Catalysis Communications*, **2003**, *4*, 417-422.
- (75) Chibani, S.; Michel, C.; Delbecq, F.; Pinel, C.; Besson, M. *Catalysis Science & Technology*, **2013**, *3*, 339-350.
- (76) Gangwal, V. R.; Van Wachem, B. G. M.; Kuster, B. F. M.; Schouten, J. C. *Chemical engineering science*, **2002**, *57*, 5051-5063.
- (77) Wang, X.; Wang, C.; Liu, Y.; Xiao, J. *Green Chemistry*, **2016**, *18*, 4605-4610.
- (78) Sankar, M.; Nowicka, E.; Tiruvalam, R.; He, Q.; Taylor, S. H.; Kiely, C. J.; Knight, D.W.; Hutchings, G. J. *Chemistry—A European Journal*, **2011**, *17*, 6524-6532.
- (79) Biella, S.; Rossi, M. *Chemical communications*, **2003**, 378-379.
- (80) McCann, S. D.; Stahl, S. S. *Accounts of Chemical Research*, **2015**, *48*, 1756-1766.
- (81) Gamez, P.; Arends, I. W.; Reedijk, J.; Sheldon, R. A. *Chemical communications*, **2003**, 2414-2415.

- (82) Rogan, L.; Hughes, N. L.; Cao, Q.; Dornan, L. M.; Muldoon, M. J. *Catalysis Science & Technology*, **2014**, *4*, 1720-1725.
- (83) Xu, B.; Lumb, J. P.; Arndtsen, B. A. *Angewandte Chemie*, **2015**, *127*, 4282-4285
- (84) Marko, I. E.; Gautier, A.; Dumeunier, R.; Doda, K.; Philippart, F.; Brown, S. M.; Urch, C. J. *Angewandte Chemie International Edition*, **2004**, *43*, 1588-1591.
- (85) Punniyamurthy, T.; Iqbal, J. *Tetrahedron letters*, **2014**, *35*, 4007-4010.
- (86) Iyer, S.; Varghese, J. P. *Synthetic communications*, **1995**, *25*, 2261-2266.
- (87) Conte, V.; Floris, B. *Dalton Transactions*, **2011**, *40*, 1419-1436.
- (88) Velusamy, S.; Ahamed, M.; Punniyamurthy, T. *Organic letters*, **2004**, *6*, 4821-4824.
- (89) Giannandrea, R.; Mastroilli, P.; Nobile, C. F.; Suranna, G. P. *Journal of molecular catalysis*, **1994**, *94*, 27-36.
- (90) Kunisu, T.; Oguma, T.; Katsuki, T. *Journal of the American Chemical Society*, **2011**, *133*, 12937-12939.
- (91) Mazza, S.; Scopelliti, R.; Hu, X. *Organometallics*, **2015**, *34*, 1538-1545.
- (92) Wang, L.; Shang, S.; Li, G.; Ren, L.; Lv, Y.; Gao, S. *The Journal of organic chemistry*, **2016**, *81*, 2189-2193.
- (93) Joshi, S. R.; Kataria, K. L.; Sawant, S. B.; Joshi, J. B. *Industrial & engineering chemistry research*, **2005**, *44*, 325-333.
- (94) Nutting, J. E.; Mao, K.; Stahl, S. S. *Journal of the American Chemical Society*, **2021**, *143*, 10565-10570.
- (95) Guðmundsson, A.; Schlipkoeter, K. E.; Bäckvall, J. E. *Angewandte Chemie International Edition*, **2020**, *59*, 5403-5406.
- (96) Jiang, X.; Zhang, J.; Ma, S. *Journal of the American Chemical Society*, **2016**, *138*, 8344-8347.

- (97) McElroy, C. R.; Constantinou, A.; Jones, L. C.; Summerton, L.; Clark, J. H. *Green Chemistry*, **2015**, *17*, 3111-3121.
- (98) Jiang, X.; Zhang, J.; S. Ma, S. *J. Am. Chem. Soc.* **2016**, *138*, 8344– 8347.
- (99) Tanaka, S.; Kon, Y.; Ogawa, A.; Uesaka, Y.; Tamura, M.; Sato, K.; *ChemCatChem* **2016**, *8*, 2930–2938.
- (100) Tanaka, S.; Kon, Y.; Uesaka, R. Y.; Morioka, Tamura, M.; Sato, K.; *Chem. Lett.* **2016**, *45*, 188–190.
- (101) Lagerblom, K.; Wrigstedt, P.; Keskiaväli, J.; Parviainen, A.; Repo, T. *ChemPlusChem*, **2016**, *81*, 1160-1165.
- (102) Pinto, M. F.; Cardoso, B. D. P.; Barroso, S.; Martins, A. M.; Royo, B. *Dalton Transactions*, **2016**, *45*, 13541-13546.
- (103) Bae, J. M.; Lee, M. M.; Lee, S. A.; Lee, S. Y.; Bok, K. H.; Kim, J.; Kim, C. *Inorganica Chimica Acta*, **2016**, *451*, 8-15.
- (104) Chàvez, J. E.; Crotti, C.; Zangrando, E.; Farnetti, E. *Journal of Molecular Catalysis A: Chemical*, **2016**, *421*, 189-195.
- (105) Yalymov, A. I.; Bilyachenko, A. N.; Levitsky, M. M.; Korlyukov, A. A.; Khrustalev, V. N.; Shul'pina, L. S.; Shul'pin, G. B. *Catalysts*, **2017**, *7*, 101.
- (106) Martins, N. M.; Mahmudov, K. T.; da Silva, M. F. C. G.; Martins, L. M.; Pombeiro, A. J. *New Journal of Chemistry*, **2016**, *40*, 10071-10083.
- (107) Olivo, G.; Giosia, S.; Barbieri, A.; Lanzalunga, O.; Di Stefano, S. *Organic & Biomolecular Chemistry*, **2016**, *14*, 10630-10635.
- (108) Crotti, C.; E. Farnetti, E.; *J. Mol. Catal. A* **2015**, *396*, 353–359.
- (109) De Araújo, M. L.; Mandelli, D.; Kozlov, Y. N.; Carvalho, W. A.; Shul'pin, G. B. *Journal of Molecular Catalysis A: Chemical*, **2016**, *422*, 103-114.
- (110) Sheldon, R. A. *Green Chem.*, **2007**, *9*, 1273–1283.

- (111) L. Hladnik, F. A. Vicente, U. Novak, M. Grilc and B. Likozar, *Ind. Crops Prod.*, **2021**, *164*, 113359.
- (112) A. Bjelić, B. Hočevár, M. Grilc, U. Novak and B. Likozar, *Rev. Chem. Eng.*, **2022**, *38*, 243-272.
- (113) T. Ročnik, B. Likozar, E. Jasiukaitytė-Grojzdek and M. Grilc, *Chem. Eng. J.*, **2022**, *448*, 137309.

## Chapter 2

### Transfer Hydrogenation of Aldehydes and Ketones in Air with Methanol and Ethanol by an Air-stable Ruthenium-triazole Complex

#### 2.1 ABSTRACT:

Coordination of 1,4-disubstituted 1,2,3-triazoles L1 and L2 with [(p-cymene)RuCl<sub>2</sub>]<sub>2</sub> followed by dehydrochlorination in the presence of a base resulted in the formation of complexes 1 and 2, respectively. Both were tested for the transfer hydrogenation of aldehydes and ketones in air using ecologically benign and cheap ethanol as the hydrogen source in the presence of a catalytic amount of a base. Air-stable complex 1 was proved to be an active catalyst for the transfer hydrogenation of a wide variety of aromatic and aliphatic aldehydes and ketones bearing various functionalities. Catalyst 1 was also effective for the transfer hydrogenation of carbonyls using the simplest primary alcohol, methanol, under aerobic conditions. Under the present catalytic protocol, labile or reducible functionalities such as nitro, cyano, and ester groups were tolerated. Good selectivity was also observed for acyclic  $\alpha,\beta$ -unsaturated carbonyls. However, this catalytic protocol was not selective for 2-cyclohexen-1-one as both alkene and keto moieties were reduced. The transfer hydrogenations are believed to proceed via a ruthenium-hydride intermediate. Finally, transfer hydrogenation of acetophenone using isopropanol as a commonly used hydrogen source was also performed and the sustainable and green credentials of these catalytic protocols utilizing methanol, ethanol, and isopropanol were compared with the help of the CHEM21 green metrics toolkit.

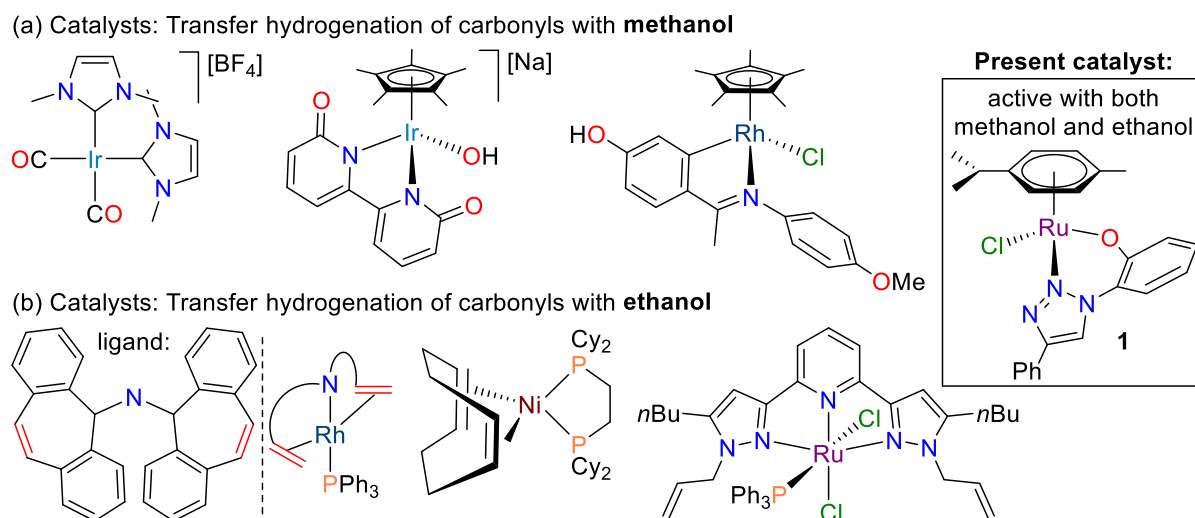
#### 2.2 INTRODUCTION:

Catalytic hydrogenation of unsaturated compounds using molecular hydrogen is one of the most fundamental transformations in synthetic chemistry, both in small lab-scale reactions and in large industrial processes.<sup>1-4</sup> To avoid the use of expensive high-pressure reactors and drastic reaction conditions for classical hydrogenation, catalytic transfer hydrogenation is considered to be an attractive alternative.<sup>5-7</sup> Transfer hydrogenation involves the transfer of a proton and a hydride from the donor molecule to the unsaturated substrate. The sacrificial hydrogen donors, such as formic acid,<sup>8-12</sup> is readily available, inexpensive, and much safer to handle. Another heavily used non-H<sub>2</sub> hydrogen source in transfer hydrogenation is isopropanol and the major side product acetone is easily recycled. The history of transfer hydrogenation dates back a century when Meerwein-Ponndorf-Verley reduction was first published in 1925 by Meerwein and Verley independently.<sup>13,14</sup> That was the first example of transfer hydrogenation of carbonyl compounds, which involved the role of aluminum alkoxide as a promoter in the reduction of a ketone in the presence of a secondary alcohol as a sacrificial hydrogen source. Although Meerwein-Ponndorf-Verley reduction has been widely utilized in both academic and industrial processes, the major drawbacks of this protocol are the requirement of a large amount of aluminum alkoxide reagent, unwanted side reactions, and moisture sensitivity of aluminum alkoxides. Over the last few decades, transfer hydrogenation of multiple bonds between carbon and heteroatoms (such as oxygen and nitrogen in carbonyls and imines, respectively) is a very active field of research and a large variety of homogeneous transition metal catalysts based on iron,<sup>15-20</sup> ruthenium,<sup>21-26</sup> osmium,<sup>27-31</sup> cobalt,<sup>32-34</sup> rhodium,<sup>35-38</sup> iridium,<sup>39-43</sup> nickel,<sup>44-48</sup> palladium,<sup>49-52</sup> and gold<sup>53,54</sup> have been developed. However, most of the efficient transfer hydrogenation protocols utilized ruthenium-, rhodium-, or iridium-based catalysts. In these processes, mostly formic acid and isopropanol are used as the hydrogen source as well as solvent. Catalytic transfer hydrogenations are equilibrium reactions and a large amount of reagents such as isopropanol

is required to shift the equilibrium toward right. In catalytic transfer hydrogenation, the use of primary alcohols as the hydrogen source is very rare in contrast to isopropanol, mainly due to their unfavorable redox potential. Density functional theory calculations gave a  $\Delta G$  value of +4.4 kJ/mol for the transfer hydrogenation of acetophenone with isopropanol to 1-phenylethanol at 40 °C.<sup>55</sup> When ethanol was used as the hydrogen source, the equilibrium was even more unfavorable with  $\Delta G = +24.2$  kJ/mol. In addition, primary alcohols are oxidized to give aldehyde as the side product in contrast to ketone obtained from secondary alcohol; aldehydes are much reactive than ketone and can undergo side reactions such as  $\alpha$ -alkylation under basic conditions.<sup>56–59</sup> However, primary alcohols such as methanol and ethanol are very attractive in the context of sustainable chemistry. Methanol is an excellent hydrogen carrier (ca. 12.5 wt % hydrogen) and is accessible from natural gas, carbon dioxide, and renewable biomass. However, the use of methanol in transfer hydrogenations is very limited (Figure 2.2.1). Garcí'a et al. described the use of a nickel(I)–hydride complex for the transfer hydrogenation of  $\alpha,\beta$ -unsaturated enones with methanol at 180 °C; however, selective reduction of C=C occurred keeping the C=O bond unaltered.<sup>60</sup> Zhang and Chen reported a hydrotalcite-derived copper catalyst for the selective transfer hydrogenation of biomass-based furfural to furfuryl alcohol and 2-methyl furan using methanol as a hydrogen source at 240 °C.<sup>61</sup> Recently, Xiao et al. described the transfer hydrogenation of aromatic aldehydes with methanol at 90 °C utilizing a cyclometalated rhodium(III) complex.<sup>62</sup> Surprisingly, the cyclometalated rhodium(III) species was not an effective transfer hydrogenation catalyst with ethanol as a hydrogen donor. Crabtree et al. reported the use of an iridium(I)–Nheterocyclic carbene (NHC) complex for the transfer hydrogenation of aromatic ketones and imines with methanol at 120 °C.<sup>63</sup> Very recently, Li et al. effectively utilized an anionic iridium(III) complex for the transfer hydrogenation of ketones and imines in refluxing methanol under base-free conditions.<sup>64</sup> However, methanol produces

formaldehyde as the side product, which, under harsh reaction conditions, can form either carbon monoxide that can poison the catalyst or produce formic acid that can neutralize the base often used in transfer hydrogenations. On the other hand, ethanol is also obtained from natural sources and it is an attractive hydrogen carrier. However, ethanol has been barely utilized in transfer hydrogenations (Figure 2.2.1). Transfer hydrogenation with ethanol was first reported by Grützmacher et al.<sup>65</sup> He reported a highly efficient, but air-sensitive rhodium(I)-phosphine catalyst with a fancy amide ligand having two bulky olefin arms for the transfer hydrogenation of ketones. Grützmacher et al. also described similar rhodium(I) complexes with a chiral bis(olefin)amine ligand for asymmetric transfer hydrogenation of acetophenone with ethanol, however, they did not give impressive results (maximum ee  $\approx$  60%). García et al.<sup>66</sup> described the use of a nickel(0)-COD complex in the presence of a bisphosphine ligand for the transfer hydrogenation of ketones with ethanol at 130 °C.<sup>67</sup> Asymmetric transfer hydrogenation of ketone in ethanol was also reported using an in situ generated ruthenium catalyst by combining [Ru(p-cymene)Cl<sub>2</sub>]<sub>2</sub> and an amino acid hydroxyamide ligand.<sup>68</sup> Khaskin et al. described the transfer hydrogenation of esters with ethanol by employing a ruthenium(II)-phosphine complex with a tridentate SNS ligand.<sup>69</sup> A similar ruthenium(II)-phosphine complex with a tridentate NNN ligand was utilized by Weingart and Thiel for the transfer hydrogenation of aldehydes and ketones under constant N<sub>2</sub> flow.<sup>70</sup> Recently, Huang et al. described selective transfer hydrogenation of alkynes to E-alkenes with ethanol catalyzed by an iridium complex and a color change was elegantly used for endpoint detection to avoid over reduction to unwanted alkanes.<sup>71</sup> Very recently, the same group reported efficient transfer hydrogenation of unactivated alkene with ethanol under an argon atmosphere using an iridium(III)-PCN complex.<sup>72</sup> In recent years, significant attention has been devoted to develop phosphine-free air-stable catalytic systems.<sup>73-78</sup> To the best of our knowledge, ruthenium catalyzed transfer hydrogenation of carbonyls utilizing

**Figure 2.2.1.** Transition metal catalysts for the transfer hydrogenation of carbonyls using methanol and ethanol as hydrogen source.



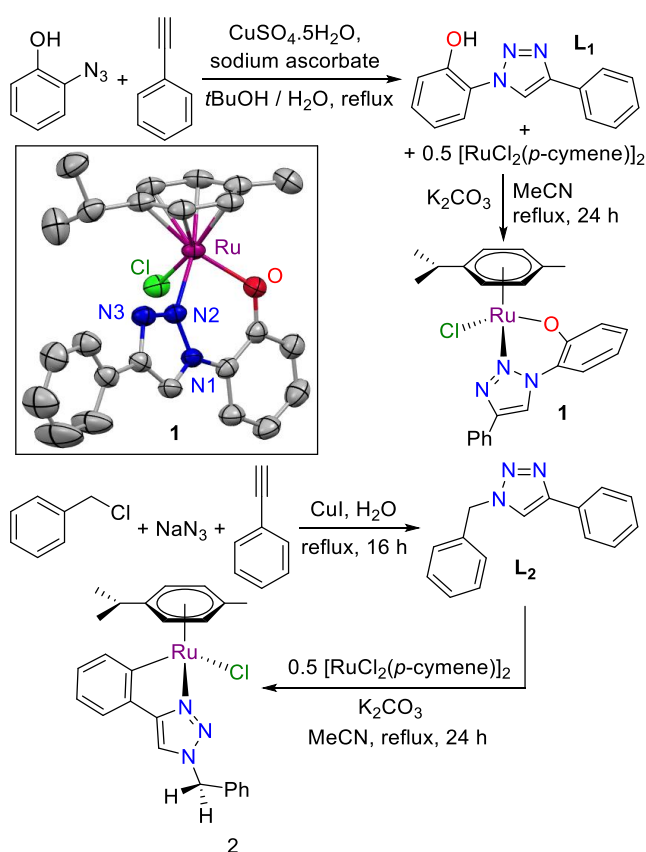
methanol as the hydrogen source is yet to be explored. In addition, no catalytic protocol for the transfer hydrogenation of carbonyls with ethanol in air is reported. Herein, we address the use of a phosphine-free air-stable ruthenium(II) complex with readily available triazole-based ligand as an effective catalyst for the transfer hydrogenation of a large number of aldehydes and ketones bearing various functional groups using both methanol and ethanol under aerobic conditions. The green aspect is the replacement of molecular dihydrogen as a reducing agent by a sacrificial hydrogen donor as well as a solvent such as ethanol is safer and easier to handle. Relating to hydrogen-donor solvents that meet green chemistry principles, ethanol is a promising candidate due to its nontoxicity, low cost, bioabundance, and good solvation properties (ability to dissolve organic compounds, metal complexes, salts, acids, and bases). Methanol is an equally important (however, toxic) source of hydrogen. Therefore, the use of this present catalytic protocol is significant for the transfer hydrogenation of carbonyls with challenging primary alcohols in the context of sustainability. We also report the use of isopropanol in this catalytic transfer hydrogenation of carbonyls. Finally, the green credentials of the use of methanol, ethanol, and isopropanol in this catalytic protocol are addressed.

## 2.3 RESULT AND DISCUSSION:

Ligand design is a key feature in the development of transition metal catalysts. NHCs have been recognized as a prominent force in the field of catalysis.<sup>79–86</sup> A wide range of transition metal catalysts decorated with various NHCs have been employed for various catalytic applications including the transfer hydrogenation of unsaturated molecules. In recent past, 1,2,3-triazolyliidenes as abnormal NHCs have been utilized very efficiently for the development of a wide variety of transition metal catalysts.<sup>87–92</sup> However, transition metal catalysts with 1,2,3-triazolyliidenes require a multistep synthesis, which commonly involves: (i) synthesis of 1,2,3-triazole commonly utilizing copper-catalyzed azide–alkyne cycloaddition, (ii) alkylation at the N3-position by using alkylating reagents such as MeI, MeOTf, MeBF<sub>4</sub>, and so forth, (iii) synthesis of silver(I) triazolylidene by reaction with Ag<sub>2</sub>O, and (iv) transmetalation with transition metal salts. To avoid these multistep syntheses, we wanted to examine if triazoles could be utilized as effective ligands for transition metal-catalyzed transfer hydrogenations. Our plan was to design a readily available bidentate triazole ligand with a pendant anionic arm. Therefore, L1 was a good choice as it can be synthesized in a single-step process from commercially available reagents and the phenolic-OH proton can easily be removed to generate an anionic arm in the presence of a base. The same arguments are also valid for L2. Therefore, we first synthesized triazole ligands L1<sup>93</sup> and L2<sup>94</sup> by employing copper-catalyzed azide–alkyne cycloaddition using the reported literature protocols (Scheme 2.3.1). The regioselective reactions produced 1,4-disubstituted 1,2,3-triazoles L1 and L2 in good yields. Facile coordination of L1 with [RuCl<sub>2</sub>(p-cymene)]<sub>2</sub> followed by smooth dehydrochlorination in the presence of a base resulted in the formation of complex 1 as an air-stable red solid (Scheme 2.3.1). Similarly, the reaction of L2 with [RuCl<sub>2</sub>(p-cymene)]<sub>2</sub> in the presence of base yielded complex 2 as a yellow solid (Scheme 2.3.1).<sup>95</sup> The C–H-activated species 2 is air-stable in the solid state for weeks; however, it

slowly decomposed in solution. Both 1 and 2 were characterized by  $^1\text{H}$  and  $^{13}\text{C}$  NMR spectroscopy and mass analysis. As expected, the  $^1\text{H}$  and  $^{13}\text{C}$  NMR spectra of 1 and 2 are consistent with  $C_1$  symmetry on the NMR time scale. Four doublets in the range of 5–6 ppm (1: 5.35, 5.42, 5.64, and 5.68 ppm; 2: 5.24, 5.26, 5.46, and 5.56 ppm) were observed for the *p*-cymene moiety in the  $^1\text{H}$  NMR spectra of 1 and 2. The benzylic  $\text{CH}_2$  protons appear as two doublets (ppm) in the  $^1\text{H}$  NMR spectra of 2. Complex 1 was further characterized by single-crystal X-ray analysis, which confirmed the connectivity of the triazole moiety at the N2-position and the pendant phenolato arm with the ruthenium metal center. In this half-sandwich complex 1, the geometry around the ruthenium metal center is pseudotetrahedral, which is best described as a three-legged “piano-stool” structure. The bond distances and bond angles are consistent with those of similar ruthenium–triazole complexes.<sup>96–100</sup>

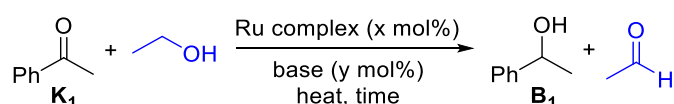
**Scheme 2.3.1. Synthesis of ruthenium-triazole complexes 1 and 2 with the molecular structure of 2 showing 50% ellipsoids<sup>a</sup>**



<sup>a</sup>Hydrogen atoms are omitted for clarity. Two molecules of **1** are present in the unit cell. Selected bond distances (Å) and angles (deg): Ru1-O1 2.053(3), Ru1'-O1' 2.044(3); Ru1-N2 2.111(3), Ru1'-N2' 2.093(3); Ru1-C11 2.429(10), Ru1'-C11' 2.432(10); Ru1-C<sub>pcentroid</sub> 1.657, Ru1'-C<sub>pcentroid</sub> 1.663 and O1-Ru1-N2 82.37(11), O1'-Ru1'-N2' 82.55(11); N2-Ru1-C11 86.01(9), N2'-Ru1'-C11' 85.09(9); C11-Ru1-O1 86.77(8), C11'-Ru1'-O1' 88.03(9).

Thereafter, we explored the catalytic activities of complexes **1** and **2** for the transfer hydrogenation of acetophenone (**K1**) as a model substrate using ethanol as a hydrogen source in a closed vial (entries 1–10 in Table 2.3.1). Upon heating a solution of **K1** in ethanol (4 mL) in air in the presence of 10 mol % of KOH and 3 mol % of complex **1**, we observed approximately 70% conversion to the corresponding alcohol **B1** in 24 h (entry 1). If complex **2** is used as a catalyst, very poor conversion (less than 15%) was obtained under identical reaction conditions (entry 2). If KOH was replaced by K<sub>2</sub>CO<sub>3</sub>, complex **2** showed slightly better activity with 28% conversion of **B1** in 24 h (entry 3). On the other hand, complex **1** gave full conversion with 98% isolated yield of **B1** under identical conditions (entry 4). If the catalyst loading of **1** is reduced to 2 mol %, full conversion of **K1** was observed in 24 and 18 h (entry 5). However, approximately 80% conversion to **B1** was observed in 12 h under identical reaction conditions (entry 6). Further reduction of the catalyst loading to 1 mol % gave full conversion of **K1** in 24 h (entry 7) and 76% conversion of **K1** in 18 h (entry 8). If the amount of base is reduced to 5 mol %, the reaction was far from completion in 24 h (entry 9). Thereafter, the reaction was performed at lower temperature; a small amount of unreacted starting material (less than 10%) was observed at 80 °C (entry 10). Hence, entry 6 ([**1**]: 1 mol %, [K<sub>2</sub>CO<sub>3</sub>]: 10 mol %, 100 °C, 24 h, and a closed vial) was concluded as an optimized reaction condition. We also performed the transfer hydrogenation of acetophenone in an open flask under refluxing conditions (entries 11–15 in Table 2.3.1)

**Table 2.3.1. Catalytic performance of ruthenium-triazole complexes **1** and **2** for transfer hydrogenation of acetophenone with ethanol<sup>a</sup>**



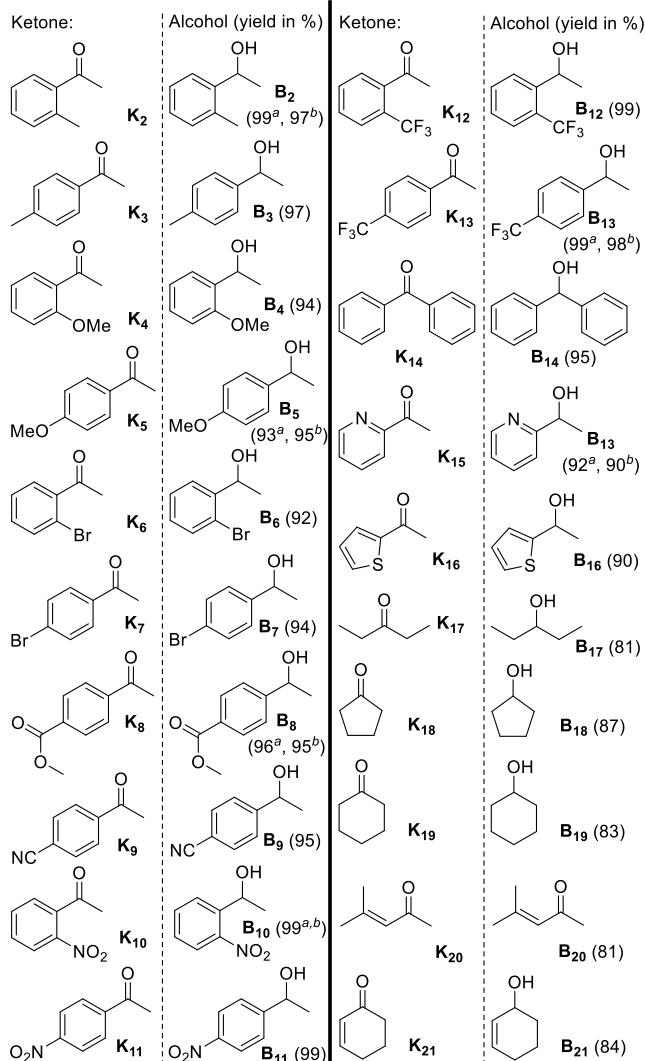
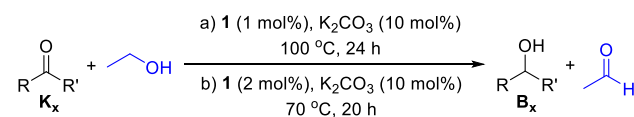
ent.	cat.	base	temp.	time	yield <sup>b</sup>
	(mol%)	(mol%)	(°C)	(h)	(%)
1 <sup>a</sup>	1 (3)	KOH (10)	100	24	69
2 <sup>a</sup>	2 (3)	KOH (10)	100	24	<15
3 <sup>a</sup>	2 (3)	K <sub>2</sub> CO <sub>3</sub> (10)	100	24	28
4 <sup>a</sup>	1 (3)	K <sub>2</sub> CO <sub>3</sub> (10)	100	24	>99 (98 <sup>c</sup> )
5 <sup>a</sup>	1 (2)	K <sub>2</sub> CO <sub>3</sub> (10)	100	24/ 18	>99
6 <sup>a</sup>	1 (2)	K <sub>2</sub> CO <sub>3</sub> (10)	100	12	78
7 <sup>a</sup>	1 (1)	K <sub>2</sub> CO <sub>3</sub> (10)	100	24	>99 (99 <sup>c</sup> )
8 <sup>a</sup>	1 (1)	K <sub>2</sub> CO <sub>3</sub> (10)	100	18	76
9 <sup>a</sup>	1 (1)	K <sub>2</sub> CO <sub>3</sub> (5)	100	24	62
10 <sup>a</sup>	1 (1)	K <sub>2</sub> CO <sub>3</sub> (10)	80	24	93
11 <sup>d</sup>	1 (1)	K <sub>2</sub> CO <sub>3</sub> (10)	80	24	80
12 <sup>d</sup>	1 (1)	K <sub>2</sub> CO <sub>3</sub> (10)	80	32	>99
13 <sup>d</sup>	1 (2)	K <sub>2</sub> CO <sub>3</sub> (10)	80	18	>99
14 <sup>d</sup>	1 (2)	K <sub>2</sub> CO <sub>3</sub> (10)	70	18	89
15 <sup>d</sup>	1 (2)	K <sub>2</sub> CO <sub>3</sub> (10)	70	20	>99
16 <sup>a</sup>	2 (1)	K <sub>2</sub> CO <sub>3</sub> (10)	100	24	25

<sup>a</sup>Reactions conducted in a closed vial (10 ml) with 0.50 mmol **K**<sub>1</sub>, 4 ml of ethanol, 5/10 mol% of base and 3/2/1 mol% of complex **1/2**. <sup>b</sup>Yields of **B**<sub>1</sub> were determined by <sup>1</sup>H NMR spectroscopy using 1,3,5-trimethoxybenzene (0.17 mmol) as internal standard. <sup>c</sup>Isolated yields. <sup>d</sup>Reactions conducted in an open flask (25 ml) with reflux condenser with 0.50 mmol **K**<sub>1</sub>, 4 ml of ethanol, 10 mol% of base and 1/2 mol% of complex **1**.

Upon heating a solution of **K**<sub>1</sub> in ethanol in open air in the presence of 10 mol % of K<sub>2</sub>CO<sub>3</sub> and 1 mol % of complex **1** at 80 °C, we observed approximately 80% conversion to **B**<sub>1</sub> in 24 h (entry 11) and complete conversion to **B**<sub>1</sub> in 32 h (entry 12). Increasing the catalyst loading to 2 mol %, complete conversion of **K**<sub>1</sub> to **B**<sub>1</sub> was observed in 18 h (entry 13). A further reduction of reaction temperature to 70 °C gave slower reactions (entries 14 and 15). Complete conversion of acetophenone was observed in 20 h at 70 °C in the presence of 2 mol % catalyst and 10 mol % base (entry 15). Entry 15 ([**1**]: 2 mol %, [K<sub>2</sub>CO<sub>3</sub>]: 10 mol %, 70 °C,

20 h, and an open flask) was utilized as another optimized reaction condition for substrate screening. We finally checked the catalytic activity of complex 2 using one optimized reaction condition as presented in entry 7. Upon heating a solution of K1 in ethanol (4 mL) in air for 24 h in the presence of 10 mol % of KOH and 1 mol % of complex 2, we observed approximately 30% conversion to the corresponding alcohol with ca. 70% unreacted starting material (entry 16). Therefore, complex 2 showed much reduced catalytic activity as compared to complex 1. Complex 2 is not air-stable and it slowly decomposes in air. Therefore, much reduced catalytic activity of complex 2 is expected as the catalytic transfer hydrogenation was performed in air. Stimulated by the above encouraging results, we thereafter tested various other ketones under optimized reaction conditions (entry 7 in Table 2.3.2: 1 mol % of 1, 10 mol % of K<sub>2</sub>CO<sub>3</sub>, 100 °C, 24 h, and a closed vial) to expand the substrate scope (Scheme 2.3.2). At first, acetophenones bearing various electron-donating and electron-withdrawing functionalities were examined. Acetophenones with electron-donating methyl and methoxy groups at either ortho or para positions (K2, K3, K4, and K5)

**Scheme 2.3.2. Transfer hydrogenation of ketones using ethanol catalyzed by complex 1<sup>a</sup>**



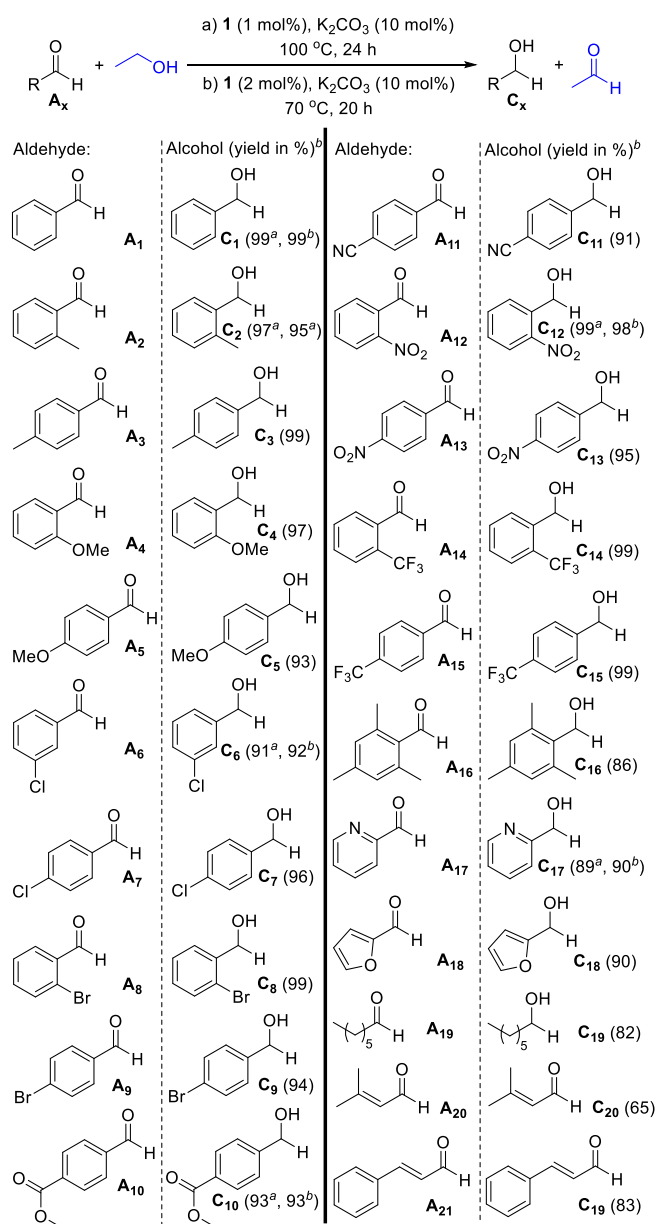
<sup>a</sup>Reactions conducted in a vial (10 ml) with 0.50 mmol ketone (**K<sub>x</sub>**), 4 ml of ethanol, 10 mol% of K<sub>2</sub>CO<sub>3</sub> and 1 mol% of complex **1** at 100 °C. <sup>b</sup>Reactions conducted in a flask (25 ml) with 0.50 mmol ketone (**K<sub>x</sub>**), 4 ml of ethanol, 10 mol% of K<sub>2</sub>CO<sub>3</sub> and 2 mol% of complex **1** at 70 °C. <sup>c</sup>Isolated yields.

gave complete conversion with excellent isolated yields (B2: 99%, B3: 97%, B4: 94%, and B5: 93%). Full conversions were also observed for substrates with mild electron-withdrawing bromo (K6, K7), moderate electronwithdrawing ester and cyano (K8, K9), and strong electronwithdrawing nitro (K10, K11) and trifluoromethyl groups (K12, K13) and the corresponding alcohols were isolated in excellent isolated yields (B6: 92%, B7: 94%, B8: 96%, B9: 95%, B10: 99%, B11: 99%, B12: 99%, and B13: 99%). Therefore, the electronic

nature of the substituents on the aryl moiety has little or no effect on the outcome of the transfer hydrogenations. This catalytic protocol is equally effective for nonmethyl ketone, benzophenone (K14), giving the desired reduced product diphenylmethanol (B14) in 95% yield. In addition, heteroaryl ketones such as 2-acetylpyridine (K15) and 2-benzoylthiophene (K16) were successfully converted to corresponding alcohols 1-(2-pyridinyl)ethanol (B15: 92%) and 1-(2-thienyl)ethanol (B16: 90%), respectively, in excellent yields. This catalytic system was also successfully applied to acyclic and cyclic aliphatic ketones, 3-pentanone (K17), cyclopentanone (K18), and cyclohexanone (K19). Under standard conditions, K17, K18, and K19 afforded the corresponding alcohols 3-pentanol (B17: 81%), cyclopentanol (B18: 87%), and cyclohexanol (B19: 83%) in good yields. Thereafter, we tested cyclic and acyclic  $\alpha,\beta$ unsaturated ketones. Selective reduction of the keto group was observed for 4-methyl-3-penten-2-one (K20) with more than 80% isolated product (B20). However, this catalytic protocol did not show any selectivity when cyclic species 2-cyclohexen-1-one (K21) was subjected to transfer hydrogenation and the completely reduced cyclohexanol (B21: 84%) was isolated. We also performed the transfer hydrogenation of several ketones (K2, K5, K8, K10, K15, and K18) in an open flask using the second optimized conditions (entry 15 in Table 2.3.1: 2 mol % of 1, 10 mol % of  $K_2CO_3$ , 70 °C, 20 h, and an open flask) and very similar yields of alcohols (B2: 97%, B5: 95%, B8: 95%, B10: 99%, B15: 98%, and B18: 90%) were obtained. Thereafter, we examined the transfer hydrogenations of a series of aldehydes under standard reaction conditions (Scheme 2.3.2). At first, benzaldehyde (A1) was tested and complete conversion with quantitative yield of benzylalcohol (C1: 99%) was obtained. Then, we examined various substituted benzaldehydes with electron-donating functionalities (A2, A3, A4, and A5) and a complete conversion with excellent isolated yields was obtained (C2: 97%, C3: 99%, C4: 97%, and C5: 93%). Thereafter, substituted benzaldehyde bearing various electron-withdrawing groups such as halides, ester, cyano,

nitro, and trifluoromethyl (A6, A7, A8, A9, A10, A11, A12, A13, A14, and A15) were subjected to this catalytic protocol and similar results were obtained (C6: 91%, C7: 96%, C8: 99%, C9: 94%, C10: 93%, C11: 91%, C12: 99%, C13: 95%, C14: 99%, and C15: 99%). Like ketones, the catalytic transfer hydrogenations of aldehydes were also insensitive to the electronic nature of the substituents.

### Scheme 2.3.3. Transfer hydrogenation of aldehydes using ethanol catalyzed by 1<sup>a</sup>



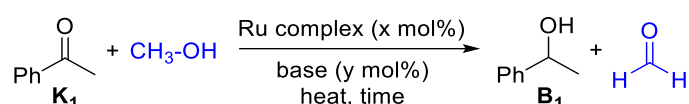
<sup>a</sup>Reactions conducted in a vial (10 ml) with 0.50 mmol ketone (**K<sub>x</sub>**), 4 ml of ethanol, 10 mol% of K<sub>2</sub>CO<sub>3</sub> and 1 mol% of complex **1** at 100 °C. <sup>b</sup>Reactions conducted in a flask (25 ml)

with 0.50 mmol ketone (**K<sub>x</sub>**), 4 ml of ethanol, 10 mol% of K<sub>2</sub>CO<sub>3</sub> and 2 mol% of complex **1** at 70 °C. <sup>a</sup>Isolated yields.

This catalytic system is equally efficient for sterically bulky 2,4,6-mesitaldehyde (A16), affording excellent yield of the corresponding alcohol (C16: 96%). When heteroaryl aldehydes such as picolinaldehyde (A17) and 2-furaldehyde (A18) were subjected to this catalytic protocol, we also obtained good yields of the corresponding products (C17: 89% and C18: 90%). Aliphatic aldehyde hexanal (A19) was also successfully converted to 1-heptanol (C19) with 82% yield. Thereafter,  $\alpha,\beta$ -unsaturated aldehydes were tested. When 3-methyl-2-butenal (A20) was subjected to transfer hydrogenation, a little more than 70% conversion to 3-methyl-2-butene-1-ol (C20: 65%) was observed. Notably, the alkene moiety was unreacted. Finally, cinnamaldehyde (A21) was tested and complete conversion of the substrate was observed. The expected product (C21: 83%) with an unreacted alkene moiety was isolated in good yield. However, a small amount of (ca. 10%) of the completely reduced product was detected. We also performed the transfer hydrogenation of several aldehydes (A1, A2, A6, A10, A12, and A17) in an open flask using the second optimized conditions (entry 15 in Table 2.3.1: 2 mol % of **1**, 10 mol % of K<sub>2</sub>CO<sub>3</sub>, 70 °C, 20 h, and an open flask) and very similar yields of products (C1: 99%, C2: 95%, C6: 92%, C10: 93%, C12: 98%, and C17: 90%) were obtained. Inspired by the successful utilization of ethanol, we set out to investigate catalytic transfer hydrogenation of carbonyls using methanol as a more challenging hydrogen donor. As complex **2** did not show promising results with ethanol, we explored the catalytic activity of only complex **1** using acetophenone as a model substrate (Table 2.3.2). We started with the exact optimized conditions previously used for ethanol. Upon heating a solution of K1 in methanol (4 mL) in air in the presence of 10 mol % of K<sub>2</sub>CO<sub>3</sub> and 1 mol % of complex **1**, we observed more than 70% conversion to the corresponding alcohol B1 in 24 h (entry 1). Increasing the catalyst loading to 2 mol %, a complete conversion of K1 was obtained in 24 h (entry 2) and 18 h (entry 3). A further

reduction of time to 12 h gave 60% conversion of **K1** (entry 4). If the amount of base is reduced from 10 to 5 mol %, almost 50% conversion to **B1** was obtained in 18 h (entry 5). Finally, a reaction was performed at 80 °C and approximately 70% conversion to **B1** was obtained in 18 h (entry 6). Hence, entry 3 ([**1**]: 2 mol %, [**K**<sub>2</sub>CO<sub>3</sub>]: 10 mol %, 100 °C, and 18 h) was concluded as the optimized reaction condition for the catalytic transfer hydrogenation of carbonyls using methanol as the hydrogen source. Thereafter, catalytic transfer hydrogenation of various

**Table 2.3.4. Catalytic performance of complexes 1 for the transfer hydrogenation of acetophenone with methanol<sup>a</sup>**



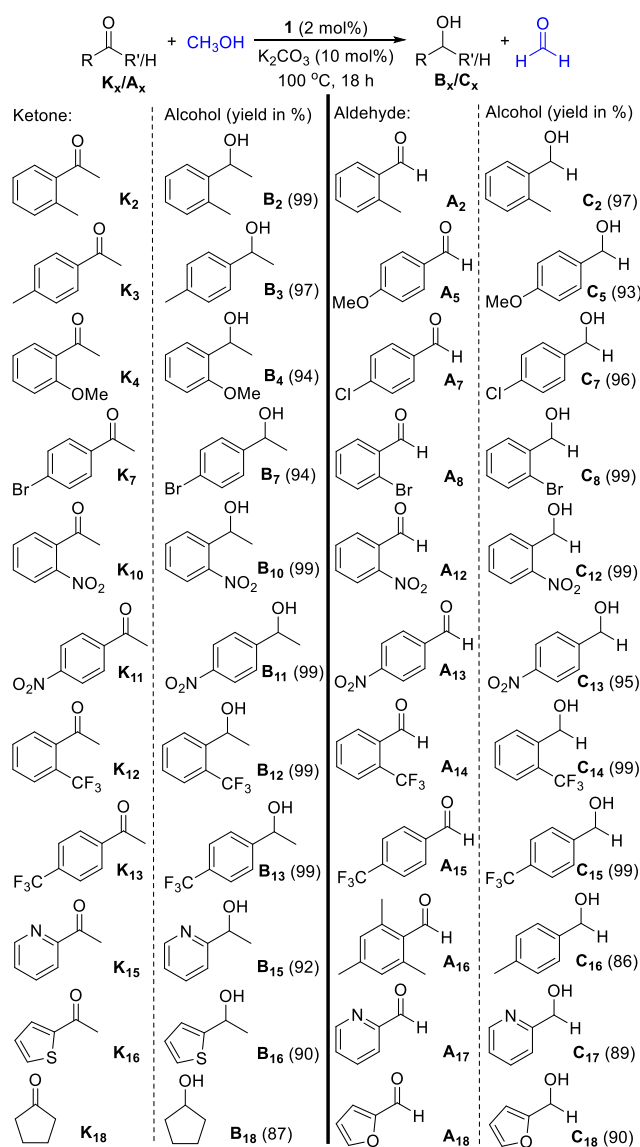
ent.	cat. (mol%)	base (mol%)	temp. (°C)	time (h)	yield <sup>b</sup> (%)
1	<b>1</b> (1)	K <sub>2</sub> CO <sub>3</sub> (10)	100	24	74
2	<b>1</b> (2)	K <sub>2</sub> CO <sub>3</sub> (10)	100	24	>99
3	<b>1</b> (2)	K <sub>2</sub> CO <sub>3</sub> (10)	100	18	>99
4	<b>1</b> (2)	K <sub>2</sub> CO <sub>3</sub> (10)	100	12	60
5	<b>1</b> (2)	K <sub>2</sub> CO <sub>3</sub> (5)	100	18	48
6	<b>1</b> (2)	K <sub>2</sub> CO <sub>3</sub> (10)	80	18	71

<sup>a</sup>Reactions conducted in a vial (10 ml) with 0.50 mmol **K1**, 4 ml of methanol, 5/10 mol% of base and 2/1 mol% of complex **1**. <sup>b</sup>Yields of **B1** were determined by <sup>1</sup>H NMR spectroscopy using 1,3,5-trimethoxybenzene (0.17 mmol) as internal standard. <sup>c</sup>Isolated yields.

ketones and aldehydes using methanol was carried out to expand the substrate scope (Scheme 2.3.4). We selected eleven ketones and eleven aldehydes from the list of various ketones and aldehydes tested previously with ethanol. Aromatic ketones and aldehydes with various electron-donating and electron-withdrawing functionalities such as methyl, methoxy, chloro, bromo, nitro, and trifluoromethyl were tested under optimized reaction conditions and the corresponding alcohols were isolated in excellent yields (**B2**: 99%, **B3**: 97%, **B4**: 94%, **B7**:

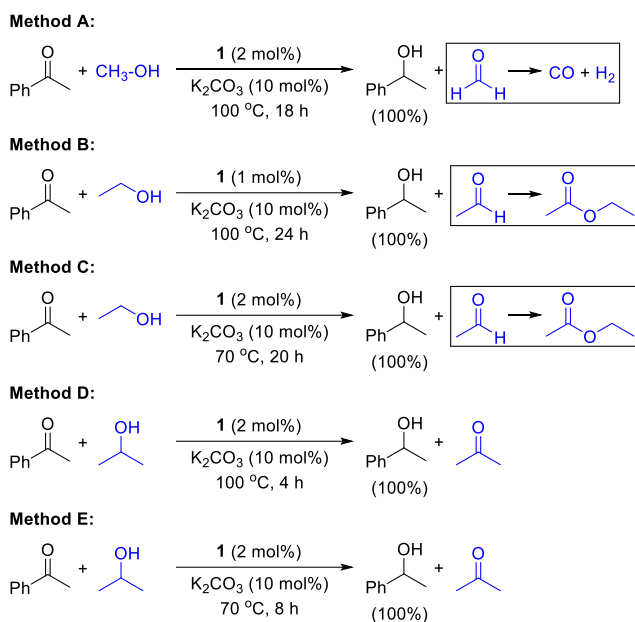
94%, B10: 99%, B11: 99%, B12: 99%, B13: 99%, C2: 97%, C5: 93%, C7: 96%, C8: 99%, C12: 99%, C13: 95%, C14: 99%, and C15: 99%). Aromatic aldehyde with a bulky mesityl group was also successfully tested (C16: 86%). Similarly, methanol was also utilized efficiently for the transfer hydrogenation of heteroaryl aldehydes and ketones such as picolinaldehyde (A17), 2-furaldehyde (A18), 2-acetylpyridine (K15), and 2-benzoylthiophene (K16) with excellent isolated yields of the corresponding alcohols (C17: 89%, C18: 90%, B15: 92%, and B16: 90%). Cyclic aliphatic ketone such as cyclopentanone was also tested successfully (B18: 87%). To investigate the application potential of the present catalytic methodology and the robustness of complex 1, we performed several gram scale reactions with 10.0 mmol of either aldehydes or ketones. Benzophenone (K1), 2-methylbenzophenone (K2), 2-nitrobenzaldehyde (A12), and 4-trifluoromethylbenzaldehyde (A15) were subjected to transfer hydrogenation using ethanol as the hydrogen source in the presence of 1 mol % of complex 1 and 10 mol % of  $K_2CO_3$  at 100 °C and the corresponding alcohols were obtained in quantitative yields in 24 h. We also tested isopropanol as the hydrogen source for the transfer hydrogenation of acetophenone as the standard substrate (see Supporting Information for details). As expected, a complete reduction of acetophenone was observed in 4 h at 100 °C using 2 mol % catalyst loading or in 8 h at 70 °C using 2 mol % catalyst loading.

**Scheme 2.3.5. Transfer hydrogenation of ketones and aldehydes with methanol catalyzed by 1<sup>a</sup>**



<sup>a</sup>Reactions conducted in a closed vial (10 ml) with 0.50 mmol ketone (**K<sub>x</sub>**) or aldehyde (**A<sub>x</sub>**), 4 ml of methanol, 10 mol% of K<sub>2</sub>CO<sub>3</sub> and 1 mol% of complex **1** at 100 °C. <sup>b</sup>Isolated yields.

### Scheme 2.3.5.A Transfer hydrogenation of Acetophenone using different optimized condition



In modern days, it is extremely important to evaluate the advantages and drawbacks of catalytic chemical transformations with the environmental and green aspects based on “The 12 Principles of Green Chemistry”.<sup>101–108</sup> To analyze the sustainable and green credentials of the one-step transformation of carbonyl to alcohol, we have selected five different optimized methods for the transfer hydrogenation of acetophenone to 1-phenylethanol using methanol (Method A), ethanol (Methods B and C), and isopropanol (Methods D and E) as the sacrificial hydrogen sources as well as solvents (Scheme 2.3.5.A). The five methods were evaluated with the CHEM21 green metrics toolkit developed by Clark et al.<sup>109</sup> The CHEM21 green metrics toolkit is considered as a quantitative extension of “The 12 Principles of Green Chemistry” and many chemical transformations were analyzed using this toolkit.<sup>110–114</sup> All those transfer hydrogenations

In modern days, it is extremely important to evaluate the advantages and drawbacks of catalytic chemical transformations with the environmental and green aspects based on “The 12 Principles of Green Chemistry”.<sup>101–108</sup> To analyze the sustainable and green credentials of the one-step transformation of carbonyl to alcohol, we have selected five different optimized methods for the transfer hydrogenation of acetophenone to 1-phenylethanol using methanol (Method A), ethanol (Methods B and C), and isopropanol (Methods D and E) as the sacrificial hydrogen sources as well as solvents

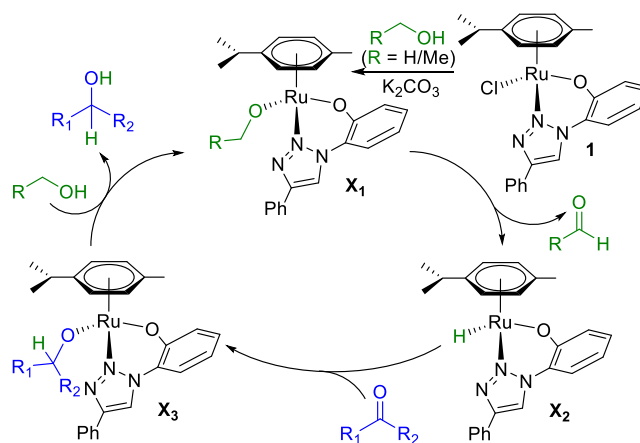
(Scheme 2.3.5.A). The five methods were evaluated with the CHEM21 green metrics toolkit developed by Clark et al.<sup>109</sup> The CHEM21 green metrics toolkit is considered as a quantitative extension of “The 12 Principles of Green Chemistry” and many chemical transformations were analyzed using this toolkit.<sup>110-114</sup> All those transfer hydrogenations quantitative yield and selectivity, and therefore all methods earn green flags for yield, conversion, and selectivity. However, atom economy and reaction mass efficiency are the highest for Method A with methanol (80.3) and the lowest for Methods D and E with isopropanol (67.8). As expected, atom economy and reaction mass efficiency for Methods B and C with ethanol (73.5) stand in the middle. Solvents (methanol, ethanol, and isopropanol) for all five methods receive green flags. Common and easy workup techniques (filtration and evaporation) were adopted and again all methods earn green flags. We did not adopt a continuous flow process and as the reactions were performed in batches, all methods receive amber flag. All five methods utilized the ruthenium catalyst, and therefore they receive red flags considering the abundance of the element and related geo-political issues. However, ruthenium is much cheaper compared to the costs of other noble metals such as rhodium, iridium, palladium, platinum, and gold. All five methods were also evaluated using energy norms. In Methods A, B, and D, transfer hydrogenations were conducted at 100 °C. If a reaction is performed above 70 °C (up to 140 °C), it should receive an amber flag under energy. However, Methods A, B, and D receive red flags as the reactions were conducted at 5 °C or more above the boiling point of solvents (methanol, ethanol, and isopropanol). Fulfilling all energy measures, Methods C and E receive green flags. Finally, health and safety concerns of all methods were evaluated. As the side product in Method A is carbon monoxide, it receives a red flag. Similarly, Methods B and C receive green flags as ethyl acetate is produced from acetaldehyde as a stable byproduct. Similarly, all reagents, catalysts, solvents, and products in Methods D and E do not have any health and safety concerns, and

hence they earn green flags. At the end, it can be concluded that the selected five methods can be differentiated by atom economy/ reaction mass efficiency, solvent, energy, and health and safety.

**Table 3. Comparison of the five different methods of transfer hydrogenations from the CHEM21 Green Metrics Toolkit Calculation**

Metric	Method A	Method B	Method C	Method D	Method E
Yield	100 	100 	100 	100 	100 
Conversion	100 	100 	100 	100 	100 
Selectivity	100 	100 	100 	100 	100 
Atom economy	80.3	73.5	73.5	67.8	67.8
Reaction mass efficiency	80.3	73.5	73.5	67.8	67.8
Solvent	MeOH 	EtOH 	EtOH 	<i>i</i> PrOH 	<i>i</i> PrOH 
Catalyst	Yes 	Yes 	Yes 	Yes 	Yes 
Element	Ru 	Ru 	Ru 	Ru 	Ru 
Reactor	Batch 	Batch 	Batch 	Batch 	Batch 
Work up	Filtration  Evaporation	Filtration  Evaporation	Filtration  Evaporation	Filtration  Evaporation	Filtration  Evaporation
Energy	100 °C 	100 °C 	70 °C 	100 °C 	70 °C 
Health & safety	H372 				

**Scheme 2.3.5. (a) Proposed catalytic cycle for the transfer hydrogenation of carbonyls with methanol/ethanol catalyzed by complex 1**



Based on the published reports, we propose a catalytic cycle for the transfer hydrogenation of carbonyls with methanol/ ethanol (Scheme 2.3.5). At first, complex 1 reacts with alcohol in the presence of a base to form a ruthenium-alkoxide (methoxide or ethoxide) complex X1. Thereafter,  $\beta$ -hydride elimination from the alkoxide complex leads to the formation of a ruthenium-hydride complex X2 with the elimination of either formaldehyde or acetaldehyde as a byproduct. Thereafter, hydride transfer to the carbonyl substrate results in the formation of a ruthenium-alkoxide complex X3. Finally, hydrogen transfer from methanol/ethanol to the alkoxy moiety releases the product with the regeneration of complex X1. To gain support on the suggested reaction pathway, a solution of complex 1 in ethanol was heated at 100 °C in the presence of a base. This resulted in the formation of ruthenium-hydride species X2 and the hydride resonance was observed at  $-10.18$  ppm in the  $^1\text{H}$  NMR spectrum of complex X2. However, complex X2 could not be isolated in pure form.

## 2.4 CONCLUSION

In conclusion, a readily accessible triazole ligand was utilized to synthesize an air-stable ruthenium complex (1), which displayed good catalytic activity for the transfer hydrogenation of various aldehydes and ketones using both methanol and ethanol as sustainable sources of hydrogen donors. To the best of our knowledge, this is the first example of a catalytic

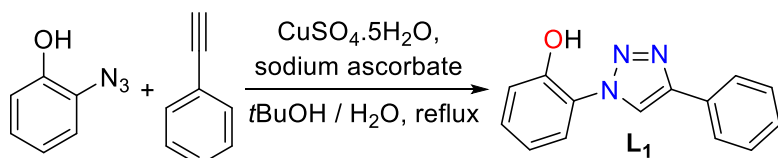
protocol, which utilized challenging primary alcohols, methanol and ethanol, both under aerobic conditions. This catalytic system showed good chemoselectivity toward the reduction of carbonyls in the presence of readily reducible or labile functionalities. The catalytic pathway is believed to proceed through a ruthenium–hydride intermediate. Furthermore, the catalytic system was proved to be robust as it was successfully applied for the gram-scale transfer hydrogenations of several aldehydes and ketones. Five optimized catalytic methods (Methods A, B, C, D, and E) were evaluated using the CHEM21 green metrics toolkit. Despite the fact that atom economy/reaction mass efficiency is the highest in Method A, this method (in methanol at 100 °C) cannot be considered as a preferred one as this method is not energetically favorable and there are health and safety concerns (red flags). However, the use of methanol is most challenging thermodynamically. Method B (in ethanol at 100 °C) should be avoided for the same unfavorable energy factor. Method D (in isopropanol at 100 °C) is equally unfavorable energetically. Method C (in ethanol at 70 °C) and Method E (in isopropanol at 70 °C) are two favored methods. Method E has an advantage over method C as Method E is faster. However, the use of primary alcohol in Method C is much more challenging than the use of a secondary alcohol in Method E. Method C is also better than Method E in terms of atom economy/reaction mass efficiency. In addition, ethanol as the hydrogen source is much more attractive, ecologically benign, and sustainable as compared to isopropanol. Thus, Method C can be concluded as the most favored catalytic protocol. Notably, this robust catalytic protocol might be realistic for possible future application particularly because of the nonrequirement of an inert atmosphere and the utilization of sustainable primary alcohol (ethanol) as the non-H<sub>2</sub> hydrogen source.

## **2.5 EXPERIMENTAL SECTION**

### **General experimental**

All experiments were performed in air. All solvents (acetonitrile, dichloromethane, diethyl ether, hexanes, ethyl acetate, acetone, methanol, ethanol and tert-butanol,) and chemicals were purchased from commercial suppliers and used without further purification. For recording NMR spectra, CDCl<sub>3</sub> was purchased from Sigma-Aldrich and used without further purification. <sup>1</sup>H and <sup>13</sup>C NMR spectra were recorded at Bruker AV-400 and JEOL-400 (<sup>1</sup>H at 400 MHz and <sup>13</sup>C at 101 MHz). <sup>1</sup>H NMR chemical shifts are referenced in parts per million (ppm) with respect to tetramethylsilane (δ 0.00 ppm) and <sup>13</sup>C{<sup>1</sup>H} NMR chemical shifts are referenced in ppm with respect to CDCl<sub>3</sub> (δ 77.16 ppm). The coupling constants (*J*) are reported in hertz (Hz). The following abbreviations are used to describe multiplicity: s = singlet, bs = broad signal, d = doublet, t = triplet, q = quadrate, m = multiplate. High resolution mass spectra were recorded on a Bruker micrOTOF-Q II Spectrometer. Elemental analysis was carried out on a EuroEA Elemental Analyser. Infrared (IR) spectra were recorded on a Perkin-Elmer FT-IR spectrophotometer.

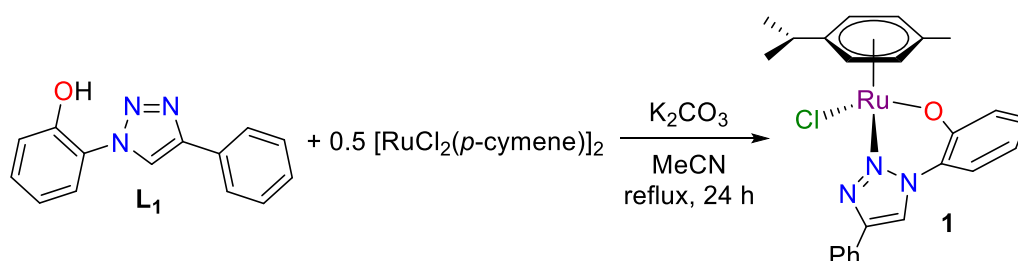
### Synthesis and NMR data of L<sub>1</sub>, L<sub>2</sub>, 1 and 2



**Synthesis of L<sub>1</sub>:** Ligand L<sub>1</sub> was synthesized according to the literature procedure. Sodium ascorbate (0.200 g, 1.0 mmol) and CuSO<sub>4</sub>·5H<sub>2</sub>O (.025 g, 0.1 mmol) was added to a solution of 2-azido phenol (1.340 g, 10.0 mmol) in 1:1 mixture of water and tert-butanol (90 mL). Thereafter, phenylacetylene (1.32 mL, 11.0 mmol) was added dropwise. The reaction mixture was stirred at 90 °C in an oil bath for 24 h. Then the resultant mixture was added to ice-cold water (100 mL) which resulted in the formation of dark-red precipitate. The dark red solid was isolated after filtration and dried to give the crude product. The crude product was purified by column chromatography (silica gel as stationary phase and 1:1 mixture of ethyl

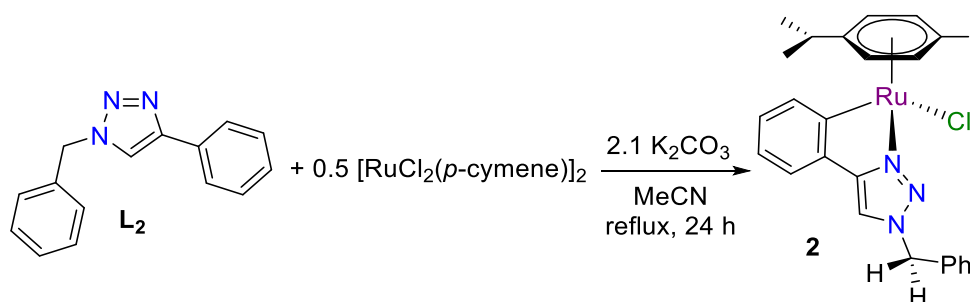
acetate and hexanes as eluent) to give red solid (1.76 g, 74%) as pure product.  $^1\text{H}$  NMR ( $\text{CDCl}_3$ ): 9.90 (s, 1H), 8.30 (s, 1H), 7.95–7.89 (d,  $J = 8$  Hz, 2H), 7.48 (m, 3H), 7.41 (m, 1H), 7.36 – 7.30 (m, 1H), 7.22 (m, 1H), 7.06 – 7.01 (m, 1H).

**Synthesis of  $\text{L}_2$ :** Ligand  $\text{L}_1$  was synthesized according to the literature procedure. A mixture of benzyl chloride (0.630 g, 5.0 mmol), phenylacetylene (0.555 g, 5.5 mmol),  $\text{NaN}_3$  (0.390 g, 6.0 mmol) and  $\text{CuI}$  (0.010 g, 1 mol%) in distilled water (15 mL) was stirred at 100 °C in an oil bath for 16 h resulting in grey chunks of solid. The grey solid was washed with distilled water ( $3 \times 10$  mL) and hexane ( $3 \times 5$  mL) and dried under vacuum. The dry solid was dissolved in  $\text{CH}_2\text{Cl}_2$  (10 mL) resulting in a pale yellow solution, which was washed with dilute  $\text{NH}_4\text{OH}$  ( $5 \times 5$  mL) and distilled water ( $3 \times 10$  mL). Thereafter, the solution was dried over  $\text{MgSO}_4$  and all volatiles were removed under high vacuum yielding an off-white solid. The solid was dissolved in minimum amount of  $\text{CH}_2\text{Cl}_2$  and the solution was added dropwise to hexanes (100 mL) while stirring vigorously, which resulted in the formation of white precipitate. The precipitate was filtered off and dried under high vacuum to give pure product (0.861 g, 73%).  $^1\text{H}$  NMR ( $\text{CDCl}_3$ ):  $\delta$  7.80 (d,  $J = 7.3$  Hz, 2H), 7.67 (s, 1H), 7.42–7.36 (m, 5H), 7.34–7.29 (m, 3H), 5.57 (s, 2H).



**Synthesis of **1**:** A mixture of **L1** (0.498 g, 2.10 mmol),  $[\text{RuCl}_2(p\text{-cymene})]_2$  (0.612 g, 1.0 mmol) and  $\text{K}_2\text{CO}_3$  (0.290 g, 2.10 mmol) in  $\text{MeCN}$  (25 mL) was refluxed in an oil bath for 24 h resulting in a red solution. All volatiles were removed under high vacuum to give a red solid which was extracted with  $\text{CH}_2\text{Cl}_2$  (20 mL). The solution was dried under high vacuum to give a red solid as crude product. The crude product was purified by column

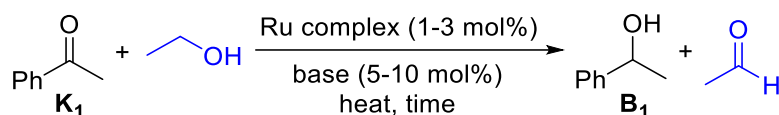
chromatography (silica gel as stationary phase and 4:3 mixture of CH<sub>2</sub>Cl<sub>2</sub> and acetone as eluent) to give a red solid as pure complex **1** (0.806 g, 79%). X-ray quality single crystals were obtained by slow evaporation of Et<sub>2</sub>O into a solution of **1** in CH<sub>2</sub>Cl<sub>2</sub>. <sup>1</sup>H NMR (CDCl<sub>3</sub>): δ 8.13 (s, 1H), 7.85 (d, *J* = 7.5 Hz, 2H), 7.50 (t, *J* = 7.5 Hz, 2H), 7.42 (t, *J* = 7.5 Hz, 1H), 7.05–6.98 (m, 3H), 6.53 (m, *J* = 7.5, 3.9 Hz, 1H), 5.66 (d, *J* = 5.8 Hz, 1H), 5.62 (d, *J* = 5.8 Hz, 1H), 5.40 (d, *J* = 5.8 Hz, 1H), 5.33 (d, *J* = 5.8 Hz, 1H), 3.19–3.07 (m, 1H), 2.33 (s, 3H), 1.35 (d, *J* = 7.2 Hz, 6H), 1.32 (d, *J* = 7.2 Hz, 6H). <sup>13</sup>C{<sup>1</sup>H} NMR (CDCl<sub>3</sub>): δ 160.53, 148.51, 129.75, 129.24, 126.21, 125.90, 123.46, 119.35, 118.40, 115.50, 102.75, 99.34, 84.98, 83.99, 81.23, 81.01, 65.94, 30.74, 22.5, 18.06, 15.38. HRMS (ESI-TOF) *m/z*: [M<sup>+</sup> – Cl] calcd for C<sub>24</sub>H<sub>25</sub>N<sub>3</sub>ORu 473.1042; found 473.1011. Anal. Calcd for C<sub>24</sub>H<sub>25</sub>ClN<sub>3</sub>ORu (508.00): C, 56.74; H, 4.96; N, 8.27. Found: C, 56.48; H, 5.05; N, 8.27.



**Synthesis of 2:** Complex **2** is a known compound; however, **2** was synthesized by using a slightly modified procedure. A mixture of **L2** (0.588 g, 2.10 mmol), [RuCl<sub>2</sub>(*p*-cymene)]<sub>2</sub> (0.612 g, 1.0 mmol) and K<sub>2</sub>CO<sub>3</sub> (0.291 g, 2.10 mmol) in MeCN (25 mL) was refluxed in an oil bath for 48 h resulting in an orange solution. All volatiles were removed under high vacuum to give an orange solid which was extracted with CH<sub>2</sub>Cl<sub>2</sub> (20 mL). The solution was dried under high vacuum to give an orange solid as crude product. The crude product was purified by column chromatography (silica gel as stationary phase and 9:1 mixture of CH<sub>2</sub>Cl<sub>2</sub> and acetone as eluent) to give a yellow solid as pure complex **2** (0.614 g, 60%). <sup>1</sup>H NMR (CDCl<sub>3</sub>): δ 8.16 (d, *J* = 7.4 Hz, 1H), 7.59 (s, 1H), 7.29 (dd, *J* = 5.0, 1.6 Hz, 3H), 7.20 (dd, *J* = 7.5, 5.5 Hz, 3H), 7.13 – 7.07 (m, 1H), 6.98 (t, *J* = 7.1 Hz, 1H), 5.54 (d, *J* = 6.0 Hz, 1H), 5.49

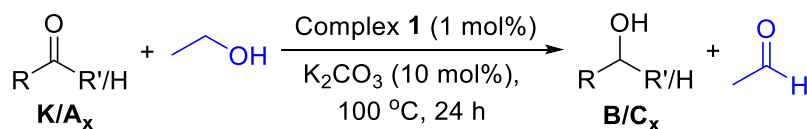
(d,  $J = 6.0$  Hz, 1H), 5.43 (d,  $J = 5.8$  Hz, 1H), 5.24 (d,  $J = 4.6$  Hz, 1H), 5.21 (d,  $J = 4.3$  Hz, 1H), 5.05 (d,  $J = 14.9$  Hz, 1H), 2.35 (m,  $J = 13.8, 6.9$  Hz, 1H), 2.01 (s, 3H), 0.90 (d,  $J = 6.9$  Hz, 3H), 0.80 (d,  $J = 6.9$  Hz, 3H).  $^{13}\text{C}\{^1\text{H}\}$  NMR ( $\text{CDCl}_3$ ):  $\delta$  155.28, 139.64, 135.41, 134.79, 128.99, 128.68, 128.18, 127.61, 122.76, 122.40, 117.84, 99.40, 98.61, 89.18, 87.09, 85.73, 83.53, 54.69, 30.77, 22.16, 18.80 HRMS (ESI-TOF)  $m/z$ :  $[\text{M}^+ - \text{Cl}]$  calcd for  $\text{C}_{25}\text{H}_{26}\text{N}_3\text{ORu}$  471.1198; found 471.1243.

## General procedure for the transfer hydrogenation of ketones and aldehydes



**General condition for reaction optimization using ethanol (Procedure 1a):** A solution of acetophenone (0.060 g, 0.5 mmol), complex **1** or **2** (3/ 2/ 1 mol%) and internal standard 1,3,5-trimethoxybenzene (0.028 g, 0.017 mmol) in ethanol (4 mL) was transferred into a pressure tube fitted with a magnetic stir-bar. The reaction mixture was heated at appropriate temperature (80/ 100 °C) in an oil bath for appropriate time (24/ 18/ 12 h). Thereafter, the reaction mixture was cooled down to r.t. and dried under high vacuum. The resultant oily mixture was dissolved in ethylacetate (3 mL) and passed through a short silica column to remove metal complex. All volatile was removed under high vacuum to give crude product. The crude product was analysed by  $^1\text{H}$  NMR spectroscopy. Occasionally the crude product was purified by column chromatography using silica as stationary phase and a 9:1 mixture of hexanes and ethylacetate as eluent.

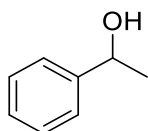
Following are the representative  $^1\text{H}$  NMR spectra of the crude product:



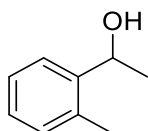
**General condition for substrate screening using ethanol (Procedure 1b):** A solution of ketone or aldehyde (0.50 mmol) and complex **1** (2.5 mg, 1 mol%) in ethanol (4 mL) was transferred into a pressure tube fitted with a magnetic stir-bar. The reaction mixture was heated at 100 °C in an oil bath for 24 h. Thereafter, the reaction mixture was cooled down to r.t. and dried under high vacuum. The resultant oily mixture was dissolved in ethylacetate (3 mL) and passed through a short silica column to remove metal complex. All volatile was removed under high vacuum to give the product. Most of the time, no further purification was needed. Occasionally the crude product was purified by column chromatography using silica as stationary phase and a mixture of hexanes and ethylacetate as eluent.

### NMR data of alcohols

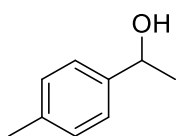
Following products are obtained by transfer hydrogenation of aldehydes and ketones with alcohols using standard catalytic protocol. Known compounds are characterized by  $^1\text{H}$  and  $^{13}\text{C}\{^1\text{H}\}$  NMR spectroscopies and new compounds are characterized by  $^1\text{H}$  and  $^{13}\text{C}\{^1\text{H}\}$  NMR spectroscopies and HRMS:



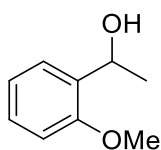
**1-Phenylethanol (B<sub>1</sub>).** Compound **B<sub>1</sub>** was synthesized according to the general procedure **1b**. Crude product was purified by column chromatography (silica as stationary phase and a mixture of hexane and ethyl acetate 9:1 as eluent) to give pure product as brown oil (60 mg, 99%).  $^1\text{H}$  NMR (400 MHz,  $\text{CDCl}_3$ ):  $\delta$  7.36 (q,  $J = 8.0$  Hz, 4H), 7.29 (dd,  $J = 5.2, 3.1$  Hz, 1H), 4.91 (q,  $J = 6.4$  Hz, 1H), 1.73 (s, 1H), 1.51 (d,  $J = 6.4$  Hz, 3H).  $^{13}\text{C}\{^1\text{H}\}$  NMR (101 MHz,  $\text{CDCl}_3$ ):  $\delta$  145.91, 128.51, 127.45, 125.47, 70.34, 25.17.



**1-(*o*-Tolyl)ethan-1-ol (B<sub>2</sub>).** Compound **B<sub>2</sub>** was synthesized according to the general procedure **1b**. Crude product was purified by column chromatography (silica as stationary phase and a mixture of hexane and ethyl acetate 9:1 as eluent) to give pure product as colourless oil (67 mg, 99%). <sup>1</sup>H NMR (400 MHz, CDCl<sub>3</sub>): δ 7.55 – 7.46 (m, 1H), 7.24 (dd, *J* = 10.3, 4.0 Hz, 1H), 7.21 – 7.11 (m, 2H), 5.11 (q, *J* = 6.4 Hz, 1H), 2.35 (s, 3H), 2.07 (s, 1H), 1.46 (d, *J* = 6.4 Hz, 3H). <sup>13</sup>C{<sup>1</sup>H} NMR (101 MHz, CDCl<sub>3</sub>): δ 143.94, 134.30, 130.45, 127.24, 126.45, 124.58, 66.86, 24.00, 18.99.

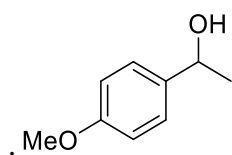


**1-(*p*-Tolyl)ethan-1-ol (B<sub>3</sub>).** Compound **B<sub>3</sub>** was synthesized according to the general procedure **1b**. Crude product was purified by column chromatography (silica as stationary phase and a mixture of hexane and ethyl acetate 9:1 as eluent) to give pure product as faint yellow liquid (65 mg, 97%). <sup>1</sup>H NMR (400 MHz, CDCl<sub>3</sub>): δ 7.27 (d, *J* = 8.0 Hz, 2H), 7.18 (d, *J* = 8.0 Hz, 2H), 4.83 (q, *J* = 6.5 Hz, 1H), 2.68 (s, 1H), 2.38 (s, 3H), 1.48 (d, *J* = 6.4 Hz, 3H). <sup>13</sup>C{<sup>1</sup>H} NMR (101 MHz, CDCl<sub>3</sub>): δ 142.98, 136.94, 129.09, 125.41, 70.05, 25.07, 21.08.

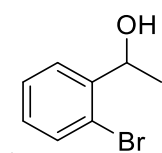


**1-(2-Methoxyphenyl)ethan-1-ol (B<sub>4</sub>).** Compound **B<sub>4</sub>** was synthesized according to the general procedure **1b**. Crude product was purified by column chromatography (silica as stationary phase and a mixture of hexane and ethyl acetate 9:1 as eluent) to give pure product as colourless oil (71 mg, 94%). <sup>1</sup>H NMR (400 MHz, CDCl<sub>3</sub>): δ 7.32 – 7.23 (m, 2H), 6.92 – 6.82 (m, 2H), 4.82 (q, *J* = 6.4 Hz, 1H), 3.79 (s, 3H), 2.18 (s, 1H), 1.46 (d, *J* = 6.4 Hz, 3H).

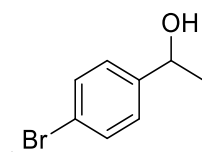
$^{13}\text{C}\{^1\text{H}\}$  NMR (101 MHz,  $\text{CDCl}_3$ ):  $\delta$  156.58, 133.44, 128.31, 126.12, 120.82, 110.45, 66.58, 55.27, 22.86.



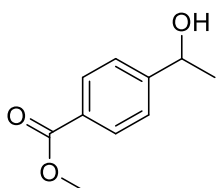
**1-(4-Methoxyphenyl)ethan-1-ol (B<sub>5</sub>)**. Compound **B<sub>5</sub>** was synthesized according to the general procedure **1b**. Crude product was purified by column chromatography (silica as stationary phase and a mixture of hexane and ethyl acetate 9:1 as eluent) to give pure product as colourless oil (70 mg, 93%).  $^1\text{H}$  NMR (400 MHz,  $\text{CDCl}_3$ ):  $\delta$  7.30 (d,  $J = 8.6$  Hz, 2H), 6.88 (d,  $J = 8.7$  Hz, 2H), 4.85 (q,  $J = 6.4$  Hz, 1H), 3.80 (s, 3H), 1.85 (s, 1H), 1.48 (d,  $J = 6.4$  Hz, 3H).  $^{13}\text{C}\{^1\text{H}\}$  NMR (101 MHz,  $\text{CDCl}_3$ ):  $\delta$  159.12, 138.14, 126.79, 113.98, 70.10, 55.42, 25.14.



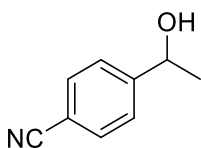
**1-(2-Bromophenyl)ethan-1-ol (B<sub>6</sub>)**. Compound **B<sub>6</sub>** was synthesized according to the general procedure **1b**. Crude product was purified by column chromatography (silica as stationary phase and a mixture of hexane and ethyl acetate 9:1 as eluent) to give pure product as faint yellow oil (92 mg, 92%).  $^1\text{H}$  NMR (400 MHz,  $\text{CDCl}_3$ ):  $\delta$  7.60 (dd,  $J = 7.8, 1.6$  Hz, 1H), 7.51 (dd,  $J = 8.0, 1.0$  Hz, 1H), 7.35 (t,  $J = 7.6$  Hz, 1H), 7.13 (td,  $J = 7.7, 1.7$  Hz, 1H), 5.25 (q,  $J = 6.4$  Hz, 1H), 1.70 (s, 1H), 1.49 (d,  $J = 6.4$  Hz, 3H).  $^{13}\text{C}\{^1\text{H}\}$  NMR (101 MHz,  $\text{CDCl}_3$ ):  $\delta$  144.74, 132.82, 128.93, 128.00, 126.81, 121.88, 69.36, 23.72.



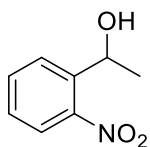
**1-(4-Bromophenyl)ethan-1-ol (B7).** Compound **B7** was synthesized according to the general procedure **1b**. Crude product was purified by column chromatography (silica as stationary phase and a mixture of hexane and ethyl acetate 9:1 as eluent) to give pure product as colourless oil (93 mg, 94%).  $^1\text{H}$  NMR (400 MHz,  $\text{CDCl}_3$ ):  $\delta$  7.43 (d,  $J = 8.4$  Hz, 2H), 7.18 (d,  $J = 8.4$  Hz, 2H), 4.77 (q,  $J = 6.5$  Hz, 1H), 2.67 (s, 1H), 1.41 (d,  $J = 6.4$  Hz, 3H).  $^{13}\text{C}\{^1\text{H}\}$  NMR (101 MHz,  $\text{CDCl}_3$ ):  $\delta$  144.90, 131.67, 127.28, 121.27, 69.88, 25.35.



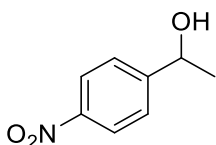
**Methyl 4-(1-hydroxyethyl)benzoate (B8).** Compound **B8** was synthesized according to the general procedure **1b**. Crude product was purified by column chromatography (silica as stationary phase and a mixture of hexane and ethyl acetate 9:1 as eluent) to give pure product as colourless yellow oil (86.4 mg, 96%).  $^1\text{H}$  NMR (400 MHz,  $\text{CDCl}_3$ ):  $\delta$  8.09 – 7.86 (m, 2H), 7.41 (d,  $J = 8.2$  Hz, 2H), 4.93 (q,  $J = 6.5$  Hz, 1H), 3.89 (s, 3H), 2.20 (s, 1H), 1.48 (d,  $J = 6.4$  Hz, 3H).  $^{13}\text{C}\{^1\text{H}\}$  NMR (101 MHz,  $\text{CDCl}_3$ ):  $\delta$  167.13, 151.12, 129.93, 129.22, 125.40, 70.03, 52.20, 25.38.



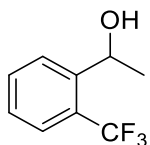
**4-(1-Hydroxyethyl)benzonitrile (B9).** Compound **B9** was synthesized according to the general procedure **1b**. Crude product was purified by column chromatography (silica as stationary phase and a mixture of hexane and ethyl acetate 9:1 as eluent) to give pure product as colourless yellow oil (70 mg, 95%).  $^1\text{H}$  NMR (400 MHz,  $\text{CDCl}_3$ ):  $\delta$  7.54 (d,  $J = 8.3$  Hz, 2H), 7.42 (d,  $J = 8.1$  Hz, 2H), 4.87 (q,  $J = 6.5$  Hz, 1H), 3.18 (s, 1H), 1.42 (d,  $J = 6.4$  Hz, 3H).  $^{13}\text{C}\{^1\text{H}\}$  NMR (101 MHz,  $\text{CDCl}_3$ ):  $\delta$  151.51, 132.25, 126.13, 118.92, 110.62, 69.38, 25.29.



**1-(2-Nitrophenyl)ethan-1-ol (B<sub>10</sub>).** Compound **B<sub>10</sub>** was synthesized according to the general procedure **1b**. Crude product was purified by column chromatography (silica as stationary phase and a mixture of hexane and ethyl acetate 9:1 as eluent) to give pure product as yellow liquid (82 mg, 99%). <sup>1</sup>H NMR (400 MHz, CDCl<sub>3</sub>): δ 7.83 (dd, *J* = 18.8, 8.0, 1.1 Hz, 2H), 7.64 – 7.57 (m, 1H), 7.42 – 7.35 (m, 1H), 5.38 (q, *J* = 6.4 Hz, 1H), 2.49 (s, 1H), 1.53 (d, *J* = 6.4 Hz, 3H). <sup>13</sup>C{<sup>1</sup>H} NMR (101 MHz, CDCl<sub>3</sub>): δ 141.05, 133.73, 128.22, 127.69, 124.40, 65.66, 24.32.

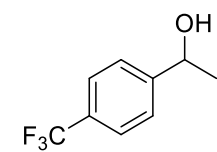


**1-(4-Nitrophenyl)ethan-1-ol (B<sub>11</sub>).** Compound **B<sub>11</sub>** was synthesized according to the general procedure **1b**. Crude product was purified by column chromatography (silica as stationary phase and a mixture of hexane and ethyl acetate 9:1 as eluent) to give pure product as colourless oil (95 mg, 99%). <sup>1</sup>H NMR (400 MHz, CDCl<sub>3</sub>): δ 8.17 (d, *J* = 8.8 Hz, 2H), 7.53 (d, *J* = 8.5 Hz, 2H), 5.00 (q, *J* = 6.5 Hz, 1H), 2.05 (s, 1H), 1.51 (d, *J* = 6.4 Hz, 4H). <sup>13</sup>C{<sup>1</sup>H} NMR (101 MHz, CDCl<sub>3</sub>): δ 153.20, 129.45, 126.26, 123.96, 69.65, 25.65.

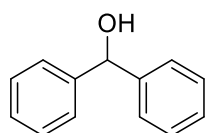


**1-(2-(Trifluoromethyl)phenyl)ethan-1-ol (B<sub>12</sub>).** Compound **B<sub>12</sub>** was synthesized according to the general procedure **1b**. Crude product was purified by column chromatography (silica as stationary phase and a mixture of hexane and ethyl acetate 9:1 as eluent) to give pure product

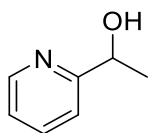
as colourless oil (94 mg, 99%).  $^1\text{H}$  NMR (400 MHz,  $\text{CDCl}_3$ ):  $\delta$  7.79 (d,  $J = 7.9$  Hz, 1H), 7.57 (dd,  $J = 15.9, 7.8$  Hz, 2H), 7.34 (t,  $J = 7.6$  Hz, 1H), 5.30 (q,  $J = 6.1$  Hz, 1H), 2.56 (s, 1H), 1.44 (d,  $J = 6.4$  Hz, 3H).  $^{13}\text{C}\{^1\text{H}\}$  NMR (101 MHz,  $\text{CDCl}_3$ ):  $\delta$  145.22, 132.47, 127.31, 126.69, 126.39, 125.37 (q,  $J = 5.9$  Hz), 123.16, 65.74, 25.49.



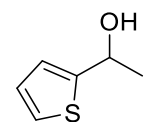
**1-(4-(Trifluoromethyl)phenyl)ethan-1-ol (B<sub>13</sub>)**. Compound **B<sub>13</sub>** was synthesized according to the general procedure **1b**. Crude product was purified by column chromatography (silica as stationary phase and a mixture of hexane and ethyl acetate 9:1 as eluent) to give pure product as colourless liquid (94 mg, 99%).  $^1\text{H}$  NMR (400 MHz,  $\text{CDCl}_3$ ):  $\delta$  7.59 (d,  $J = 8.1$  Hz, 2H), 7.46 (d,  $J = 8.1$  Hz, 2H), 4.92 (q,  $J = 6.5$  Hz, 1H), 2.30 (s, 1H), 1.48 (d,  $J = 6.4$  Hz, 3H).  $^{13}\text{C}\{^1\text{H}\}$  NMR (101 MHz,  $\text{CDCl}_3$ ):  $\delta$  149.83, 129.89, 129.57, 125.87 – 125.39 (m), 122.95, 69.90, 25.43.



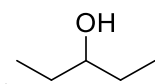
**Diphenylmethanol (B<sub>14</sub>)**. Compound **B<sub>14</sub>** was synthesized according to the general procedure **1b**. Crude product was purified by column chromatography (silica as stationary phase and a mixture of ethyl acetate and hexane 1:9 as eluent) to give pure product as colourless oil (87.4 mg, 95%).  $^1\text{H}$  NMR (400 MHz,  $\text{CDCl}_3$ ):  $\delta$  7.44 – 7.30 (m, 8H), 7.28 (dd,  $J = 7.0, 3.8, 1.7$  Hz, 2H), 5.85 (s, 1H), 1.99 (s, 1H).  $^{13}\text{C}\{^1\text{H}\}$  NMR (101 MHz,  $\text{CDCl}_3$ ):  $\delta$  143.94, 128.64, 127.72, 126.68, 76.41.



**1-(Pyridin-2-yl)ethan-1-ol (B<sub>15</sub>)**. Compound **B<sub>15</sub>** was synthesized according to the general procedure **1b**. Crude product was purified by column chromatography (silica as stationary phase and a mixture of hexane and ethyl acetate 9:1 as eluent) to give pure product as colourless oil (56 mg, 92%). <sup>1</sup>H NMR (400 MHz, CDCl<sub>3</sub>): δ 8.53 (d, *J* = 4.1 Hz, 1H), 7.69 (dd, *J* = 12.1, 4.4 Hz, 1H), 7.31 – 7.25 (m, 1H), 7.20 (t, *J* = 5.9 Hz, 1H), 4.89 (q, *J* = 6.5 Hz, 1H), 1.50 (d, *J* = 6.4 Hz, 3H). <sup>13</sup>C{<sup>1</sup>H} NMR (101 MHz, CDCl<sub>3</sub>): δ 163.49, 148.17, 136.86, 122.21, 119.83, 69.15, 24.18.

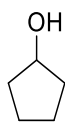


**1-(Thiophen-2-yl)ethan-1-ol (B<sub>16</sub>)**. Compound **B<sub>16</sub>** was synthesized according to the general procedure **1b**. Crude product was purified by column chromatography (silica as stationary phase and a mixture of hexane and ethyl acetate 9:1 as eluent) to give pure product colourless oil (57 mg, 90%). <sup>1</sup>H NMR (400 MHz, CDCl<sub>3</sub>): δ 7.26 (dd, *J* = 5.0, 3.0 Hz, 1H), 7.15 – 7.12 (m, 1H), 7.07 (dd, *J* = 5.0, 1.2 Hz, 1H), 4.90 (q, *J* = 6.4 Hz, 1H), 2.79 (s, 1H), 1.48 (d, *J* = 6.4 Hz, 3H). <sup>13</sup>C{<sup>1</sup>H} NMR (101 MHz, CDCl<sub>3</sub>): δ 147.41, 125.95, 125.73, 120.09, 66.34, 24.39.

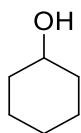


**Pentan-3-ol (B<sub>17</sub>)**. Compound **B<sub>17</sub>** was synthesized according to the general procedure **1b**. Crude product was purified by column chromatography (silica as stationary phase and a mixture of hexane and ethyl acetate 9:1 as eluent) to give pure product as colourless liquid (34 g, 81%). <sup>1</sup>H NMR (400 MHz, CDCl<sub>3</sub>): δ 3.43 – 3.33 (m, 1H), 2.36 – 2.14 (m, 1H), 1.52 –

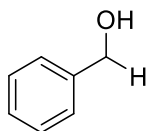
1.31 (m, 4H), 0.88 (dd,  $J = 10, 6.9, 2.5$  Hz, 6H).  $^{13}\text{C}\{^1\text{H}\}$  NMR (101 MHz,  $\text{CDCl}_3$ ):  $\delta$   $^{13}\text{C}$  74.68, 29.61, 9.86.



**Cyclopentanol (B18).** Compound **B18** was synthesized according to the general procedure **1b**. Crude product was purified by column chromatography (silica as stationary phase and a mixture of hexane and ethyl acetate 9:1 as eluent) to give pure product as colourless liquid (37 mg, 87%).  $^1\text{H}$  NMR (400 MHz,  $\text{CDCl}_3$ ):  $\delta$  4.32 (s, 1H), 1.83 – 1.68 (m, 4H), 1.59 – 1.51 (m, 4H).  $^{13}\text{C}\{^1\text{H}\}$  NMR (101 MHz,  $\text{CDCl}_3$ ):  $\delta$  74.20, 35.70, 23.41.



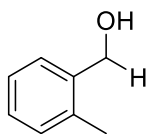
**Cyclohexanol (B19).** Compound **B19** was synthesized according to the general procedure **1b**. Crude product was purified by column chromatography (silica as stationary phase and a mixture of hexane and ethyl acetate 9:1 as eluent) to give pure product as colourless liquid (41 mg, 83%).  $^1\text{H}$  NMR (400 MHz,  $\text{CDCl}_3$ ):  $\delta$  3.61 (dt,  $J = 8.9, 4.2$  Hz, 1H), 1.88 (dd,  $J = 9.1, 3.7$  Hz, 2H), 1.75 – 1.50 (m, 4H), 1.31 – 1.19 (m, 4H).  $^{13}\text{C}\{^1\text{H}\}$  NMR (101 MHz,  $\text{CDCl}_3$ ):  $\delta$  70.47, 35.67, 25.59, 24.26.



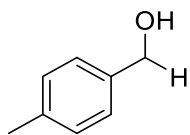
**Phenylmethanol (C1).** Compound **C1** was synthesized according to the general procedure **2b**. Crude product was purified by column chromatography (silica as stationary phase and a mixture of hexane and ethyl acetate as 9:1 as eluent) to give pure product as yellow oil (53

mg, 99%).  $^1\text{H}$  NMR (400 MHz,  $\text{CDCl}_3$ ):  $\delta$  7.43 – 7.19 (m, 5H), 4.64 (s, 2H), 2.62 (s, 1H).

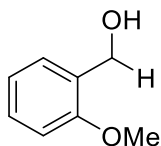
$^{13}\text{C}\{^1\text{H}\}$  NMR (101 MHz,  $\text{CDCl}_3$ ):  $\delta$  140.92, 128.59, 127.65, 127.07, 65.20.



***o*-Tolylmethanol (C<sub>2</sub>).** Compound **C<sub>2</sub>** was synthesized according to the general procedure **2b**. Crude product was purified by column chromatography (silica as stationary phase and a mixture of hexane and ethyl acetate 9:1 as eluent) to give pure product as colourless liquid (60 mg, 99%).  $^1\text{H}$  NMR (400 MHz,  $\text{CDCl}_3$ ):  $\delta$  7.38 – 7.31 (m, 1H), 7.27 – 7.15 (m, 3H), 4.64 (s, 2H), 2.53 (s, 1H), 2.35 (s, 3H).  $^{13}\text{C}\{^1\text{H}\}$  NMR (101 MHz,  $\text{CDCl}_3$ ):  $\delta$  138.77, 136.07, 130.30, 127.72, 127.53, 126.05, 63.27, 18.65.

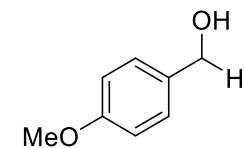


***p*-Tolylmethanol (C<sub>3</sub>).** Compound **C<sub>3</sub>** was synthesized according to the general procedure **2b**. Crude product was purified by column chromatography (silica as stationary phase and a mixture of hexane and ethyl acetate 9:1 as eluent) to give pure product as colourless oil (59 mg, 97%).  $^1\text{H}$  NMR (400 MHz,  $\text{CDCl}_3$ ):  $\delta$  7.16–7.24 (dd,  $J = 7.9$  Hz, 4H), 4.62 (s, 2H), 2.36 (s, 3H), 1.98 (s, 1H).  $^{13}\text{C}\{^1\text{H}\}$  NMR (101 MHz,  $\text{CDCl}_3$ ):  $\delta$  138.02, 137.45, 129.32, 127.22, 65.27, 21.24.

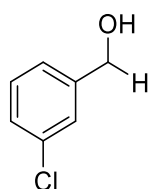


**(2-Methoxyphenyl)methanol (C<sub>4</sub>).** Compound **C<sub>4</sub>** was synthesized according to the general procedure **2b**. Crude product was purified by column chromatography (silica as stationary

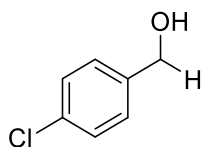
phase and a mixture of hexane and ethyl acetate 9:1 as eluent) to give pure product as colourless liquid (64 mg, 94%).  $^1\text{H}$  NMR (400 MHz,  $\text{CDCl}_3$ ):  $\delta$  7.28 (m,  $J = 5.2, 1.6$  Hz, 2H), 6.95 (m,  $J = 7.4, 1.0$  Hz, 1H), 6.91 – 6.87 (m, 1H), 4.68 (s, 2H), 3.86 (s, 3H), 2.34 (s, 1H).  $^{13}\text{C}\{^1\text{H}\}$  NMR (101 MHz,  $\text{CDCl}_3$ ):  $\delta$  157.50, 129.14, 129.02, 128.80, 120.73, 110.29, 62.07, 55.33.



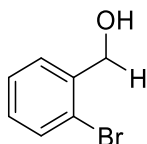
**(4-Methoxyphenyl)methanol (C<sub>5</sub>).** Compound C<sub>5</sub> was synthesized according to the general procedure **2b**. Crude product was purified by column chromatography (silica as stationary phase and a mixture of hexane and ethyl acetate 9:1 as eluent) to give pure product as colourless liquid (63 mg, 93%).  $^1\text{H}$  NMR (400 MHz,  $\text{CDCl}_3$ ):  $\delta$  7.27 (d,  $J = 8.3$  Hz, 2H), 6.89 (dd,  $J = 9.0, 2.3$  Hz, 2H), 4.57 (s, 2H), 3.80 (s, 3H), 2.47 (s, 1H).  $^{13}\text{C}\{^1\text{H}\}$  NMR (101 MHz,  $\text{CDCl}_3$ ):  $\delta$  159.28, 133.26, 128.75, 114.04, 65.05, 55.38.



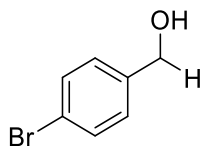
**(3-Chlorophenyl)methanol (C<sub>6</sub>).** Compound C<sub>6</sub> was synthesized according to the general procedure **2b**. Crude product was purified by column chromatography (silica as stationary phase and a mixture of hexane and ethyl acetate 9:1 as eluent) to give pure product as colourless oil (64 mg, 91%).  $^1\text{H}$  NMR (400 MHz,  $\text{CDCl}_3$ ):  $\delta$  7.37 – 7.25 (m, 4H), 4.68 (s, 2H), 1.74 (s, 1H).  $^{13}\text{C}\{^1\text{H}\}$  NMR (101 MHz,  $\text{CDCl}_3$ ):  $\delta$  142.97, 134.59, 129.96, 127.85, 127.10, 124.98, 64.70.



**(4-Chlorophenyl)methanol (C<sub>7</sub>).** Compound C<sub>7</sub> was synthesized according to the general procedure **2b**. Crude product was purified by column chromatography (silica as stationary phase and a mixture of hexane and ethyl acetate 9:1 as eluent) to give pure product as white solid (68mg, 96%). <sup>1</sup>H NMR (400 MHz, CDCl<sub>3</sub>): δ 7.33–7.27 (m, *J* = 8.4, 4.9 Hz, 4H), 4.63 (dd, *J* = 4.8, 2.3 Hz, 2H), 1.93 (s, 1H). <sup>13</sup>C{<sup>1</sup>H} NMR (101 MHz, CDCl<sub>3</sub>): δ 139.45, 133.49, 128.79, 128.38, 64.60.

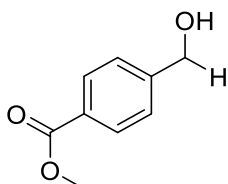


**(2-Bromophenyl)methanol (C<sub>8</sub>).** Compound C<sub>8</sub> was synthesized according to the general procedure **2b**. Crude product was purified by column chromatography (silica as stationary phase and a mixture of hexane and ethyl acetate 9:1 as eluent) to give pure product as colourless liquid (92 mg, 99%). <sup>1</sup>H NMR (400 MHz, CDCl<sub>3</sub>): δ 7.55 (dd, *J* = 8.0, 1.0 Hz, 1H), 7.48 (dd, *J* = 7.6, 1.5 Hz, 1H), 7.33 (td, *J* = 7.5, 1.0 Hz, 1H), 7.16 (td, *J* = 7.7, 1.7 Hz, 1H), 4.76 (s, 2H), 1.82 (s, 1H). <sup>13</sup>C{<sup>1</sup>H} NMR (101 MHz, CDCl<sub>3</sub>): δ 139.84, 132.70, 129.22, 129.00, 127.77, 122.67, 65.15.

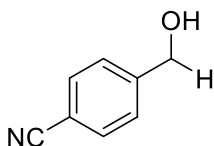


**(4-Bromophenyl)methanol (C<sub>9</sub>).** Compound C<sub>9</sub> was synthesized according to the general procedure **2b**. Crude product was purified by column chromatography (silica as stationary phase and a mixture of hexane and ethyl acetate 9:1 as eluent) to give pure product as white

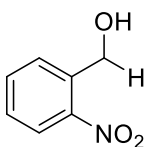
liquid (86 g, 99%).  $^1\text{H}$  NMR (400 MHz,  $\text{CDCl}_3$ ):  $\delta$  7.50 – 7.39 (m, 2H), 7.19 (d,  $J = 8.3$  Hz, 2H), 4.58 (s, 2H), 2.35 (s, 1H).  $^{13}\text{C}\{^1\text{H}\}$  NMR (101 MHz,  $\text{CDCl}_3$ ):  $\delta$  139.82, 131.68, 128.67, 121.49, 64.50.



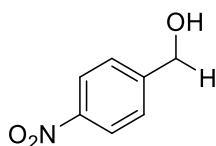
**Methyl 4-(hydroxymethyl)benzoate ( $\text{C}_{10}$ ).** Compound  $\text{C}_{10}$  was synthesized according to the general procedure **2b**. Crude product was purified by column chromatography (silica as stationary phase and a mixture of hexane and ethyl acetate 9:1 as eluent) to give pure product as white liquid (77mg, 93%).  $^1\text{H}$  NMR (400 MHz,  $\text{CDCl}_3$ ):  $\delta$  7.97 (d,  $J = 8.3$  Hz, 2H), 7.38 (d,  $J = 8.3$  Hz, 2H), 4.71 (s, 2H), 3.88 (s, 3H), 2.55 (s, 1H).  $^{13}\text{C}\{^1\text{H}\}$  NMR (101 MHz,  $\text{CDCl}_3$ ):  $\delta$  167.19, 146.25, 129.87, 129.22, 126.52, 64.60, 52.21.



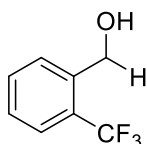
**4-(Hydroxymethyl)benzonitrile ( $\text{C}_{11}$ ).** Compound  $\text{C}_{11}$  was synthesized according to the general procedure **2b**. Crude product was purified by column chromatography (silica as stationary phase and a mixture of hexane and ethyl acetate 9:1 as eluent) to give pure product as white liquid (40mg, 91%).  $^1\text{H}$  NMR (400 MHz,  $\text{CDCl}_3$ ):  $\delta$  7.55 (d,  $J = 8.3$  Hz, 2H), 7.41 (d,  $J = 8.3$  Hz, 2H), 4.68 (s, 2H), 3.35 (s, 1H).  $^{13}\text{C}\{^1\text{H}\}$  NMR (101 MHz,  $\text{CDCl}_3$ ):  $\delta$  167.19, 146.25, 129.87, 129.93, 110.58, 64.60.



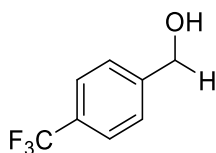
**(2-Nitrophenyl)methanol (C<sub>12</sub>).** Compound C<sub>12</sub> was synthesized according to the general procedure **2b**. Crude product was purified by column chromatography (silica as stationary phase and a mixture of hexane and ethyl acetate 9:1 as eluent) to give pure product as brown oil (75.7 mg, 99%). <sup>1</sup>H NMR (400 MHz, CDCl<sub>3</sub>): δ 8.09 (dd, *J* = 8.2, 1.1 Hz, 1H), 7.74 (d, *J* = 7.0 Hz, 1H), 7.67 (td, *J* = 7.6, 1.2 Hz, 1H), 7.51 – 7.41 (m, 1H), 4.97 (s, 2H), 2.43 (s, 1H). <sup>13</sup>C{<sup>1</sup>H} NMR (101 MHz, CDCl<sub>3</sub>): δ 147.59, 136.97, 134.21, 129.83, 128.50, 125.04, 62.44.



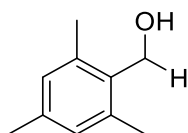
**(4-Nitrophenyl)methanol (C<sub>13</sub>).** Compound C<sub>13</sub> was synthesized according to the general procedure **2b**. Crude product was purified by column chromatography (silica as stationary phase and a mixture of hexane and ethyl acetate 9:1 as eluent) to give pure product as colourless oil (0.72 mg, 95%). <sup>1</sup>H NMR (400 MHz, CDCl<sub>3</sub>): δ 7.62 (d, *J* = 8.0 Hz, 2H), 7.48 (d, *J* = 8.0 Hz, 2H), 4.77 (s, 2H), 2.05 (s, 1H). <sup>13</sup>C{<sup>1</sup>H} NMR (101 MHz, CDCl<sub>3</sub>): δ 148.44, 147.26, 127.08, 123.77, 63.98.



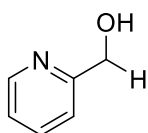
**(2-(Trifluoromethyl)phenyl)methanol (C<sub>14</sub>).** Compound C<sub>14</sub> was synthesized according to the general procedure **2b**. Crude product was purified by column chromatography (silica as stationary phase and a mixture of hexane and ethyl acetate 9:1 as eluent) to give pure product as colourless liquid (87mg, 99%). <sup>1</sup>H NMR (400 MHz, CDCl<sub>3</sub>): δ 7.65 (dd, *J* = 7.8 Hz, 2H), 7.54 (t, *J* = 7.6 Hz, 1H), 7.37 (t, *J* = 7.6 Hz, 1H), 4.84 (s, 2H), 2.49 (s, 1H). <sup>13</sup>C{<sup>1</sup>H} NMR (101 MHz, CDCl<sub>3</sub>): δ 139.34, 132.26, 128.83, 127.49, 127.15, 125.84 (q, *J* = 10.0, 4.4 Hz), 123.19, 61.34.



**(4-(Trifluoromethyl)phenyl)methanol (C<sub>15</sub>).** Compound C<sub>15</sub> was synthesized according to the general procedure **2b**. Crude product was purified by column chromatography (silica as stationary phase and a mixture of hexane and ethyl acetate 9:1 as eluent) to give pure product as colourless oil (87 mg, 99%). <sup>1</sup>H NMR (400 MHz, CDCl<sub>3</sub>): δ 7.62 (d, *J* = 8.0 Hz, 2H), 7.48 (d, *J* = 8.0 Hz, 2H), 4.77 (s, 2H), 1.84 (s, 1H). <sup>13</sup>C{<sup>1</sup>H} NMR (101 MHz, CDCl<sub>3</sub>): δ 144.76, 129.86, 129.54, 125.38 (q, *J* = 3.8 Hz), 122.95, 63.95.

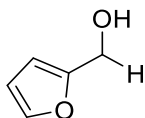


**Mesitylmethanol (C<sub>16</sub>).** Compound C<sub>16</sub> was synthesized according to the general procedure **2b**. Crude product was purified by column chromatography (silica as stationary phase and a mixture of hexane and ethyl acetate 9:1 as eluent) to give pure product as white crystalline solid (64.5 mg, 86%). <sup>1</sup>H NMR (400 MHz, CDCl<sub>3</sub>): δ 6.88 (s, 2H), 4.71 (s, 2H), 2.40 (s, 6H), 2.27 (s, 3H), 1.39 (s, 1H). <sup>13</sup>C{<sup>1</sup>H} NMR (101 MHz, CDCl<sub>3</sub>): δ 137.84, 137.41, 133.86, 129.27, 59.29, 21.08, 19.45.

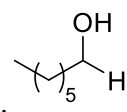


**Pyridin-2-ylmethanol (C<sub>17</sub>).** Compound C<sub>17</sub> was synthesized according to the general procedure **2b**. Crude product was purified by column chromatography (silica as stationary phase and a mixture of hexane and ethyl acetate 9:1 as eluent) to give pure product as colourless liquid (48 mg, 89%). <sup>1</sup>H NMR (400 MHz, CDCl<sub>3</sub>): δ 8.49 (s, 1H), 7.65 (t, *J* = 7.4

Hz, 1H), 7.29 (d,  $J = 7.5$  Hz, 1H), 7.16 (s, 1H), 4.73 (s, 2H), 4.60 – 3.70 (s, 1H).  $^{13}\text{C}\{^1\text{H}\}$  NMR (101 MHz,  $\text{CDCl}_3$ ):  $\delta$  160.05, 148.22, 136.95, 122.21, 120.85, 64.27.



**Furan-2-ylmethanol (C<sub>18</sub>).** Compound **C<sub>18</sub>** was synthesized according to the general procedure **2b**. Crude product was purified by column chromatography (silica as stationary phase and a mixture of hexane and ethyl acetate 9:1 as eluent) to give pure product as colourless oil (44 g, 90%).  $^1\text{H}$  NMR (400 MHz,  $\text{CDCl}_3$ ):  $\delta$  7.40 (dd,  $J = 1.8$  Hz, 1H), 6.34 (dd,  $J = 3.1$  Hz, 1H), 6.29 (d,  $J = 3.2$  Hz, 1H), 4.60 (s, 2H), 1.96 (s, 1H).  $^{13}\text{C}\{^1\text{H}\}$  NMR (101 MHz,  $\text{CDCl}_3$ ):  $\delta$  154.12, 142.72, 110.49, 107.90, 57.59.



**Heptan-1-ol (C<sub>19</sub>).** Compound **C<sub>19</sub>** was synthesized according to the general procedure **2b**. Crude product was purified by column chromatography (silica as stationary phase and a mixture hexane and ethyl acetate 9:1 as eluent as eluent) to give pure product as colourless oil. (47 mg, 82%).  $^1\text{H}$  NMR (400 MHz,  $\text{CDCl}_3$ ):  $\delta$  1H NMR (400 MHz,  $\text{CDCl}_3$ ) 3.64 (m,  $J = 6.6$  Hz, 1H), 1.81 – 1.52 (m, 3H), 1.51 – 1.03 (m, 9H), 0.89 (m,  $J = 6.8$  Hz, 3H).  $^{13}\text{C}\{^1\text{H}\}$  NMR (101 MHz,  $\text{CDCl}_3$ ):  $\delta$  63.07, 32.81, 31.79, 29.06, 25.69, 22.55, 13.99.

**NMR spectra of Ligand, complex 1,2 and some products:**

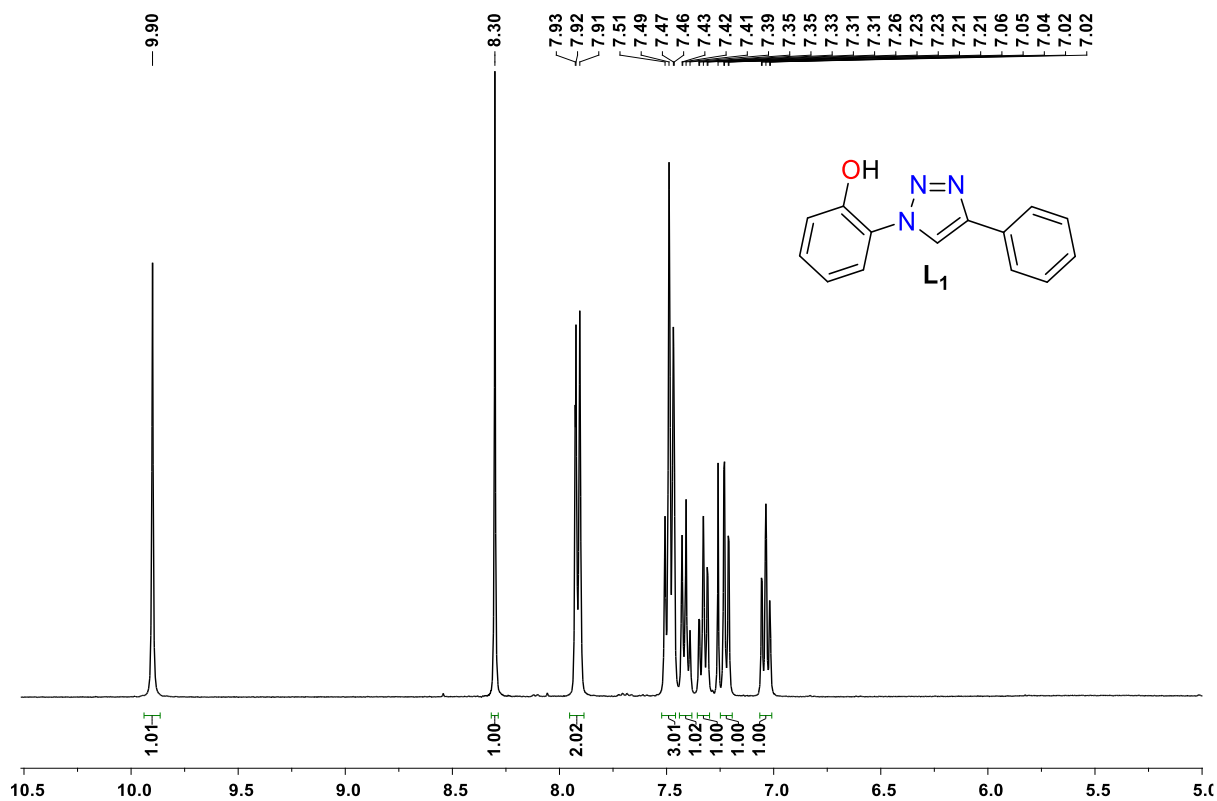


**Figure 2.5.1.**  $^1\text{H}$  NMR (400 MHz) spectrum of **L<sub>1</sub>** in  $\text{CDCl}_3$  at r.t.

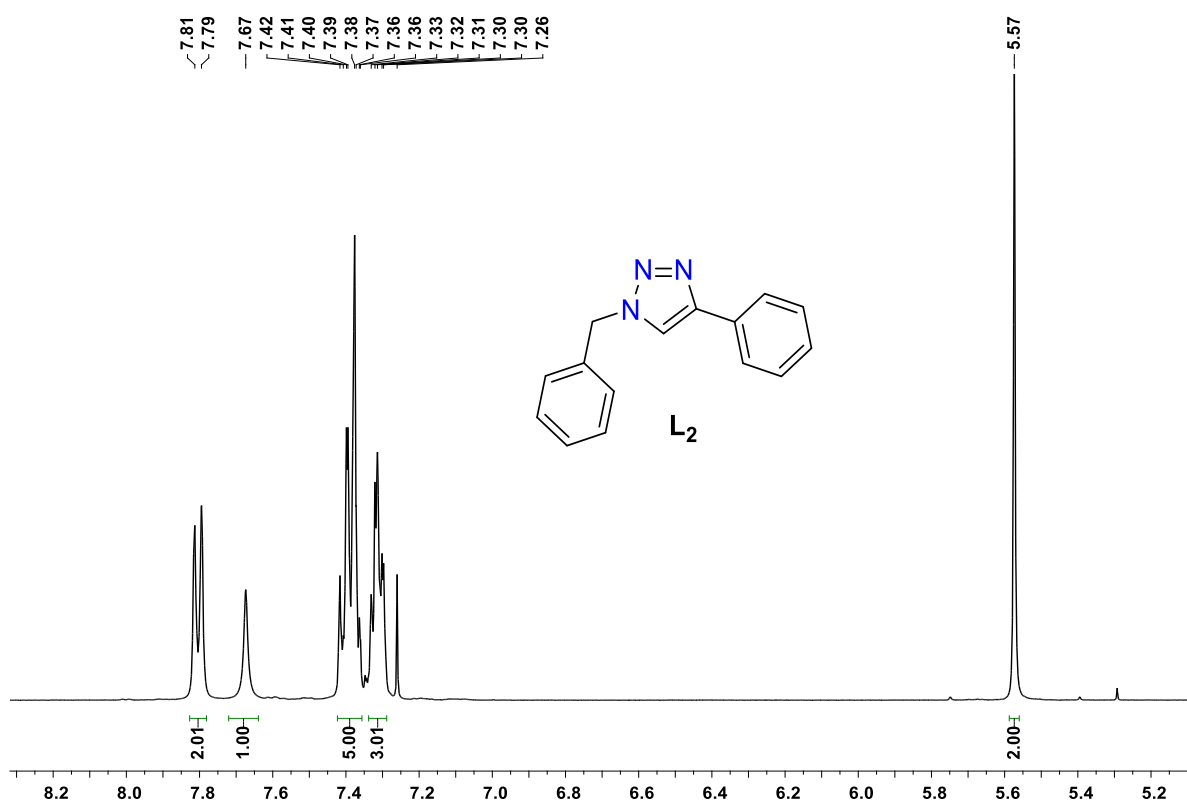


**Figure 2.5.2.**  $^1\text{H}$  NMR (400 MHz) spectrum of **L<sub>2</sub>** in  $\text{CDCl}_3$  at r.t.

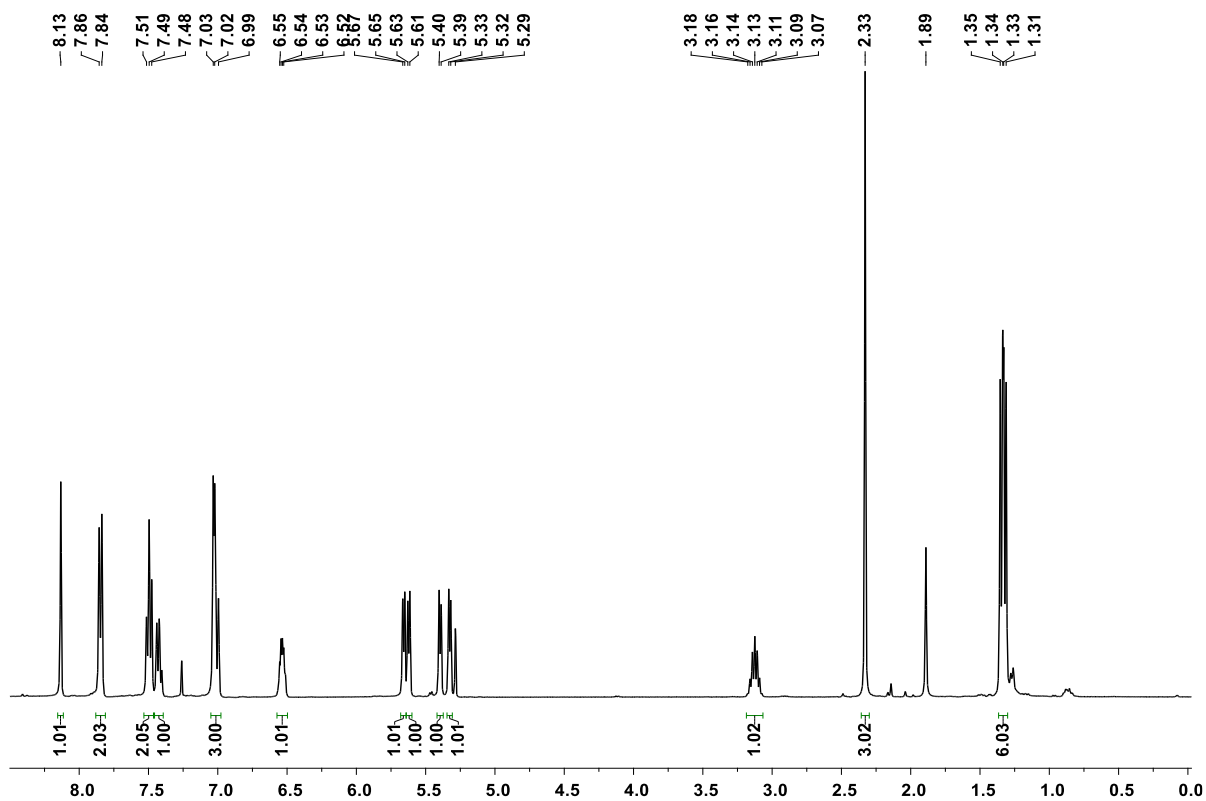


**Figure 2.5.3.**  $^1\text{H}$  NMR (400 MHz) spectrum of complex **1** in  $\text{CDCl}_3$  at r.t. (\* indicates  $\text{H}_2\text{O}$ ).

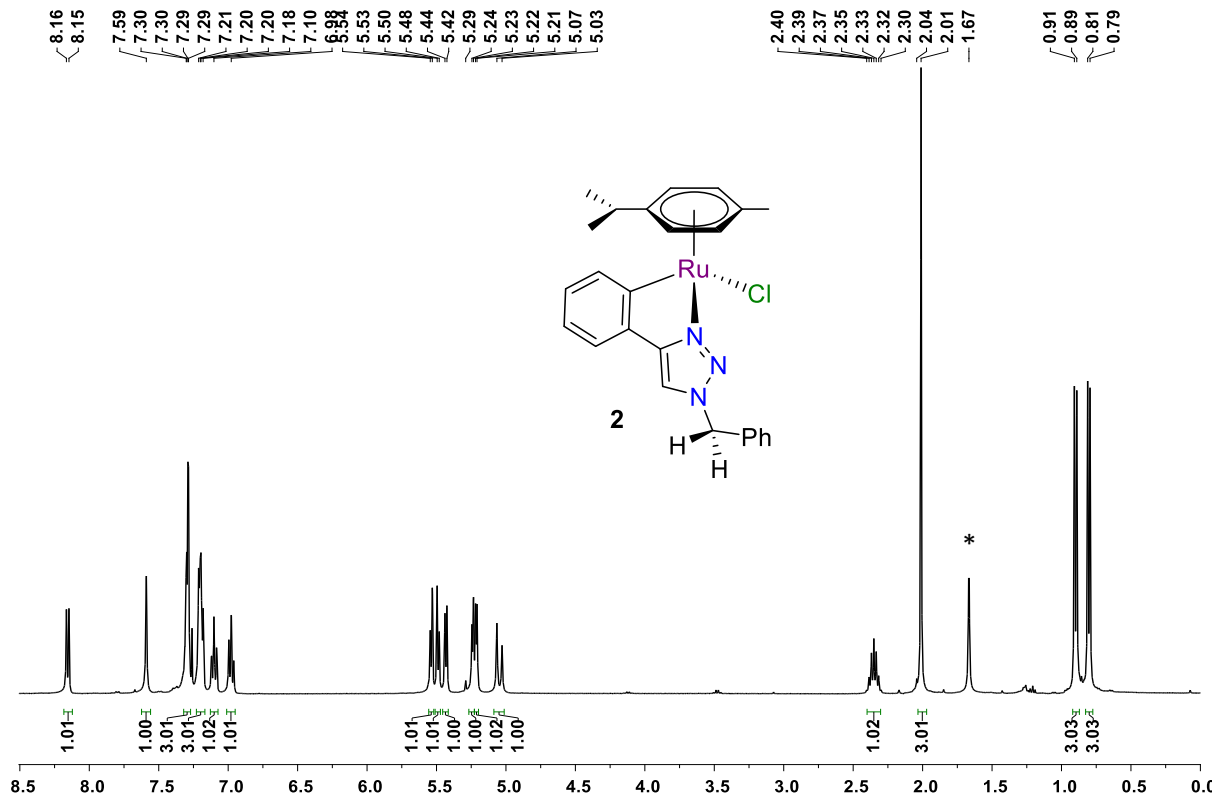


**Figure 2.5.4.**  $^1\text{H}$  NMR (400 MHz) spectrum of complex **2** in  $\text{CDCl}_3$  at r.t. (\* indicates  $\text{H}_2\text{O}$ ).

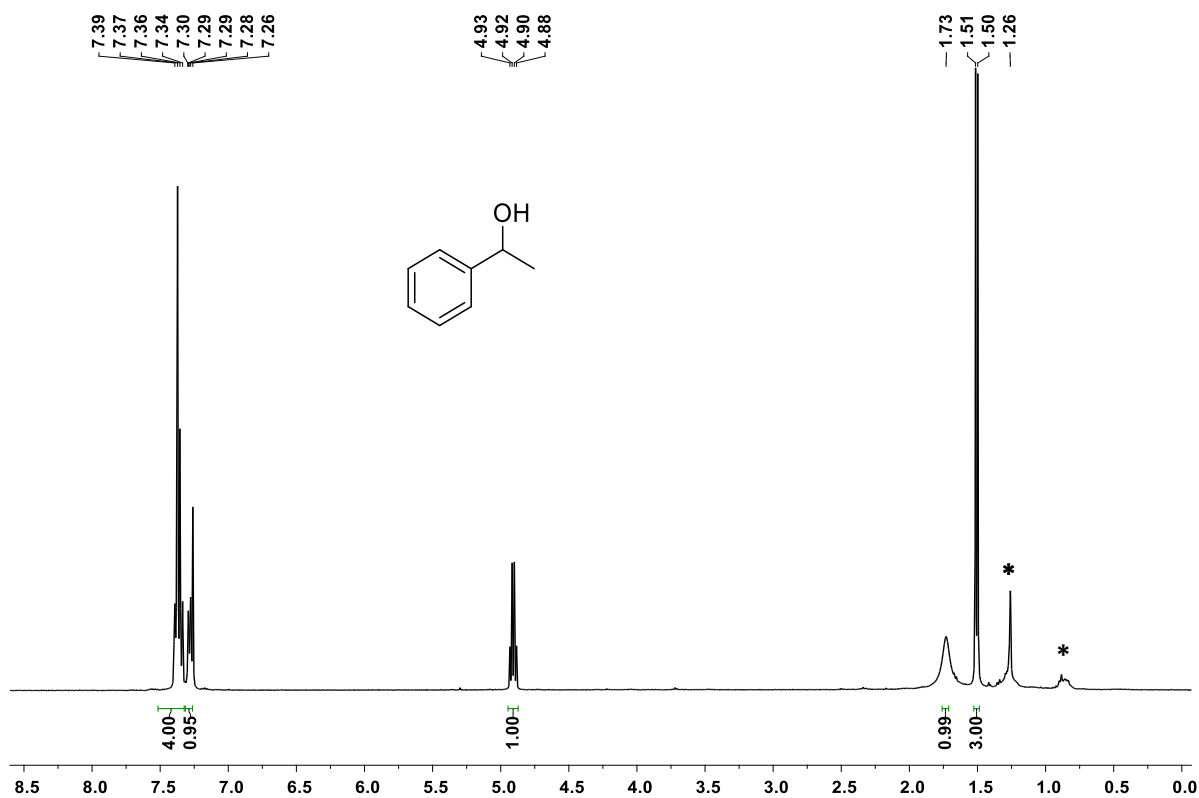


**Figure 2.5.5.**  $^1\text{H}$  NMR (400 MHz) spectrum of 1-Phenylethan-1-ol ( $\text{B}_1$ ) in  $\text{CDCl}_3$  at r.t. (\* indicates H-grease).

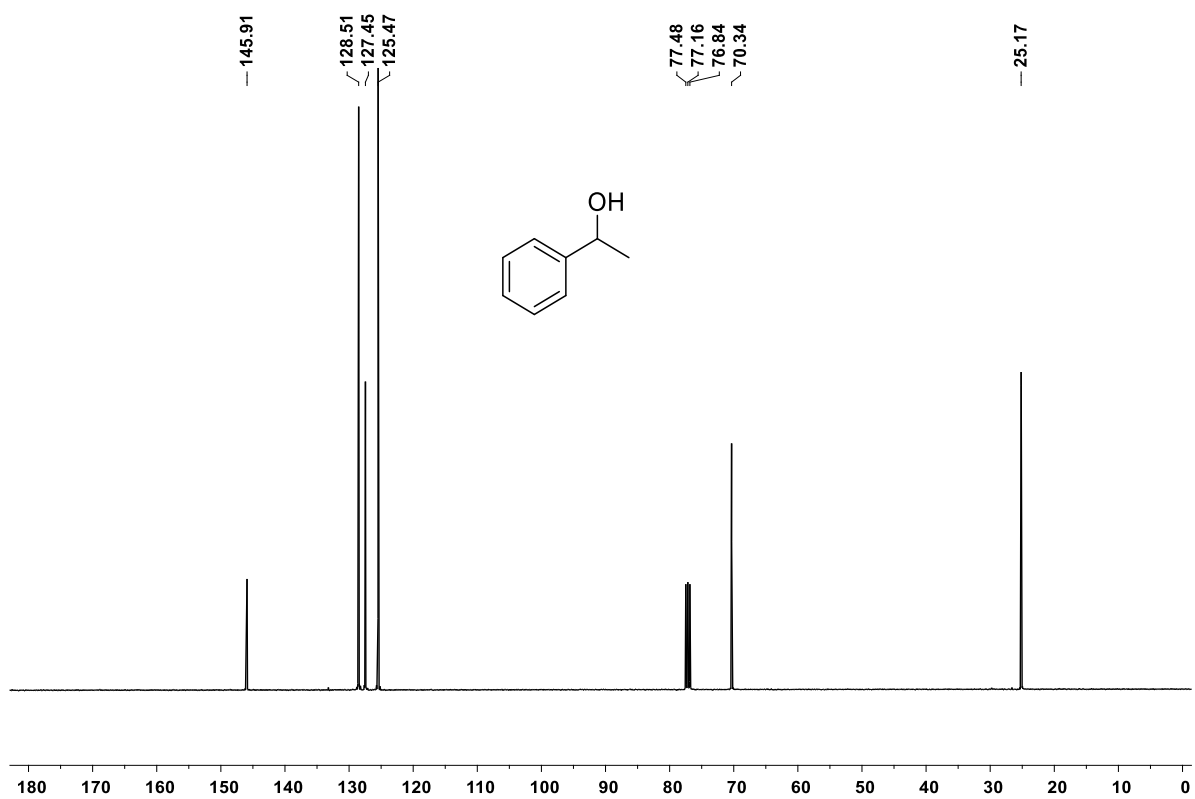


**Figure 2.5.6.**  $^{13}\text{C}\{^1\text{H}\}$  NMR (101 MHz) spectrum of 1-Phenylethan-1-ol ( $\text{B}_1$ ) in  $\text{CDCl}_3$  at r.t.

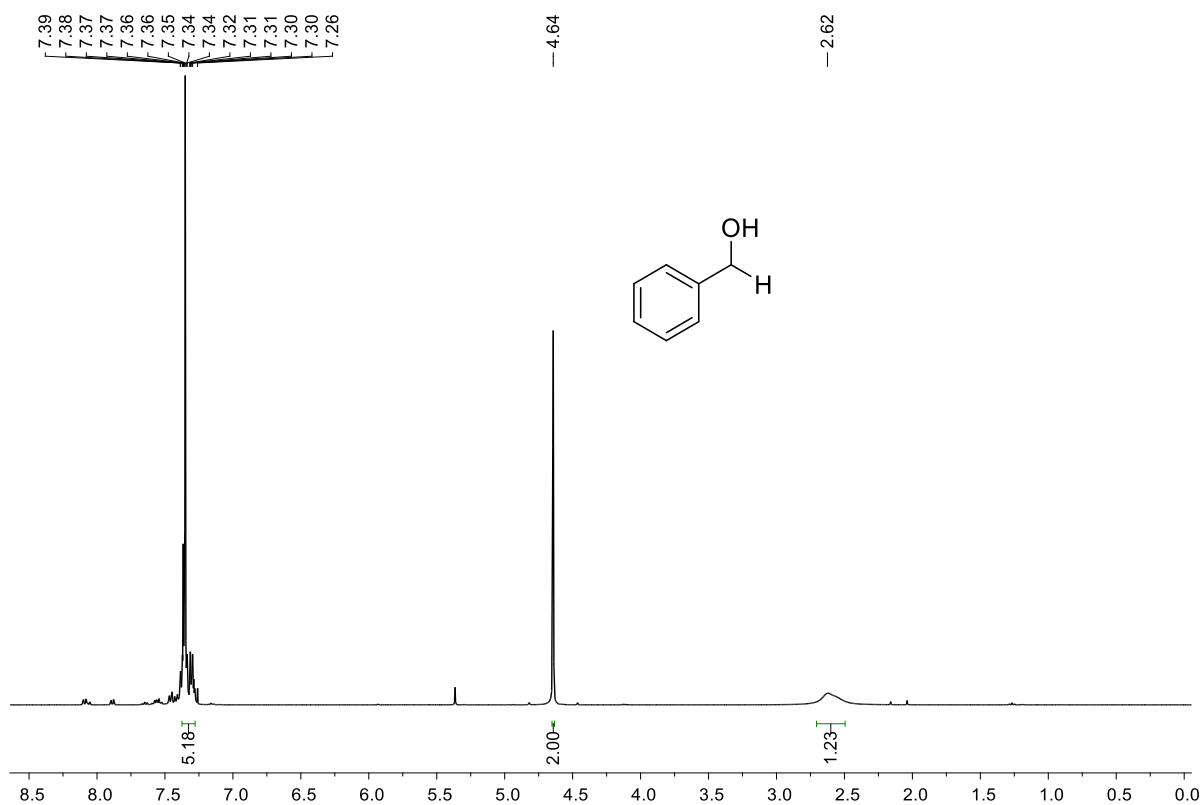


**Figure 2.5.7.**  $^1\text{H}$  NMR (400 MHz) spectrum of Phenylmethanol ( $\text{C}_1$ ) in  $\text{CDCl}_3$  at r.t.

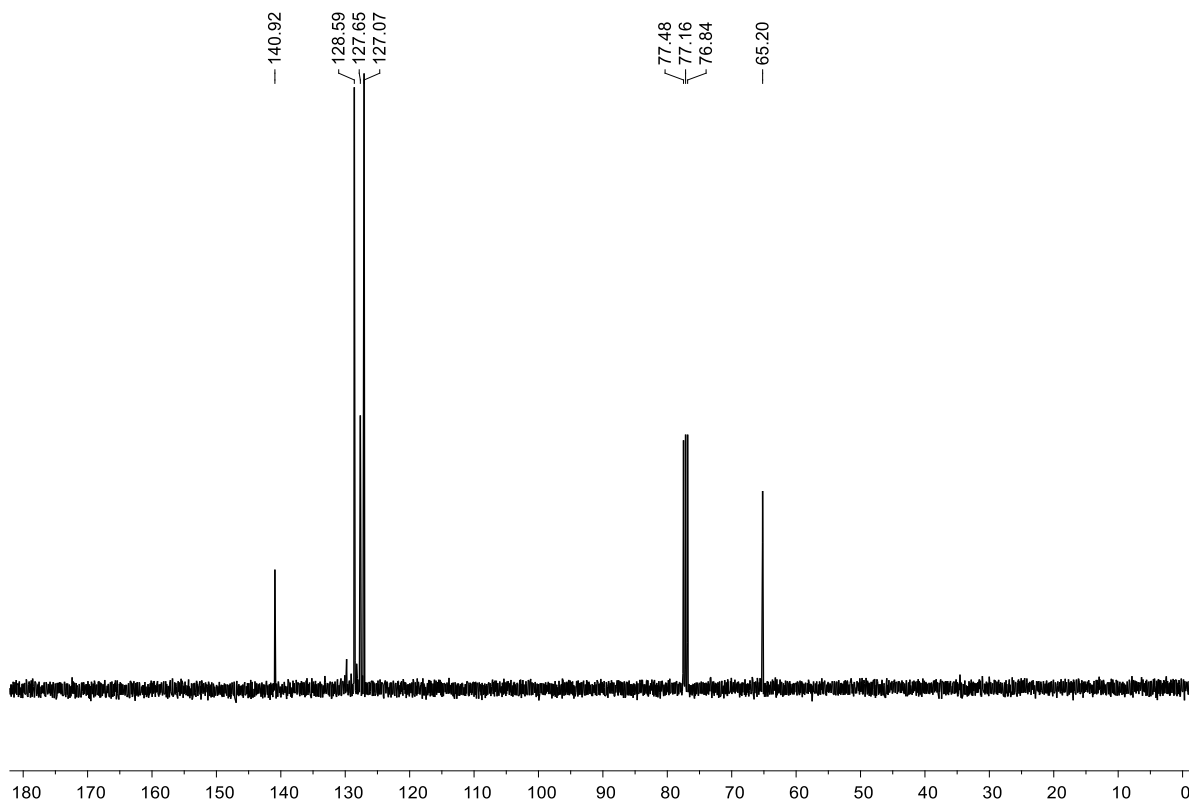


**Figure 2.5.8.**  $^{13}\text{C}\{^1\text{H}\}$  NMR (101 MHz) spectrum of Phenylmethanol ( $\text{C}_1$ ) in  $\text{CDCl}_3$  at r.t.

## 2.6 REFERENCES:

- (6) Cerveny, L., Ed. *Catalytic Hydrogenation*; Elsevier: Amsterdam, 1986.
- (7) de Vries, J. G., Elsevier, C. J., Eds. *The Handbook of Homogeneous Hydrogenation*; Wiley-VCH: Weinheim, 2007.
- (8) Andersson, P. G., Munslow, I. J., Eds. *Modern Reduction Methods*; Wiley-VCH Verlag GmbH & Co. KGaA: Weinheim, 2008.
- (9) Magano, J.; Dunetz, J. R. Large-Scale Carbonyl Reductions in the Pharmaceutical Industry. *Org. Process Dev.* **2012**, *16*, 1156–1184.
- (10) Robertson, A.; Matsumoto, T.; Ogo, S. The development of aqueous transfer hydrogenation catalysts. *Dalton Trans.* **2011**, *40*, 10304–10310.
- (11) Wang, D.; Astruc, D. The Gold-en Age of Transfer Hydrogenation. *Chem. Rev.* **2015**, *115*, 6621–6686.
- (12) Romero, A. H. Reduction of Nitroarenes via Catalytic Transfer Hydrogenation Using Formic Acid as Hydrogen Source: A Comprehensive Review. *ChemistrySelect* **2020**, *5*, 13054–13075.
- (13) Yang, P.; Xu, H.; Zhou, J. Nickel-Catalyzed Asymmetric Transfer Hydrogenation of Olefins for the Synthesis of  $\alpha$ - and  $\beta$ -Amino Acids. *Angew. Chem. Int. Ed.* **2014**, *53*, 12210–12213.
- (14) Zieliński, G. K.; Samojłowicz, C.; Wdowik, T.; Grela, K. In tandem or alone: a remarkably selective transfer hydrogenation of alkenes catalyzed by ruthenium olefin metathesis catalysts. *Org. Biomol. Chem.* **2015**, *13*, 2684–2688.

- (15) Nie, R.; Peng, X.; Zhang, H.; Yu, X.; Lu, X.; Zhou, D.; Xia, Q. Transfer hydrogenation of bio-fuel with formic acid over biomass-derived N-doped carbon supported acid-resistant Pd catalyst. *Catal. Sci. Technol.* **2017**, *7*, 627–634.
- (16) Jiang, L.; Zhou, P.; Zhang, Z.; Jin, S.; Chi, Q. Synthesis of Secondary Amines from One-Pot Reductive Amination with Formic Acid as the Hydrogen Donor over an Acid-Resistant Cobalt. *Catalyst. Ind. Eng. Chem. Res.* **2017**, *56*, 12556–12565.
- (17) Wang, S.; Huang, H.; Dorcet, V.; Roisnel, T.; Bruneau, C.; Fischmeister, C. Efficient Iridium Catalysts for Base-Free Hydrogenation of Levulinic Acid. *Organometallics* **2017**, *36*, 3152–3162.
- (18) Verley, A. Sur l'échange de groupements fonctionnels entre deux molécules. Passage de la fonction alcool à la fonction aldéhyde et inversement. *Bull. Soc. Chim. Fr.* **1925**, *37*, 537–542.
- (19) Meerwein, H.; Schmidt, R. Ein neues Verfahren zur Reduktion von Aldehyden und Ketonen. *Liebigs Ann. Chem.* **1925**, *444*, 221–238.
- (20) Bigler, R.; Huber, R.; Mezzetti, A. Highly Enantioselective Transfer Hydrogenation of Ketones with Chiral (NH)<sub>2</sub>P<sub>2</sub> Macrocyclic Iron(II) Complexes. *Angew. Chem. Int. Ed.* **2015**, *54*, 5171–5174.
- (21) Bigler, R.; Huber, R.; Stöckli, M.; Mezzetti, A. Iron(II)/(NH)<sub>2</sub>P<sub>2</sub> Macrocycles: Modular, Highly Enantioselective Transfer Hydrogenation Catalysts. *ACS Catalysis* **2016**, *6*, 6455–6464.
- (22) Funk, T. W.; Mahoney, A. R.; Sponenburg, R. A.; Zimmerman, K. P.; Kim, D. K., Harrison, E. E. Synthesis and Catalytic Activity of (3,4-

Diphenylcyclopentadienone)Iron Tricarbonyl Compounds in Transfer Hydrogenations and Dehydrogenations. *Organometallics* **2018**, *37*, 1133–1140.

- (23) Xue, Q.; Wu, R.; Wang, D.; Zhu, M.; Zuo, W. The Stabilization Effect of  $\pi$ -backdonation Ligands on the Catalytic Reactivities of Amido-ene (amido) Iron Catalysts in the Asymmetric Transfer Hydrogenation of Ketones. *Eur. J. Inorg. Chem.* **2020**, *32*, 3103–3110.
- (24) Huo, S.; Wang, Q.; Zuo, W. An Iron Variant of the Noyori Hydrogenation Catalyst for the Asymmetric Transfer Hydrogenation of Ketones. *Dalton Trans.* **2020**, *49*, 7959–7967.
- (25) Lopes, R.; Raya-Barón, Á.; Robalo, M. P.; Vinagreiro, C.; Barroso, S.; Romão, M. J.; Fernández, I.; Pereira, M. M.; Royo, B. Donor Functionalized Iron(II) N-Heterocyclic Carbene Complexes in Transfer Hydrogenation Reactions. *Eur. J. Inorg. Chem.* <https://doi.org/10.1002/ejic.202000868>.
- (26) Chang, Y.-H.; Leu, W.-J.; Datta, A.; Hsiao, H.-C.; Lin, C.-H.; Guh, J.-H.; Huang, J.-H. Catalytic transfer hydrogenation and anticancer activity of arene–ruthenium compounds incorporating bi-dentate precursors. *Dalton Trans.* **2015**, *44*, 16107–16118.
- (27) Dubey, A., Khaskin, E. Catalytic Ester Metathesis Reaction and Its Application to Transfer Hydrogenation of Esters. *ACS Catal.* **2016**, *6*, 3998–4002.
- (28) Paul, B.; Chakrabarti, K.; Kundu, S. Optimum bifunctionality in a 2-(2-pyridyl-2-ol)-1, 10-phenanthroline based ruthenium complex for transfer hydrogenation of ketones and nitriles: impact of the number of 2-hydroxypyridine fragments. *Dalton Trans.* **2016**, *45*, 11162–11171.

- (29) Barrios-Rivera, J.; Xu, Y.; Wills, M. Probing the Effects of Heterocyclic Functionality in [(Benzene)Ru(TsDPENR)Cl] Catalysts for Asymmetric Transfer Hydrogenation. *Org. Lett.* **2019**, *21*, 7223–7227.
- (30) Figliolia, R.; Cavigli, P.; Comuzzi, C.; Zotto, A. D.; Lovison, D.; Strazzolini, P.; Susmel, S.; Zuccaccia, D.; Ballico, M.; Baratta, W. CNN pincer ruthenium complexes for efficient transfer hydrogenation of biomass-derived carbonyl compounds. *Dalton Trans.* **2020**, *49*, 453–465.
- (31) Melle, P.; Thiede, J.; Hey, D. A.; Albrecht, M. Highly Efficient Transfer Hydrogenation Catalysis with Tailored Pyridylidene Amide Pincer Ruthenium Complexes. *Chem. Eur. J.* **2020**, *26*, 13226–13234.
- (32) Park, B. Y.; Luong, T.; Sato, H.; Krische, M. J. Osmium (0)-Catalyzed C–C Coupling of Ethylene and  $\alpha$ -Olefins with Diols, Ketols, or Hydroxy Esters via Transfer Hydrogenation. *J. Org. Chem.* **2016**, *81*, 8585–8594.
- (33) Gichumbi, J. M.; Omondi, B.; Friedrich, H. B. Half-Sandwich Osmium (II) Complexes with Bidentate N, N-Chelating Ligands and Their Use in the Transfer Hydrogenation of Ketones. *Eur. J. Inorg. Chem.* **2017**, 915–924.
- (34) Biswas, S.; Roy, P. Jana, S. Mondal, T. K. Osmium-hydride-carbonyl complex with thioether containing Schiff base ligand: Synthesis, crystal structure, electrochemistry and catalytic transfer hydrogenation. *J. of Organomet. Chem.* **2017**, *846*, 201–207.
- (35) de Julián, E.; Fernández, N.; Díez, J.; Lastra, E.; Gamasa, M. P. Osmium(II)/R-pybox vs ruthenium(II)/R-pybox complexes in the catalytic asymmetric transfer hydrogenation of arylketones. *Mol. Catal.* **2018**, *456*, 75–86.

- (36) Wang, W.; Yang, X. Mechanistic insights into asymmetric transfer hydrogenation of pyruvic acid catalysed by chiral osmium complexes with formic acid assisted proton transfer. *Chem. Commun.* **2019**, *55*, 9633–9636.
- (37) Zhang, G.; Yin, Z.; Tan, J. Cobalt (II)-catalysed transfer hydrogenation of olefins. *RSC Adv.* **2016**, *6*, 22419–22423.
- (38) Chen, F.; Sahoo, B.; Kreyenschulte, C.; Lund, H.; Zeng, M.; He, L.; Junge, K.; Beller, M. Selective cobalt nanoparticles for catalytic transfer hydrogenation of N-heteroarenes. *Chem. Sci.* **2017**, *8*, 6239–6246.
- (39) Jiang, B.-L.; Ma, S.-S.; Wang, M.-L.; Liu, D.-S.; Xu, B.-H.; Zhang, S.-J. Cobalt-Catalyzed Chemoselective Transfer Hydrogenation of C=C and C=O Bonds with Alkanols. *ChemCatChem* **2017**, *11*, 1701–1706.
- (40) Koto, Y.; Shibahara, F.; Murai, T. 1-Substituted-imidazo[1,5-a]pyridin-3-ylidenes as Highly Efficient Ligands for Rh- and Ir-catalyzed Transfer Hydrogenation of Carbonyl Compounds. *Chem. Lett.* **2016**, *45*, 1327–1329.
- (41) Zhang X.; Chen J.; Khan R.; Shen G.; He Z.; Zhou Y.; Fan B. Rhodium-catalyzed transfer hydrogenation of quinoxalines with water as a hydrogen source. *Org. Biomol. Chem.* **2019**, *17*, 10142–10147.
- (42) Wang, F.; Zheng, L.-S.; Lang, Q.-W.; Yin, C.; Wu, T.; Phansavath, P.; Chen, G.-Q.; Ratovelomanana-Vidal, V.; Zhang, X. Rh(III)-Catalyzed diastereoselective transfer hydrogenation: an efficient entry to key intermediates of HIV protease inhibitors. *Chem. Commun.* **2020**, *56*, 3119–3122.

- (43) Lin, X.; Wang, Y.; Hu, Y.; Zhu, W.; Dou, X. Diboron-Mediated Rhodium-Catalysed Transfer Hydrogenation of Alkenes and Carbonyls. *Eur. J. Org. Chem.* **2020**, 1046–1049.
- (44) Chen, S.-j.; Lu, G.-p.; Cai, C. A base-controlled chemoselective transfer hydrogenation of  $\alpha$ ,  $\beta$ -unsaturated ketones catalyzed by  $[\text{IrCp}^*\text{Cl}_2]_2$  with 2-propanol. *RSC Adv.* **2015**, 5, 13208–13211.
- (45) Xu, C.; Zhang, L.; Dong, C.; Xu, J.; Pan, Y.; Li, Y.; Zhang, H.; Li, H.; Yu, Z.; Xu, L. Iridium-Catalyzed Transfer Hydrogenation of 1,10-Phenanthrolines using Formic Acid as the Hydrogen Source. *Adv. Synth. Catal.* **2016**, 358, 567–572.
- (46) Wang, R.; Tang, Y.; Xu, M.; Meng, C.; Li, F. Transfer Hydrogenation of Aldehydes and Ketones with Isopropanol under Neutral Conditions Catalyzed by a Metal–Ligand Bifunctional Catalyst  $[\text{Cp}^*\text{Ir}(2,2'\text{-bpyO})(\text{H}_2\text{O})]$ . *J. Org. Chem.* **2018**, 83, 2274–2281.
- (47) Zhang, D.; Iwai, T.; Sawamura, M. Iridium-Catalyzed Alkene-Selective Transfer Hydrogenation with 1,4-Dioxane as Hydrogen Donor. *Org. Lett.* **2019**, 21, 5867–5872.
- (48) Murayama, H.; Heike, Y.; Higashida, K.; Shimizu, Y.; Yodsinn, N.; Wongnongwa, Y.; Jungsuttiwong, S.; Mori, S.; Sawamura, M. Iridium-Catalyzed Enantioselective Transfer Hydrogenation of Ketones Controlled by Alcohol Hydrogen-Bonding and  $\text{sp}^3\text{-C-H}$  Noncovalent Interactions. *Adv. Synth. Catal.* **2020**, 362, 4655–4661.
- (49) Xu, H.; Yang, P.; Chuanprasit, P.; Hirao, H.; Zhou, J. Nickel-Catalyzed Asymmetric Transfer Hydrogenation of Hydrazones and Other Ketimines. *Angew. Chem. Int. Ed.* **2015**, 127, 5201–5205.

- (50) Sabater, S.; Page, M. J.; Mahon, M. F.; Whittlesey, M. K. Stoichiometric and Catalytic Reactivity of Ni(6-Mes)(PPh<sub>3</sub>)<sub>2</sub>. *Organometallics* **2017**, *36*, 1776–1783.
- (51) Garduno, J. A.; Garcia, J. J. Nickel-Catalyzed Transfer Hydrogenation of Benzonitriles with 2-Propanol and 1,4-Butanediol as the Hydrogen Source. *ACS Omega* **2017**, *2*, 2337–2343.
- (52) Hu, X.; Wang, G.; Qin, C.; Xie, X.; Zhang, C.; Xu, W.; Liu, Y. Ligandless nickel-catalyzed transfer hydrogenation of alkenes and alkynes using water as the hydrogen donor. *Org. Chem. Front.* **2019**, *6*, 2619–2623.
- (53) Segizbayev, M.; Öztopçu, Ö.; Hayrapetyan, D.; Shakhman, D.; Lyssenko, K. A.; Khalimon, A. Y. Transfer hydrogenation of aldehydes and ketones catalyzed using an aminophosphinite POCN<sup>H</sup> pincer complex of Ni(II). *Dalton Trans.* **2020**, *49*, 11950–11957.
- (54) Cummings, S. P.; Le, T.-N.; Fernandez, G. E.; Quiambao, L. G.; Stokes, B. J. Tetrahydroxydiboron-Mediated Palladium-Catalyzed Transfer Hydrogenation and Deuteration of Alkenes and Alkynes Using Water as the Stoichiometric H or D Atom Donor. *J. Am. Chem. Soc.* **2016**, *138*, 6107–6110.
- (55) Xuan, Q.; Song, Q. Diboron-Assisted Palladium-Catalyzed Transfer Hydrogenation of N-Heteroaromatics with Water as Hydrogen Donor and Solvent. *Org. Lett.* **2016**, *18*, 4250–4253.
- (56) Cao, B.; Wei, Y.; Shi, M. Palladium-catalyzed intramolecular transfer hydrogenation & cycloaddition of *p*-quinaminedethered alkylidenecyclopropanes to synthesize perhydroindole scaffolds. *Chem. Commun.* **2018**, *54*, 14085–14088.

- (57) Zhao, C.; Zhang, Z., Liu, Y.; Shang, N.; Wang, H.-J. ;Wang, C., Gao, Y. Palladium Nanoparticles Anchored on Sustainable Chitin for Phenol Hydrogenation to Cyclohexanone. *ACS Sustainable Chem. Eng.* **2020**, *8*, 12304–12312.
- (58) Bhattacharjee, R.; Datta, A. Supported Sub-Nanometer Gold Cluster Catalyzed Transfer Hydrogenation of Aldehydes to Alcohols. *J. Phys. Chem. C* **2016**, *120*, 24449–24456.
- (59) Vysakh, A. B; Shebin, K. J.; Jain, R.; Sumanta, P.; Gopinath, C. S.; Vinod, C. P. Surfactant free synthesis of Au@Ni core-shell nanochains in aqueous medium as efficient transfer hydrogenation catalyst. *Appl. Catal. A-Gen.* **2019**, *575*, 93–100.
- (60) Weingart, P.; Thiel, W. R. Applying Le Chatelier's Principle for a Highly Efficient Catalytic Transfer Hydrogenation with Ethanol as the Hydrogen Source. *ChemCatChem* **2018**, *10*, 4844–4848.
- (61) Kuwahara, T.; Fukuyama, T.; Ryu, I. RuHCl(CO)(PPh<sub>3</sub>)<sub>3</sub>-Catalyzed  $\alpha$ -Alkylation of Ketones with Primary Alcohols. *Org. Lett.* **2012**, *14*, 4703–4705.
- (62) Kovalenko, O. O.; Lundberg, H.; Hübner, D.; Adolfsson, H. Tandem  $\alpha$ -Alkylation/Asymmetric Transfer Hydrogenation of Acetophenones with Primary Alcohols. *Eur. J. Org. Chem.* **2014**, *30*, 6639–6642.
- (63) Chan, L. K. M.; Poole, D. L.; Shen, D.; Healy, M. P.; Donohoe, T. J. Rhodium-Catalyzed Ketone Methylation Using Methanol Under Mild Conditions: Formation of  $\alpha$ -Branched Products. *Angew.Chem. Int. Ed.* **2014**, *53*, 761–765.

- (64) Xiao, H.; Wang, G.; Krische, M. J. Regioselective Hydrohydroxyalkylation of Styrene with Primary Alcohols or Aldehydes via Ruthenium-Catalyzed C–C Bond Forming Transfer Hydrogenation. *Angew. Chem. Int. Ed.* **2016**, *55*, 16119–16122.
- (65) Castellanos-Blanco, N.; Flores-Alamo, M.; García, J. J. Nickel Catalyzed Alkylation and Transfer Hydrogenation of  $\alpha,\beta$ -Unsaturated Enones with Methanol. *Organometallics* **2012**, *31*, 680–686.
- (66) Zhang, J.; Chen, J. Selective Transfer Hydrogenation of Bi-omass Based Furfural and 5-Hydroxymethylfurfural over Hydrotalcite Derived Copper Catalysts Using Methanol as a Hydrogen Donor. *ACS Sustainable Chem. Eng.* **2017**, *5*, 5982–5993.
- (67) Aboo, A. H.; Bennett, E. L.; Deeprose, M.; Robertson, C. M.; Iggo, J. A.; Xiao, J. Methanol as hydrogen source: Transfer Hydrogenation of Aromatic Aldehydes with a Rhodacycle. *Chem. Commun.* **2018**, *54*, 11805–11808.
- (68) Campos, J.; Sharninghausen, L. S.; Manas, M. G.; Crabtree, R. H. Methanol Dehydrogenation by Iridium N-Heterocyclic Carbene Complexes. *Inorg. Chem.* **2015**, *54*, 5079–5084.
- (69) Wang, R.; Han, X.; Xu, J.; Liu, P. Li, F. Transfer Hydrogenation of Ketones and Imines with Methanol under Base-Free Conditions Catalyzed by an Anionic Metal-Ligand Bifunctional Iridium Catalyst. *J. Org. Chem.* **2020**, *85*, 2242–2249.
- (70) Zweifel, T.; Naubron, J.-V.; Büttner, T.; Ott, T.; Grützmacher, H. Ethanol as Hydrogen Donor: Highly Efficient Transfer Hydrogenations with Rhodium(I) Amides. *Angew. Chem. Int. Ed.* **2008**, *47*, 3245–3249.

- (71) Castellanos-Blanco, N.; Arévalo, A.; García, J. J. Nickel-catalyzed transfer hydrogenation of ketones using ethanol as a solvent and a hydrogen donor. *Dalton Trans.* **2016**, *45*, 13604–13614.
- (72) Dubey, A.; Khaskin, E. Catalytic Ester Metathesis Reaction and Its Application to Transfer Hydrogenation of Esters. *ACS Catal.* **2016**, *6*, 3998–4002.
- (73) Weingart, P.; Thiel, W. R. Applying Le Chatelier's Principle for a Highly Efficient Catalytic Transfer Hydrogenation with Ethanol as the Hydrogen Source. *ChemCatChem* **2018**, *10*, 4844–4848.
- (74) Wang, Y.; Huang, Z.; Leng, X.; Zhu, H.; Liu, G.; Huang, Z. Transfer Hydrogenation of Alkenes Using Ethanol Catalyzed by a NCP Pincer Iridium Complex: Scope and Mechanism. *J. Am. Chem. Soc.* **2018**, *140*, 4417–4429.
- (75) He, Y.-M.; Fan, Q.-H. Phosphine-free chiral metal catalysts for highly effective asymmetric catalytic hydrogenation. *Org. Biomol. Chem.* **2010**, *8*, 2497–2504.
- (76) Zhang, C.; Liu, J.; Xia, C. Aryl-palladium-NHC complex: efficient phosphine-free catalyst precursors for the carbonylation of aryl iodides with amines or alkynes. *Org. Biomol. Chem.* **2014**, *12*, 9702–9706.
- (77) Puylaert, P.; Dell'Acqua, A.; Ouahabi, F. E.; Spannenberg, A.; Roisnel, T.; Lefort, L.; Hinze, S.; Tin, S.; de Vries, J. G. Phosphine-free cobalt catalyst precursors for the selective hydrogenation of olefins. *Catal. Sci. Technol.* **2019**, *9*, 61–64.
- (78) Guo, B.; Yu, T.-Q.; Li, H.-X.; Zhang, S.-Q.; Braunstein, P.; Young, D. J.; Li, H.-Y.; Lang, J.-P. Phosphine Ligand-Free Ruthenium Complexes as Efficient Catalysts for

the Syn-thesis of Quinolines and Pyridines by Acceptorless Dehydrogenative Coupling Reactions. *ChemCatChem* **2019**, *11*, 2500–2510.

(79) Wu, X.-J.; Wang, H.-J.; Yang, Z.-Q.; Tang, X.-S.; Yuan, Y.; Su, W.; Chen, C.; Verpoort, F. Efficient and phosphine-free bidentate N-heterocyclic carbene/ruthenium catalytic systems for the dehydrogenative amidation of alcohols and amines. *Org. Chem. Front.* **2019**, *6*, 563–570.

(80) Jana, A.; Das, K.; Kundu, A.; Thorve, P. R.; Adhikari, D.; Maji, B. A Phosphine-Free Manganese Catalyst Enables Stereoselective Synthesis of (1 + n)-Membered Cycloalkanes from Methyl Ketones and 1,n-Diols. *ACS Catal.* **2020**, *10*, 2615–2626.

(81) Johnson, C.; Albrecht, M. Piano-stool N-heterocyclic carbene iron complexes: Synthesis, reactivity and catalytic applications. *Coord. Chem. Rev.* **2017**, *352*, 1-14.

(82) Vivancos, Á.; Segarra, C.; Albrecht, M. Mesoionic and Related Less Heteroatom-Stabilized N-Heterocyclic Carbene Complexes: Synthesis, Catalysis, and Other Applications. *Chem. Rev.* **2018**, *118*, 9493–9586.

(83) Smith, C. A.; Narouz, M. R.; Lummis, P. A.; Singh, I. Nazemi, A.; Li, C.-H.; Crudden, C. M. N-Heterocyclic Carbenes in Materials Chemistry. *Chem. Rev.* **2019**, *119*, 4986–5056.

(84) Sau, S. C.; Hota, P. K.; Mandal, S. K.; Soleilhavoup, M.; Bertrand, G. Stable abnormal N-heterocyclic carbenes and their applications. *Chem. Soc. Rev.* **2020**, *49*, 1233–1252.

- (85) Budagumpi, S.; Keri, R. S.; Achar, G.; Brinda, K. N. Coinage Metal Complexes of Chiral N-Heterocyclic Carbene Ligands: Syntheses and Applications in Asymmetric Catalysis. *Adv. Synth. Catal.* **2020**, *362*, 970–997.
- (86) Rufino-Felipe, E.; Valdes, H.; German-Acacio, J. M.; Reyes-Marquez, V.; Morales-Morales, D. Fluorinated N-Heterocyclic carbene complexes. Applications in catalysis. *J. Organomet. Chem.* **2020**, *921*, 121364.
- (87) Ohmiya, H. N-Heterocyclic Carbene-Based Catalysis Enabling Cross-Coupling Reactions. *ACS Catal.* **2020**, *10*, 6862–6869.
- (88) Hoveyda, A. H.; Zhou, Y.; Shi, Y.; Brown, M. K.; Wu, H.; Torker, S. Sulfonate N-Heterocyclic Carbene–Copper Complexes: Uniquely Effective Catalysts for Enantioselective Synthesis of C–C, C–B, C–H, and C–Si Bonds. *Angew. Chem. Int. Ed.* **2020**, *59*, 21304–21359.
- (89) Schuster, O.; Yang, L.; Raubenheimer, H. G.; Albrecht, M. Beyond Conventional N-Heterocyclic Carbenes: Abnormal, Remote, and Other Classes of NHC Ligands with Reduced Heteroatom Stabilization. *Chem. Rev.* **2009**, *109*, 3445–3478.
- (90) Krueger, A.; Albrecht, M. Abnormal N-heterocyclic Carbenes: More than Just Exceptionally Strong Donor Ligands. *Aust. J. Chem.* **2011**, *64*, 1113–1117.
- (91) Crowley, J. D.; Lee, A.-L.; Kilpin, K. J. 1,3,4-Trisubstituted-1,2,3-triazol-5-ylidene click carbene ligands. Synthesis, catalysis, and self-assembly. *Aust. J. Chem.* **2011**, *64*, 1118–1132.
- (92) Crabtree, R. H. Abnormal, mesoionic and remote N-heterocyclic carbene complexes. *Coord. Chem. Rev.* **2013**, *257*, 755–766.

- (93) Albrecht, M. Normal and abnormal N-heterocyclic carbene ligands: similarities and differences of mesoionic C-donor complexes. *Adv. Organomet. Chem.* **2014**, *62*, 111–158.
- (94) Sau, S. C.; Hota, P. K.; Mandal, S. K.; Soleilhavoup, M.; Bertrand, G. Stable abnormal N-heterocyclic carbenes and their applications. *Chem. Soc. Rev.* **2020**, *49*, 1233–1252.
- (95) Ghosh, D.; Rhodes, S.; Hawkins, K.; Winder, D.; Atkinson, A.; Ming, W.; Padgett, C.; Orvis, J.; Aiken, K.; Landge, S. A simple and effective 1, 2, 3-triazole based “turn-on” fluorescence sensor for the detection of anions. *New J. Chem.* **2015**, *39*, 295–303.
- (96) Bagh, B.; McKinty, A. M.; Lough, A. J.; Stephan, D. W. 1, 2, 3-Triazolylidene ruthenium (II) ( $\eta^6$ -arene) complexes: synthesis, metallation and reactivity. *Dalton Trans.* **2014**, *43*, 12842–12850.
- (97) Riedl, C. A.; Flocke, L. S.; Hejl, M.; Roller, A.; Klose, M. H. M.; Jakupec, M. A.; Kandioller, W.; Keppler, B. K. Introducing the 4-Phenyl-1,2,3-Triazole Moiety as a Versatile Scaffold for the Development of Cytotoxic Ruthenium(II) and Osmium(II) Arene Cyclometalates. *Inorg. Chem.* **2017**, *56*, 528–541.
- (98) Saleem, F.; Rao, G. K.; Kumar, A.; Mukherjee, G.; Singh, A. K. Half-Sandwich Ruthenium(II) Complexes of Click Generated 1,2,3-Triazole Based Organosulfur/-selenium Ligands: Structural and Donor Site Dependent Catalytic Oxidation and Transfer Hydrogenation Aspects. *Organometallics* **2013**, *32*, 3595–3603.
- (99) Lo, W. K. C.; Huff, G. S.; Cubanski, J. R.; Kennedy, A. D. W.; McAdam, C. J.; McMorran, D. A.; Gordon, K. C.; Crowley, J. D. Comparison of Inverse and Regular

2-Pyridyl-1,2,3-triazole “Click” Complexes: Structures, Stability, Electrochemical, and Photophysical Properties. *Inorg. Chem.* **2015**, *54*, 1572–1587.

- (100) Riedl, C. A.; Hejl, M.; Klose, M. H. M.; Roller, A.; Jakupec, M. A.; Kandioller, W.; Keppler, B. K. N- and S-donor leaving groups in triazole-based ruthena(II)cycles: potent anticancer activity, selective activation, and mode of action studies. *Dalton Trans.* **2018**, *47*, 4625–4638.
- (101) Wu, Q.; Pan, L.; Du, G.; Zhang, C.; Wang, D. Preparation of pyridyltriazole ruthenium complexes as effective catalysts for the selective alkylation and one-pot C–H hydroxylation of 2-oxindole with alcohols and mechanism exploration. *Org. Chem. Front.* **2018**, *5*, 2668–2675.
- (102) Rono, C. K.; Chu, W. K.; Darkwa, J.; Meyer, D.; Makhubela, B. C. E. Triazolyl Ru<sup>II</sup>, Rh<sup>III</sup>, Os<sup>II</sup>, and Ir<sup>III</sup> Complexes as Potential Anticancer Agents: Synthesis, Structure Elucidation, Cytotoxicity, and DNA Model Interaction Studies. *Organometallics* **2019**, *38*, 3197–3211.
- (103) Riedl, C. A.; Hejl, M.; Klose, M. H. M.; Roller, A.; Jakupec, M. A.; Kandioller, W.; Keppler, B. K. N- and S-donor leaving groups in triazole-based ruthena(II)cycles: potent anticancer activity, selective activation, and mode of action studies. *Dalton Trans.* **2018**, *47*, 4625–4638
- (104) Wu, Q.; Pan, L.; Du, G.; Zhang, C.; Wang, D. Preparation of pyridyltriazole ruthenium complexes as effective catalysts for the selective alkylation and one-pot C–H hydroxylation of 2-oxindole with alcohols and mechanism exploration. *Org. Chem. Front.* **2018**, *5*, 2668–2675.

- (105) Rono, C. K.; Chu, W. K.; Darkwa, J.; Meyer, D.; Makhubela, B. C. E. Triazolyl RuII, RhIII, OsII, and IrIII Complexes as Potential Anticancer Agents: Synthesis, Structure Elucidation, Cytotoxicity, and DNA Model Interaction Studies. *Organometallics*. **2019**, *38*, 3197–3211.
- (106) Anastas, P.; Eghbali, N. Green Chemistry: Principles and Practice. *Chem. Soc. Rev.* **2010**, *39*, 301–312.
- (107) Sheldon, R. A. Fundamentals of green chemistry: efficiency in reaction design. *Chem. Soc. Rev.* **2012**, *41*, 1437–1451
- (108) Anastas, P.; Warner, J. Green Chemistry: Theory and Practice; Oxford University Press: New York, **2000**.
- (109) Lefferts, L.; Sheldon, R. A. Green Chemistry and Catalysis; Wiley: Weinheim, **2007**.
- (110) Prat, D.; Hayler, J.; Wells, A. A survey of solvent selection guides. *Green Chem.* **2014**, *16*, 4546–4551.
- (111) Prat, D.; Wells, A.; Hayler, J.; Sneddon, H.; McElroy, C. R.; Abou-Shehada, S.; Dunne, P. J. CHEM21 selection guide of classical and less classical-solvents. *Green Chem.* **2016**, *18*, 288–296
- (112) Allen, D. T.; Gathergood, N.; Licence, P.; Subramaniam, B. Expectations for Manuscripts Contributing to the Field of Solvents in ACS Sustainable Chemistry & Engineering. *ACS Sustainable Chem. Eng.* **2020**, *8*, 14627–14629.

- (113) Hii, K. K.; Moores, A.; Pradeep, T.; Sels, B.; Allen, D. T.; Licence, P.; Subramaniam, B. Expectations for Manuscripts on Catalysis in ACS Sustainable Chemistry & Engineering. *ACS Sustainable Chem. Eng.* **2020**, *8*, 4995–4996.
- (114) McElroy, C. R.; Constantinou, A.; Jones, L. C.; Summerton, L.; Clark, J. H. Towards a Holistic Approach to Metrics for the 21st Century Pharmaceutical Industry. *Green Chem.* **2015**, *17*, 3111–3121.
- (115) Allen, D. T.; Carrier, D. J.; Gong, J.; Hwang, B.-J.; Licence, P.; Moores, A.; Pradeep, T.; Sels, B.; Subramaniam, B.; Tam, M. K. C.; Zhang, L.; Williams, R. M. Advancing the Use of Sustainability Metrics in ACS Sustainable Chemistry and Engineering. *ACS Sustainable Chem. Eng.* **2018**, *6*, 1.
- (116) Dreesbeke, M. A.; Du Prez, F. E. Sustainable Synthesis of Renewable Terpenoid-Based (Meth)acrylates Using the CHEM21 Green Metrics Toolkit. *ACS Sustainable Chem. Eng.* **2019**, *7*, 11633–11639
- (117) Prieschl, M.; García-Lacuna, J.; Munday, R.; Leslie, K.; O’Kearney-McMullan, A.; Hone, C. A.; Kappe, C. O. Optimization and sustainability assessment of a continuous flow Ru-catalyzed ester hydrogenation for an important precursor of a  $\beta$ 2-adrenergic receptor agonist. *Green Chem.* **2020**, *22*, 5762–5770.
- (118) Dalidovich, T.; Mishra, K. A.; Shalima, T.; Kudrjasova, M.; Kananovich, D. G.; Aav, R. Mechanochemical Synthesis of Amides with Uronium-Based Coupling Reagents: A Method for Hexaamidation of Biotin[6]uril. *ACS Sustainable Chem. Eng.* **2020**, *8*, 15703–15715.
- (119) Zhu, Z.; Wang, Z.; Jian, Y.; Sun, H.; Zhang, G.; Lynam, J. M.; McElroy, C. R.; Burden, T. J.; Inight, R. L.; Fairlamb, I. J. S.; Zhang, W.; Gao, Z. Pd-Catalysed

carbonylative Suzuki–Miyaura crosscouplings using  $\text{Fe}(\text{CO})_5$  under mild conditions: generation of a highly active, recyclable and scalable ‘Pd–Fe’ nanocatalyst. *Green Chem.* **2021**, *23*, 920–926.

## Chapter 3

### Catalytic Transfer Hydrogenation of Lignocellulosic Biomass Model Compounds Furfural and Vanillin with Ethanol by an Air-stable Iron(II) Complex

#### 3.1 ABSTRACT:

The chemical transformation of biomass for the synthesis of various fine chemicals is the necessity for the sustainable developments in the present age. Various components of lignocellulosic biomass can be chemically reduced to numerous value added products and this field of research has attracted enormous attentions. The scientific community has devoted a significant research interest to develop catalysts for the reduction of cellulose and lignin model compounds furfural and vanillin, respectively. In this context, an iron(II) catalyst (**1**) was readily synthesized by the facile coordination of NNO pincer ligand with  $\text{FeCl}_2 \cdot 4\text{H}_2\text{O}$  salt as precursor. The air-stable complex **4** was utilized for the catalytic transfer hydrogenation of cellulose and lignin model compounds furfural and vanillin, respectively, using ecologically benign but challenging primary alcohol ethanol as the hydrogen source in presence of catalytic amount of base. Secondary alcohol isopropanol was also utilized as the sacrificial hydrogen donor. Complex **4** as a sustainable iron compound was proved to be a very efficient catalyst for the transfer hydrogenation of furfural and vanillin under ambient conditions with both primary and secondary alcohols as hydrogen donors. Under the present catalytic protocol, various other biomass model carbonyl compounds and structurally related aldehydes were effectively reduced to the corresponding alcohols. Kinetic studies for transfer hydrogenation of vanillin with ethanol suggested first order kinetics in catalyst (complex **4**) and zeroth order in substrate vanillin. Based on the experimental evidences (isolation of

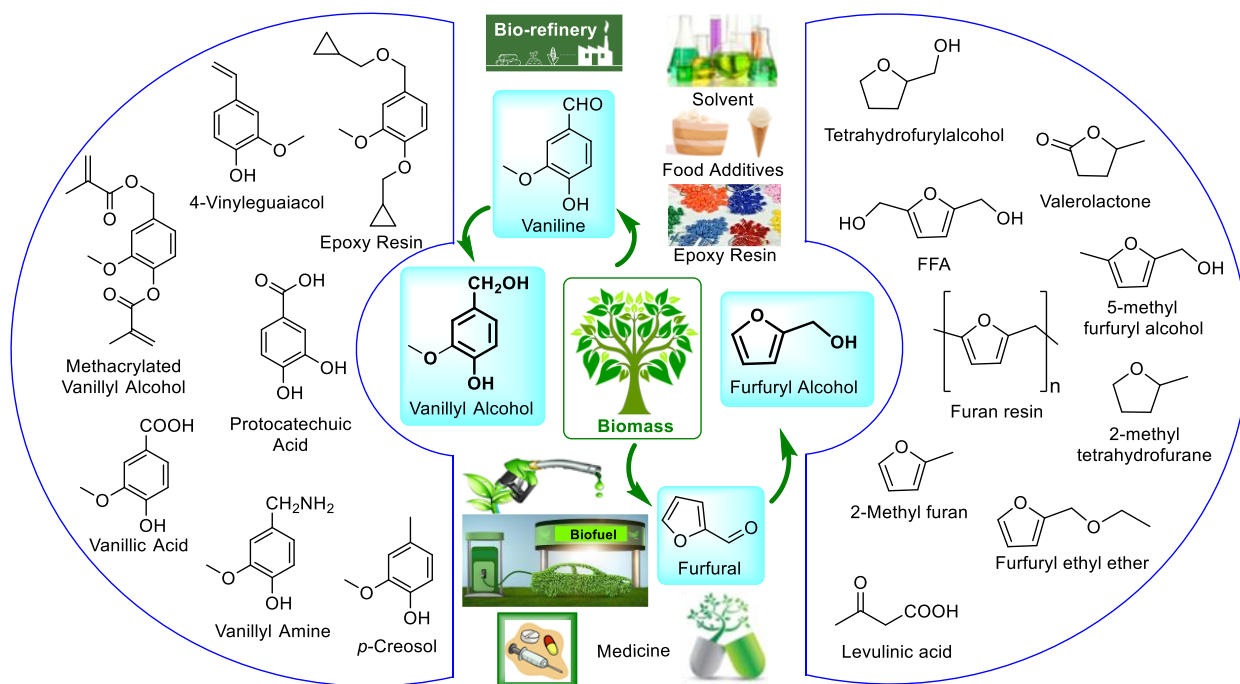
intermediate by stoichiometric reactions and kinetic studies) and published reports, a catalytic cycle for the transfer hydrogenations is proposed which proceed via iron(II)-dialkoxides and alkoxide-hydride intermediates. Finally, CHEM21 green metrics toolkit was utilized to evaluate the sustainable and green credentials of the catalytic protocols.

### **3.2 INTRODUCTION:**

In the present era, fossil fuels are extremely essential in every aspect of modern life as fossil fuels are the most important sources for most important organic chemicals. The huge growth of global population, enhancement of living standards and resultant ever-growing demand for materials will certainly create shortage of petro-based resources which have limited reserves and are shrinking day by day. Therefore, it is extremely vital for the humanity to search alternatives to nonrenewable fossil fuels. In addition, increasing concerns on global warming and related global climate change demand a serious reduction of the use of fossil fuel. Hence, the effective use of sustainable biomass feedstock presents an indispensable opportunity and the importance of bio-refineries is growing significantly.<sup>1, 2</sup> In present age, it is extremely vital to transform renewable biomass into effective biofuels and varieties of valuable fine chemicals.<sup>3-5</sup> The chemical conversions of biomass into useful chemicals is ever expanding, however, challenging field of research.<sup>6-8</sup> Every year the production of biomass worldwide is near about  $1.7 \times 10^{11}$  metric tons out of which a significant amount is lignocellulosic biomass which has three major components (hemicellulose, cellulose and lignin). Lignocellulosic biomass may be established as one of the most promising carbon feedstocks for the sustainable development of biofuel and fine chemicals. Maximum numbers of bio-based fine chemicals are obtained from cellulose and hemicellulose. One of the important examples is furfural, a furan derived heterocyclic aromatic aldehyde which is one of the oldest renewable chemicals besides sugar, ethanol and acetic acid. Approximately  $2.5 \times 10^5$  metric tons of

furfural is produced per anum from biomass and furfural is the direct source of furfuryl alcohol obtained by partial reduction of furfural. Roughly 60 to 70% of total furfural production is converted into furfuryl alcohol with wide applications. One of the major uses of furfuryl alcohol is the syntheses of furan resins which have found wide applications. Furfuryl alcohol is one of the potential biofuels which has been utilized as a fuel in rocketry. In addition, furfuryl alcohol is an essential feedstock for the production of various downstream fine chemicals with wide applications in chemical industries such as food additives, solvents, fuels and pharmaceuticals (Figure 3.3.2).<sup>9-10</sup> Similar to cellulose and hemicellulose, lignin is also a source of a wide variety of important chemicals and particularly aromatic phenolic compounds are obtained from lignin. Vanillin as a monomeric aldehyde is one of the prominent examples and more than  $3 \times 10^3$  metric tons of vanillin are produced from lignin each year. Vanillyl alcohol is produced from vanillin by biological or chemical reduction of carbonyl functionality. Similar to furfuryl alcohol, vanillyl alcohol is a potential biofuel and it is a source of various downstream fine chemicals (Figure 3.3.2). Furfuryl alcohol is industrially produced by hydrogenation of furfural under high temperature and pressure in presence of noble metal (e.g., Ru,<sup>11-12</sup> Pd<sup>13</sup>, Au<sup>14</sup> and Pt<sup>15-17</sup>) and base metal (e.g., Fe<sup>18</sup>, Co<sup>19-21</sup> and Cu<sup>22-27</sup>) heterogeneous catalysts. Heterogeneous catalysts also dominate the reduction of vanillin to vanillyl alcohol and reactions were performed under harsh conditions.<sup>28-29</sup> In this context, there is a genuine need for the development homogeneous catalytic system that can selectively reduce the aldehyde functionalities in furfural and vanillin to the corresponding alcohols furfuryl alcohol and vanillyl alcohol, respectively, under mild conditions maintaining the green sustainable aspects.

**Figure 3.2.1. Furfural, furfuryl alcohol, vanillin, vanillyl alcohol and important downstream fine chemicals by biomass valorization.**



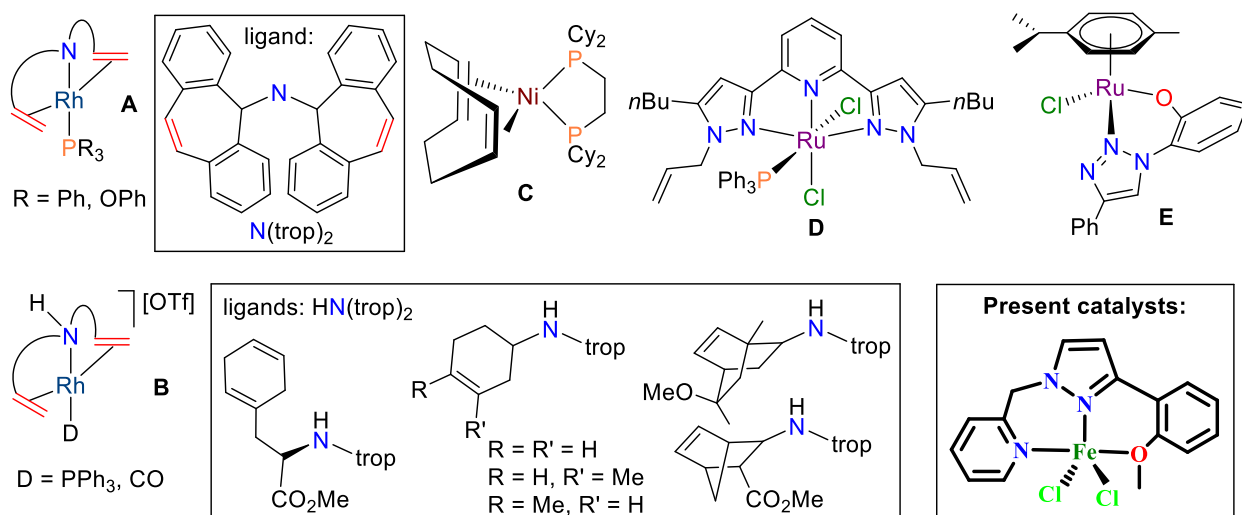
The reduction of carbonyl compounds represents one of the most frequently utilized fundamental transformations in small scale laboratory reactions as well as in large scale industrial syntheses.<sup>30-34</sup> Various hydride reducing reagents such as  $\text{LiBH}_4$ ,  $\text{NaBH}_4$ ,  $\text{LiAlH}_4$  and DIBAL-H are commonly used reducing agents for carbonyl compounds in organic syntheses. However, hydride reducing reagents are often hazardous and require stoichiometric amounts (or excess). In addition, stoichiometric amount of byproducts is formed and the production of a large amount of chemical waste is not acceptable from the environmental point of view.<sup>35</sup> With an ever growing global environmental concern, transition metal-catalyzed hydrogenation of carbonyls with molecular hydrogen presents an effective waste-free process in chemical and pharmaceutical syntheses.<sup>36-37</sup> However, classical hydrogenation requires pressurized hydrogen, a very elaborate instrumental setup and often high temperature for the reduction of carbonyl compounds. On the other hand, transfer hydrogenation presents an easy alternative for the carbonyl reductions and interest is immensely growing in industrial research as well as in academia.<sup>38-41</sup> In recent times, catalytic transfer hydrogenation is becoming the center of active research in this field due to

the non-necessity of hazardous pressurized H<sub>2</sub> gas, extreme conditions and expensive instrumental setup.<sup>42-45</sup> In addition, the frequently used hydrogen donors used in transfer hydrogenations are nicely available, very cheap, easy to handle and the side products can be recycled in most of cases.<sup>46-47</sup> Transfer hydrogenation involves the transfer of proton and hydride to the substrate from a non-H<sub>2</sub> hydrogen source. In 1925 Meerwein and Verley independently reported the first example of transfer hydrogenation (also known as Meerwein–Ponndorf–Verley reaction), in which aluminum alkoxide promoted the reduction of carbonyl compound in the presence of secondary alcohol utilized as a sacrificial hydrogen source.<sup>48-49</sup> Although Meerwein–Ponndorf–Verley reaction has found wide applications in both academic and industrial syntheses, presently the acceptability of this reaction has declined significantly due to the use of large amount of moisture sensitive aluminium alkoxides and undesirable side reactions. As an easy reduction alternative, transfer hydrogenations of carbon-heteroatoms such as carbon-oxygen and carbon-nitrogen multiple bonds have attracted a significant research interest and a wide variety of homogeneous transition metal catalysts based on iron<sup>50-55</sup>, cobalt<sup>56-58</sup>, iridium<sup>59-63</sup>, ruthenium<sup>64-69</sup>, nickel<sup>70-74</sup>, palladium<sup>75-78</sup>, etc. have been developed. Transfer hydrogenation of unsaturated compounds using formic acid and secondary alcohol isopropanol as the solvent and sacrificial hydrogen source is well established and widely used for various synthetic purpose.<sup>79-82</sup> In contrast, transfer hydrogenation using primary alcohols as hydrogen donors is a very rare and challenging reaction because of the unfavorable redox potentials of primary alcohols. DFT calculations also supported the above fact by giving a  $\Delta G$  value of + 4.4 kJ/mol for the transfer hydrogenation of acetophenone with isopropanol in contrast to a  $\Delta G$  value of + 24.2 kJ/mol for the same reaction with ethanol.<sup>83</sup> There is another setback of using primary alcohol in transfer hydrogenations. Isopropanol as secondary alcohol produce acetone as byproduct while ethanol as primary alcohol generates aldehyde which is much reactive as

compared to ketone byproduct and can undergo unwanted side reactions. However, ethanol is an excellent hydrogen carrier with high wt% of hydrogen. In addition, ethanol is available from natural sources such as natural gas, carbon dioxide and renewable biomass, which is very attractive in the context of sustainability. Despite those benefits, ethanol is very rarely utilized in the transfer hydrogenations primarily due to the unfavorable thermodynamics. In 2008, Grützmacher et al. published the first example of transfer hydrogenation utilizing ethanol as the hydrogen donor.<sup>84</sup> Air sensitive rhodium(I)-phosphine complexes with sterically bulky tridentate amido olefin ligand was highly efficient for the transfer hydrogenation of ketones. Soon after the first report, similar rhodium(I)-phosphine or carbonyl complexes with chiral bis(olefin)amine ligands were also used for the asymmetric transfer hydrogenation of ketone in presence of ethanol as a liquid hydrogen carrier.<sup>85</sup> Thereafter, Adlofson et al. reported asymmetric transfer hydrogenation of ketones in ethanol using ruthenium catalyst by combining  $[\text{Ru}(p\text{-cymene})\text{Cl}_2]_2$  and an amino acid hydroxy-amide ligand.<sup>86</sup> Thiel et al. described transfer hydrogenation of aldehydes and ketones with ruthenium(II)-phosphine complex of NNN pincer ligand under constant nitrogen flow to shift the equilibrium to the right. Very recently, we published transfer hydrogenation of aldehydes and ketones in ethanol catalyzed by air-stable ruthenium triazole complexes.<sup>87</sup> In all those five reports, noble metal catalysts were used. In contrast, García et al. described first row transition metal catalyzed transfer hydrogenation of ketones with ethanol at high temperature (130 °C).<sup>88</sup> Nickel(0)-COD complex in presence of various bisphosphine ligands were utilized for the purpose. Utilizing ethanol as the hydrogen source, transfer hydrogenation of other unsaturated substrates are also rarely reported. In 2018, Haung et al. described the transfer hydrogenation of alkene using ethanol as hydrogen source catalyzed by iridium(III)-hydride complex with NCP pincer ligand. In the following year, they reported selective transfer hydrogenation of alkynes to *E*-alkenes in ethanol catalyzed by similar NCP pincer

iridium complexes and sharp color change was utilized as a smart tool to avoid over reduction to alkanes.<sup>89</sup> Transfer hydrogenation of esters with ethanol catalyzed by ruthenium(II)-phosphine complex with tridentate SNS ligand was reported by Khaskin et al.<sup>90</sup> Most of the reports published in recent years used second and third row transition metals for the transfer hydrogenation with ethanol, but examples of first-row transition metal catalysts are very rare. To the best of our knowledge, only one report was published in 2018 by de Vries et al. They used the base metal catalyst PNP pincer iron(II)-hydride complex for the transfer hydrogenation of esters in ethanol.<sup>91</sup> Among all the other transition metals, iron is extremely attractive candidate not only for being cheap, abundant and nontoxic, but also for its unique electronic structure and catalytic activity in comparison with other transition metals.<sup>92</sup> In the context of reduction of furfural and vanillin to furfuryl alcohol and vanillyl alcohol, respectively, majority of the published reports utilized noble metal catalysts under extreme conditions and this field is highly dominated by heterogeneous catalysts.<sup>93-95</sup> This gives us the opportunity to develop a homogeneous catalyst with an earth-abundant, cheap, nontoxic transition metal catalyst and iron is an attractive candidate. Herein, we report a readily available and air-stable iron complex as an effective and sustainable catalyst for the selective transfer hydrogenation of furfural and vanillin to furfuryl alcohol and vanillyl alcohol, respectively, under mild conditions using ethanol and isopropanol as green hydrogen carriers as well as solvents (Figure 3.2.1). We also addressed the green credentials of the catalytic protocols by using CHEM21 green metrics toolkit.<sup>96-102</sup>

**Figure 3.2.2. Transition metal catalysts for the transfer hydrogenation of carbonyls using ethanol as hydrogen source.**



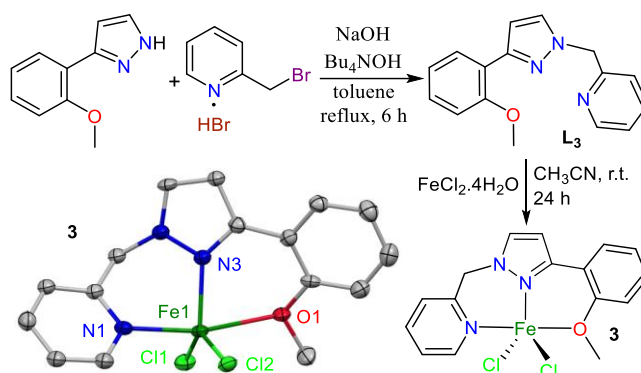
### 3.3 RESULT AND DISCUSSION

Ligand design is crucial in the development of transition metal complexes for homogeneous catalysis. In past two decades, tridentate pincer ligands have been effectively utilized for the developments of a wide variety of transition metal catalysts because of their unique properties.<sup>103</sup> Several groups such as pyridine, imidazole, triazole, ether or thioether moiety may be easily lost as a monodentate ligand; however, they are bound firmly in a well-defined meridional coordination sphere as a part of tridentate pincer ligands. In addition, pincer ligands generally result thermally stable complexes, which is a crucial feature in homogeneous catalysis. However, a large number of pincer ligands has one or multiple phosphine moieties which are air-sensitive.<sup>104-106</sup> Therefore, the development of phosphine-free ligands for the syntheses of air-stable catalysts has attracted a significant attention in recent years.<sup>107-113</sup> In this context, we designed a stable NNO pincer ligand (**L<sub>3</sub>**) which was readily synthesized in excellent yield by reacting 3-(2-methoxyphenyl)-1H-pyrazole with 2-(chloromethyl)pyridine in presence of base (Scheme 3.3.1). Ligand **L<sub>3</sub>** was characterized by mass spectrometry, elemental analysis and <sup>1</sup>H and <sup>13</sup>C NMR spectroscopy. In the <sup>1</sup>H NMR spectrum of **L<sub>3</sub>**, the methoxy and benzyl protons appear as singlets at 3.93 and 5.54 ppm, respectively. The aryl, pyrazolyl and pyridyl resonances were observed in the aromatic range

(6.87-8.68 ppm). Thereafter, facile coordination of tridentate NNO ligand **L3** with  $\text{FeCl}_2 \cdot 4\text{H}_2\text{O}$  resulted in the formation of complex **3** as yellow solid (Scheme 3.3.1). Complex **3** is air-stable and it was characterized by IR spectroscopy, mass and elemental analysis. Complex **3** is NMR inactive suggesting high spin iron(II) species. Mass spectrum of complex **3** shows the peak at 356.0230, which corresponds to  $[\text{M} - \text{Cl}]^+$ . In the IR spectrum of free ligand **L3**, a sharp band was observed at  $1665 \text{ cm}^{-1}$  which is the characteristic peak for the pyrazole stretching vibration of the N=N bond. The pyrazole N=N stretching bands are slightly shifted to  $1680 \text{ cm}^{-1}$  in complex **3**. On the other hand, medium intense bands in the range  $3000$  to  $2800 \text{ cm}^{-1}$  were found in the IR spectra of complex **1** which are assigned as symmetric and asymmetric stretching vibrations of  $\text{C}(\text{sp}^3)\text{-H}$  bonds. The same vibrational band was found at around  $3310 \text{ cm}^{-1}$  in the free ligand. The vibrational bands in the range of  $1400$  to  $1610 \text{ cm}^{-1}$  are assigned for pyridyl (C=N) and phenyl (C=C) ring stretching for both ligands and complex **3**. The identity of complex **3** was further confirmed by single crystal X-ray analysis (Scheme 3.3.1). Single crystal XRD study revealed that complex **3** crystallized in the monoclinic system with  $P2_1/c$  space group.<sup>114</sup> A neutral  $[\text{Fe}^{\text{II}}(\text{NNO})\text{Cl}_2]$  unit is present in the asymmetric unit of the crystal structure. The coordination geometry around the metal center in complex **3** can be best describe as distorted trigonal bipyramidal as supported by the Addison parameter  $\tau$  of 0.55 (square pyramid,  $\tau = 0$ ; trigonal bipyramid,  $\tau = 1$ ;  $\tau = (\alpha - \beta)/60^\circ$ , where  $\alpha$  and  $\beta$  are the two major angles around the metal coordination sphere). It is found that pyrazolyl nitrogen atom (N3) of the tridentate pincer ligand and two terminal chloride ions occupy the trigones. The pyridyl nitrogen (N1) and methoxy oxygen (O1) axially coordinate the metal center. Axial Fe–O1 ( $2.360 \text{ \AA}$ ) and Fe–N1 ( $2.171 \text{ \AA}$ ) bond lengths and equatorial Fe–N3 ( $2.051 \text{ \AA}$ ) and Fe–Cl ( $2.294 \text{ \AA}$ ) bond lengths are in the expected range. The bond lengths and bond angles in complex **4** are very consistent with reported high spin iron(II) complexes with trigonal bipyramidal geometry.<sup>115-117</sup> The solid-

state packing of this complex is mainly stabilized by extensive  $\pi\cdots\pi$  stacking interaction between pyrazole and phenyl rings of two neighboring molecules with a centroid-to-centroid distance of 3.947 Å. In addition, C–H $\cdots$ Cl hydrogen bonding interactions and C–H $\cdots\pi$  interactions contribute to the solid-state stability of complex **3**.

**Scheme 3.3.1. Synthesis of complex 3 with the molecular structure showing 50% ellipsoids<sup>a</sup>**

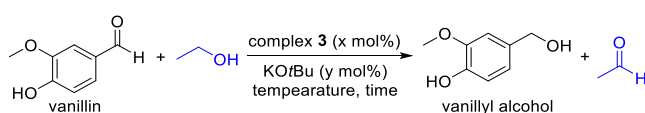


<sup>a</sup>Hydrogen atoms are omitted for clarity. Selected bond distances (Å) and angles (deg): Fe1–O1 2.360(3), Fe1–N1 2.171(3); Fe1–N3 2.051(3), Fe1–Cl1 2.294(3); Fe1–Cl2 2.294(10) and O1–Fe1–N3 166.239(1), N1–Fe1–N3 90.340(9), Cl1–Fe1–Cl2 133.153(9); N3–Fe1–Cl1 110.473(8), N3–Fe1–Cl2 110.473(9).

Thereafter, we tested the catalytic activities of complex **3** for the transfer hydrogenation of vanillin using ethanol as a sacrificial hydrogen source as well as a solvent (Table 3.3.1). As *KOtBu* was widely used base in successful transfer hydrogenations,<sup>118–121</sup> we selected this base in the following transfer hydrogenations. The first reduction of vanillin was conducted at r.t. for 12 h with 5 mol% of catalyst **3** and 10 mol% of *KOtBu* as base and vanillin was completely reduced to vanillyl alcohol (entry 1). Further reduction of reaction time to 8 h also gave complete conversion (entry 1). Same result was obtained with lower base loading of 5 mol% (entry 2). Thereafter, catalyst loading was gradually reduced to 2 mol% and full conversion was obtained in 8 h (entry 4) and roughly 90% yield was obtained in 7 h (entry 5). Further reduction of catalyst loading to 1 mol% gave a little less than 70% yield (entry 6). Transfer hydrogenations of vanillin either in the absence of base (entry 8) or complex **4** (entry 7) gave very poor yield or no yield at all. At r.t., the optimized reduction condition is

following: 2 mol% complex **1**, 5 mol% KO<sup>t</sup>Bu, 8 h (entry 4). Thereafter, we tested the effect of temperature on the transfer hydrogenation of vanillin with ethanol. Under same catalyst and base loading, complete conversions of vanillin to vanillyl alcohol were observed in 6 (entry 9) and 4 h (entry 11) at 50 and 70 °C, respectively. At 70 °C, the catalyst and base loading was further reduced from 2 and 5 mol%, respective (entry 13, 14, 15 and 16). Following condition was optimized at 70 °C for full conversion: 1 mol% complex **1**, 3 mol% KO<sup>t</sup>Bu, 6 h (entry 15). If the reaction temperature was increased to 100 °C, only 4 h was required for 100% yield under same catalyst and base loading (entry 17). Therefore, three conditions were optimized for the complete reduction of vanillin to vanillyl alcohol at various temperatures: A. 2 mol% complex **1**, 5 mol% KO<sup>t</sup>Bu, 8 h, r.t. (entry 4); B. 1 mol% complex **1**, 3 mol% KO<sup>t</sup>Bu, 6 h, 70 °C (entry 15) and C. 1 mol% complex **1**, 3 mol% KO<sup>t</sup>Bu, 4 h, 100 °C (entry 17).

**Table 3.3.1. Catalytic performance of **3** for transfer hydrogenation of vanillin with ethanol**



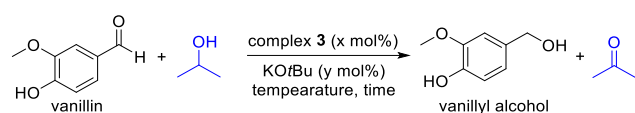
ent.	<b>3</b> (mol%)	KO <sup>t</sup> Bu (mol%)	temp. (°C)	time (h)	yield <sup>b</sup> (%)
1	5	10	r.t.	12/10/8	>99
2	5	5	r.t.	8	>99 (98 <sup>c</sup> )
3	3	5	r.t.	8	>99
<b>4</b>	<b>2</b>	<b>5</b>	<b>r.t.</b>	<b>8</b>	<b>&gt;99 (99<sup>c</sup>)</b>
5	2	5	r.t.	7/6/5/4/3/2/1	94/83/71/58/41/26/14
6	1	5	r.t.	8	67
7	No	5	r.t.	8	0
8	1	no	r.t.	8	>10
9	2	5	50	8/6	>99

10	2	5	50	4	70
11	2	5	70	4	>99 (99 <sup>c</sup> )
12	2	5	70	3	73
13	1	5	70	4	88
14	1	5	70	6	>99 (98 <sup>c</sup> )
<b>15</b>	<b>1</b>	<b>3</b>	<b>70</b>	<b>6</b>	<b>&gt;99</b>
16	1	2	70	6	80
<b>17</b>	<b>1</b>	<b>3</b>	<b>100</b>	<b>4</b>	<b>&gt;99</b>
18	1	3	100	3	92

<sup>a</sup>Reactions conducted in a vial (10 ml) with 0.50 mmol vanillin, 4 ml of ethanol, 10/5/3/2 mol% of KO<sup>t</sup>Bu and 5/3/2/1 mol% of complex **3**. <sup>b</sup>Yields of vanillyl alcohol were determined by <sup>1</sup>H NMR spectroscopy using THF (0.25 mmol) as standard. <sup>c</sup>Isolated yields.

Thereafter, catalytic activity of complex **3** was tested for the transfer hydrogenation of vanillin using isopropanol as a frequently used non-H<sub>2</sub> source of hydrogen (Table 3.3.2). We started with the last optimized condition obtained using ethanol as hydrogen source (entry 17 of Table 3.3.1). Using 1 mol% catalyst and 3 mol% base loading, a complete conversion of vanillin with quantitative isolated yield of vanillyl alcohol was obtained in 4 h at 100 °C in isopropanol (entry 1 of Table 3.3.2). Full conversion of vanillin into vanillyl alcohol was also obtained in 3 h under identical conditions (entry 2). However, a small amount of unreacted starting vanillin was observed after 2 h of heating at 100 °C (entry 3). Reaction times of 4 and 5 h were required for the complete reduction of vanillin to vanillyl alcohol with same catalyst and base loading at 70 (entry 5) and 50 °C, respectively. If the transfer hydrogenation was conducted at r.t., the complete reduction of vanillin was achieved in 6 h with same catalyst and base loading. Hence, milder reaction condition was needed for the room temperature reduction of vanillin with isopropanol as reagent as well as reaction media.

**Table 3.3.2. Catalytic performance of **3** for transfer hydrogenation of vanillin with isopropanol**



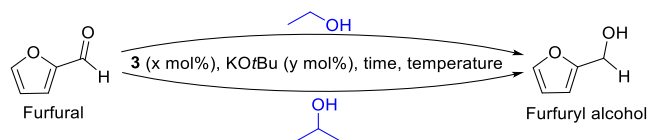
ent.	<b>3</b>	KO <sup>t</sup> Bu	temp.	time	yield <sup>b</sup>
	(mol%)	(mol%)	(°C)	(h)	(%)
1	1	3	100	4	>99 (99 <sup>c</sup> )
2	1	3	100	3	>99 (98 <sup>c</sup> )
3	1	3	100	2	84
4	1	3	70	3	88
5	1	3	70	4	>99
6	1	3	50	4	87
7	1	3	50	5	>99
8	1	3	r.t.	5	89
9	1	3	r.t.	6	>99 (98 <sup>c</sup> )

<sup>a</sup>Reactions conducted in a vial (10 ml) with 0.50 mmol vanillin, 4 ml of isopropanol, 3 mol% of KO<sup>t</sup>Bu and 1 mol% of complex **1**. <sup>b</sup>Yields of vanillyl alcohol were determined by <sup>1</sup>H NMR spectroscopy using THF (0.25 mmol) as standard. <sup>c</sup>Isolated yields.

Generally, transfer hydrogenations of carbonyls are easier with secondary alcohol isopropanol than primary alcohol ethanol. As expected, milder reaction condition such as lower catalyst loading was needed for the room temperature reduction of vanillin with isopropanol (entry 9 of Table 3.3.2: 1 mol% of **3**, 3 mol% of KO<sup>t</sup>Bu, 8 h) as compared to challenging primary alcohol ethanol (entry 4 of Table 3.3.1: 2 mol% of **3**, 5 mol% of KO<sup>t</sup>Bu, 8 h). Thereafter, influence of the nature of alcohols as hydrogen donors was tested at various temperature and transfer hydrogenation of vanillin with ethanol and isopropanol was conducted for 3 h at various temperature (r.t., 50, 70 and 100 °C) under identical catalyst (1 mol%) and base loading (3 mol%) (Table 3.3.3 and Figure 3.3.3). As expected, better conversion of vanillin to vanillyl alcohol was observed at all temperatures. For example, vanillin was completely reduced to vanillyl alcohol in 3 h at 100 °C using isopropanol (entry

8) and approximately 10% unreacted vanillin was left in ethanol as media under identical conditions (entry 7).

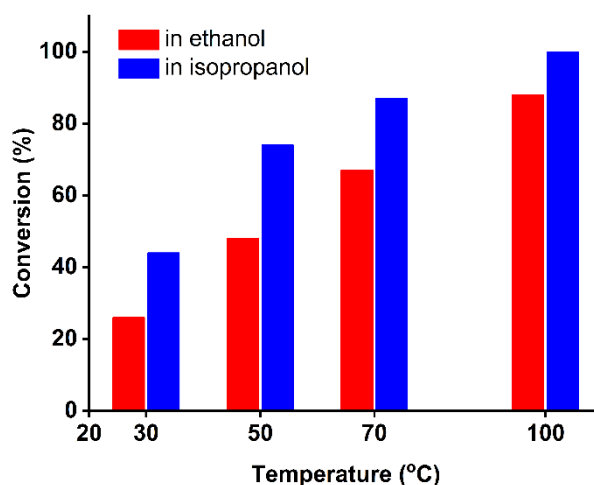
**Table 3.3.3. Catalytic performance of 4 for transfer hydrogenation of vanillin with isopropanol**



ent.	3 (mol%)	KO <sup>t</sup> Bu (mol%)	Alcohol	temp. (°C)	time (h)	yield <sup>b</sup> (%)
1	1	3	Ethanol	r.t.	3	26
2	1	3	isopropanol	r.t.	3	44
3	1	3	Ethanol	50	3	48
4	1	3	isopropanol	50	3	74
5	1	3	Ethanol	70	3	67
6	1	3	isopropanol	70	3	88
7	1	3	Ethanol	100	3	91
8	1	3	isopropanol	100	3	>99

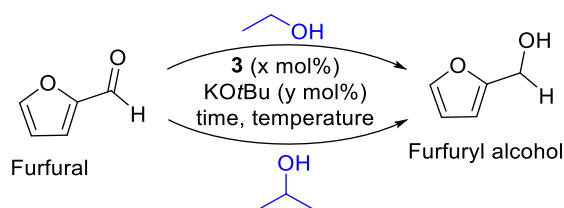
<sup>a</sup>Reactions conducted in a vial (10 ml) with 0.50 mmol vanillin, 4 ml of ethanol or isopropanol, 3 mol% of KO<sup>t</sup>Bu and 1 mol% of complex 1. <sup>b</sup>Yields of vanillyl alcohol were determined by <sup>1</sup>H NMR spectroscopy using THF (0.25 mmol) as standard.

**Figure 3.3.3 Reduction of vanillin to vanillyl alcohol in ethanol and isopropanol at various temperatures in 3 h using 1 mol% of complex 3 and 3 mol% KO<sup>t</sup>Bu.**



Encouraged by the successful utilization of complex **3** for the reduction of vanillin to vanillyl alcohol, we used complex **3** for the transfer hydrogenation of another biomass model compound furfural using both ethanol and isopropanol (Table 3.3.4). Utilizing ethanol as hydrogen donor (entry 1 to 9), we started with the optimized conditions used for the transfer hydrogenation of vanillin at room temperature. Using 2 mol% catalyst and 5 mol% base loading, furfural was completely reduced to furfuryl alcohol in 8 h at r.t. (entry 1). Further decrease of reaction time gave incomplete reduction, a little less than 10% unreacted furfural was noted (entry 2). Thereafter, higher temperatures (50, 70 and 100 °C) were tested. Using identical catalyst and base loading, furfural was totally reduced to furfuryl alcohol in 6, 5 and 4 h at 50, 70 and 100 °C, respectively (entry 3, 5 and 7). Reducing catalyst loading (1 mol% complex **1** and 3 mol% base), full conversion of furfural was observed in 5 h at 100 °C (entry 9). Thereafter, we used isopropanol (entry 10 to 14) and better catalytic activity was observed. Using 2 mol% catalyst and 5 mol% base loading, complete reductions of furfural to furfuryl alcohol were noted in 4, 3, 2 and 1 h at r.t., 50, 70 and 100 °C, respectively. In summary, complex **3** displayed similar catalytic performances for the reduction of both vanillin and furfural to the corresponding alcohols.

**Table 3.3.4. Catalytic performance of **3** for transfer hydrogenation of furfural with ethanol and isopropanol**



ent.	3 (mol%)	KO <sup>t</sup> Bu (mol%)	alcohol	temp. (°C)	time (h)	yield <sup>b</sup> (%)
1	2	5	ethanol	r.t.	8	>99 (98 <sup>c</sup> )
2	2	5	ethanol	r.t.	7	93
3	2	5	ethanol	50	7/6	>99

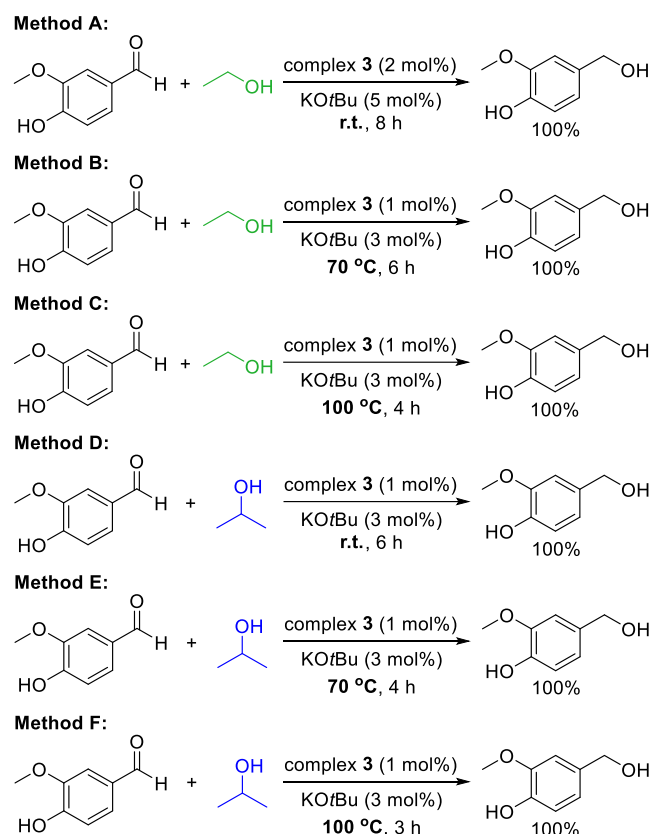
4	2	5	ethanol	50	5	91
5	2	5	ethanol	70	5	>99 (98 <sup>c</sup> )
6	2	5	ethanol	70	4	94
7	2	5	ethanol	100	4	>99
8	2	5	ethanol	100	3	93
9	1	3	ethanol	100	5	>99 (99 <sup>c</sup> )
10	2	5	isopropanol	r.t.	4	>99
11	2	5	isopropanol	50	3	>99
12	2	5	isopropanol	70	2	>99
13	2	5	isopropanol	100	1	>99
14	1	3	isopropanol	100	4	>99

<sup>a</sup>Reactions conducted in a vial (10 ml) with 0.50 mmol furfural, 4 ml of ethanol or isopropanol, 5/3 mol% of KO<sup>t</sup>Bu and 2/1 mol% of complex **4**. <sup>b</sup>Yields of furfuryl alcohol were determined by <sup>1</sup>H NMR spectroscopy using THF (0.25 mmol) as standard.

In our present time, it is extremely vital for the research community to develop new synthetic protocol which is greener and hence, more sustainable as compared to the existing synthetic processes. Therefore, we feel the obligation to evaluate the disadvantages and benefits of the present catalytic protocols for the transfer hydrogenation of vanillin to vanillyl alcohol and furfural to furfuryl alcohol with the green credentials based on “The 12 Principles of Green Chemistry”.<sup>121</sup> To evaluate the green aspects of the reduction of vanillin, six previously optimized reaction conditions were considered for the transfer hydrogenation of vanillin to vanillyl alcohol with ethanol (Method A, B and C) and isopropanol (Method D, E and F) as the hydrogen sources and solvents (Scheme 3.3.2). Similarly, several optimized reactions for the transfer hydrogenations of furfural were also analyzed (see ESI for details). For all the chosen methods, gram-scale reactions were performed which is important to express the practical potential of these transfer hydrogenations. Method A, B and C were performed in ethanol at r.t., 70 and 100 °C, respectively. Similarly, method D, E and F were carried out in isopropanol at r.t., 70 and 100 °C, respectively. We used 2 mol% catalysts and

5 mol% base loading in method A. All other methods were conducted using 1 mol% catalysts and 3 mol% base loading. Product vanillyl alcohol was isolated in all above methods and purity of product was confirmed by  $^1\text{H}$  NMR spectroscopy.

**Scheme 3.3.2. Gram-scale transfer hydrogenation of vanillin to vanillyl alcohol using different optimized reaction conditions<sup>a, b</sup>**



<sup>a</sup>Reactions conducted in a flask (100 ml) with 10.0 mmol vanillin, 50 ml of ethanol/isopropanol, 3/5 mol% of KOtBu and 1/2 mol% of complex 3. <sup>b</sup>Yields of vanillyl alcohol were determined by isolation of pure product.

Above six optimized catalytic protocols for the transfer hydrogenations of vanillin (Method A, B, C, D, E and F) were evaluated using the CHEM21 green metrics toolkit which is essentially a quantitative reflection of “The 12 Principles of Green Chemistry” (Table 3.3.5). At first, we calculated the yield, conversion, selectivity, atom economy and reaction mass efficiency as functions of all six methods with the used mass of reagents and solvent and isolated mass of product vanillyl alcohol. Complete conversion, quantitative yield and excellent selectivity were obtained in all six methods and all these methods earn green flags

for yield, conversion and selectivity. Very good atom economy and reaction mass efficiency were also found. A little less than 80% atom economy and reaction mass efficiency were obtained for method A, B and C with ethanol as solvent. Lower atom economy and reaction mass efficiency were obtained for method D, E and F with solvent isopropanol with higher molecular weight. Both ethanol and isopropanol are considered green solvents and all methods receive green flags for solvents. We utilized iron catalyst for these catalytic transfer hydrogenations of vanillin. As iron is one of most abundant (thus sustainable) metal, all methods again receive green flags. All six methods receive amber flag for reactor as we carried out the reductions in batches (not continuous flow process). We utilized simple workup techniques commonly used for organic syntheses and thus, all methods earn green flags for work up. Thereafter, these six transfer hydrogenation methods were analyzed using energy norms. Acceptable temperature range is 0 to 70 °C. In addition, adequate reaction temperature is expected to be 5 °C or more below the boiling point of solvents. Therefore, method A and D earn green flags as these reactions were performed at r.t. Similarly, method B and E also gets green flags as the reactions were conducted at 70 °C. In contrast, method C and F receive red flags as these catalytic reactions were conducted at 100 °C which is outside the acceptable temperature range and also higher than the reflux temperatures of both solvents. Finally, health and safety measures were taken into account and all six methods were evaluated. As the reagents, solvent, catalyst and products in all catalytic protocols do not have any health and safety concerns, all six methods earn green flags. In summary, we can say that these six optimized methods have mostly green and sustainable features. However, method C and F are energetically most unfavorable as reflected by red flags. Although, rest four methods are green under energy parameter, method A and C are most favored as they were carried out at ambient temperature. Between method A and C, method A is more attractive as this method has slightly higher atom economy and reaction mass

efficiency although slightly higher catalyst loading was used in method A. In addition, using ethanol as a sustainable source of hydrogen is very attractive for method A.

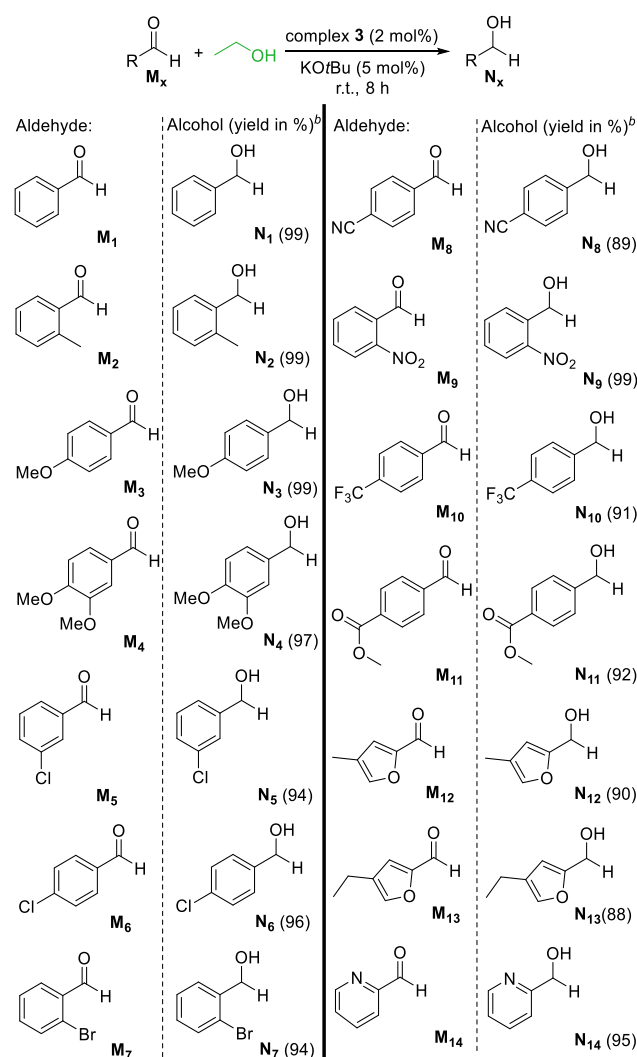
**Table 3.3.5. Comparison of the five different methods of transfer hydrogenations from the CHEM21 Green Metrics Toolkit Calculation**

Metric	Method A	Method B	Method C	Method D	Method E	Method F
Yield	100	100	100	100	100	100
Conversion	100	100	100	100	100	100
Selectivity	100	100	100	100	100	100
Atom economy	77.8	77.8	77.8	72.6	72.6	72.6
Reaction mass efficiency	77.8	77.8	77.8	72.6	72.6	72.6
Solvent	EtOH	EtOH	EtOH	<i>i</i> PrOH	<i>i</i> PrOH	<i>i</i> PrOH
Catalyst	Yes	Yes	Yes	Yes	Yes	Yes
Element	Fe	Fe	Fe	Fe	Fe	Fe
Reactor	Batch	Batch	Batch	Batch	Batch	Batch
Work up	Filtration evaporation	Filtration evaporation	Filtration evaporation	Filtration Evaporation	Filtration Evaporation	Filtration Evaporation
Energy	r.t.	70 °C	100 °C	r.t.	70 °C	100 °C
Health & safety						

Thereafter, we utilized the most favored optimization conditions (method A: 2 mol% complex **1**, 5 mol% KO<sup>t</sup>Bu, ethanol, r.t., 8 h) for the transfer hydrogenation of structurally related aldehydes and biomass model aldehyde compounds (Scheme 3.3.3). As vanillin is a substituted benzaldehyde, we performed the transfer hydrogenation of benzaldehydes with a wide variety of substituents. Under stated conditions, benzaldehyde (**M**<sub>1</sub>) was completely reduced to benzyl alcohol (**N**<sub>1</sub>) with quantitative isolated yield. Similarly, benzaldehydes with electron donating substituents (**M**<sub>2</sub>, **M**<sub>3</sub>) were complete converted to the corresponding

substituted benzyl alcohols (**N**<sub>2</sub>: 99%, **N**<sub>3</sub>: 99%). A structurally related biomass model compound veratraldehyde (**M**<sub>4</sub>), a widely used flavorant and odorant, was also reduced to the corresponding alcohol (**N**<sub>4</sub>: 97%) in excellent yield. Thereafter, various substituted benzaldehyde with a various electron withdrawing functionalities (**M**<sub>5</sub>, **M**<sub>6</sub>, **M**<sub>7</sub>, **M**<sub>8</sub>, **M**<sub>9</sub>, **M**<sub>10</sub> and **M**<sub>11</sub>) were subjected to transfer hydrogenation using above reaction conditions. Substituted benzaldehyde with mild electron withdrawing halo (**M**<sub>5</sub>, **M**<sub>6</sub> and **M**<sub>7</sub>), moderate electron withdrawing ester and cyano (**M**<sub>8</sub> and **M**<sub>11</sub>) and strong electron withdrawing nitro and trifluoromethyl groups (**M**<sub>9</sub> and **M**<sub>10</sub>) were completely reduced to the corresponding alcohols in excellent isolated yields (**N**<sub>5</sub>: 94%, **N**<sub>6</sub>: 96%, **N**<sub>7</sub>: 94%, **N**<sub>8</sub>: 89%, **N**<sub>9</sub>:99%, **N**<sub>10</sub>: 91% and **N**<sub>11</sub>: 92%). The transfer hydrogenation is selective to aldehyde and other reducible functionalities such as cyano, nitro and ester were unaltered. Thereafter, we successfully tested a couple of furfural derivatives 5-methyl furfural (**M**<sub>12</sub>) and 5-ethyl furfural (**M**<sub>13</sub>) which are also biomass model compounds. In addition, another heteroaryl aldehyde 2-pyridinecarboxaldehyde (**M**<sub>14</sub>) was successfully reduced to the corresponding alcohols 2-pyridinemethanol (**N**<sub>14</sub>: 95%) in excellent yields.

**Scheme 3.3.3. Transfer hydrogenation of structurally related aldehydes and biomass model aldehyde compounds using ethanol catalyzed by 1<sup>a</sup>**

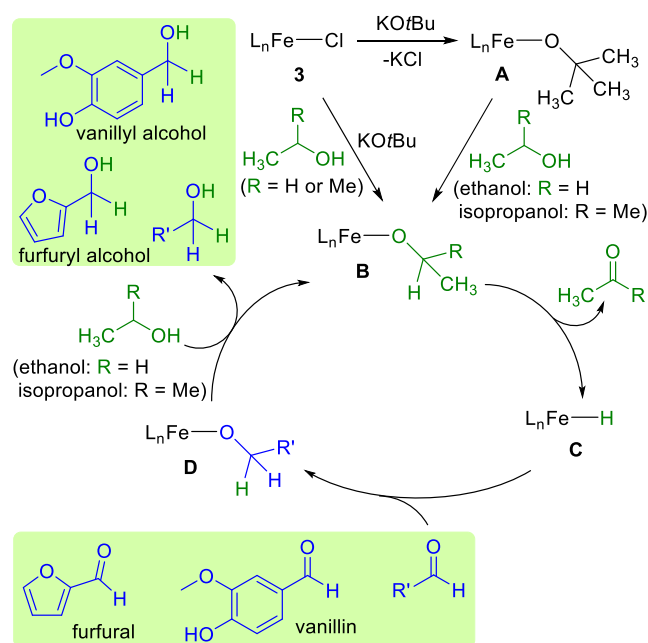


<sup>a</sup>Reactions conducted in a vial (10 ml) with 0.50 mmol aldehyde substrate, 4 ml of ethanol, 5 mol% of KOtBu and 2 mol% of complex **1**. <sup>c</sup>Isolated yields.

The catalytic pathway for the transfer hydrogenation of carbonyls using alcohol is well established.<sup>87</sup> Based on the previous reports, we propose a plausible reaction mechanism for the transfer hydrogenation of vanillin or furfural or related aldehydes with ethanol or isopropanol as hydrogen source and solvent (Scheme 3.3.4). At first, precatalyst complex **1** reacts with base (KOtBu) and transmetalation results in the formation of iron(II)-tert-butoxide complex **A** with the elimination of KCl. Thereafter, intermediate **A** reacts with alcohol solvent (ethanol or isopropanol) to form the corresponding iron(II)-alkoxide (ethoxide or isopropoxide) species **B** as the active catalyst. Hence, the catalytic cycle starts with the activation of precatalyst **1** with KOtBu and alcohol to yield active alkoxide (ethoxide

or isopropoxide) complex **B**. In the following step,  $\alpha$ -hydride elimination from the alkoxide complex **B** resulted in the formation of iron(II)-hydride complex **C** with the elimination of the corresponding carbonyl compound (either acetaldehyde or acetone) as byproduct. Thereafter, hydride transfer takes place to the aldehyde substrate which leads to the formation of iron(II)-alkoxide complex **D**. In the final step, hydrogen transfer from ethanol/isopropanol to the alkoxy moiety **D** discharges the reduced product with the regeneration of active catalyst **B**.

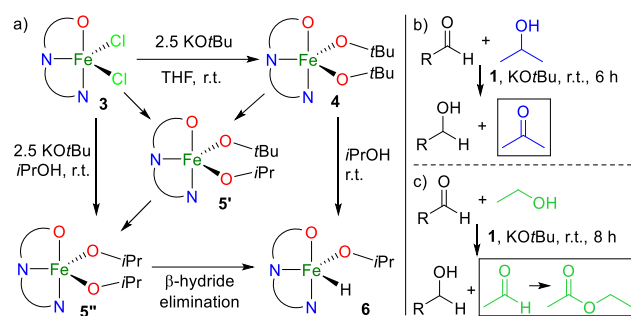
**Scheme 3.3.4. Proposed catalytic cycle for the transfer hydrogenation of carbonyls with methanol/ethanol catalyzed by complex 3**



A stoichiometric reactivity study was performed to shed light on the suggested reaction mechanism (Scheme 3.3.4). At first a stoichiometric reaction of complex **3** with base was performed in the absence of alcohol isopropanol. Addition of  $KOtBu$  to a solution of complex **3** in THF at r.t. showed an instant color change from yellow to red. This reaction resulted in the formation of a NMR inactive iron(II) di-tert-butoxide species **4** as red solid which was characterized by HRMS and elemental analysis. Thereafter, complex **3** was reacted with  $KOtBu$  in presence of excess isopropanol (in the absence of aldehyde substrate). The reaction is expected to proceed via iron(II) iso-propoxide species which ultimately gives iron(II)

hydride species by  $\beta$ -hydride elimination. Mass analysis was performed from the above reaction mixture at very early stage, which clearly showed characteristic mass peaks for iron(II) di-iso-propoxide species **5** ( $m/z$  439.1538) and iron(II) isopropoxide hydride species **6** ( $m/z$  381.1094). Mass spectrum also showed a peak for iron(II) iso-propoxide tert-butoxide species (**5'**) which clearly indicates that above reaction proceeds via iron(II) di-tert-butoxide (**5**) intermediate. Finally, iron(II) isopropoxide hydride species **6** was isolated as the final product which was again characterized by HRMS and elemental analysis. Iron(II) isopropoxide hydride species **6** was also isolated if iron(II) di-tert-butoxide species **5** was treated with excess isopropanol (a very similar mass spectrum was also observed). Despite many attempts, we could not get structural data of **4** and **6** by single crystal X-ray analysis due to the poor quality of crystals. In addition, we were interested to determine the nature of byproducts coming from the secondary and primary alcohol as hydrogen source (Scheme 3.3.4) and 5c). It is well established that acetone is formed as byproduct if isopropanol is used. However, ketone or aldehyde byproduct might undergo further changes in the reaction media and it is important to verify it. Therefore, we performed a transfer hydrogenation of vanillin in isopropanol and at the end we analyzed the content of the reaction by mass analysis (Scheme 3.3.4). We detected only acetone as byproduct. Similarly, transfer hydrogenation of vanillin in ethanol was performed and we analyzed the reaction mixture by mass analysis (Scheme 3.3.5). Acetaldehyde is the expected byproduct in this reaction with ethanol, however, the mass analysis did not detect acetaldehyde. Instead, we detected ethyl acetate as byproduct which is not surprising as reactive acetaldehyde formed ethyl acetate as a highly stable byproduct. Formation of ethyl acetate byproduct for transfer hydrogenation in ethanol was also reported previously.<sup>87,89</sup>

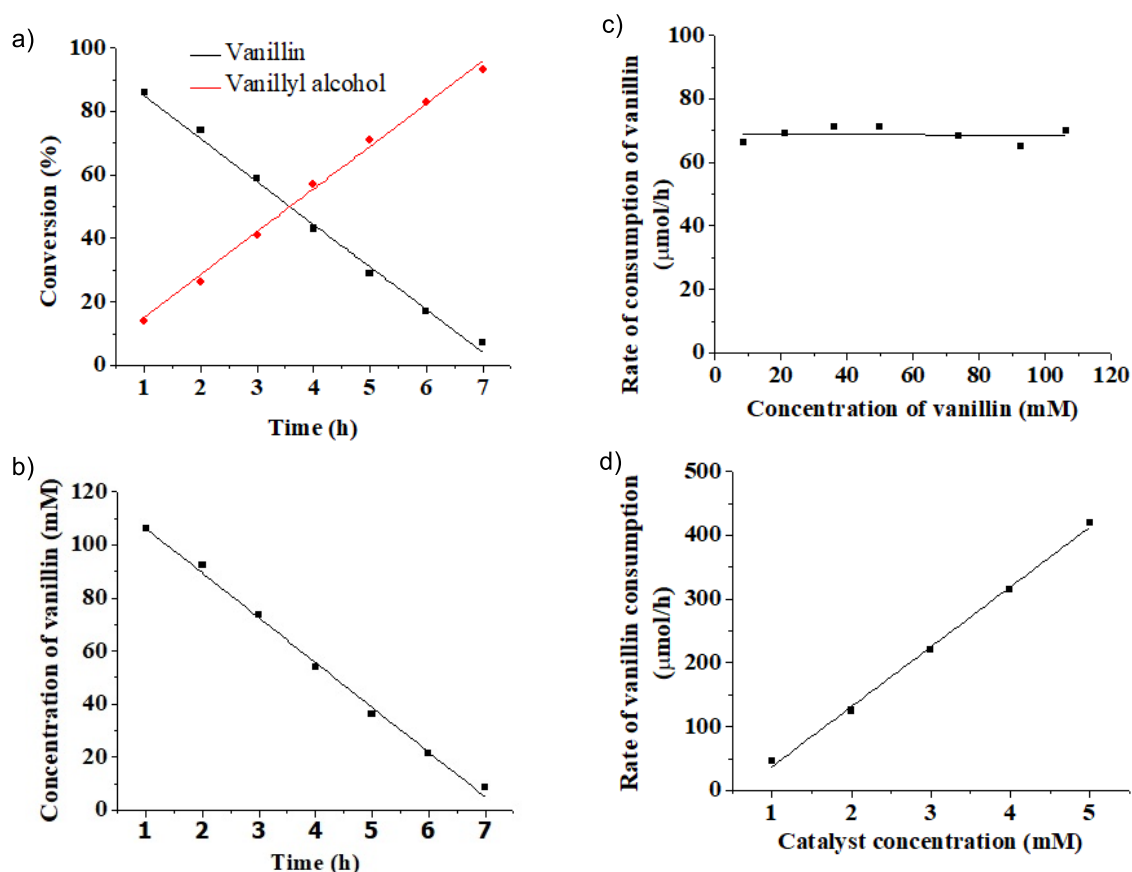
**Scheme 3.3.5 a) Stoichiometric reactivity study with complex 3; b) and c) formation of byproducts from alcohols as hydrogen source.**



In addition to the above mentioned stoichiometric reactions, we wanted to check the reaction kinetics. A detailed kinetic analysis was carried out for the transfer hydrogenation of vanillin as a model substrate. At first, we checked the influence of the concentration of base on the rate of the catalytic transfer hydrogenation of vanillin. Transfer hydrogenation of vanillin was performed using various base loading (5, 7.5, 10, 12.5, 15, 17.5 and 20 mol%) keeping other parameter constant (2 mol% complex **3**, r.t., 4 h, isopropanol). With respect to the iron complex **1**, 2.5 to 10 equivalent of base was used; however, no effect on the reaction rate was observed (see ESI for details). This clearly suggests that base only acts as the activator of the precatalyst (complex **3**) and the role of base in the catalytic cycle is insignificant. Similar observation was reported by the Pidko et al. in their study on manganese-catalyzed transfer hydrogenation of ketone.<sup>123</sup> Thereafter, the reaction progress i.e. the conversion of vanillin and formation of vanillyl alcohol at r.t. were monitored using 2 mol% of catalyst loading (Figure 3.3.4 a). The linear fall of the amount of vanillin or linear growth of the amount of vanillyl alcohol is indicative of zeroth order kinetics in substrate vanillin. The respective concentrations of vanillin were also plotted against time (Figure 3.3.4 b) and we observed a linear decrease of substrate concentration with time which suggested saturation kinetics or zero-order kinetics in substrate (rate constant = 16.9 mM h<sup>-1</sup>). The rate of consumption of substrate was also plotted against the concentration of substrate (Figure 3.3.4 c) and we observed a constant rate (69.1 mmol h<sup>-1</sup>) of substrate consumption. The reaction kinetics with respect to alcohol was not studied as alcohol was used as solvent (huge excess). Finally, we investigated the influence of the concentration of catalyst (complex **3**) on

the rate of the transfer hydrogenation of vanillin. Transfer hydrogenations of vanillin in ethanol with 1, 2, 3, 4 and 5 mol% catalyst loading were performed for 1 h (see ESI for details) and the rate of consumption of vanillin was plotted against concentration of catalyst (Figure 3.3.4 d). The reaction rate increased linearly with the catalyst concentration and this is in agreement with first order kinetic in catalyst. Zeroth order kinetics in substrate and first order kinetics in catalyst was also reported previously for transfer hydrogenation of carbonyls. The zeroth order kinetic in substrate suggests that substrate binding and activation is not the rate-limiting step. The  $\beta$ -hydride elimination step to convert iron-alkoxide species **B** (isopropoxide and ethoxide for isopropanol and ethanol donor, respectively) to iron-hydride species **C** is expected to be the rate-determining step in the catalytic cycle.

**Figure 3.3.4. Kinetic analyses for the conversion of vanillin to vanillyl alcohol.**



### 3.4 CONCLUSIONS:

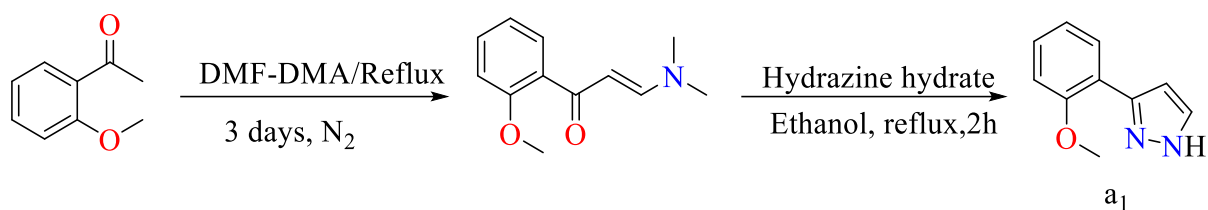
In conclusion, a readily accessible tridentate NNO pincer ligand (**L1**) was developed and utilized for the synthesis of an air-stable iron(II) complex (**1**) from a cheap precursor iron(II) chloride tetrahydrate. Complex **3** proved to be an efficient catalyst for the transfer hydrogenation of cellulose and lignin model compounds furfural and vanillin, respectively, using environmentally benevolent and economically sustainable but challenging primary alcohol ethanol as the hydrogen source in presence of catalytic amount of base. Ecologically benign secondary alcohol isopropanol was also used effectively for the same purpose. The substrate scope was easily extended to various other biomass model carbonyl compounds and structurally related aldehydes. In presence of other reducible functionalities such as cyano, nitro and ester group, good chemoselectivity towards the reduction of aldehyde moiety was observed. Stoichiometric reactivity and kinetic studies were performed to shed light on the proposed reaction pathway which is believed to proceed via iron(II)-alkoxide (**B**), -hydride (**C**) and -alkoxide (**D**) intermediates with  $\beta$ -hydride elimination step for the formation of iron-hydride species **C** as the rate-determining step. This catalytic system is robust as several gram-scale transfer hydrogenations were successfully concluded. Several optimized catalytic methods (method A to F) were selected and the green and sustainable credentials were analyzed by using the CHEM21 green metrics toolkit. Method A (2 mol% complex **1**, 5 mol% KO $t$ Bu, ethanol, r.t., 8 h) was concluded as the most favored one. To the best of our knowledge, this is the first example of iron-catalyst for the transfer hydrogenation of carbonyls using challenging primary alcohol ethanol. For the reduction of biomass model compound furfural and vanillin, most of the previous works reported noble metal catalysts under extreme conditions and this field is highly dominated by heterogeneous catalysts. Hence, utilizing iron complex as an effective homogeneous catalyst is valuable as this non-toxic first row transition metal is the most abundant transition metal on earth crust. In

addition, it is extremely crucial to convert renewable biomass into effective biofuels and fine chemicals. Therefore, this catalytic protocol for the transfer hydrogenation of biomass model compounds furfural and vanillin is an important development in the field of biomass valorization. Notably, present green catalytic system might be realistic for possible future application particularly because of the use of environmentally benign and sustainable hydrogen source ethanol and the utilization of non-toxic, cheap, earth-abundant and thus, sustainable iron catalyst.

### 3.5 EXPERIMENTAL SECTION

**General experimental.** Syntheses of ligand and iron complex were carried out in air. All solvents (acetonitrile, dichloromethane, diethyl ether, hexanes, ethyl acetate, Isopropanol, ethanol, DMF-DMA and toluene) and chemicals were purchased from commercial suppliers and used without further purification. All THs were performed under inert condition and degassed ethanol and isopropanol were used. For recording NMR spectra,  $\text{CDCl}_3$  and  $\text{DMSO-d}_6$  was purchased from Sigma-Aldrich and used without further purification.  $^1\text{H}$  and  $^{13}\text{C}$  NMR spectra were recorded at Bruker AV-400 and JEOL-400 ( $^1\text{H}$  at 400 MHz and  $^{13}\text{C}$  at 101 MHz).  $^1\text{H}$  NMR chemical shifts are referenced in parts per million (ppm) with respect to tetramethylsilane ( $\delta$  0.00 ppm) and  $^{13}\text{C}\{^1\text{H}\}$  NMR chemical shifts are referenced in ppm with respect to  $\text{CDCl}_3$  ( $\delta$  77.16 ppm). The coupling constants ( $J$ ) are reported in hertz (Hz). The following abbreviations are used to describe multiplicity: s = singlet, bs = broad signal, d = doublet, t = triplet, q = quadrate, m = multiplate. High resolution mass spectra were recorded on a Bruker micrOTOF-Q II Spectrometer. Elemental analysis was carried out on a EuroEA Elemental Analyser. Infrared (IR) spectra were recorded on a Perkin-Elmer FT-IR spectrophotometer. Crystal data were collected with a Rigaku Oxford diffractometer and with an INCOATEC micro source (Mo- $\text{K}\alpha$  radiation,  $\lambda = 0.71073 \text{ \AA}$ , multilayer optics) at 293 K

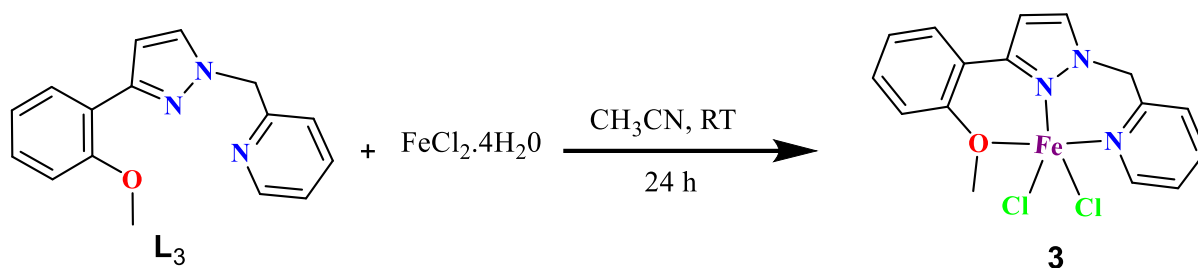
## Synthesis and characterisation of L<sub>3</sub> and 3



**Synthesis of a<sub>1</sub>:** Compound 3-(2-methoxyphenyl)-1H-pyrazole is a known compound and was synthesized using following procedure. A solution of 2-Methoxy acetophenone (3.00 g, 20.0 mmol) in a 1:1 mixture of DMF-DMA (20 ml) was reflux for 3 days under inert condition to give an orange brown solution. Removal of solvents under vacuum gave brown oil. Thereafter, ethanol (8.0 mL) and hydrazine hydrate (1.28 g, 40 mmol) was added and the reaction mixture was refluxed for 2 hours. The resulting yellow solution was cooled to room temperature and cold water (15 mL) was added giving an off-white precipitate. The mixture was kept at 0-4 °C overnight to allow complete precipitation and the solid was collected after filtration. The solid was washed with cold water (3 x 20 mL) to give a white solid as pure product (3.34 g, 96%). <sup>1</sup>H NMR (CDCl<sub>3</sub>): δ 12.50 (br, 1H), 7.73 (m, 1H), 7.69 (s, 1H), 7.09 (m, 2H), 6.67 (s, 1H), 4.02 (s, 3H).

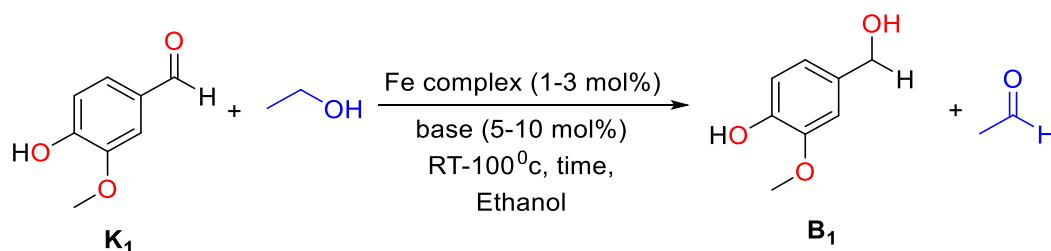
**Synthesis of L<sub>3</sub>:** In a pressure tube, 3-(2-methoxyphenyl)-1H-pyrazole (1.74 g, 10.0 mmol), 2-(chloromethyl) pyridine hydrochloride (1.64 g, 10.0 mmol), NaOH solution (40%, 5.0 mL) and toluene (15 mL) were added and the reaction mixture was stirred at r.t. for 15 mins. Then tert-butylammonium hydroxide (4.0 mL) was added and the reaction mixture was stirred at 130°C temperature for 24 h. The resulting red mixture was cooled down to r.t. and extracted with ethyl acetate (3 x 50 mL). All volatiles were removed under high vacuum to give **L<sub>1</sub>** as pure procedure (2.27 g, 73%). <sup>1</sup>H NMR (CDCl<sub>3</sub>): δ 8.58 (s, 1H), 8.0 (d, *J* = 6.0 Hz, 1H), 7.6 (t, *J* = 8.0 Hz, 3H), 7.31–7.09 (m, 2H), 7.03–6.9 (m, 3H), 6.88 (s, 1H), 5.54 (s, 1H), 3.92 (s, 3H). <sup>13</sup>C{<sup>1</sup>H} NMR (CDCl<sub>3</sub>): 155.26, 148.22, 147.39, 134.79, 130.10, 129.33, 123.45,

121.29, 122.25, 122.76, 121.79, 121.27, 113.75, 56.11, 55.22 HRMS (ESI-TOF)  $m/z$ :  $[M - H]^+$  calcd for  $C_{16}H_{15}N_3O$  265.1256; found 265.1289. Anal. Calcd for  $C_{16}H_{15}N_3O$  (265.12): C, 72.43; H, 5.70; N, 15.89. Found: C, 72.41; H, 5.65; N, 15.71.



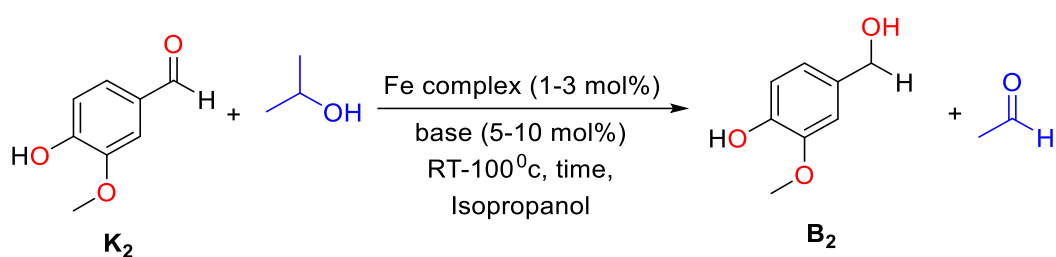
**Synthesis of 3:** A mixture of **L1** (0.267 g, 1.00 mmol) and  $FeCl_2 \cdot 4H_2O$  (0.126 g, 1.00 mmol) in acetonitrile (25 mL) was stirred at r.t. for 24 h resulting in a yellow precipitate. All volatiles were removed under high vacuum to give a light yellow solid which was extracted with dichloromethane (20 mL). All volatiles were removed under high vacuum to give a yellow solid as pure complex **4** (0.321 g, 79%). X-ray quality single crystals were obtained by slow diffusion of diethyl ether into a solution of **1** in dichloromethane. HRMS (ESI-TOF)  $m/z$ :  $[M - Cl]^+$  calcd for  $C_{16}H_{15}ClFeN_3O$  356.0248; found 356.0230. Anal. Calcd for  $C_{16}H_{15}Cl_2FeN_3O$  (390.54): C, 49.02; H, 3.86; N, 8.08. Found: C, 49.21; H, 3.87; N, 8.01.

### General procedure for the transfer hydrogenation of vanillin and furfural

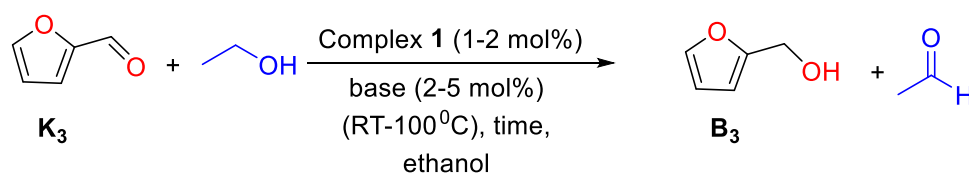


**General condition for reaction optimization using ethanol (Procedure 1a):** A solution of Vanillin (0.076 g, 0.5 mmol), complex **3** (3/ 2/ 1 mol %) and  $KOtBu$  (10/ 5/ 3 mol%) in ethanol (4 mL) was transferred into a pressure tube fitted with a magnetic stir-bar. The

reaction mixture was heated at appropriate temperature (r.t. / 50 °C/ 70 °C/ 100 °C) in an oil bath for appropriate time (1 to 12 h). Thereafter, the reaction mixture was cooled down to r.t. and dried under high vacuum. The resultant oily mixture was dissolved in ethyl acetate (3 mL) and passed through a short silica column to remove metal complex. All volatile was removed under high vacuum to give crude product. The crude product was analysed by <sup>1</sup>H NMR spectroscopy. Occasionally the crude product was purified by column chromatography using silica as stationary phase and a 9:1 mixture of hexanes and ethyl acetate as eluent.



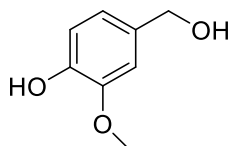
**General condition for reaction optimization using isopropanol (Procedure 1b):** A solution of Vanillin (0.076 g, 0.5 mmol), complex **3** (3/ 2/ 1 mol %) and KO<sup>t</sup>Bu (10/ 5/ 3 mol %) in isopropanol (4 mL) was transferred into a pressure tube fitted with a magnetic stir-bar. The reaction mixture was heated at appropriate temperature (r.t. / 50 °C/ 70 °C/ 100 °C) in an oil bath for appropriate time (1 to 12 h). Thereafter, the reaction mixture was cooled down to r.t. and dried under high vacuum. The resultant oily mixture was dissolved in ethyl acetate (3 mL) and passed through a short silica column to remove metal complex. All volatile was removed under high vacuum to give crude product. The crude product was analysed by <sup>1</sup>H NMR spectroscopy. Occasionally the crude product was purified by column chromatography using silica as stationary phase and a 9:1 mixture of hexanes and ethyl acetate as eluent.



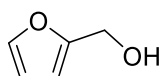
**General condition for reaction optimization furfural using ethanol (Procedure 2a):** A solution of Furfural (0.048 g, 0.5 mmol), complex **3** (3/ 2/ 1 mol %) and KO<sup>t</sup>Bu (10/ 5/ 3 mol%) in ethanol (4 mL) was transferred into a pressure tube fitted with a magnetic stir-bar. The reaction mixture was heated at appropriate temperature (r.t. / 50 °C/ 70 °C/ 100 °C) in an oil bath for appropriate time (1 to 12 h). Thereafter, the reaction mixture was cooled down to r.t. and dried under high vacuum. The resultant oily mixture was dissolved in ethyl acetate (3 mL) and passed through a short silica column to remove metal complex. All volatile was removed under high vacuum to give crude product. The crude product was analysed by <sup>1</sup>H NMR spectroscopy. Occasionally the crude product was purified by column chromatography using silica as stationary phase and a 9:1 mixture of hexanes and ethyl acetate as eluent.

**General condition for reaction optimization furfural using isopropanol (Procedure 2b):** A solution of Furfuryl (0.048 g, 0.5 mmol), complex **3** (3/ 2/ 1 mol %) and KO<sup>t</sup>Bu (10/ 5/ 3 mol %) in isopropanol (4 mL) was transferred into a pressure tube fitted with a magnetic stir-bar. The reaction mixture was heated at appropriate temperature (r.t. / 50 °C/ 70 °C/ 100 °C) in an oil bath for appropriate time (1 to 12 h). Thereafter, the reaction mixture was cooled down to r.t. and dried under high vacuum. The resultant oily mixture was dissolved in ethyl acetate (3 mL) and passed through a short silica column to remove metal complex. All volatile was removed under high vacuum to give crude product. The crude product was analysed by <sup>1</sup>H NMR spectroscopy. Occasionally the crude product was purified by column chromatography using silica as stationary phase and a 9:1 mixture of hexanes and ethyl acetate as eluent.

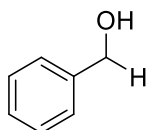
## **NMR data of products**



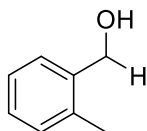
**Vanillyl alcohol.** Vanillyl alcohol as white solid (76 mg, 99%) was synthesized according to the general procedure.  $^1\text{H}$  NMR (400 MHz, DMSO- $d_6$ ):  $\delta$  8.81 (br, 1H), 6.89 (d,  $J = 6$  Hz, 1H), 6.75 (d,  $J = 6$  Hz, 1H), 5.03 (m, 1H), 3.75 (s, 3H).  $^{13}\text{C}\{^1\text{H}\}$  NMR (101 MHz, DMSO- $d_6$ ):  $\delta$  147.75, 119.59, 115.48, 111.48, 63.43, 55.93.



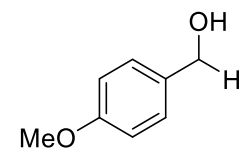
**Furfuryl alcohol.** Vanillyl alcohol as colourless liquid (47 mg, 99%) was synthesized according to the general procedure.  $^1\text{H}$  NMR (400 MHz,  $\text{CDCl}_3$ ):  $\delta$  7.40 (m, 1H), 6.35 (m, 1H), 6.28 (m, 1H).  $^{13}\text{C}\{^1\text{H}\}$  NMR (101 MHz,  $\text{CDCl}_3$ ):  $\delta$  154.01, 142.25, 116.38, 110.72, 57.28.



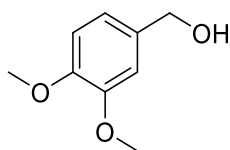
**Phenylmethanol (N<sub>1</sub>).** Compound N<sub>1</sub> as yellow oil (53 mg, 99%) was synthesized according to the general procedure.  $^1\text{H}$  NMR (400 MHz,  $\text{CDCl}_3$ ):  $\delta$  7.43 – 7.19 (m, 5H), 4.64 (s, 2H), 2.62 (s, 1H).  $^{13}\text{C}\{^1\text{H}\}$  NMR (101 MHz,  $\text{CDCl}_3$ ):  $\delta$  140.92, 128.59, 127.65, 127.07, 65.20.



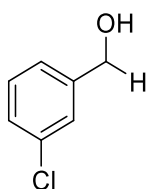
***o*-Tolylmethanol (N<sub>2</sub>).** Compound N<sub>2</sub> as colourless liquid (60 mg, 99%) was synthesized according to the general procedure.  $^1\text{H}$  NMR (400 MHz,  $\text{CDCl}_3$ ):  $\delta$  7.38 – 7.31 (m, 1H), 7.27 – 7.15 (m, 3H), 4.64 (s, 2H), 2.53 (s, 1H), 2.35 (s, 3H).  $^{13}\text{C}\{^1\text{H}\}$  NMR (101 MHz,  $\text{CDCl}_3$ ):  $\delta$  138.77, 136.07, 130.30, 127.72, 127.53, 126.05, 63.27, 18.65.



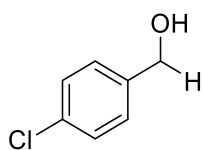
**(4-Methoxyphenyl)methanol (N<sub>3</sub>).** Compound N<sub>3</sub> as colourless liquid (68 mg, 99%) was synthesized according to the general procedure. <sup>1</sup>H NMR (400 MHz, CDCl<sub>3</sub>): δ 7.27 (d, *J* = 8.3 Hz, 2H), 6.89 (dd, *J* = 9.0, 2.3 Hz, 2H), 4.57 (s, 2H), 3.80 (s, 3H), 2.47 (s, 1H). <sup>13</sup>C{<sup>1</sup>H} NMR (101 MHz, CDCl<sub>3</sub>): δ 159.28, 133.26, 128.75, 114.04, 65.05, 55.38.



**(3,4-Dimethoxyphenyl)methanol (N<sub>4</sub>).** Compound N<sub>4</sub> as colourless liquid (82 mg, 97%) was synthesized according to the general procedure. <sup>1</sup>H NMR (400 MHz, CDCl<sub>3</sub>): δ 6.93-6.84 (m, 3H), 4.62 (s, 2H), 3.89 (s, 3H), 3.88 (s, 3H). <sup>13</sup>C{<sup>1</sup>H} NMR (101 MHz, CDCl<sub>3</sub>): δ 149.10, 133.41, 119.40, 110.07, 110.48, 65.75, 55.38.

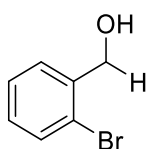


**(3-Chlorophenyl)methanol (N<sub>5</sub>).** Compound N<sub>5</sub> as colourless oil (67 mg, 94%) was synthesized according to the general procedure. <sup>1</sup>H NMR (400 MHz, CDCl<sub>3</sub>): δ 7.37 – 7.25 (m, 4H), 4.68 (s, 2H), 1.74 (s, 1H). <sup>13</sup>C{<sup>1</sup>H} NMR (101 MHz, CDCl<sub>3</sub>): δ 142.97, 134.59, 129.96, 127.85, 127.10, 124.98, 64.70.

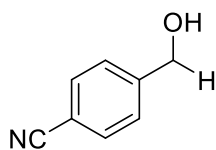


**(4-Chlorophenyl)methanol (N<sub>6</sub>).** Compound N<sub>6</sub> was synthesized according to the general procedure. Crude product was purified by column chromatography (silica as stationary phase

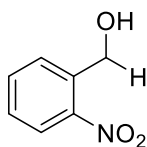
and a mixture of hexane and ethyl acetate 9:1 as eluent) to give pure product as white solid (68mg, 96%).  $^1\text{H}$  NMR (400 MHz,  $\text{CDCl}_3$ ):  $\delta$  7.33–7.27 (m,  $J = 8.4, 4.9$  Hz, 4H), 4.63 (dd,  $J = 4.8, 2.3$  Hz, 2H), 1.93 (s, 1H).  $^{13}\text{C}\{^1\text{H}\}$  NMR (100 MHz,  $\text{CDCl}_3$ ):  $\delta$  139.45, 133.49, 128.79, 128.38, 64.60.



**(2-Bromophenyl)methanol (N7).** Compound N7 as colourless liquid (86 mg, 94%) was synthesized according to the general procedure.  $^1\text{H}$  NMR (400 MHz,  $\text{CDCl}_3$ ):  $\delta$  7.55 (dd,  $J = 8.0, 1.0$  Hz, 1H), 7.48 (dd,  $J = 7.6, 1.5$  Hz, 1H), 7.33 (td,  $J = 7.5, 1.0$  Hz, 1H), 7.16 (td,  $J = 7.7, 1.7$  Hz, 1H), 4.76 (s, 2H), 1.82 (s, 1H).  $^{13}\text{C}\{^1\text{H}\}$  NMR (101 MHz,  $\text{CDCl}_3$ ):  $\delta$  139.84, 132.70, 129.22, 129.00, 127.77, 122.67, 65.15.



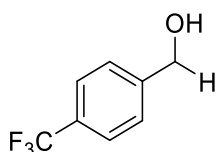
**4-(Hydroxymethyl)benzonitrile (N8).** Compound N8 as white liquid (59 mg, 89%) was synthesized according to the general procedure.  $^1\text{H}$  NMR (400 MHz,  $\text{CDCl}_3$ ):  $\delta$  7.55 (d,  $J = 8.3$  Hz, 2H), 7.41 (d,  $J = 8.3$  Hz, 2H), 4.68 (s, 2H), 3.35 (s, 1H).  $^{13}\text{C}\{^1\text{H}\}$  NMR (101 MHz,  $\text{CDCl}_3$ ):  $\delta$  167.19, 146.25, 129.87, 129.93, 110.58, 64.60.



**(2-Nitrophenyl)methanol (N9).** Compound N9 was synthesized according to the general procedure. Crude product was purified by column chromatography (silica as stationary phase and a mixture of hexane and ethyl acetate 9:1 as eluent) to give pure product as brown oil (75.7 mg, 99%).  $^1\text{H}$  NMR (400 MHz,  $\text{CDCl}_3$ ):  $\delta$  8.09 (dd,  $J = 8.2, 1.1$  Hz, 1H), 7.74 (d,  $J =$

7.0 Hz, 1H), 7.67 (td,  $J = 7.6, 1.2$  Hz, 1H), 7.51 – 7.41 (m, 1H), 4.97 (s, 2H), 2.43 (s, 1H).

$^{13}\text{C}\{^1\text{H}\}$  NMR (101 MHz,  $\text{CDCl}_3$ ):  $\delta$  147.59, 136.97, 134.21, 129.83, 128.50, 125.04, 62.44.

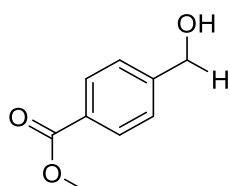


**(4-(Trifluoromethyl)phenyl)methanol (N<sub>10</sub>)**. Compound N<sub>10</sub> as colourless oil (80 mg, 91%)

was synthesized according to the general procedure.  $^1\text{H}$  NMR (400 MHz,  $\text{CDCl}_3$ ):  $\delta$  7.62 (d,

$J = 8.0$  Hz, 2H), 7.48 (d,  $J = 8.0$  Hz, 2H), 4.77 (s, 2H), 1.84 (s, 1H).  $^{13}\text{C}\{^1\text{H}\}$  NMR (101

MHz,  $\text{CDCl}_3$ ):  $\delta$  144.76, 129.86, 129.54, 125.38 (q,  $J = 3.8$  Hz), 122.95, 63.95.

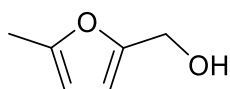


**Methyl 4-(hydroxymethyl)benzoate (N<sub>11</sub>)**. Compound N<sub>11</sub> as colourless liquid (76 mg,

92%) was synthesized according to the general procedure.  $^1\text{H}$  NMR (400 MHz,  $\text{CDCl}_3$ ): 7.97

(d,  $J = 8.3$  Hz, 2H), 7.38 (d,  $J = 8.3$  Hz, 2H), 4.71 (s, 2H), 3.88 (s, 3H), 2.55 (s, 1H).  $^{13}\text{C}\{^1\text{H}\}$

NMR (101 MHz,  $\text{CDCl}_3$ ):  $\delta$  167.19, 146.25, 129.87, 129.22, 126.52, 64.60, 52.21.

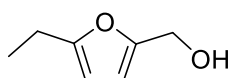


**(5-Methylfuran-2-yl)methanol (N<sub>12</sub>)**. Compound N<sub>12</sub> as colourless liquid (52.50 mg, 90%)

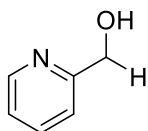
was synthesized according to the general procedure.  $^1\text{H}$  NMR (400 MHz,  $\text{CDCl}_3$ ):  $\delta$  6.18 (d,

$J = 4$  Hz, 1H), 5.99 (d,  $J = 4$  Hz, 1H), 4.53 (s, 2H).  $^{13}\text{C}\{^1\text{H}\}$  NMR (101 MHz,  $\text{CDCl}_3$ ):  $\delta$

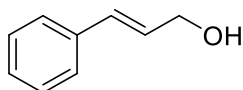
155.34, 108.43, 106.20, 57.15, 13.40.



**(5-Ethylfuran-2-yl)methanol (N<sub>13</sub>).** Compound N<sub>13</sub> as colourless oil (55 mg, 88%) was synthesized according to the general procedure. <sup>1</sup>H NMR (400 MHz, CDCl<sub>3</sub>): δ 6.14 (d, *J* = 4 Hz, 1H), 6.15 (d, *J* = 4 Hz, 1H), 4.51 (s, 2H), 2.42 (q, 2H), 2.55 (t, *J* = 8 Hz, 3H). <sup>13</sup>C{<sup>1</sup>H} NMR (101 MHz, CDCl<sub>3</sub>): δ 157.94, 132.25, 108.19, 104.58, 57.20, 21.13, 12.04.



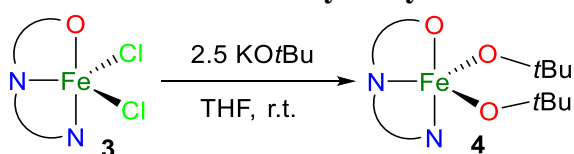
**Pyridin-2-ylmethanol (N<sub>14</sub>).** Compound N<sub>14</sub> was synthesized according to the general procedure. Crude product was purified by column chromatography (silica as stationary phase and a mixture of hexane and ethyl acetate 9:1 as eluent) to give pure product as colourless liquid (48 mg, 89%). <sup>1</sup>H NMR (400 MHz, CDCl<sub>3</sub>): δ 8.49 (s, 1H), 7.65 (t, *J* = 7.4 Hz, 1H), 7.29 (d, *J* = 7.5 Hz, 1H), 7.16 (s, 1H), 4.73 (s, 2H), 4.60 – 3.70 (s, 1H). <sup>13</sup>C{<sup>1</sup>H} NMR (101 MHz, CDCl<sub>3</sub>): δ 160.05, 148.22, 136.95, 122.21, 120.85, 64.27



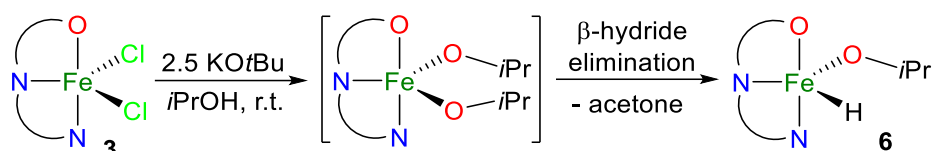
**(E)-3-phenylprop-2-en-1-ol (N<sub>15</sub>).** Compound N<sub>15</sub> as colourless oil (55 mg, 84%) was synthesized according to the general procedure. <sup>1</sup>H NMR (400 MHz, CDCl<sub>3</sub>): δ 7.24–7.41 (m, 5H), 6.63 (d, *J* = 15.9 Hz, 1H), 6.37 (m, 1H), 4.33 (d, *J* = 5.7 Hz, 2H), 2.04 (s, 1H). <sup>13</sup>C{<sup>1</sup>H} NMR (101 MHz, CDCl<sub>3</sub>) δ 136.87, 131.19, 128.68, 128.70, 127.75, 126.57, 63.68.

## Mechanistic analysis

### Stoichiometric reactivity study.



**Synthesis of iron(II) di-tert-butoxide species 5.** Solid KO $t$ Bu (0.028 g, 0.25 mmol) was added to a solution of complex **1** (0.039 g, 0.1 mmol) in THF (5.0 mL) at r.t., which shows an instant color change from yellow to red. The reaction mixture was stirred at r.t. for 1 h. All volatiles were removed from the mixture under high vacuum resulting in a red solid. The solid was extracted with dichloromethane (3 x 5 mL) and dried under high vacuum to give red solid as pure complex **2** (0.035 g, 76%). HRMS (ESI-TOF)  $m/z$ : [M – H]<sup>+</sup> calcd for C<sub>24</sub>H<sub>32</sub>FeN<sub>3</sub>O<sub>3</sub> 466.1788; found 466.1788. Anal. Calcd for C<sub>24</sub>H<sub>33</sub>FeN<sub>3</sub>O<sub>3</sub> (467.14): C, 61.68; H, 7.12; N, 8.99. Found: C, 61.67; H, 7.16; N, 8.97.



**Synthesis of iron(II) isopropoxide hydride species 6.** Solid KO $t$ Bu (0.028 g, 0.25 mmol) was added to a solution of complex **1** (0.039 g, 0.01 mmol) in isopropanol (3 mL) at r.t. The reaction mixture was stirred for 5 mins and subjected for ESI-mass analysis. The reaction mixture was stirred for 16 h at r.t. and subjected for ESI-mass analysis. All volatiles were removed from the mixture under high vacuum resulting in an orange-yellow solid. The solid was extracted with dichloromethane (3 x 5 mL). and dried under high vacuum to give yellow-orange solid as pure complex **4** (0.030 g, 80%). HRMS (ESI-TOF)  $m/z$ : [M – H]<sup>+</sup> calcd for C<sub>19</sub>H<sub>23</sub>FeN<sub>3</sub>O<sub>2</sub> 381.1094; found 381.1134. Anal. Calcd for C<sub>19</sub>H<sub>24</sub>FeN<sub>3</sub>O<sub>2</sub> (382.10.): C, 59.86; H, 6.08; N, 14.65. Found: C, 59.89; H, 6.05; N, 8.97.

### X-ray structure determination

Crystallographic data and structure determinations details are compiled in Table 3.5.1. The crystals were obtained by slow diffusion of diethyl ether into a solution of **1** in DCM at r.t. The crystals were coated with silicon oil on a glass slide and a suitable single crystal was

mounted on a glass fibre. Crystal data were collected with a Rigaku Oxford diffractometer and with an INCOATEC micro source (Mo-K $\alpha$  radiation,  $\lambda = 0.71073$  Å, multilayer optics) at 293 K. The structure was determined using direct methods employed in ShelXT,<sup>S4</sup> OleX,<sup>S5</sup> and refinement was carried out using least-square minimization implemented in ShelXL.<sup>S6</sup> All nonhydrogen atoms were refined with anisotropic displacement parameters. Hydrogen atom positions were fixed geometrically in idealized positions and were refined using a riding model. CCDC 2157166 (for complex **3**) contains the supplementary crystallographic data for this paper.

**Table 3.5.1.** Crystallographic Data and Refinement Parameters for complex **3**

Empirical formula	C <sub>16</sub> H <sub>15</sub> Cl <sub>2</sub> FeN <sub>3</sub> O
CCDC	2157166
Formula weight (g mol <sup>-1</sup> )	392.07
Temperature	100.00(10)
Wavelength	0.71073
Crystal system	Monoclinic
Space group	P2 <sub>1</sub> /c
<i>a</i> (Å)	13.1315(6)
<i>b</i> (Å)	16.5901(8)
<i>c</i> (Å)	8.1561(4)
$\alpha$ (deg)	90
$\beta$ (deg)	102.191(5)
$\gamma$ (deg)	90
volume (Å <sup>3</sup> )	1736.76(15)
Z	4
<i>D</i> <sub>calc</sub> (g cm <sup>-3</sup> )	1.4993
$\mu$ (mm <sup>-1</sup> )	9.845
<i>F</i> (000)	200.2
Crystal Size	0.2 x 0.1 x 0.1 mm <sup>3</sup>
$\theta$ Range (deg)	6.88-136.5
Index Ranges	-16 $\leq$ h $\leq$ 7, -20 $\leq$ k $\leq$ 20, -10 $\leq$ l $\leq$ 10
Reflections collected	12691
Independent reflections ( <i>R</i> <sub>int</sub> )	3160 (0.0890)
Completeness to theta = 25.07 <sup>o</sup>	99.60
Refinement method	Full-matrix least-squares on <i>F</i> <sup>2</sup>
Data/Restraints/parameters	3160/0/209
Goodness-of-fit on <i>F</i> <sup>2</sup>	1.025
Final <i>R</i> indices [ <i>I</i> > 2 $\sigma$ ( <i>I</i> )]	<i>R</i> <sub>1</sub> = 0.0716, w <i>R</i> <sub>2</sub> = 0.1670
<i>R</i> indices (all data)	<i>R</i> <sub>1</sub> = 0.0974,

	wR <sub>2</sub> = 0.1815
Largest diff. peak/hole (e Å <sup>-3</sup> )	1.39/-1.06

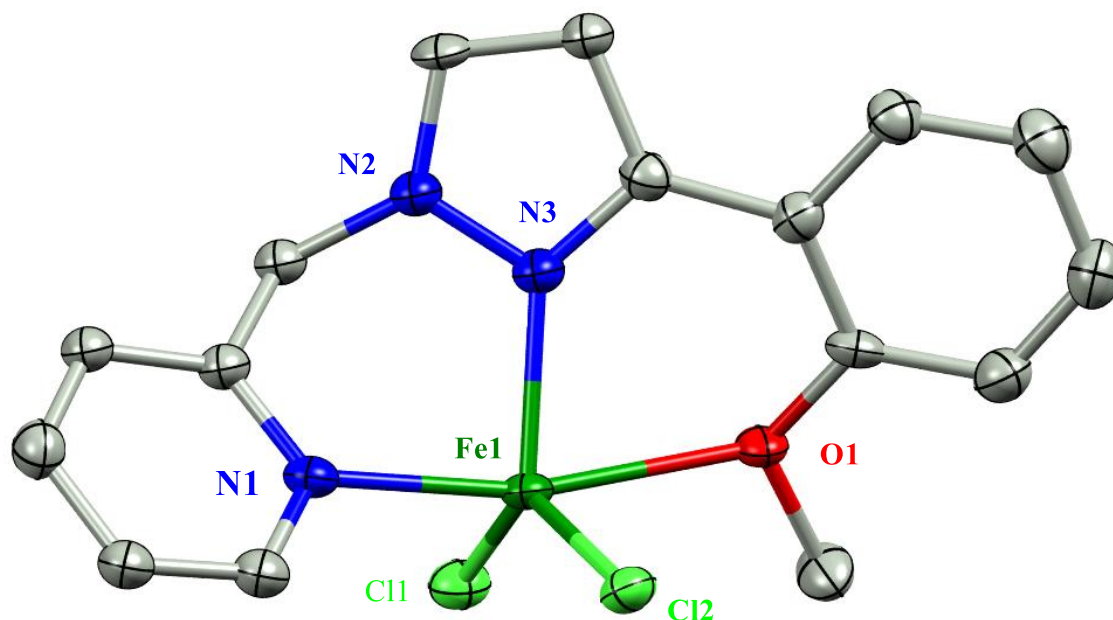


**Figure 3.5.1.** Molecular Structure of complex **3** showing 50% Ellipsoids [Hydrogen atoms are omitted for clarity. Selected bond distances (Å) and angles (deg): Fe1-O1 2.360(3), Fe1-N1 2.171(3); Fe1-N3 2.051(3), Fe1-Cl1 2.294(3); Fe1-Cl2 2.294(10) and O1-Fe1-N3 166.239(1), N1-Fe1-N3 90.340(9), Cl1-Fe1-Cl2 133.153(9); N3-Fe1-Cl1 110.473(8), N3-Fe1-Cl2 110.473(9)

**<sup>1</sup>H AND <sup>13</sup>C NMR spectra of ligand L3 and some products:**

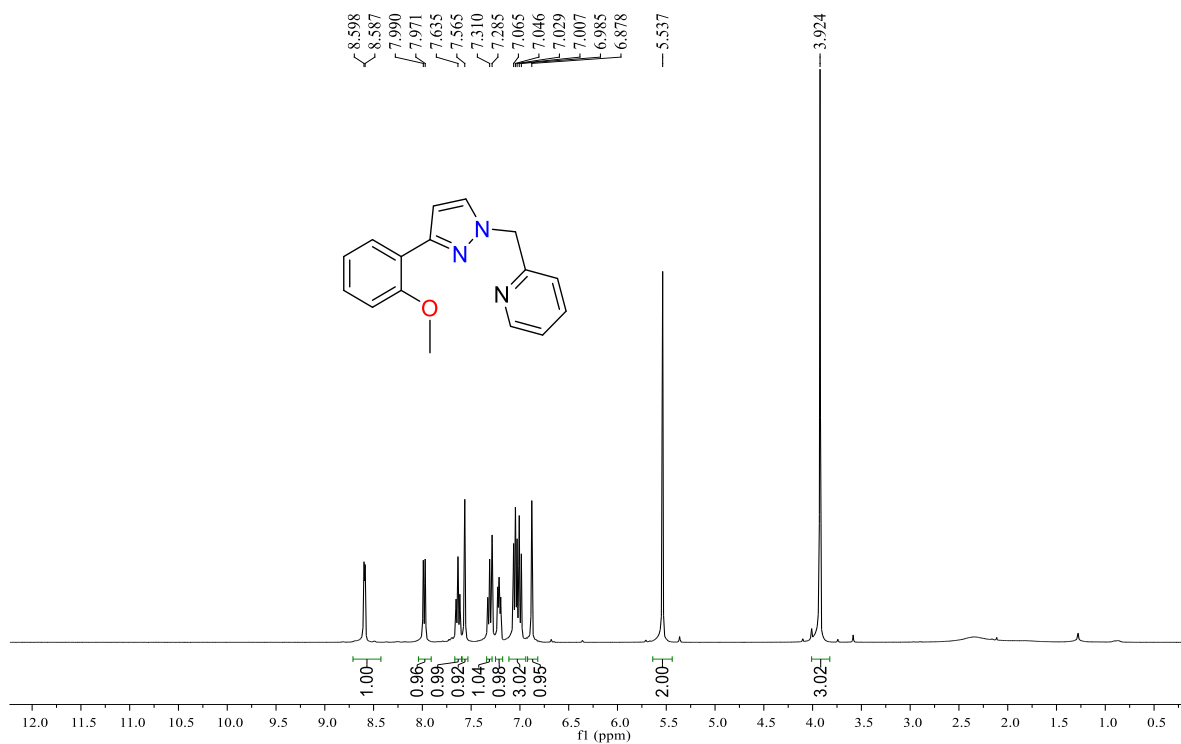


**Figure 3.5.2.** <sup>1</sup>H NMR (400 MHz) spectrum of L<sub>4</sub> in CDCl<sub>3</sub> at r.t.

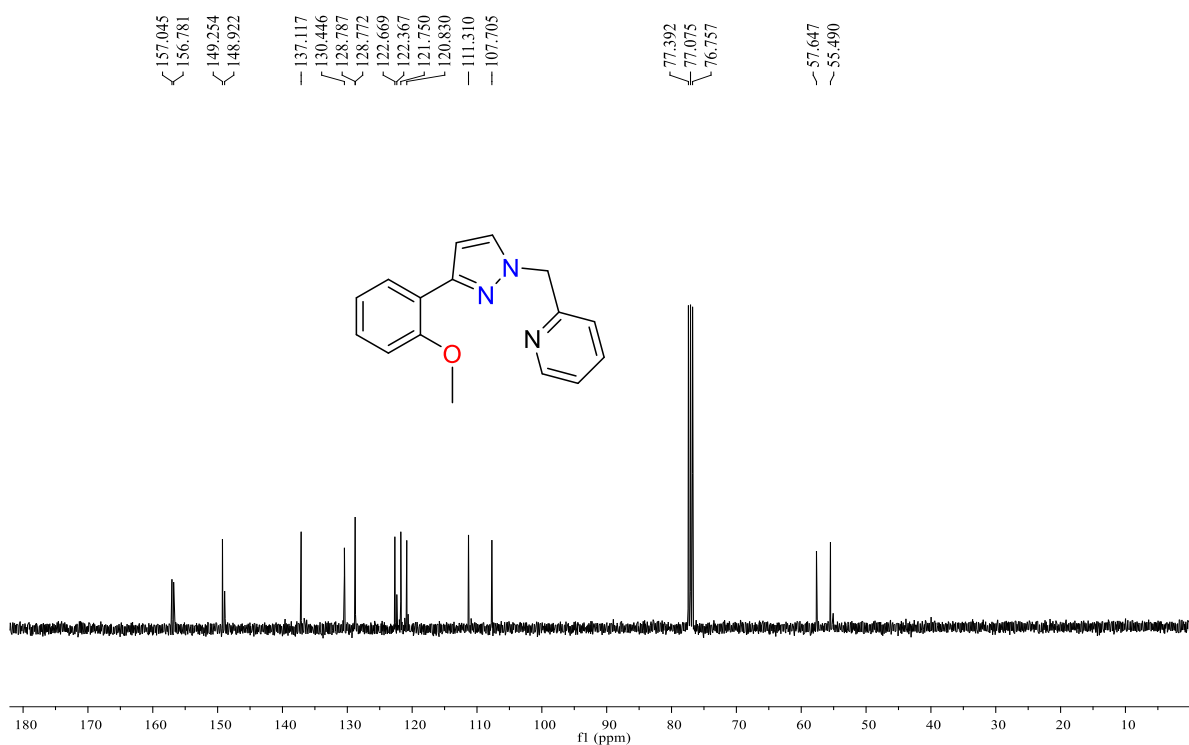


**Figure 3.5.2.** <sup>13</sup>C NMR (400 MHz) spectrum of L<sub>2</sub> in CDCl<sub>3</sub> at r.t.

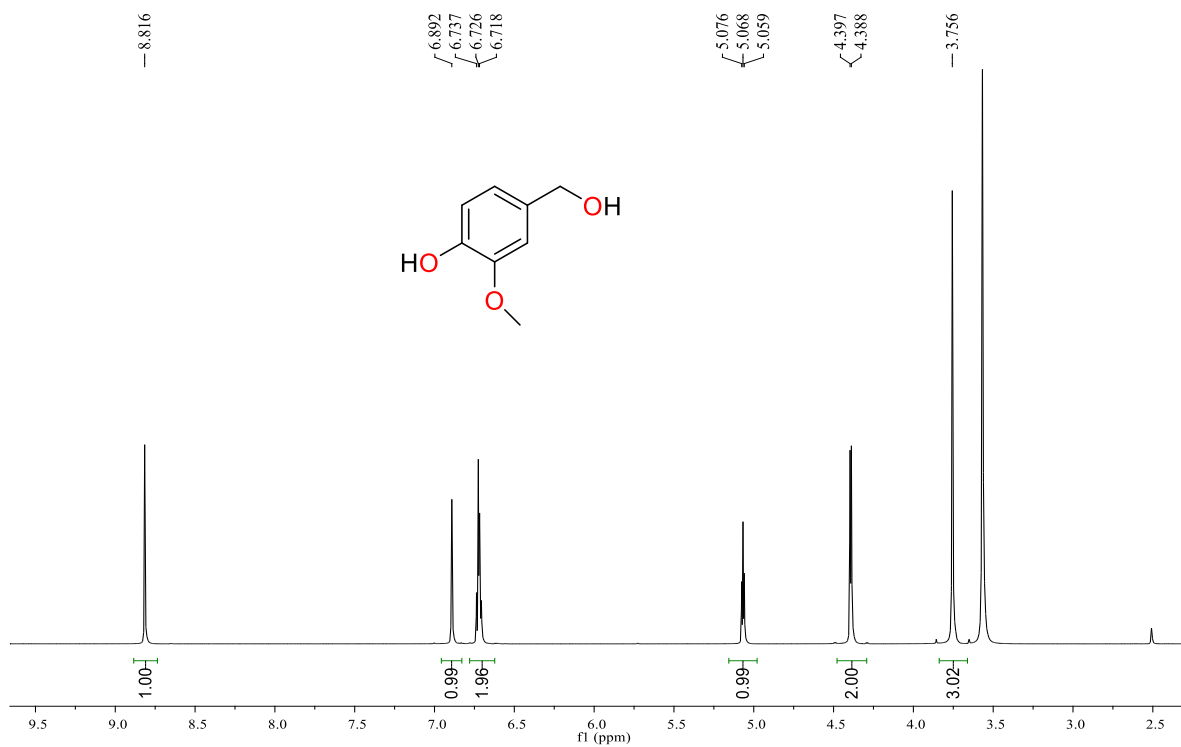


**Figure 3.5.3.**  $^1\text{H}$  NMR (400 MHz) spectrum of vanillyl alcohol in  $\text{CDCl}_3$  at r.t.

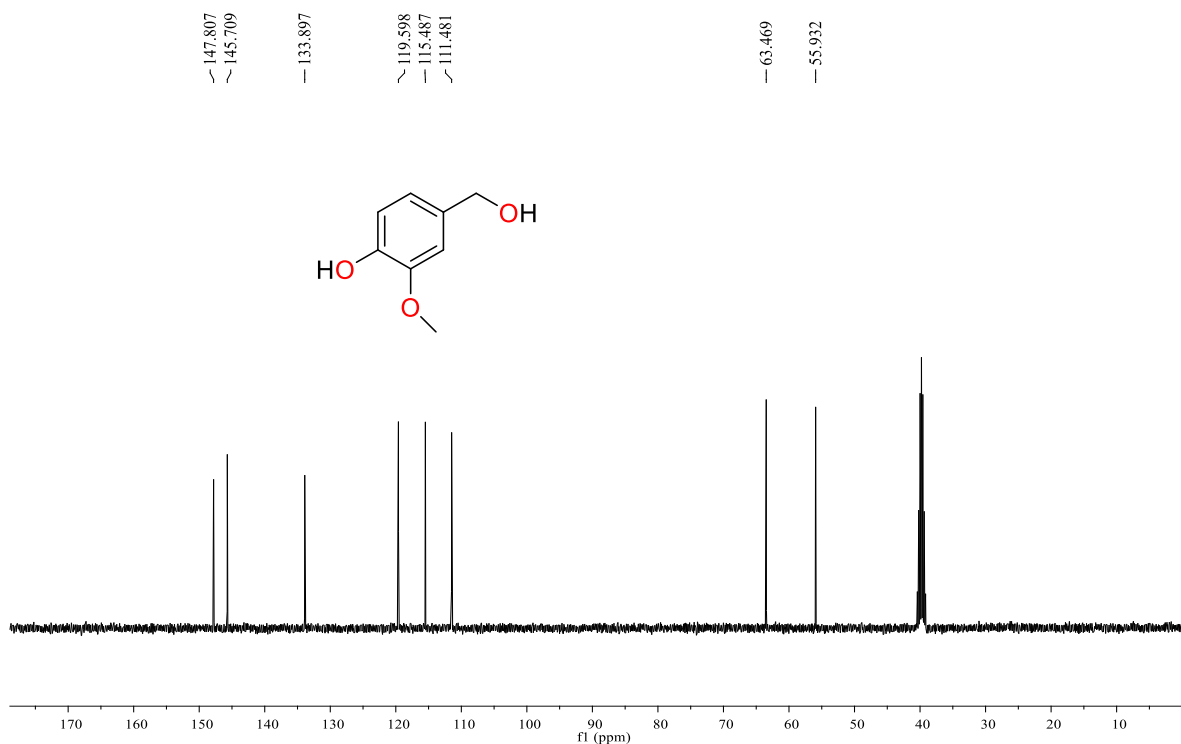


**Figure 3.5.4.**  $^{13}\text{C}$   $\{^1\text{H}\}$  NMR (101 MHz) spectrum of vanillyl alcohol in  $\text{CDCl}_3$  at r.t.

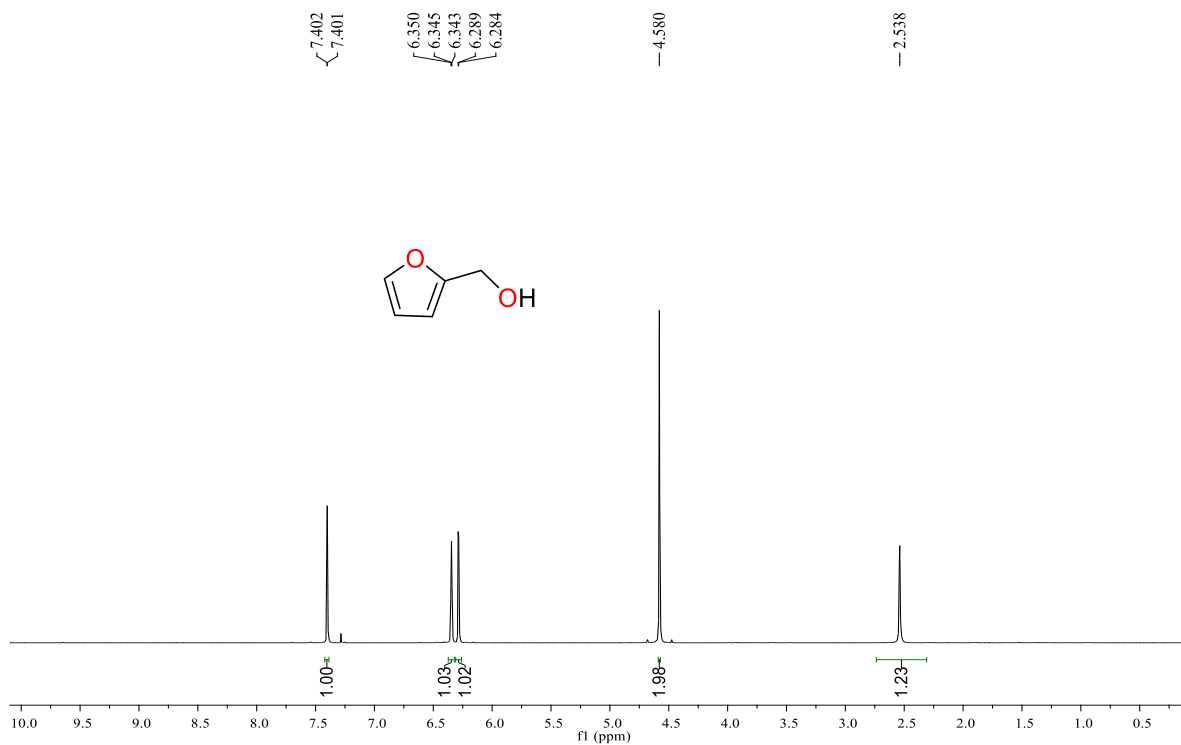


**Figure 3.5.5.**  $^1\text{H}$  NMR (400 MHz) spectrum of furfuryl alcohol in  $\text{CDCl}_3$  at r.t.

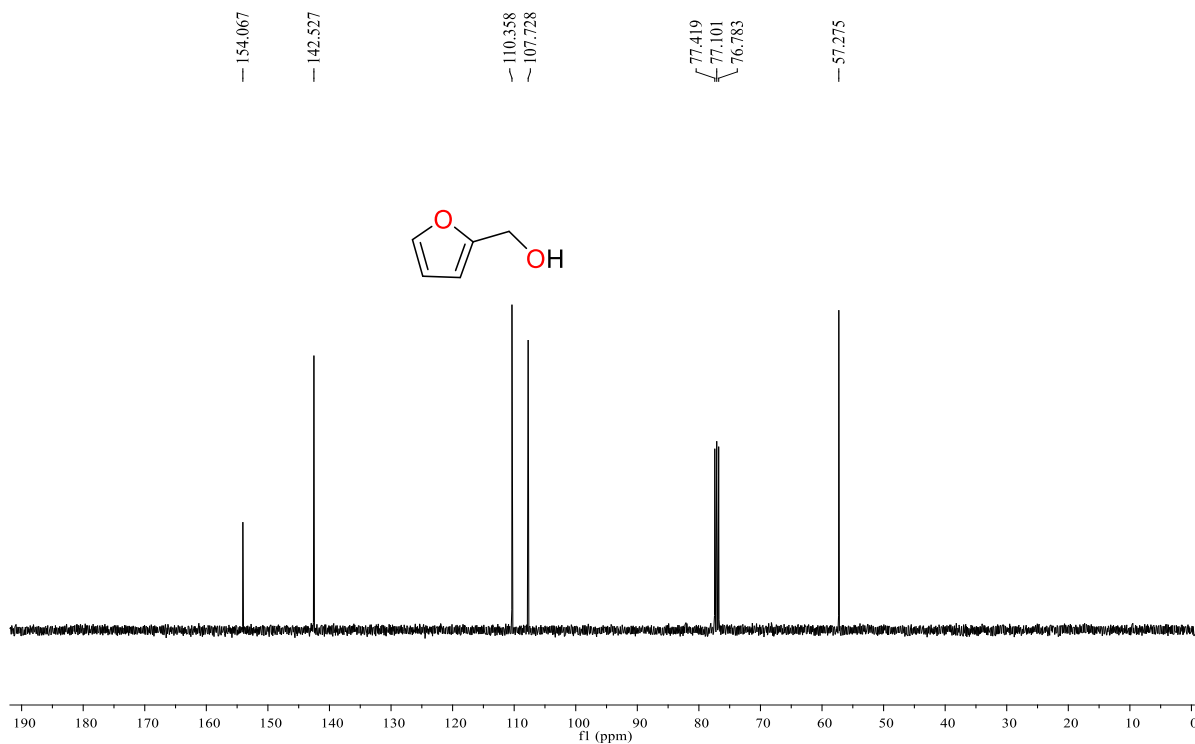


**Figure 3.5.6.**  $^{13}\text{C}$   $\{^1\text{H}\}$  NMR (100 MHz) spectrum of furfuryl alcohol in  $\text{CDCl}_3$  at r.t.

### 3.6 REFERENCES:

- (1) Clark, J. H.; Luque, R.; Matharu, A. S. Green chemistry, biofuels, and biorefinery. *Annu. Rev. Chem. Biomol. Eng.* **2012**, *3*, 183-207.
- (2) Kamm, B.; Gruber, P. R.; Kamm, M. *Biorefineries-industrial processes and products*. Wiley-VCH Weinheim, Germany: 2006.
- (3) Dutta, S.; De, S.; Saha, B.; Alam, M. I. Advances in conversion of hemicellulosic biomass to furfural and upgrading to biofuels. *Catal. Sci. Technol.* **2012**, *2*, 2025-2036.
- (4) Wang, Y.; De, S.; Yan, N. Rational control of nano-scale metal-catalysts for biomass conversion. *Chem. Commun.* **2016**, *52*, 6210-6224.
- (5) Safarian, S.; Unnpórsson, R.; Richter, C. A review of biomass gasification modelling. *Renewable Sustainable Energy Rev.* **2019**, *110*, 378-391.
- (6) He, J.; Li, H.; Riisager, A.; Yang, S. Catalytic transfer hydrogenation of furfural to furfuryl alcohol with recyclable Al-Zr@ Fe mixed oxides. *ChemCatChem.* **2018**, *10*, 430-438.
- (7) Wang, F.; Zhang, Z. Catalytic transfer hydrogenation of furfural into furfuryl alcohol over magnetic  $\gamma$ -Fe<sub>2</sub>O<sub>3</sub>@ HAP catalyst. *ACS Sustainable Chem. Eng.* **2017**, *51*, 942-947.
- (8) Wang, X.; Qiu, M.; Smith Jr, R. L.; Yang, J.; Shen, F.; Qi, X. Ferromagnetic Lignin-Derived Ordered Mesoporous Carbon for Catalytic Hydrogenation of Furfural to Furfuryl Alcohol. *ACS Sustainable Chem. Eng.* **2020**, *8*, 18157-18166.

- (9) Chaffey, D. R.; Davies, T. E.; Taylor, S. H.; Graham, A. E. Etherification reactions of furfuryl alcohol in the presence of Orthoesters and ketals: application to the synthesis of furfuryl ether Biofuels *ACS Sustainable Chem. Eng.* **2018**, *6*, 4996-5002.
- (10) Kung, Y.; Runguphan, W.; Keasling, J. D. From Fields to Fuels: Recent Advances in the Microbial Production of Biofuels. *ACS Synthetic Biology.* **2012**, *1*, 498-513.
- (11) Ramirez-Barria, C.; Isaacs, M.; Wilson, K.; Guerrero-Ruiz, A.; Rodríguez-Ramos, I. Optimization of ruthenium based catalysts for the aqueous phase hydrogenation of furfural to furfuryl alcohol. *Applied Catalysis A: General.* **2018**, *563*, 177-184.
- (12) Tukacs, J. M.; Bohus, M.; Dibó, G.; Mika, L. T. Ruthenium-catalyzed solvent-free conversion of furfural to furfuryl alcohol. *RSC Adv.* **2017**, *7*, 3331-3335.
- (13) Zhao, Y. Facile synthesis of Pd nanoparticles on SiO<sub>2</sub> for hydrogenation of biomass-derived furfural. *Environ. Chem. Lett.* **2014**, *12*, 185-190.
- (14) Li, M.; Hao, Y.; Cárdenas-Lizana, F.; Keane, M. A. Selective production of furfuryl alcohol via gas phase hydrogenation of furfural over Au/Al<sub>2</sub>O<sub>3</sub>. *Catal. Commun.* **2015**, *69*, 119-122.
- (15) Gao, X.; Tian, S.; Jin, Y.; Wan, X.; Zhou, C.; Chen, R.; Dai, Y.; Yang, Y. Bimetallic PtFe-Catalyzed Selective Hydrogenation of Furfural to Furfuryl Alcohol: Solvent Effect of Isopropanol and Hydrogen Activation. *ACS Sustainable Chem. Eng.* **2020**, *8*, 12722-12730.
- (16) Chen, X.; Zhang, L.; Zhang, B.; Guo, X.; Mu, X. Highly selective hydrogenation of furfural to furfuryl alcohol over Pt nanoparticles supported on gC<sub>3</sub>N<sub>4</sub> nanosheets catalysts in water. *Scientificreports.* **2016**, *6*, 1-13.

- (17) Nakagawa, Y.; Takada, K.; Tamura, M.; Tomishige, K. Total hydrogenation of furfural and 5-hydroxymethylfurfural over supported Pt–Ir alloy catalyst. *ACS Catal.* **2014**, *4*, 2718-2726.
- (18) Zhang, Z.; Tong, X.; Zhang, H.; Li, Y. Versatile catalysis of iron: tunable and selective transformation of biomass-derived furfural in aliphatic alcohol. *Green Chem.* **2018**, *20*, 3092-3100.
- (19) Xu, L.; Nie, R.; Lyu, X.; Wang, J.; Lu, X. Selective hydrogenation of furfural to furfuryl alcohol without external hydrogen over N-doped carbon confined Co catalysts. *Fuel Process. Technol.* **2020**, *197*, 106-205.
- (20) Xu, C.; Paone, E.; Rodríguez-Padrón, D.; Luque, R.; Mauriello, F. Recent catalytic routes for the preparation and the upgrading of biomass derived furfural and 5-hydroxymethylfurfural. *Chem. Soc. Rev.* **2020**, *49*, 4273-4306.
- (21) Kalong, M.; Hongmanorom, P.; Ratchahat, S.; Koo-amornpattana, W.; Faungnawakij, K.; Assabumrungrat, S.; Srifa, A.; Kawi, S. Hydrogen-free hydrogenation of furfural to furfuryl alcohol and 2-methylfuran over Ni and Co-promoted Cu/ $\gamma$ -Al<sub>2</sub>O<sub>3</sub> catalysts. *Fuel Process. Technol.* **2021**, *214*, 106-721.
- (22) Jiménez-Gómez, C. P.; Cecilia, J. A.; Durán-Martín, D.; Moreno-Tost, R.; Santamaría-González, J.; Mérida-Robles, J.; Mariscal, R.; Maireles-Torres, P. Gas-phase hydrogenation of furfural to furfuryl alcohol over Cu/ZnO catalysts. *J. Mol. Catal.* **2016**, *336*, 107-115.
- (23) Zhang, M.; Li, Z. Cu/Cu<sub>2</sub>O-MC (MC= mesoporous carbon) for highly efficient hydrogenation of furfural to furfuryl alcohol under visible light. *ACS Sustainable Chem. Eng.* **2019**, *7*, 11485-11492.

- (24) Gong, W.; Chen, C.; Zhang, Y.; Zhou, H.; Wang, H.; Zhang, H.; Zhang, Y.; Wang, G.; Zhao, H. Efficient synthesis of furfuryl alcohol from H<sub>2</sub>-hydrogenation/transfer hydrogenation of furfural using sulfonate group modified Cu catalyst. *ACS Sustainable Chem. Eng.* **2017**, *5*, 2172-2180.
- (25) Yuan, J.; Li, S.-S.; Yu, L.; Liu, Y.-M.; Cao, Y.; He, H.-Y.; Fan, K.-N. Copper-based catalysts for the efficient conversion of carbohydrate biomass into  $\gamma$ -valerolactone in the absence of externally added hydrogen. *Energy Environ. Sci.* **2013**, *6*, 3308-3313.
- (26) Thongratkaew, S.; Luadthong, C.; Kiatphuengporn, S.; Khemthong, P.; Hirunsit, P.; Faungnawakij, K. Cu-Al spinel-oxide catalysts for selective hydrogenation of furfural to furfuryl alcohol. *Catal. Today.* **2021**, *367*, 177-188.
- (27) Frainier, L. J.; Fineberg, H. H. Copper chromite catalyst for preparation of furfuryl alcohol from furfural. Patents: 1981.
- (28) Arora, S.; Gupta, N.; Singh, V. Improved Pd/Ru metal supported graphene oxide nano-catalysts for hydrodeoxygenation (HDO) of vanillyl alcohol, vanillin and lignin. *Green Chem.* **2020**, *22*, 2018-2027.
- (29) Rahmanivahid, B.; Pinilla-de Dios, M.; Haghighi, M.; Luque, R. Mechanochemical synthesis of CuO/MgAl<sub>2</sub>O<sub>4</sub> and MgFe<sub>2</sub>O<sub>4</sub> spinels for vanillin production from isoeugenol and vanillyl alcohol. *Molecules.* **2019**, *24*, 25-97.
- (30) Robertson, A.; Matsumoto, T.; Ogo, S. The development of aqueous transfer hydrogenation catalysts. *Dalton Trans.* **2011**, *40*, 10304-10310.
- (31) Magano, J.; Dunetz, J. R. Large-scale carbonyl reductions in the pharmaceutical industry. *Org. Process Res. Dev.* **2012**, *16*, 1156-1184.

- (32) Cervený, L. *Catalytic hydrogenation*. Elsevier: 1986.
- (33) de Vries, J. G.; Elsevier, C. J. *Handbook of homogeneous hydrogenation*. WeinheimWiley-VCH: 2007.
- (34) Andersson, P. G.; Munslow, I. J. *Modern reduction methods*. John Wiley & Sons: 2008.
- (35) Wang, D.; Astruc, D., The golden age of transfer hydrogenation. *Chem. Rev.* **2015**, *115*, 6621-6686.
- (36) Zhong, R.; Wei, Z.; Zhang, W.; Liu, S.; Liu, Q. A practical and stereoselective in situ NHC-cobalt catalytic system for hydrogenation of ketones and aldehydes. *Chem.* **2019**, *5*, 1552-1566.
- (37) Zeng, L.; Yang, H.; Zhao, M.; Wen, J.; Tucker, J. H.; Zhang, X. C1-Symmetric PNP ligands for manganese-catalyzed enantioselective hydrogenation of ketones: reaction scope and enantioinduction model. *ACS Catal.* **2020**, *10*, 13794-13799.
- (38) Farrar-Tobar, R. A.; Dell'Acqua, A.; Tin, S.; de Vries, J. G. Metal-catalysed selective transfer hydrogenation of  $\alpha$ ,  $\beta$ -unsaturated carbonyl compounds to allylic alcohols. *GreenChem.* **2020**, *22*, 3323-3357.
- (39) Jiang, L.; Zhou, P.; Zhang, Z.; Jin, S.; Chi, Q. Synthesis of Secondary Amines from one-pot reductive amination with formic acid as the hydrogen donor over an acid-resistant cobalt catalyst. *Ind. Eng. Chem. Res.* **2017**, *56*, 12556-12565.
- (40) Wang, S.; Huang, H.; Dorcet, V.; Roisnel, T.; Bruneau, C.; Fischmeister, C. Efficient Iridium catalysts for base-free hydrogenation of levulinic acid. *Organometallics.* **2017**, *36*, 3152-3162.

- (41) Zielinski, G. K.; Samojłowicz, C.; Wdowik, T.; Grela, K. In tandem or alone: a remarkably selective transfer hydrogenation of alkenes catalyzed by ruthenium olefin metathesis catalysts. *Org. Biomol. Chem.* **2015**, *13*, 2684–2688.
- (42) Everaere, K.; Mortreux, A.; Carpentier, J. F. Ruthenium (II)-Catalyzed Asymmetric Transfer Hydrogenation of Carbonyl Compounds with 2-Propanol and Ephedrine-Type Ligands. *Adv. Synth. Catal.* **2003**, *345*, 67-77.
- (43) Gladiali, S.; Alberico, E. Asymmetric transfer hydrogenation: chiral ligands and applications. *Chem. Soc. Rev.* **2006**, *35*, 226-236.
- (44) Ikariya, T.; Blacker, A. J. Asymmetric transfer hydrogenation of ketones with bifunctional transition metal-based molecular catalysts. *Acc. Chem. Res.* **2007**, *40*, 1300-1308.
- (45) Wang, C.; Wu, X.; Xiao, J. Broader, greener, and more efficient: Recent advances in asymmetric transfer hydrogenation. *Chem. - Asian.* **2008**, *3*, 1750-1770.
- (46) Wu, X.; Xiao, J. Aqueous-phase asymmetric transfer hydrogenation of ketones—a greener approach to chiral alcohols. *Chem. Commun.* **2007**, *24*, 2449-2466.
- (47) Ganguli, K.; Shee, S.; Panja, D.; Kundu, S. Cooperative Mn(i)-complex catalyzed transfer hydrogenation of ketones and imines. *Dalton Trans.* **2019**, *48*, 7358-7366.
- (48) Verley, A. Exchange of functional groups between two molecules. Exchange of alcohol and aldehyde groups. *Bull. Soc. Chim. Fr.* **1925**, *37*, 537-542.
- (49) Meerwein, H.; Schmidt, R. Ein neues verfahren zur reduktion von aldehyden und ketonen. *Liebigs Ann. Chem.* **1925**, *444*, 221-238.

- (50) Bigler, R.; Huber, R.; Mezzetti, A. Highly enantioselective transfer hydrogenation of ketones with chiral (NH)<sub>2</sub>P<sub>2</sub> macrocyclic iron (II) complexes. *Angew. Chem., Int. Ed.* **2015**, *127*, 5260-5263.
- (51) Gggg Espinal-Viguri, M.; Neale, S. E.; Coles, N. T.; Macgregor, S. A.; Webster, R. L. Room Temperature Iron-Catalyzed Transfer Hydrogenation and Regioselective Deuteration of Carbon–Carbon Double Bonds. *J. Am. Chem. Soc.* **2019**, *141*, 572-582.
- (52) Lopes, R.; Raya-Barón, Á.; Robalo, M. P.; Vinagreiro, C.; Barroso, S.; Romão, M. J.; Fernández, I.; Pereira, M. M.; Royo, B. Donor Functionalized Iron (II) N-Heterocyclic Carbene Complexes in Transfer Hydrogenation Reactions. *Eur. J. Inorg. Chem.* **2021**, *31*, 22-29.
- (53) Huo, S.; Wang, Q.; Zuo, W. An iron variant of the Noyori hydrogenation catalyst for the asymmetric transfer hydrogenation of ketones. *Dalton Trans.* **2020**, *49*, 7959-7967.
- (54) Funk, T. W.; Mahoney, A. R.; Sponenburg, R. A.; Zimmerman, K. P.; Kim, D. K.; Harrison, E. E. Synthesis and Catalytic Activity of (3, 4-Diphenylcyclopentadienone) Iron Tricarbonyl Compounds in Transfer Hydrogenations and Dehydrogenations. *Organometallics.* **2018**, *37*, 1133-1140.
- (55) Xue, Q.; Wu, R.; Wang, D.; Zhu, M.; Zuo, W. The Stabilization Effect of  $\pi$ -Backdonation Ligands on the Catalytic Reactivities of Amido-Ene (amido) Iron Catalysts in the Asymmetric Transfer Hydrogenation of Ketones. *Eur. J. Inorg. Chem.* **2020**, *51*, 3103-3110.
- (56) Zhang, G.; Yin, Z.; Tan, J. Cobalt (II)-catalysed transfer hydrogenation of olefins. *RSC Adv.* **2016**, *6*, 22419-22423.

- (57) Chen, F.; Sahoo, B.; Kreyenschulte, C.; Lund, H.; Zeng, M.; He, L.; Junge, K.; Beller, M. Selective cobalt nanoparticles for catalytic transfer hydrogenation of N-heteroarenes. *Chem.Sci.* **2017**, *8*, 6239-6246.
- (58) Jiang, B. L.; Ma, S. S.; Wang, M. L.; Liu, D. S.; Xu, B. H.; Zhang, S. J. Cobalt-Catalyzed Chemoselective Transfer Hydrogenation of C=C and C=O Bonds with Alkanols. *ChemCatChem.* **2019**, *11*, 1701-1706.
- (59) Chen, S.-j.; Lu, G.-p.; Cai, C. A base-controlled chemoselective transfer hydrogenation of  $\alpha$ ,  $\beta$ -unsaturated ketones catalyzed by  $[\text{IrCp}^*\text{Cl}_2]_2$  with 2-propanol. *RSC Adv.* **2015**, *5*, 13208 –13211.
- (60) Xu, C.; Zhang, L.; Dong, C.; Xu, J.; Pan, Y.; Li, Y.; Zhang, H.; Li, H.; Yu, Z.; Xu, L. Iridium-Catalyzed Transfer Hydrogenation of 1,10-Phenanthrolines using Formic Acid as the Hydrogen Source. *Adv. Synth. Catal.* **2016**, *358*, 567 –572.
- (61) Wang, R.; Tang, Y.; Xu, M.; Meng, C.; Li, F. Transfer Hydrogenation of Aldehydes and Ketones with Isopropanol under Neutral Conditions Catalyzed by a Metal–Ligand Bifunctional Catalyst  $[\text{Cp}^*\text{Ir}(2,2'\text{-bpy})(\text{H}_2\text{O})]$ . *J. Org. Chem.* **2018**, *83*, 2274 –2281.
- (62) Zhang, D.; Iwai, T.; Sawamura, M. Iridium-Catalyzed Alkene-Selective Transfer Hydrogenation with 1,4-Dioxane as Hydrogen Donor. *Org. Lett.* **2019**, *21*, 5867 –5872.
- (63) Murayama, H.; Heike, Y.; Higashida, K.; Shimizu, Y.; Yodsinsin, N.; Wongnongwa, Y.; Jungsuttiwong, S.; Mori, S.; Sawamura, M. Iridium-Catalyzed Enantioselective Transfer Hydrogenation of Ketones Controlled by Alcohol Hydrogen-Bonding and C(sp<sup>3</sup>)-H Noncovalent Interactions. *Adv. Synth. Catal.* **2020**, *362*, 4655 –4661.

- (64) Shee, S.; Paul, B.; Kundu, S. Counter Anion Controlled Reactivity Switch in Transfer Hydrogenation: A Case Study between Ketones and Nitroarenes. *ChemistrySelect*. **2017**, *2*, 1705-1710.
- (65) Bauri, S.; Donthireddy, S. N. R.; Illam, P. M.; Rit, A., Effect of Ancillary Ligand in Cyclometalated Ru(II)–NHC-Catalyzed Transfer Hydrogenation of Unsaturated Compounds. *Inorganic Chemistry* 2018, *57*, 14582-14593.
- (66) Paul, B.; Chakrabarti, K.; Kundu, S. Optimum bifunctionality in a 2-(2-pyridyl-2-ol)-1, 10-phenanthroline based ruthenium complex for transfer hydrogenation of ketones and nitriles: impact of the number of 2-hydroxypyridine fragments. *Dalton Trans.* **2016**, *45*, 11162 –11171.
- (67) Barrios-Rivera, J.; Xu, Y.; Wills, M. Probing the Effects of Heterocyclic Functionality in [(Benzene)Ru(TsDPENR)Cl] Catalysts for Asymmetric Transfer Hydrogenation. *Org. Lett.* **2019**, *21*, 7223 –7227.
- (68) Figliolia, R.; Cavigli, P.; Comuzzi, C.; Zotto, A. D.; Lovison, D.; Strazzolini, P.; Susmel, S.; Zuccaccia, D.; Ballico, M.; Baratta, W. CNN pincer ruthenium complexes for efficient transfer hydrogenation of biomass-derived carbonyl compounds. *Dalton Trans.* **2020**, *49*, 453 –465.
- (69) Melle, P.; Thiede, J.; Hey, D. A.; Albrecht, M. Highly Efficient Transfer Hydrogenation Catalysis with Tailored Pyridylidene Amide Pincer Ruthenium Complexes. *Chem. Eur. J.* **2020**, *26*, 13226 – 13234.
- (70) Xu, H.; Yang, P.; Chuanpravit, P.; Hirao, H.; Zhou, J. NickelCatalyzed Asymmetric Transfer Hydrogenation of Hydrazones and Other Ketimines. *Angew. Chem., Int. Ed.* **2015**, *127*, 5201 –5205.

- (71) Sabater, S.; Page, M. J.; Mahon, M. F.; Whittlesey, M. K. Stoichiometric and Catalytic Reactivity of Ni(6-Mes)(PPh<sub>3</sub>)<sub>2</sub>. *Organometallics*. **2017**, *36*, 1776–1783.
- (72) Garduno, J. A.; Garcia, J. J. Nickel-Catalyzed Transfer Hydrogenation of Benzonitriles with 2-Propanol and 1,4-Butanediol as the Hydrogen Source. *ACS Omega*. **2017**, *2*, 2337–2343
- (73) Hu, X.; Wang, G.; Qin, C.; Xie, X.; Zhang, C.; Xu, W.; Liu, Y. Ligandless nickel-catalyzed transfer hydrogenation of alkenes and alkynes using water as the hydrogen donor. *Org. Chem. Front.* **2019**, *6*, 2619–2623.
- (74) Segizbayev, M.; Öztöpcü, O. .; Hayrapetyan, D.; Shakhman, D.; Lyssenko, K. A.; Khalimon, A. Y. Transfer hydrogenation of aldehydes and ketones catalyzed using an aminophosphinite POCNH pincer complex of Ni(II). *Dalton Trans.* **2020**, *49*, 11950–11957.
- (75) Cummings, S. P.; Le, T.-N.; Fernandez, G. E.; Quiambao, L. G.; Stokes, B. J. Tetrahydroxydiboron-Mediated Palladium-Catalyzed Transfer Hydrogenation and Deuteration of Alkenes and Alkynes Using Water as the Stoichiometric H or D Atom Donor. *J. Am. Chem. Soc.* **2016**, *138*, 6107–6110.
- (76) Xuan, Q.; Song, Q. Diboron-Assisted Palladium-Catalyzed Transfer Hydrogenation of N-Heteroaromatics with Water as Hydrogen Donor and Solvent. *Org. Lett.* **2016**, *18*, 4250–4253.
- (77) Cao, B.; Wei, Y.; Shi, M. Palladium-catalyzed intramolecular transfer hydrogenation & cycloaddition of p-quinaminedethered alkylidenecyclopropanes to synthesize perhydroindole scaffolds. *Chem. Commun.* **2018**, *54*, 14085–14088.

- (78) Zhao, C.; Zhang, Z.; Liu, Y.; Shang, N.; Wang, H.-J.; Wang, C.; Gao, Y. Palladium Nanoparticles Anchored on Sustainable Chitin for Phenol Hydrogenation to Cyclohexanone. *ACS Sustainable Chem. Eng.* **2020**, *8*, 12304–12312.
- (79) Nishimura, S. *Handbook of Heterogeneous Catalytic Hydrogenation for Organic Synthesis*. John Wiley & Sons, 2001.
- (80) Tomar, P.; Nozoe, Y.; Ozawa, N.; Nishimura, S.; Ebitani, K. Formic Acid as a Hydrogen Source for the Additive-Free Reduction of Aromatic Carbonyl and Nitrile Compounds at Reusable Supported Pd Catalysts. *Catalysts*. **2020**, *10*, 875.
- (81) Eppinger, J.; Huang, K. Formic acid as a hydrogen energy carrier. *ACS Energy Lett.* **2017**, *2*, 188–195.
- (82) Zhang, D.; Ye, F.; Xue, T.; Guan, Y.; Wang, Y. M. Transfer hydrogenation of phenol on supported Pd catalysts using formic acid as an alternative hydrogen source. *Catal. Today*. **2014**, *234*, 133–138.
- (83) Weingart, P.; Thiel, W. R. Applying Le Chatelier's Principle for a Highly Efficient Catalytic Transfer Hydrogenation with Ethanol as the Hydrogen Source. *ChemCatChem*. **2018**, *10*, 4844–4848.
- (84) Zweifel, T.; Naubron, J. V.; Büttner, T.; Ott, T.; Grützmacher, H. Ethanol as hydrogen donor: highly efficient transfer hydrogenations with rhodium (I) amides. *Angew. Chem., Int. Ed.* **2008**, *47*, 3245–3249.
- (85) Zweifel, T.; Scheschkewitz, D.; Ott, T.; Vogt, M.; Grützmacher, H. Chiral [Bis(olefin)amine]rhodium(I) Complexes; Transfer Hydrogenation in Ethanol. *Eur. J. Inorg. Chem.* **2009**, *2009*, 5561–5576.

- (86) Lundberg, H.; Adolfsson, H. Ruthenium-catalyzed asymmetric transfer hydrogenation of ketones in ethanol. *Tetrahedron Letts.* **2011**, *52*, 2754-2758.
- (87) Ghosh, R.; Jana, N. C.; Panda, S.; Bagh, B. Transfer Hydrogenation of Aldehydes and Ketones in Air with Methanol and Ethanol by an Air-Stable Ruthenium–Triazole Complex. *ACS Sustainable Chem. Eng.* **2021**, *9*, 4903-4914.
- (88) Castellanos-Blanco, N.; Arévalo, A.; García, J. J., Nickel-catalyzed transfer hydrogenation of ketones using ethanol as a solvent and a hydrogen donor. *Dalton Trans.* 2016, *45*, 13604-13614.
- (89) Wang, Y., Huang, Z., Leng, X., Zhu, H., Liu, G., & Huang, Z. Transfer hydrogenation of alkenes using ethanol catalyzed by a NCP pincer iridium complex: scope and mechanism. *J. Am. Chem. Soc.*, **2018**, *140*, 4417-4429.
- (90) Dubey, A.; Khaskin, E. Catalytic Ester Metathesis Reaction and Its Application to Transfer Hydrogenation of Esters. *ACS Catal.* **2016**, *6*, 3998–4002.
- (91) Farrar-Tobar, R. A.; Wozniak, B.; Savini, A.; Hinze, S.; Tin, S.; de Vries, J. G. Base-Free Iron Catalyzed Transfer Hydrogenation of Esters Using EtOH as Hydrogen Source. *Angew. Chem., Int. Ed.* **2019**, *58*, 1129-1133.
- (92) Mazza, S.; Scopelliti, R.; Hu, X. Chemoselective hydrogenation and transfer hydrogenation of aldehydes catalyzed by iron (II) PONOP pincer complexes. *Organometallics.* **2015**, *34*, 1538-1545.
- (93) He, J.; Li, H.; Riisager, A.; Yang, S. Catalytic transfer hydrogenation of furfural to furfuryl alcohol with recyclable Al–Zr@ Fe mixed oxides. *ChemCatChem.* **2018**, *10*, 430-438.

- (94) Li, J.; Liu, J. I.; Zhou, H. J.; Fu, Y. Catalytic Transfer Hydrogenation of Furfural to Furfuryl Alcohol over Nitrogen-Doped Carbon-Supported Iron Catalysts. *ChemSusChem*. **2016**, *9*, 1339-1347.
- (95) Ma, M.; Hou, P.; Zhang, P.; Cao, J.; Liu, H.; Yue, H.; Tian, G.; Feng, S. Magnetic Fe<sub>3</sub>O<sub>4</sub> nanoparticles as easily separable catalysts for efficient catalytic transfer hydrogenation of biomass-derived furfural to furfuryl alcohol. *Appl. Catal., A*. **2020**, *602*, 117-709.
- (96) McElroy, C. R.; Constantinou, A.; Jones, L. C.; Summerton, L.; Clark, J. H. Towards a Holistic Approach to Metrics for the 21st Century Pharmaceutical Industry. *Green Chem*. **2015**, *17*, 3111–3121.
- (97) Allen, D. T.; Carrier, D. J.; Gong, J.; Hwang, B.-J.; Licence, P.; Moores, A.; Pradeep, T.; Sels, B.; Subramaniam, B.; Tam, M. K. C.; Zhang, L.; Williams, R. M. Advancing the Use of Sustainability Metrics in ACS Sustainable Chemistry and Engineering. *ACS Sustainable Chem. Eng*. **2018**, *6*, 2359-2360.
- (98) Driesbeke, M. A.; Du Prez, F. E. Sustainable Synthesis of Renewable Terpenoid-Based (Meth)acrylates Using the CHEM21 Green Metrics Toolkit. *ACS Sustainable Chem. Eng*. **2019**, *7*, 11633–11639.
- (99) Prieschl, M.; García-Lacuna, J.; Munday, R.; Leslie, K.; O’Kearney-McMullan, A.; Hone, C. A.; Kappe, C. O. Optimization and sustainability assessment of a continuous flow Ru-catalyzed ester hydrogenation for an important precursor of a  $\beta_2$ -adrenergic receptor agonist. *Green Chem*. **2020**, *22*, 5762–5770.

- (100) Jana, N. C.; Sethi, S.; Saha, R.; Bagh, B. Aerobic oxidation of vanillyl alcohol to vanillin catalyzed by air-stable and recyclable copper complex and TEMPO under base-free conditions. *Green Chem.* **2022**, *24*, 2542-2556.
- (101) Dalidovich, T.; Mishra, K. A.; Shalima, T.; Kudrjasova, M.; Kananovich, D. G.; Aav, R. Mechanochemical Synthesis of Amides with Uronium-Based Coupling Reagents: A Method for Hexaamidation of Biotin[6]uril. *ACS Sustainable Chem. Eng.* **2020**, *8*, 15703 –15715.
- (102) Zhu, Z.; Wang, Z.; Jian, Y.; Sun, H.; Zhang, G.; Lynam, J. M.; McElroy, C. R.; Burden, T. J.; Inight, R. L.; Fairlamb, I. J. S.; Zhang, W.; Gao, Z. Pd-Catalysed carbonylative Suzuki –Miyaura crosscouplings using Fe(CO)<sub>5</sub> under mild conditions: generation of a highly active, recyclable and scalable ‘Pd –Fe’ nanocatalyst. *Green Chem.* **2021**, *23*, 920 –926.
- (103) Peris, E.; Crabtree, R. H. Key factors in pincer ligand design. *Chem. Soc. Rev.* **2018**, *47*, 1959-1968.
- (104) Shang, R.; Ilies, L.; Nakamura, E. Iron-catalyzed ortho C–H methylation of aromatics bearing a simple carbonyl group with methylaluminum and tridentate phosphine ligand. *J. Am. Chem. Soc.* **2016**, *138*, 10132-10135.
- (105) Nishizawa, K.; Ouchi, M.; Sawamoto, M. Phosphine–ligand decoration toward active and robust iron catalysts in LRP. *Macromolecules.* **2013**, *46*, 3342-3349.
- (106) Rathke, J.; Muetterties, E. Phosphine chemistry of iron (0) and (II). *J. Am. Chem. Soc.* **1975**, *97*, 3272-3273.

- (107) He, Y.-M.; Fan, Q.-H. Phosphine-free chiral metal catalysts for highly effective asymmetric catalytic hydrogenation. *Org. Biomol. Chem.* **2010**, *8*, 2497–2504.
- (108) Zhang, C.; Liu, J.; Xia, C. Arylpalladium-NHC complex: efficient phosphine-free catalyst precursors for the carbonylation of aryl iodides with amines or alkynes. *Org. Biomol. Chem.* **2014**, *12*, 9702–9706.
- (109) Puylaert, P.; Dell'Acqua, A.; Ouahabi, F. E.; Spannenberg, A.; Roisnel, T.; Lefort, L.; Hinze, S.; Tin, S.; de Vries, J. G. Phosphine-free cobalt catalyst precursors for the selective hydrogenation of olefins. *Catal. Sci. Technol.* **2019**, *9*, 61–64.
- (110) Guo, B.; Yu, T.-Q.; Li, H.-X.; Zhang, S.-Q.; Braunstein, P.; Young, D. J.; Li, H.-Y.; Lang, J.-P. Phosphine Ligand-Free Ruthenium Complexes as Efficient Catalysts for the Synthesis of Quinolines and Pyridines by Acceptorless Dehydrogenative Coupling Reactions. *ChemCatChem.* **2019**, *11*, 2500–2510.
- (111) Wu, X.-J.; Wang, H.-J.; Yang, Z.-Q.; Tang, X.-S.; Yuan, Y.; Su, W.; Chen, C.; Verpoort, F. Efficient and phosphine-free bidentate N-heterocyclic carbene/ruthenium catalytic systems for the dehydrogenative amidation of alcohols and amines. *Org. Chem. Front.* **2019**, *6*, 563–570.
- (112) Jana, A.; Das, K.; Kundu, A.; Thorve, P. R.; Adhikari, D.; Maji, B. A Phosphine-Free Manganese Catalyst Enables Stereoselective Synthesis of (1 + n)- Membered Cycloalkanes from Methyl Ketones and 1,n-Diols. *ACS Catal.* **2020**, *10*, 2615–2626.
- (113) Panda, S.; Saha, R.; Sethi, S.; Ghosh, R.; Bagh, B. Efficient  $\alpha$ -Alkylation of Arylacetonitriles with Secondary Alcohols Catalyzed by a Phosphine-Free Air-Stable Iridium(III) Complex. *J.org.Chem.* **2020**, *85*, 15610-15621.

- (114) Steinberg, A.; Ergaz, I.; Toscano, R. A.; Glaser, R. Crystallization of a Racemate Affords a  $P2_1/c$  Chiral Crystal Structure: Asymmetric Unit of Two Opposite Handed Molecules Simulates Achiral  $P2_1/n$  Packing via Pseudosymmetry. *Cryst. Growth Des.* **2011**, *11*, 1262-1270.
- (115) A. W. Addison, T. N. Rao, J. Reedijk, J. van Rijn and G. C. Verschoor, J. *DaltonTrans.* **1984**, 1349–1356.
- (116) Singh, A.; Maji, A.; Joshi, M.; Choudhury, A. R.; Ghosh, K., Designed pincer ligand supported Co(II)-based catalysts for dehydrogenative activation of alcohols: Studies on N-alkylation of amines,  $\alpha$ -alkylation of ketones and synthesis of quinolines. *DaltonTrans.* **2021**, *50*, 8567-8587.
- (117) Schönfeld, S.; Lochenie, C.; Hörner, G.; Weber, B., Iron(II) complexes with  $N_2O_2$  coordinating Schiff base-like equatorial ligand and 1,2-bis(pyridin-2-ylethynyl)benzene as axial pincer ligand. *Journal of Physics:CondensedMatter.* **2019**, *31*, 504-002.
- (118) Waldie, K. M.; Flajslik, K. R.; McLoughlin, E.; Chidsey, C. E.; Waymouth, R. M. Electrocatalytic alcohol oxidation with ruthenium transfer hydrogenation catalysts. *J. Am. Chem. Soc.* **2017**, *139*, 738-748.
- (119) Huo, S.; Wang, Q.; Zuo, W. An iron variant of the Noyori hydrogenation catalyst for the asymmetric transfer hydrogenation of ketones. *Dalton Trans.* **2020**, *49*, 7959-7967.
- (120) Zuo, W.; Prokopchuk, D. E.; Lough, A. J.; Morris, R. H. Details of the mechanism of the asymmetric transfer hydrogenation of acetophenone using the amine (imine) diphosphine iron precatalyst: the base effect and the enantiodetermining step. *ACS Catal.* **2016**, *6*, 301-314.

- (121) Demmans, K. Z.; Olson, M. E.; Morris, R. H. Asymmetric transfer hydrogenation of ketones with well-defined manganese (I) PNN and PNNP complexes. *Organometallics*. **2018**, *37*, 4608-4618.
- (122) Prat, D.; Wells, A.; Hayler, J.; Sneddon, H.; McElroy, C. R.; Abou-Shehada, S.; Dunn, P. J. Correction: CHEM21 selection guide of classical- and less classical-solvents. *Green Chem.* **2015**, *17*, 4848-4861.

## Chapter 4

### **Base Metal Iron Catalyzed Sustainable Oxidation of Vanillyl Alcohol to Vanillic Acid in Deep Eutectic Solvent and Implementation of Vanillic Acid for Fine-Chemical Synthesis**

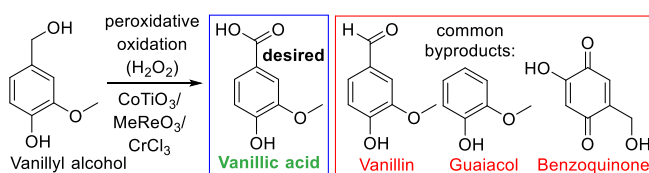
**4.1 ABSTRACT:** In the modern era, sustainable developments for the productions of fine chemicals from abundant biomass by utilizing various chemical transformations have become a strong trend of research in the scientific community. This may provide a sustainable alternative to petrochemicals as the major source of fine chemicals. Lignin is an alternative major source of monomeric phenolic compounds and the syntheses of fine chemicals by oxidising lignin-based monomeric phenolics are gaining serious attention. For instance, biomass derived vanillin or vanillyl alcohol can be oxidized to vanillic acid which has been employed as a new building block for the syntheses of various value-added products. In this context, an air-stable iron(II) complex has been synthesized and utilized as an excellent base-metal catalyst for the selective oxidation of vanillyl alcohol to vanillic acid. We used hydrogen peroxide and tert-butyl hydroperoxide as green oxidants. These peroxidative oxidations of vanillyl alcohol to vanillic acid were performed in metal-free type-III deep eutectic solvents as green and sustainable reaction media. After the first set of oxidations, the catalyst and the reaction medium were recycled five times without any noticeable change in catalytic performance. CHEM21 green metrics toolkit was also used to examine the sustainable and green features of the optimized oxidation protocol for the conversion of vanillyl alcohol to vanillic acid. Low E-factors (4.65) suggest waste minimized sustainable oxidations of vanillyl alcohol to vanillic acid. Finally, vanillic acid was used as a starting material for the syntheses of several fine chemicals with various (potential) applications such as flavorant, odorant, surfactant and bio-based plasticizer.

**4.2 INTRODUCTION:** Fossil fuels are undoubtedly the primary source of the majority of useful organic chemicals and their needs are ever growing to satisfy the demand of the rising human population with better quality of living standards. But petro-based resources have limited reserves and they are non-renewable. Hence, their exponentially growing demand will certainly cause shortage in the foreseeable future. In addition, extensive use of fossil fuels has generated various serious environmental concerns. Therefore, searching for alternatives to non-renewable petroleum resources has become a strong trend in research in present era. In this context, the proper use of biomass feedstock, which is renewable, can certainly provide a vital alternative to fossil fuels. Thus, bio-refineries may play an important role in biomass valorization and the use of biorefinery to produce a wide range of fine chemicals has attracted a serious attention.<sup>1, 2</sup> Hemicellulose, cellulose and lignin are the three primary component of lignocellulosic biomass. Most of the bio-originated fine chemicals are aliphatic in nature and cellulose is considered as their major source.<sup>3</sup> In contrast, lignin contains a wide variety of aromatic compounds and thus, the effective valorization of lignin in the biorefinery is an essential task. Already, lignin, as the second largest resource of biomass, has been established itself as a major source of aromatic fine chemicals including fuel-grade compounds and several synthetic protocols of lignin-valorization are presently operational.<sup>4, 5</sup> Lignin produced from wood and cashew nutshell liquid is an important source of aromatic phenolic compounds such as p-coumaryl, p-sinapyl, coniferyl, veratryl and vanillyl alcohol.<sup>6</sup> In this context, oxidation of lignin-based aromatic phenolic compounds to value-added products has attracted a significant research interest. Vanillyl alcohol is considered as one of the most studied lignin-derived monomeric phenolic compounds which is further oxidized to vanillin, an aroma molecule with wide application in industry.<sup>7-9</sup> In addition, reactive groups in vanillin can be functionalized easily and thus, vanillin is also an interesting building block.<sup>10, 11</sup> Various groups have developed synthetic catalytic protocols

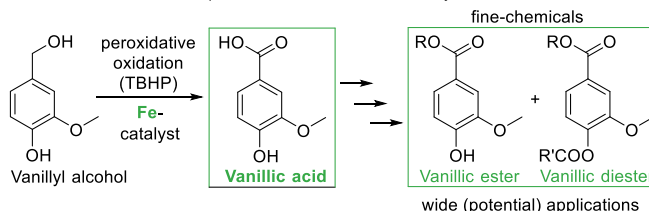
for the oxidation of vanillyl alcohol to vanillin. Recently, we reported a sustainable copper-catalyzed aerobic oxidation protocol for the selective oxidation of vanillyl alcohol to vanillin.<sup>12</sup> So far, the research community has paid little attention to the selective oxidation of vanillyl alcohol to vanillic acid which is often found as an over-oxidation product (along with other by-products) during the oxidation of vanillyl alcohol to vanillin. However, vanillic acid has a huge potential as a building block for the syntheses of various functional materials. For example, several simple esters of vanillic acids such as methyl, ethyl and butyl vanillate are effective perfuming agents in various commodities such as deodorants, room deodorizers, skin- and haircare products, cosmetics and toiletries. Ito and co-worker systematically evaluated the antioxidative properties of methyl, ethyl and butyl vanillate in multiple antioxidant assays and compared with well-known antioxidants.<sup>13</sup> Ma and co-workers utilized vanillic acid for the synthesis of thermoplastic polyesters with improved mechanical properties.<sup>14</sup> Gauthier and co-workers used vanillic acid for the synthesis of polyesters as bio-based alternative to commonly used polyethylene terephthalate (PET).<sup>15</sup> These vanillic acid-based polyesters exhibited good thermal stability. D'Arrigo and Griffini and coworkers utilized vanillic acid for the development of biobased polyurethane coatings with high biomass content, enhanced thermal stability and good adhesion performance.<sup>16</sup> Recently, Yang and coworkers synthesized vanillic diesters with different alkyl chains, which were used as effective plasticizers for poly(vinyl chloride) (PVC).<sup>17</sup> These bio-based vanillic diesters has provided good alternative to traditional phthalate plasticizers and the resulted PVC materials showed similar or better flexibility and stretchability as compared to PVC blend of dioctyl phthalate. Therefore, it is of high importance to develop efficient catalytic protocol for the selective oxidation of vanillyl alcohol to vanillic acid with high potential applicability.

#### **Scheme 4.2.1. Catalytic oxidation of vanillyl alcohol**

Previous work: Peroxidative oxidation of vanillyl alcohol to vanillic acid



Present work: Selective peroxidative oxidation of vanillyl alcohol to vanillic acid



Selective oxidation vanillyl alcohol to vanillic acid has been very much ignored in contrast to the selective oxidation vanillyl alcohol to vanillin. In a process of targeted oxidation of vanillyl alcohol to vanillin, vanillic acid has often been found as an over-oxidation product.<sup>18-25</sup> There are few reports for the selective oxidation vanillyl alcohol or vanillin to vanillic acid. In a very old report, stoichiometric amount of silver oxide (in situ generated from AgNO<sub>3</sub> and NaOH) was used as an oxidant to convert vanillin to vanillic acid.<sup>26</sup> The reaction was performed in basic aqueous solution at elevated temperature. Recently, Repo and coworkers reported heterogeneous gold nanoparticles supported on titania and alumina as catalyst for the selective oxidation of vanillin to vanillic acid.<sup>27</sup> The oxidation was performed in aqueous alkaline medium at elevated temperature (80 °C) using pressurized oxygen as oxidant. Very recently, Jiang and Wei and coworkers reported selective oxidation of vanillyl alcohol to vanillic acid (95% conversion and 86% isolated yield) using inorganic ligand-supported FeMo<sub>6</sub> system as heterogeneous catalyst.<sup>28</sup> The oxidation was performed in water at 70 °C using O<sub>2</sub> as oxidant and KCl as additive. In addition, a few reports described enzymatic oxidation of vanillin to vanillic acid using unheated milk,<sup>29</sup> soil bacteria<sup>30</sup> and freshly prepared liver slices of guinea-pig.<sup>31</sup> Compared to the oxidation of vanillin to vanillic acid, relatively difficult oxidation of vanillyl alcohol to vanillic acid is very rare and often

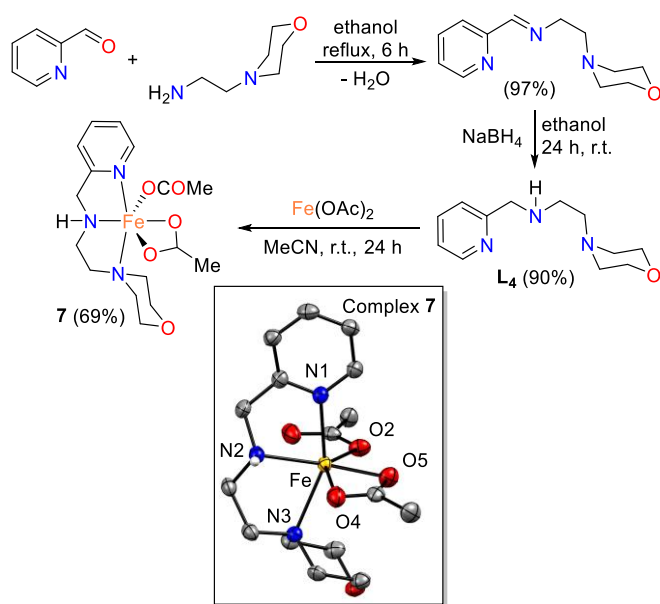
accompanied by the formation of significant amount of byproducts (Scheme 4.2.1). Ali and Hamid and coworkers used heterogeneous mixed metal oxide (CoTiO<sub>3</sub>) for the peroxidative oxidation of vanillyl alcohol in various organic solvents and high selectivity to vanillic acid could be obtained.<sup>32</sup> However, a significant amount of byproducts such as vanillin and guaiacol were also noted. Immobilized methyltrioxo rhenium has also been used as heterogeneous catalyst for the same purpose.<sup>33</sup> The peroxidative oxidation was performed in acetic acid. Microwave assisted peroxidative oxidation of vanillyl alcohol to vanillyl acid by using metal salts (particularly CrCl<sub>3</sub> and MnCl<sub>2</sub>) is also reported in a mixture of water and organic solvent.<sup>34</sup> In both cases, selectivity to either vanillic acid (10-12%) or vanillin (50-60%) was not good. In contrast to those reports, we have developed a highly selective catalytic protocol for the peroxidative oxidation of vanillyl alcohol to vanillic acid at r.t. (Scheme 4.2.1). Utilization of base metal iron catalyst (in low loading) is also advantageous. In contrast to the use of organic solvents, the use of environmentally benign deep eutectic solvent is beneficial.

The oxidation of alcohols to the corresponding carbonyl compounds or their complete oxidation to acids are among the central reactions in organic chemistry and are of interest for the development of environmentally benign processes, production of new materials and energy sources.<sup>35, 36</sup> Various hypervalent iodine compounds,<sup>37</sup> chromium salts,<sup>38</sup> activated DMSO compounds<sup>39</sup> and manganese dioxide<sup>40</sup> have been used as stoichiometric oxidants for alcohol oxidation. Stoichiometric oxidations are still in common use, despite the formation of a large amount of undesirable by-products. Therefore, there is a need of oxidants which are environmentally benign. Recent environmental compatibility and sustainable approach lead to two types of oxidations which are aerobic oxidation and peroxidative oxidation and various metal-catalysts have been developed. Mostly hydrogen peroxide<sup>41-43</sup> and tert-butyl hydrogen peroxide<sup>44-48</sup> have been used as green oxidants and the by-products are non-

hazardous. However, aerobic oxidation utilize air as the cheapest, most sustainable and green oxidant. In addition, by-products are water and hydrogen peroxide which are environmentally benign. However, pressurized oxygen cylinders are often used. Although various metal-catalysts (both homogeneous and heterogeneous) have been developed,<sup>49-59</sup> copper is a heavily used metal in aerobic oxidation of alcohols.<sup>60-64</sup> In the context of aerobic oxidation of lignin-model compound vanillyl alcohol, research community has particularly focused on the transformation of vanillyl alcohol selectively to vanillin with wide applications in commodity products. Various heterogeneous catalysts particularly a wide range of metal oxides and mixed metal oxides have been utilized for the selective aerobic oxidation of vanillyl alcohol to vanillin.<sup>65-76</sup> However, high temperature and high oxygen pressure have been used in most of the reports. In this context, the use of homogeneous catalysts is often beneficial; however, the number of reports is limited for the selective aerobic oxidation of vanillyl alcohol to vanillin.<sup>77-79</sup> We have also contributed in this field by developing air-stable and recyclable copper catalysts. Similar to aerobic oxidation, there are only a few examples of homogeneous system for peroxidative oxidation of vanillyl alcohol to vanillin.<sup>80-82</sup> Although selective aerobic oxidation of vanillyl alcohol to vanillin as an important aroma chemical has been studied extensively, selective oxidation of vanillyl alcohol to vanillic acid has been ignored. In the present report, we describe the development of a base-metal catalyzed peroxidative oxidation protocol for selective oxidation of vanillyl alcohol to vanillic acid (Scheme 4.2.1). An air-stable iron-complex has proved to be an excellent catalyst in various deep eutectic solvents at r.t. in the absence of added additives. We also demonstrated the syntheses of various vanillic esters and diesters as (potential) value-added chemicals.

**4.3 RESULT AND DISCUSSION:** Pincer ligands are considered as one of the most well-known, widely used and important class of ligands and coordination chemists have successfully utilized these tridentate ligands for the syntheses of a wide variety of transition metal complexes.<sup>83- 84</sup> A large majority of those complexes have found applications in varieties of catalytic transformations in the last twenty years. Often one or more phosphine donor arms are found in a large number of pincer ligands such as PNP, PNN and PCP and these phosphine-containing pincer ligands generally form air-sensitive metal complexes. In addition, alkylidene and carbanions are central in various other pincer ligands which also result in air-sensitive metal complexes. Therefore, phosphine-free (and carbene-free) ligand synthesis are important for the development of air-stable complexes and gaining serious attention in homogeneous catalysis.<sup>85-89</sup> Particularly, air-sensitive metal complexes are of no use in the field of oxidation of alcohol. Therefore, we wanted to use a tridentate NNN pincer ligand which is expected to give good stability of the resulted metal complex by tridentate coordination and might give an air-stable metal complex. We selected a known NNN pincer ligand **L4** which can be readily synthesized from cheap commercially available starting materials (Scheme 4.3.1). The condensation of 2-pyridinecarboxaldehyde with 2-morpholino ethylamine in ethanol under reflux yielded the Schiff base imine intermediate which was further reduced with sodium borohydride to get the desired amine ligand **L4** (Scheme 4.3.1). Ligand **L4** was characterized by standard characterization techniques such as <sup>1</sup>H and <sup>13</sup>C NMR spectroscopy. Thereafter, we focused on the synthesis of metal complex. We selected iron as it is non-toxic, cheap and earth-abundant (most abundant transition metal and second most abundant metal). Facile coordination of **L4** with cheap iron(II) acetate at r.t. in air resulted in the formation of complex **7** as an air-stable solid (Scheme 4.3.1).

**Scheme 4.3.1:** Synthesis of complex **7** (the molecular structure of complex **7** showing **70%** ellipsoids and all hydrogen atoms except N-H are omitted for clarity).



Complex 7 was NMR silent and was characterized by FT-IR, mass and elemental analysis. In the mass spectrum, a peak was observed at 395.0230 which corresponds to  $[M - H]^+$ . C(sp<sup>3</sup>)-H symmetric and asymmetric stretching bands of ligand L<sub>4</sub> were noticed at 2900-2750 cm<sup>-1</sup>. The corresponding C-H stretching bands were shifted to 3000-2900 cm<sup>-1</sup> for coordinated ligand in complex 1. Similar shifting of band from 1658 cm<sup>-1</sup> to 1632 cm<sup>-1</sup> was also observed for pyridyl C=N stretching. The broad N-H stretching appeared around 3400 cm<sup>-1</sup> in the IR spectrum of the free ligand L<sub>7</sub>, but a sharp peak at 3200 cm<sup>-1</sup> indicates the presence of a characteristic Fe-NH moiety in complex 7.<sup>90-92</sup> Further, the geometrical identity of complex 1 was confirmed by single crystal x-ray crystallography. Complex 7 crystallized in orthorhombic system with space group Pna21. X-ray analysis reveals that asymmetric unit has one  $[\text{Fe}(\text{L}1)(\text{OAc})_2]$  unit and the geometry around the iron center is distorted octahedral with the acetate groups occupied the equatorial sites. The pyridyl nitrogen (N1) and morpholine nitrogen (N3) coordinated axially to the metal center. The Fe-Npyridyl bond distance is 2.207(2) Å while the Fe-Nmorpholine distance is 2.378(2) Å. Rest of the bond distances and angles are in good agreement with previously reported similar iron(II) complexes with octahedral geometry.<sup>93-95</sup> It is worth to mention that the distance between

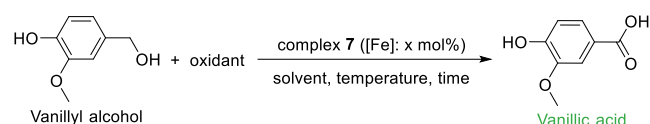
amine nitrogen(N2) and iron is 2.179(19) Å which is similar to the previously reported Fe-Namine distances.<sup>96-98</sup> Extensive N-H···O and C-H···O hydrogen bonding interactions as well as C-H···π interactions are also observed in the solid-state structure of complex 7.

With the air-stable iron complex (7) in hand, we explored the catalytic activity of complex 7 for the peroxidative oxidation of vanillyl alcohol by using tert-butyl hydroperoxide (TBHP) as standard oxidant (Table 4.3.1). Most homogeneous catalytic systems for the peroxidative/aerobic oxidation operate in hazardous organic solvents such as acetonitrile, toluene and dichloromethane. However, we wanted to perform the oxidation of vanillyl alcohol in sustainable reaction medium. Previously, we utilized mixtures of water and green organic solvents such as acetone, methanol and ethanol for the selective aerobic oxidation of vanillyl alcohol to vanillin. Finding new green reaction media for sustainable chemical transformations is important and we continued our search for other potential sustainable reaction media as alternative to water or other non-hazardous organic solvents. We fixed our attention to deep eutectic solvent (DES). In 2003, Abbott and coworkers reported DES for the first time as eutectic mixtures of urea and various quaternary ammonium salts.<sup>99</sup> DES, eutectic mixture of a hydrogen bond acceptor and a hydrogen bond donor, is considered as an emerging type of sustainable and green reaction media because of their minor economic and environmental impact. DESs come with several advantages over ionic liquids which are associated with several serious drawbacks such as high cost, high toxicity, complex synthesis and purification processes, and nonbiodegradability.<sup>100-106</sup> So far, DESs have limited use as solvents in organic reactions. With our goal of finding alternative sustainable reaction media, we decided to use a common DES, 1:2 (molar ratio) mixture of choline chloride and glycerol, as the reaction medium for the peroxidative oxidation of vanillyl alcohol (Table 4.3.1). We started using 2 eq. of TBHP as oxidant. Using 5 mol% of catalyst loading, we obtained complete conversion (with near quantitative yield) of vanillyl alcohol to vanillic acid in 3 h at

r.t. (entry 1). Reducing the catalyst loading to 3 (entry 2) and 2 mol% (entry 3) also gave full conversion to vanillic acid in 3 h at r.t. If the reaction time was shortened to just 1 h, complete conversion of vanillyl alcohol to vanillic acid was observed in presence of 2 mol% of catalyst loading (entry 3). If the catalyst loading was further reduced to just 1 mol%, vanillyl alcohol could not be completely oxidised to vanillic acid in 1 h at r.t. (entry 4). The obvious trend of decreasing catalytic activity with decreasing catalyst loading was observed from entry 3 to entry 4. 2 mol% catalyst loading is enough for full conversion of vanillyl alcohol (0.25 mmol) in 1 h, but 1 mol% catalyst loading is not capable of doing complete oxidation of 0.25 mmol vanillyl alcohol in 1h. Vanillin as intermediate oxidation product was also observed if the peroxidative oxidation of vanillyl alcohol was run for just half an hour in presence of 2 mol% catalyst loading at r.t. (entry 5). However, vanillyl alcohol was completely oxidized to vanillic acid in just half an hour if the reaction temperature was increased to 70 °C (entry 6). Thereafter, we used hydrogen peroxide instead of TBHP and much reduced yield of vanillic acid was obtained in 1 h along with decent amount of vanillin as intermediate oxidation product (entry 7). Thereafter, we increased the reaction time to 3 h in presence of hydrogen peroxide as oxidant and complete conversion of vanillyl alcohol to vanillin was noted (entry 8). If the reaction was performed in air without adding any other peroxide oxidant, we did not observe any oxidation of vanillyl alcohol to vanillic acid; less than 10% vanillin formation was noted (entry 9). So, TBHP was the best oxidant in the present system. Although slightly inferior than TBHP, hydrogen peroxide also acted as a good oxidant in the present transformation. We also carried out the peroxidative oxidation of vanillyl alcohol with TBHP in commonly used organic solvents such as acetonitrile (entry 10), toluene (entry 11) and dichloromethane (entry 12); however, poor conversion to vanillic acid was noted and presence of vanillin as well as unreacted vanillyl alcohol were also detected. Very poor conversion (<10%) was noted in absence of any iron catalyst (entry 13).

In presence of iron salts such as  $\text{Fe}(\text{NO}_3)_3$  and  $\text{Fe}(\text{OAc})_2$ , small amount of vanillic acid (<30%) was formed (entry 14 and 15). Peroxidative oxidation of vanillyl alcohol with TBHP was also performed under inert condition (in absence of dioxygen) using optimized reaction condition and complete conversion of vanillic acid was noted.

**Table 4.3.1** Catalytic performance of complex **7** for the peroxidative oxidation of vanillyl alcohol to vanillic acid in a mixture of choline chloride and glycerol (1:2 molar ratio).<sup>a</sup>

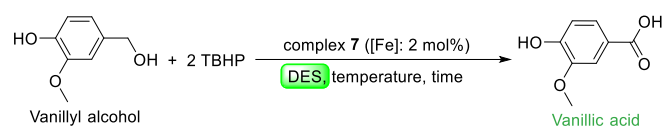


Ent.	<b>7</b> (mol%)	Oxidant (eq.)	Solvent	Temp. (°C)	Time (h)	Yield <sup>b</sup> (%)
1	5	TBHP (2)	DES	r.t.	12/6/3	>99 (96°)
2	3	TBHP (2)	DES	r.t.	3	>99 (97°)
<b>3</b>	<b>2</b>	<b>TBHP</b> <b>(2)</b>	<b>DES</b>	<b>r.t.</b>	<b>3/2/1</b>	<b>&gt;99 (97°)</b>
4	1	TBHP (2)	DES	r.t.	1	78 (75°)
5	2	TBHP (2)	DES	r.t.	0.5	72 (68°)
6	2	TBHP (2)	DES	70	0.5	>99 (96°)
7	2	H <sub>2</sub> O <sub>2</sub> (2)	DES	r.t.	1	60
<b>8</b>	<b>2</b>	<b>H<sub>2</sub>O<sub>2</sub> (2)</b>	<b>DES</b>	<b>r.t.</b>	<b>3</b>	<b>&gt;99 (97°)</b>
9	2	air	DES	r.t.	1	0
10	2	TBHP (2)	MeCN	r.t.	1	57
11	2	TBHP (2)	toluene	r.t.	1	46
12	2	TBHP (2)	DCM	r.t.	1	53
13	no	TBHP (2)	DES	r.t.	1	<10
14	Fe(NO <sub>3</sub> ) <sub>3</sub>	TBHP (2)	DES	r.t.	1	24
15	Fe(OAc) <sub>2</sub>	TBHP (2)	DES	r.t.	1	28

The best optimized reaction conditions for the peroxidative oxidation of vanillyl alcohol to vanillic acid are the following: A. 1 mol% complex **7**, 2 eq. TBHP, choline chloride/glycerol (1:2) as reaction medium, 1 h and r.t. (entry 3 in Table 4.3.1, depicted in bold) and B. 1 mol% complex **7**, 2 eq. hydrogen peroxide, choline chloride/glycerol (1:2) as reaction medium, 3 h

and r.t. (entry 8 in Table 4.3.1, depicted in bold). So, we successfully used a common DES (choline chloride/glycerol (1:2)) as a sustainable reaction media. We also wanted to check the catalytic performance of complex 1 for the peroxidative oxidation of vanillyl alcohol to vanillic acid in various other DESs. Therefore, we prepared a series of DESs (total ten) by combining various hydrogen-bond acceptor such as choline chloride (ChCl), tetramethyl ammonium chloride (TMAC), tetra butyl ammonium bromide (TBAB) and methyl triphenyl phosphonium bromide (MTPB) and various hydrogen bond donors such as glycerol, urea, thiourea and ethylene glycol. The catalytic oxidation of vanillyl alcohol was performed using TBHP as oxidant in the above DESs using previously optimized reaction condition (condition A, entry 3 in Table 4.3.1) and the results are summarized in Table 4.3.2. Complete oxidations of vanillyl alcohol to vanillic acid with almost quantitative isolated yields were observed in ChCl/glycerol (1:2) and ChCl/urea (1:2) (entry 1 and 2). Excellent yields of vanillic acid (92-93%) were also obtained in TBAB/glycerol (1:3) and ChCl/thiourea (1:2). (entry 3 and 4). Using MTPB/glycerol (1:3) and MTPB/ethylene glycol (1:2) as reaction media, we noted 76 and 65% yields of vanillic acid respectively (entry 5 and 6). A bit more than 50% yields of vanillic acid was observed if the oxidations of vanillyl alcohol were carried out in ChCl/ethylene glycol (1:2) and TMAC/ethylene glycol (1:2) (entry 7 and 8). Very poor yields (30-35%) of vanillic acid were noted in TMAC/glycerol (1:2) and TMAC/glycerol (1:3) as reaction media (entry 9 and 10). In case of incomplete oxidation to vanillic acid, we observed unreacted starting material vanillyl alcohol as well as vanillin as intermediate oxidation product. Therefore, it can be concluded that ChCl/glycerol (1:2) and ChCl/urea (1:2) are the best reaction media for the catalytic peroxidative oxidation of vanillyl alcohol to vanillic acid.

**Table 4.3.2. Catalytic performance of complex 7 for the peroxidative oxidation of vanillyl alcohol in various DESs.<sup>a</sup>**



Ent.	7 (mol%)	Solvent	Temp. (°C)	Time (h)	Yield <sup>b</sup> (%)
1	2	ChCl/ glycerol (1:2)	r.t.	1	97
2	2	ChCl/urea (1:2)	r.t.	1	95
3	2	TBAB/glycerol (1:3)	r.t.	1	93
4	2	ChCl/thiourea (1:2)	r.t.	1	92
5	2	MTPB/glycerol (1:3)	r.t.	1	76
6	2	MTPB/EG (1:2)	r.t.	1	65
7	2	ChCl/EG (1:2)	r.t.	1	56
8	2	TMAC/EG (1:2)	r.t.	1	52
9	2	TMAC/glycerol (1:2)	r.t.	1	35
10	2	TMAC/glycerol (1:3)	r.t.	1	30

<sup>a</sup>Reactions conducted in a vial (10 ml) with 0.25 mmol of vanillyl alcohol, 0.50 mmol of TBHP, 2 mol% of complex 7 in 2 mL of DES (molar ratio) as solvent at r.t. <sup>b</sup>Isolated yields of vanillic acid. ChCl, TBAB, TMAC, MTPB, MTAC and EG stand for choline chloride, tetra butyl ammonium bromide, tetramethyl ammonium chloride, methyl triphenyl phosphonium bromide and ethylene glycol, respectively.

**Table 4.3.3** Calculation of different metrics of vanillyl alcohol oxidation under optimized condition.

**Method: A**

**Method: B**

Met.	Yield	Conv.	Select.	A.E.	M.E.
A	99	100	99	68.9	49.9
B	99	100	99	89.4	75.0

Met.	Optimum Efficiency	Mass Intensity	Solvent	Catalyst	Catalyst Recovery
A	72.4	20.0	ChCl/gly c	Yes	Yes
B	83.9	19.4	ChCl/gly c	Yes	Yes

Met.	Media Recovery	Element	Reactor	Work up	Energy
A	Yes	Fe	Batch	Extraction	r.t.
B	Yes	Fe	Batch	Extraction	r.t.

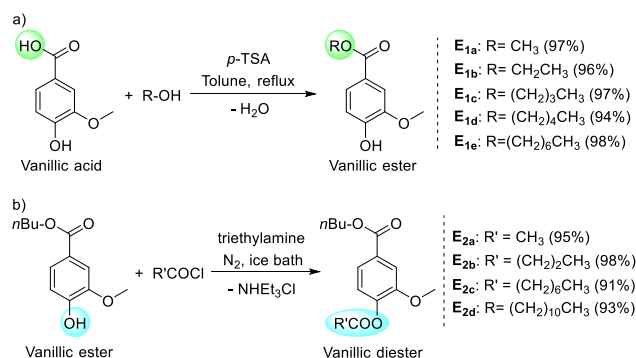
To establish the practical viability of the present catalytic protocol, we successfully performed two gram-scale reactions using two previously optimized reaction conditions and

the product vanillic acid was isolated in almost quantitative yield (Method A and B in Table 4.3.3). We also used CHEM21 green metrics toolkit to examine the green and sustainable features of the optimized catalytic protocol for the peroxidative oxidation of vanillyl alcohol to vanillic acid (see ESI for details).<sup>107-110</sup> The results are summarized in Table 4.3.3 (green flag, amber flag and red flag stand for an acceptable process, acceptable process with concerns and undesirable process, respectively). Almost quantitative yield, conversion and selectivity were noted for both Method A and B and these metrics were assigned with green flags. Method B is better than Method A in terms of atom economy (A.E.), reaction mass efficiency (M.E.) and optimum efficiency. This is due to the formation of lighter byproduct water in Method B as compared to the formation of heavier byproduct tert-butanol in Method A. Environmentally benign solvent was used for these catalytic oxidations and thus, both solvent and catalyst metrics got green flags. Base metal iron was used as catalyst and element metrics of both methods received green flags. In addition to the use of cheap and abundant base metal-based catalyst, it is important to recycle and reuse a catalyst for sustainable catalytic development. The role of solvent is equally important as solvents in a chemical reaction often produce the most amount of chemical waste. As a consequence, recycling the reaction media is even more important than catalyst recycling. Therefore, we set out to explore the possibility of catalyst and reaction media recovery and reuse. After performing the catalytic oxidation of vanillyl alcohol to vanillic acid using standard optimized reaction conditions, we extracted the product vanillic acid with ethyl acetate, another green solvent. For both Method A and B, the leftover mixture of reaction media and catalyst was reused for the second set of peroxidative oxidation of vanillyl alcohol. We did not observe any noticeable change in catalytic activity (isolated yields of vanillic acid: 97% in Method A and 96% in Method B). After the second set of reactions, the recovered reaction media and catalyst were reused for another four times without any significant change in activity for both

methods. Therefore, the solution of the iron catalyst in DES (ChCl/glycerol (1:2)) was effectively recycled five times. TON of 49 was obtained for the first run of both methods. If all six consecutive oxidations are considered, a rough TON of 290 was calculated. We also calculated the E-factor, a reliable measure to estimate the quantity of waste generated for the production of one kilogram of desired product.<sup>111-112</sup> A favourable process should have a E-factor of 1 to 5. The calculated E-factor for both Method A and B is 4.65.

In our catalytic oxidation protocol, vanillic acid was synthesized from vanillyl alcohol which is a renewable and abundant biomaterial derived from lignin biomass. Recently, vanillic acid has been utilized for the syntheses of various value-added derivatives with wide potential applications.<sup>13-17</sup> Finally, we tested the practical applicability of the present catalytic protocol for the oxidation of vanillyl alcohol to vanillic acid and the scope of this optimized oxidation protocols was extended in real-life applications. The robustness of this catalytic process motivated us to test its applicability in synthesizing various esters with proven applications (Scheme 4.3.2). At first we targeted the carboxylic moiety of vanillic acid to synthesize various vanillic esters with different alkyl chains (Scheme 4.3.2). Vanillic acid was reacted with various alcohols in presence of p toluenesulfonic acid and the corresponding vanillic esters E1a, E1b, E1c, E1d and E1e were isolated in excellent yields (E<sub>1a</sub>: 97%, E<sub>1b</sub>: 96%, E<sub>1c</sub>: 97%, E<sub>1d</sub>: 94% and E<sub>1e</sub>: 98%). Methyl, ethyl and butyl vanillate (E<sub>1a</sub>, E<sub>1b</sub> and E<sub>1c</sub>) are effective aroma chemicals used as perfuming agents in various commodities. Long chain fatty esters find possible application as surfactants. In the following step, we targeted the syntheses of several vanillic diesters which were previously used as effective plasticizers for poly(vinyl chloride). We used butyl vanillate as starting material and esterification of hydroxyl moiety of butyl vanillate with acyl chloride in presence of triethylamine resulted in the formation of various vanillic diesters (Scheme 4.3.2). Four vanillic diesters E<sub>2a</sub>, E<sub>2b</sub>, E<sub>2c</sub> and E<sub>2d</sub> were isolated in excellent yields (E<sub>2a</sub>: 95%, E<sub>2b</sub>: 98%, E<sub>2c</sub>: 91% and E<sub>2d</sub>: 93%).

**Scheme 4.3.2** Application of vanillic acid in the syntheses of vanillic esters and diesters with (potential) applications.



**4.4 CONCLUSION:** An air-stable phosphine-free NNN pincer ligand L4 was readily synthesized from cheap commercially available reagents. Facile coordination of the tridentate pincer ligand L4 with cheap iron(II) acetate resulted in the formation of a mononuclear octahedral complex 7 which was characterized by IR spectroscopy, mass spectrometry, elemental analysis and single crystal X-ray diffraction study. Complex 7 was proved to be an efficient catalyst for the selective peroxidative oxidation of vanillyl alcohol to vanillic acid (via vanillin as an intermediate oxidation product). Selective oxidation of vanillyl alcohol to vanillin as an important aroma molecule is well studied. Although vanillic acid as an abundant renewable biomaterial has proven to be an interesting building block in recent studies, selective oxidation of vanillyl alcohol to vanillic acid is ignored by research community. Developing sustainable catalytic protocol for selective oxidation of vanillyl alcohol to vanillic acid is an important development. Previously demonstrated methods, utilized heterogeneous metal oxides or metal salts based on non-abundant metal in organic solvents. Very rarely green solvent such as water was used; however, large amount of salt-additive was used. In contrast, using base metal iron catalyst is undoubtedly advantageous as iron is cheap, non-toxic and second most abundant metal on earth crust. Instead of using commonly used hazardous organic solvents for alcohol oxidations such as acetonitrile, toluene and dichloromethane, the use of environmentally friendly DES as reaction media is

also sustainable. A major setback of the previously reported processes is the generation of significant or large amount of by-products. In contrast, our catalytic oxidation method is extremely selective to desired product vanillic acid. Purification of final product was carried out by simple work-up process (extraction with ethyl acetate). Although catalyst recycle was done in a previous report, the recovery and reuse of reaction medium was not done for the oxidation of vanillyl alcohol to vanillic acid. In the present work, the catalyst and reaction media were recovered and recycled effectively without any noticeable change in catalytic activity. This helps to minimize the waste generated in the present process and it is reflected in low *E*-factors (4.65). As solvents produces huge amount of waste in most of the chemical process, the recycle of reaction medium in the present catalytic oxidation method is beneficial for the environment. In addition, the optimized condition used a metal-free type-III DES and the components glycerol and choline chloride are not harmful (as reflected by green H-codes). Gram-scale syntheses of vanillic acid shows the robust nature of this catalytic oxidation protocol. In previous reports, catalytic methods showed the oxidation of vanillyl alcohol or vanillin to vanillic acid; however, further utilization of vanillic acid was not demonstrated. In the present report, the potential applicability of this oxidation process is illustrated by synthesizing various vanillic esters and diesters with (potential) applications in real-life. This base metal catalyzed oxidation of vanillyl alcohol to vanillic acid is realistic for possible future use in industry. However, we performed the catalytic oxidant in batches. Oxidation in continuous flow reactor would be more attractive. In future, we will explore the possibility of performing this selective oxidation of vanillyl alcohol to vanillic acid in continuous flow reactor. Our peroxidative oxidation protocol requires H<sub>2</sub>O<sub>2</sub> and TBHP as oxidants and produces water and *tert*-butanol (though green) as by-product waste. Aerobic oxidation using air as most sustainable oxidant is more attractive and we will focus on developing base metal catalyst for aerobic oxidation of vanillyl alcohol to vanillic acid.

## 4.5 EXPERIMENTAL SECTION:

### Syntheses of ligand and corresponding iron complex

**General experimental.** Syntheses of ligand and iron complex were carried out in air. All solvents (acetonitrile, dichloromethane, diethyl ether, hexanes, ethyl acetate, ethanol, methanol) and chemicals were purchased from commercial suppliers and used without further purification. For recording NMR spectra,  $\text{CDCl}_3$  and  $\text{DMSO-d}_6$  was purchased from Sigma-Aldrich and used without further purification.  $^1\text{H}$  and  $^{13}\text{C}$  NMR spectra were recorded at Bruker AV-400 and JEOL-400 ( $^1\text{H}$  at 400 MHz and  $^{13}\text{C}$  at 101 MHz).  $^1\text{H}$  NMR chemical shifts are referenced in parts per million (ppm) with respect to tetramethylsilane ( $\delta$  0.00 ppm) and  $^{13}\text{C}\{^1\text{H}\}$  NMR chemical shifts are referenced in ppm with respect to  $\text{CDCl}_3$  ( $\delta$  77.16 ppm). The coupling constants ( $J$ ) are reported in hertz (Hz). The following abbreviations are used to describe multiplicity: s = singlet, bs = broad signal, d = doublet, t = triplet, q = quadrate, m = multiplate. High resolution mass spectra were recorded on a Bruker micrOTOF-Q II Spectrometer. Elemental analysis was carried out on a EuroEA Elemental Analyser. Infrared (IR) spectra were recorded on a Perkin-Elmer FT-IR spectrophotometer. Crystal data were collected with Rigaku Oxford diffractometer and with INCOATEC micro source (Mo- $K\alpha$  radiation,  $\lambda = 0.71073 \text{ \AA}$ , multilayer optics) at 293 K.

**Synthesis of (E)-N-(2-morpholinoethyl)-1-(pyridin-2-yl)methanimine.** In a pressure tube, picolinaldehyde (1.07 g, 10.0 mmol) in ethanol (5mL) was added dropwise to a solution of 2-morpholinoethan-1-amine (1.30 g, 10.0 mmol) in ethanol (15mL). The reaction mixture was allowed to stirred for 24 h at 65 °C. Then the reaction mixture was cooled down to room temperature and solvent was removed under reduced pressure to obtained the pure product as reddish liquid (2.12 g, 97%).  $^1\text{H}$  NMR ( $\text{CDCl}_3$ ):  $\delta$  7.16 (t,  $J=6$  Hz, 1H), 6.90 (d,  $J = 6.0$  Hz, 1H), 6.85 (t,  $J = 8.0$  Hz, 1H), 6.73 (t,  $J=7$  Hz, 1H), 5.85 (s, 1H), 5.54 (s, 1H), 3.43 (t,  $J=4$  Hz,

4H), 2.80 (t,  $J = 3$  Hz, 2H), 2.66 (t,  $J = 3$  Hz, 2H), 2.45 (t,  $J = 3$  Hz, 4H),  $^{13}\text{C}\{^1\text{H}\}$  NMR ( $\text{CDCl}_3$ ): 155.26, 125.34, 1123.69, 118.37, 114.56, 56.76, 44.68, 48.56, 44.27.

**Synthesis of L4.** To a solution of (E)-N-(2-morpholinoethyl)-1-(pyridin-2-yl)methanimine (2.19 g, 10.0 mmol) in methanol,  $\text{NaBH}_4$  (1.11 g, 30 mmol) was added slowly at 0 °C and the resultant reaction mixture was stirred at r.t. for 24 hours. After completion of the reaction, all the volatiles were removed under high vacuum. The product was extracted with dichloromethane (20 mL) to give a reddish liquid as pure compound (1.98 g, 90%).  $^1\text{H}$  NMR ( $\text{CDCl}_3$ ):  $\delta$  7.19 (t,  $J = 6$  Hz, 1H), 6.98 (d,  $J = 6.0$  Hz, 1H), 6.87 (t,  $J = 8.0$  Hz, 1H), 6.77 (t,  $J = 7$  Hz, 1H), 3.98 (s, 1H), 3.76 (t,  $J = 4$  Hz, 4H), 2.73 (t,  $J = 3$  Hz, 2H), 2.50 (t,  $J = 3$  Hz, 2H), 2.43 (t,  $J = 3$  Hz, 4H),  $^{13}\text{C}\{^1\text{H}\}$  NMR ( $\text{CDCl}_3$ ): 158.29, 128.66, 128.34, 122.62, 118.94, 116.34, 66.93, 57.42, 53.61, 52.41, 44.57.

Following are the  $^1\text{H}$  and  $^{13}\text{C}\{^1\text{H}\}$  NMR spectra of L1:

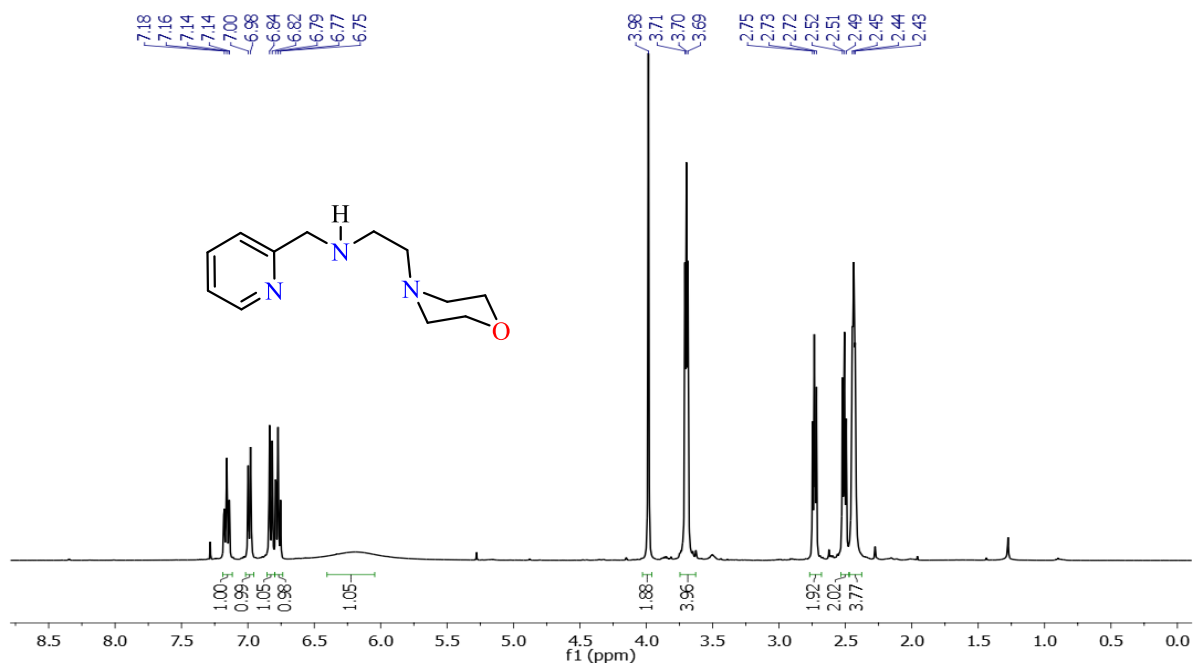


**Figure 4.5.1.**  $^1\text{H}$  NMR (400 MHz) spectrum of L4 in  $\text{CDCl}_3$  at r.t.

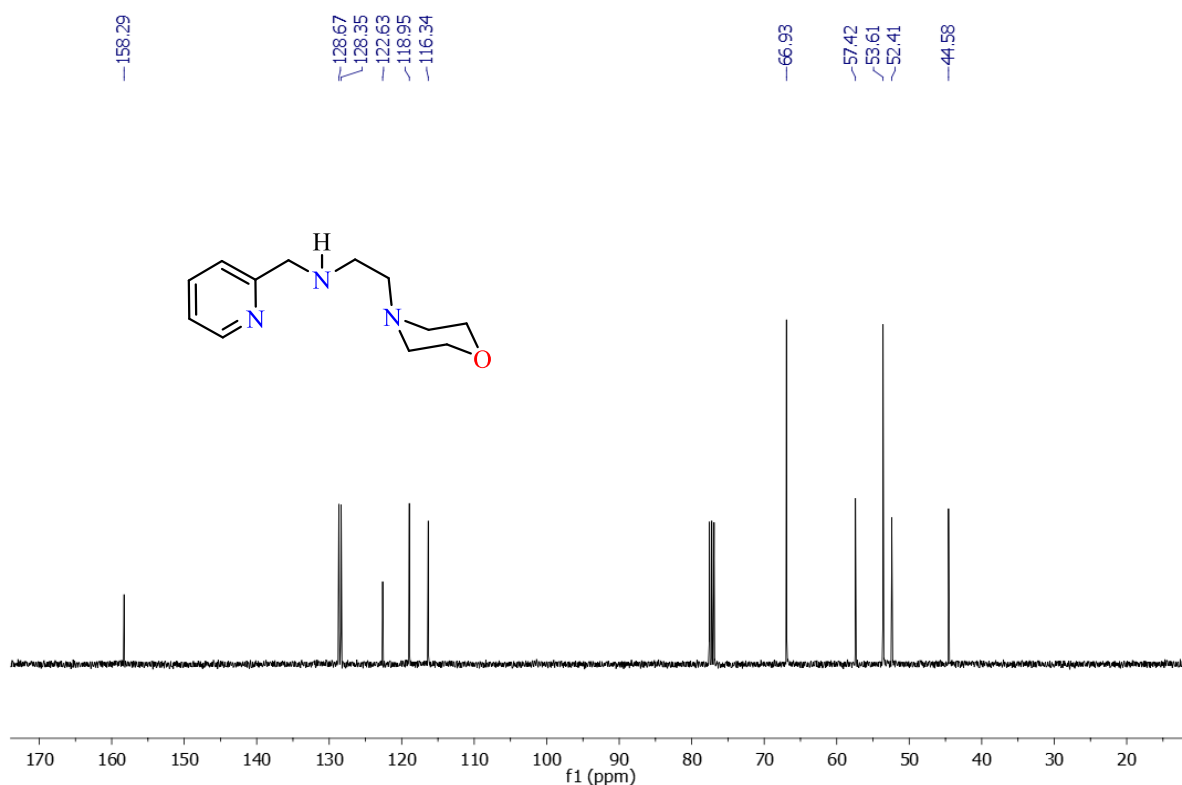


**Figure 4.5.2.**  $^{13}\text{C}\{^1\text{H}\}$  NMR (400 MHz) spectrum of **L4** in  $\text{CDCl}_3$  at r.t.

**Synthesis of 7.** A mixture of **L1** (0.221 g, 1.00 mmol) and  $\text{Fe}(\text{OAc})_2$  (0.173 g, 1.00 mmol) in acetonitrile (25 mL) under inert atmosphere was stirred at r.t. for 24 h resulting in a dark yellow precipitate. All volatiles were removed under high vacuum to give a dark yellow solid which was extracted with dichloromethane (15 mL). Then the solvent was removed under high vacuum to give a yellow solid as pure complex **1** (0.272 g, 69%). X-ray quality single crystals were obtained by slow diffusion of diethyl ether into a solution of **1** in dichloromethane. HRMS (ESI-TOF)  $m/z$ :  $[\text{M} - \text{H}]^+$  calcd for  $\text{C}_{16}\text{H}_{25}\text{FeN}_3\text{O}_5$  395.1029; found 395.0230. Anal. Calcd for  $\text{C}_{16}\text{H}_{26}\text{FeN}_3\text{O}_5$  (396.54): C, 48.50; H, 6.61; N, 10.60. Found: C, 49.21; H, 6.87; N, 10.01.

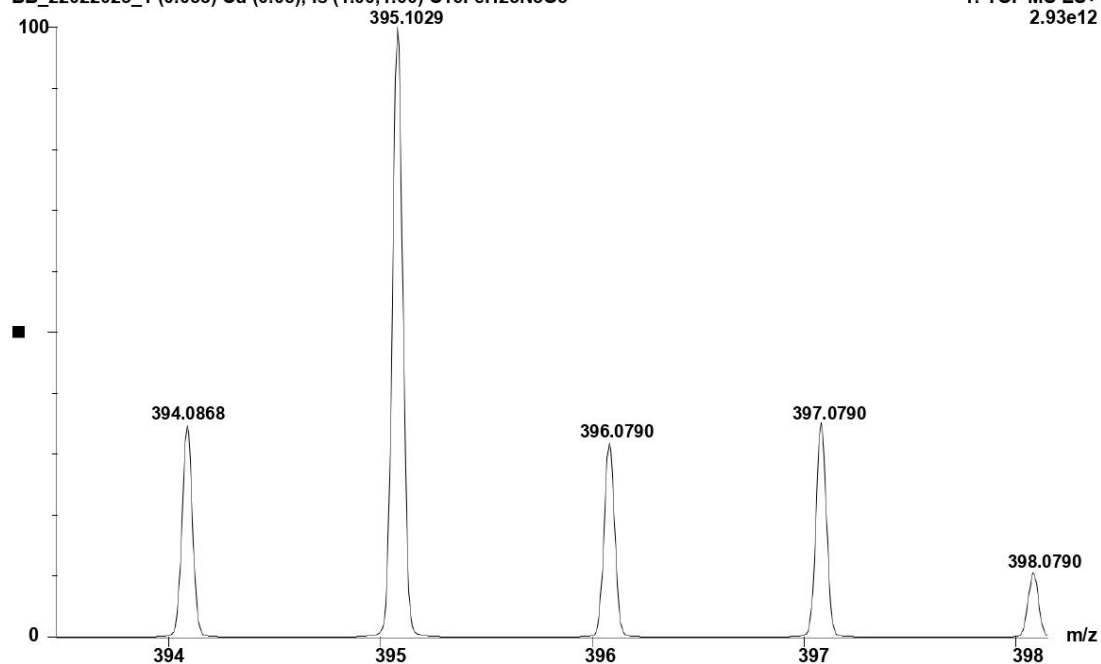
BB\_RG\_NNN\_iron complex 6

22-Feb-2023  
11:56:36

XEVO-G2XSQTOF#YFA1739

BB\_22022023\_1 (0.053) Cu (0.05); Is (1.00,1.00) C<sub>16</sub>FeH<sub>25</sub>N<sub>3</sub>O<sub>5</sub>

1: TOF MS ES+  
2.93e12



BB\_22022023\_1 25 (0.519) Cm (25:44)

1: TOF MS ES+  
2.57e6

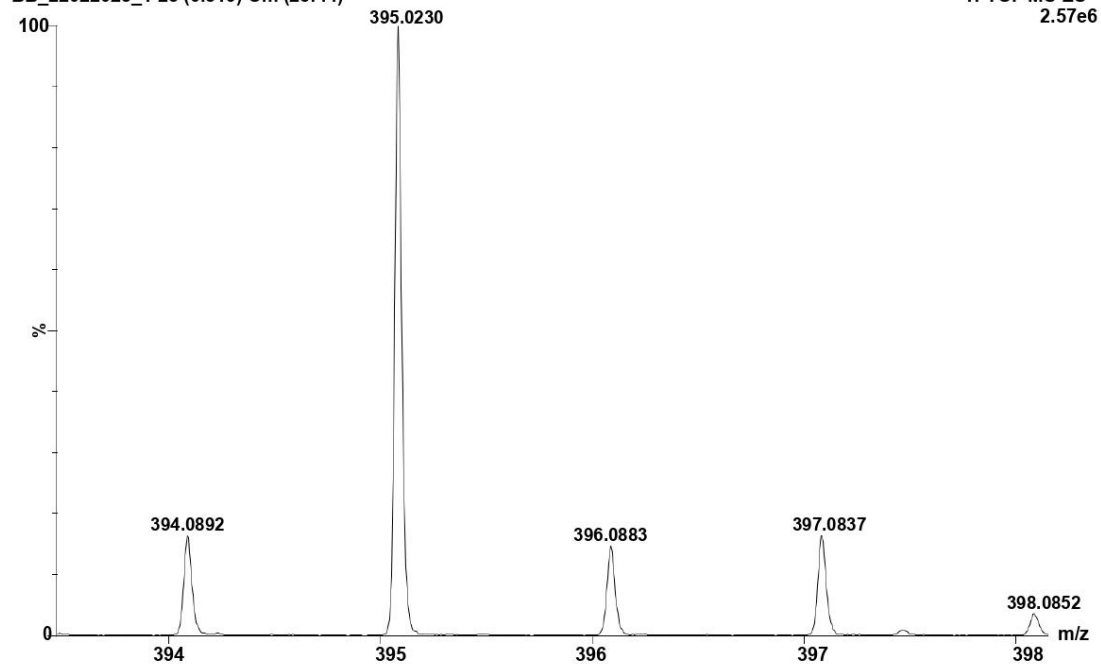


Figure 4.5.3. Mass spectrum of 7.

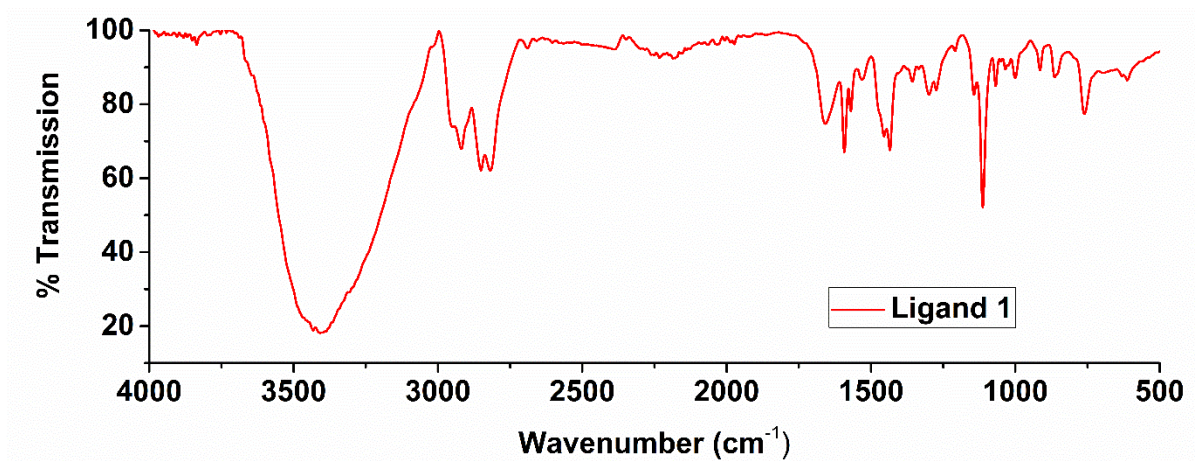


Figure 4.5.4. IR spectrum of L4.

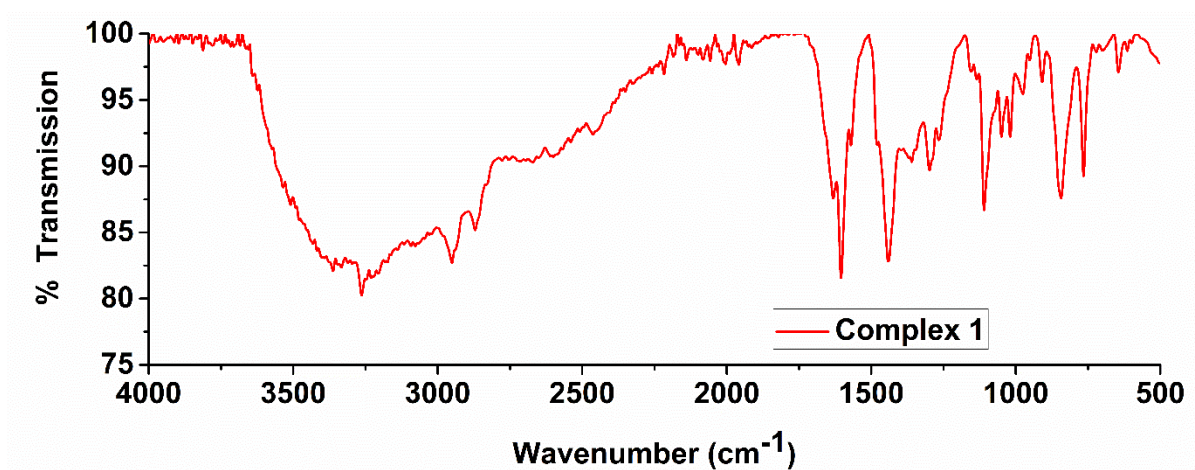


Figure 4.5.5. IR spectrum of 7.

**General procedure for oxidations (reaction optimization and).** Vanillyl alcohol (0.038 g, 0.25 mmol) and complex **7** (5/ 3/ 2/ 1 mol %) and TBHP (75  $\mu$ L, 0.50 mmol) were taken in deep eutectic solvent (ChCl/glycerol (1:2 molar ratio): 2 mL) and was transferred into a seal tube fitted with a magnetic stir-bar. The reaction mixture was heated at appropriate temperature (r.t./ 100  $^{\circ}$ C) in an oil bath for appropriate time (1 to 12 h). Thereafter, the reaction mixture was cooled down to r.t. (in case of heating) and was extracted using ethyl acetate (3 X 5 mL). All volatiles were removed under reduced pressure to give white solid as pure product. The product was analysed by  $^1$ H NMR spectroscopy using 1,3,5-trimethoxybenzene as standard.

Note: 20 mg complex **7** was dissolved in 4 mL of DES to prepare a stock solution. Required amounts of solutions were taken for oxidations using micropipette.

**General procedure for gram-scale oxidation of vanillyl alcohol.** Vanillyl alcohol (1.54 g, 10 mmol) and complex **7** (0.079 g, 0.20 mmol) and TBHP (2.8 mL) were taken in deep eutectic solvent (ChCl/glycerol (1:2 molar ratio): 20 mL) and was transferred into a seal tube fitted with a magnetic stir-bar. The reaction mixture was allowed to run for 1 hours at room temperature. Thereafter, the reaction mixture was extracted with ethyl acetate (3 X 15 mL) and all the volatiles were removed under reduced pressure to obtained white solid as pure product. The purity of product was analysed by <sup>1</sup>H NMR spectroscopy.

**General procedure for the esterification of vanillyl alcohol.** Vanillic acid (0.084 g, 0.50 mmol) and different alcohols (1.2 equivalent, 0.60 mmol) and *p*-toluenesulfonic acid (0.258 g, 1.5 mmol) were taken in dry toluene (3 mL) and transferred in a pressure tube. The reaction mixture was allowed to run for 24 h at reflux condition. After completion of the reaction the excess solvent and alcohol was removed using reduced pressure and solid was obtained. The solid was dissolved in ethyl acetate (5 mL). Then, the organic solution was washed with aqueous NaHCO<sub>3</sub> solutions and dried by anhydrous Na<sub>2</sub>SO<sub>4</sub>, filtered, and concentrated under reduced pressure to obtain oily liquid as crude product. The crude was further characterised by <sup>1</sup>H NMR spectroscopy and no further purification was needed.

**General procedure for the recycling of media and calculation of *E*-factor and TON:**

**Method A:** Vanillyl alcohol (1.54 g, 10 mmol), complex **7** (0.079 g, 0.20 mmol) and TBHP (2.8 mL, 20 mmol) were taken into a round bottom flask with a magnetic stir-bar. Thereafter, deep eutectic solvent (10 ml, (ChCl/glycerol (1:2 molar ratio))) was added into the mixture. The resultant reaction mixture was allowed to run for 1 h at r.t. After completion of the reaction, the reaction mixture was extracted using ethyl acetate (2 X 10 mL) and remaining

mixture of catalyst in DES was used for next reaction run. The ethyl acetate solution was dried under high vacuum to give pure vanillic acid (1.66 g, 99%). For the second run, vanillyl alcohol (1.52 g, 10 mmol) and TBHP (1.8 ml) were added to recovered mixture of reaction media and catalyst. The resultant reaction mixture was allowed to run for 1 h at r.t. Thereafter, entire process was repeated for five times. The yields of vanillic acid in the next five runs are the following: 2<sup>nd</sup> run (1.63 g, 97%), 3<sup>rd</sup> run (1.63 g, 97%), 4<sup>th</sup> run (1.62 g, 96%) 5<sup>th</sup> run (1.62 g, 96%) and 6<sup>th</sup> run (1.62 g, 96%). No significant change in catalytic activity was observed. Finally, used ethyl acetate was further recovered using solvent distillation technique (~80% recovered) and reused. The amount of media recovered is as follows: 1<sup>st</sup> run: 11.90 g; 2<sup>nd</sup> cycle: 11.75 g; 3<sup>rd</sup> cycle: 11.64 g; 4<sup>th</sup> cycle: 11.57 g; 5<sup>th</sup> cycle: 11.49 g; 6<sup>th</sup> cycle 11.37 g.

#### Overall E-factor for six consecutive reaction runs

**Method A:** 2 mol% of catalyst loading, r.t., 2 h in ChCl/glycerol (1:2)

Substrate:	Vanillyl alcohol (10 mmol)	= 1.54 g
	TBHP (20 mmol)	= 2.57 g
Catalyst:	Complex <b>7</b> (2 mol %)	= 0.079 g
Solvent:	ChCl/glycerol (10 mL) x 1.190	= 11.90 g
	Ethyl acetate (20 ml) x 0.90	= 18.00 g

$$E\text{-factor} = \frac{\text{mass (waste)}}{\text{mass (product)}}$$

$$= \frac{15.42 \text{ g (TBHP)} + 0.079 \text{ g (Iron catalyst)} + 11.90 \text{ g (reaction medium)} + 18.00 \text{ g (EtOAc to extract Vanillic acid)}}{1.64 \text{ g} + 1.63 \text{ g} + 1.63 \text{ g} + 1.62 \text{ g} + 1.62 \text{ g} + 1.62 \text{ g (product)}}$$

$$= \mathbf{4.65 \text{ kg waste / 1 kg of product}}$$

$$\text{TON (1st run)} = \frac{9.9 \text{ mmol (yield of vanillic acid)}}{0.2 \text{ mmol (amount of catalyst)}} = 49$$

$$\text{TON (all 6 runs)} = \frac{(9.9 + 9.7 + 9.7 + 9.6 + 9.6 + 9.6) \text{ mmol (yield of vanillic acid)}}{0.2 \text{ mmol (amount of catalyst)}} = 290$$

### **General procedure for the recycling of media and calculation of *E*-factor and TON:**

**Method B:** Vanillyl alcohol (1.52 g, 10 mmol), complex **7** (0.079 g, 0.20 mmol) and H<sub>2</sub>O<sub>2</sub> (2.4 mL, 20 mmol) were taken into a round bottom flask with a magnetic stir-bar. Thereafter, deep eutectic solvent (10 ml, (ChCl/glycerol (1:2 molar ratio))) was added into the mixture. The resultant reaction mixture was allowed to run for 3 h at r.t. After completion of the reaction, the reaction mixture was extracted using ethyl acetate (2 X 10 mL) and remaining mixture of catalyst in DES was used for next reaction run. The ethyl acetate solution was dried under high vacuum to give pure vanillic acid (1.66 g, 99%). For the second run, vanillyl alcohol (1.52 g, 10 mmol) and H<sub>2</sub>O<sub>2</sub> (0.68 mL) were added to recovered mixture of reaction media and catalyst. The resultant reaction mixture was allowed to run for 3 h at r.t. Thereafter, entire process was repeated for five times. The yields of vanillic acid in the next five runs are the following: 2<sup>nd</sup> run (1.62 g, 96%), 3<sup>rd</sup> run (1.63 g, 97%), 4<sup>th</sup> run (1.62 g, 96%) 5<sup>th</sup> run (1.62 g, 96%) and 6<sup>th</sup> run (1.61 g, 96%). No significant change in catalytic activity was observed. Finally, used ethyl acetate was further recovered using solvent distillation technique (~80% recovered) and reused. The amount of media recovered is as follows: 1<sup>st</sup> run: 11.90 g; 2<sup>nd</sup> cycle: 11.79 g; 3<sup>rd</sup> cycle: 11.65 g; 4<sup>th</sup> cycle: 11.55 g; 5<sup>th</sup> cycle: 11.50 g; 6<sup>th</sup> cycle 11.45 g.

### **Overall *E*-factor for six consecutive reaction runs**

**Method B:** 2 mol% of catalyst loading, r.t., 3 h in ChCl/glycerol (1:2)

Substrate:	Vanillyl alcohol (10 mmol)	= 1.540 g
	H <sub>2</sub> O <sub>2</sub> (20 mmol)	= 2.67 g
Catalyst:	Complex <b>1</b> (2 mol %)	= 0.079 g
Solvent:	ChCl/glycerol (10 mL) x 1.190	= 11.90 g
	Ethyl acetate (20 ml) x 0.902	= 18.00 g

$$E\text{-factor} = \frac{\text{mass (waste)}}{\text{mass (product)}}$$

$$= \frac{15.42 \text{ g (H}_2\text{O}_2) + 0.079 \text{ g (Iron catalyst)} + 11.9 \text{ g (reaction medium)} + 18.00 \text{ g (EtOAc to extract Vanillic acid)}}{1.66 \text{ g} + 1.62 \text{ g} + 1.63 \text{ g} + 1.62 \text{ g} + 1.62 + 1.61 \text{ g (product)}}$$

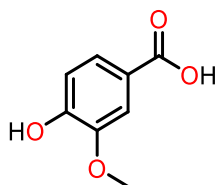
$$= \mathbf{4.65 \text{ kg waste / 1 kg of product}}$$

$$\text{TON (1st run)} = \frac{9.9 \text{ mmol (yield of vanillic acid)}}{0.2 \text{ mmol (amount of catalyst)}} = 49$$

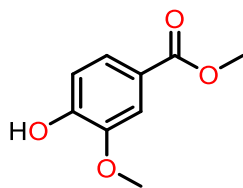
$$\text{TON (all 6 runs)} = \frac{(9.9 + 9.6 + 9.7 + 9.6 + 9.6 + 9.6) \text{ mmol (yield of vanillic acid)}}{0.2 \text{ mmol (amount of catalyst)}} = 290$$

**General procedure for the synthesis of vanillic diester:** butyl 4-hydroxy-3-methoxybenzoate (0.112 g, 0.5 mmol) and triethylamine (104  $\mu$ L, 1.5 mmol) were dissolved in dry DCM (5 mL) in a Schlenk tube under inert condition. The mixture was stirred in an ice bath and under a N<sub>2</sub> atmosphere, acetyl chlorides (1.2 equivalent, 0.60 mmol) was dropped into the reaction mixture slowly for 10 min. Then, the temperature was warmed to room temperature and the mixture was reacted for 6 h. The reaction mixture was washed three times with distilled water (15 mL) and dried over with Na<sub>2</sub>SO<sub>4</sub>. The solution was filtered and organic solvent was removed under reduced pressure to give colourless oil as pure product. The product was further dried for 1 h under reduced pressure.

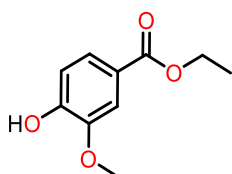
## NMR DATA OF PRODUCTS



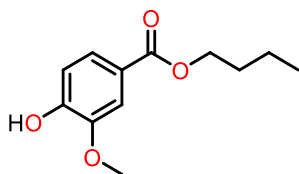
**Vanillic acid.** Vanillic acid as white solid (42 mg, 98%) was synthesized according to the general procedure. <sup>1</sup>H NMR (400 MHz, DMSO-d<sub>6</sub>)  $\delta$  12.51 (bs, 1H), 9.86 (br, 1H), 7.54 – 7.33 (m, 2H), 6.84 (d, *J* = 8.4 Hz, 1H), 3.81 (s, 3H), <sup>13</sup>C NMR (101 MHz, DMSO)  $\delta$  167.68, 151.54, 147.67, 123.93, 122.04, 115.47, 113.12, 55.97.



**Methyl 4-hydroxy-3-methoxybenzoate (E<sub>1a</sub>)** methyl 4-hydroxy-3-methoxybenzoate as colourless liquid (87 mg, 97%) was synthesized according to the general procedure. <sup>1</sup>H NMR (400 MHz, CDCl<sub>3</sub>) δ 7.52 (dd, *J* = 8.0, 1.8 Hz, 1H), 7.43 (d, *J* = 2.0 Hz, 1H), 6.83 (d, *J* = 8.0 Hz, 1H), 6.24 (bs, 1H), 3.78 (s, 3H), 3.77 (s, 3H). <sup>13</sup>C NMR (101 MHz, CDCl<sub>3</sub>) δ 167.12, 150.21, 146.33, 124.17, 122.02, 114.26, 111.86, 55.99, 52.01.

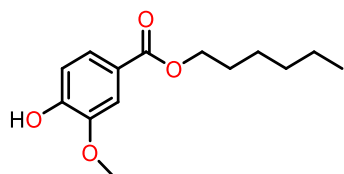


**Ethyl 4-hydroxy-3-methoxybenzoate (E<sub>1b</sub>)**. ethyl 4-hydroxy-3-methoxybenzoate as light brown liquid (94 mg, 96%) was synthesized according to the general procedure. <sup>1</sup>H NMR (400 MHz, CDCl<sub>3</sub>) δ 7.64 (dd, *J* = 8.3, 1.5 Hz, 1H), 7.55 (d, *J* = 2.0 Hz, 1H), 6.94 (d, *J* = 8.0 Hz, 1H), 5.98 (br, 1H), 4.35 (q, *J* = 7.0 Hz, 2H), 3.91 (s, 3H), 1.38 (t, *J* = 7.0 Hz, 3H) <sup>13</sup>C NMR (101 MHz, CDCl<sub>3</sub>) δ 166.59, 150.06, 146.26, 124.09, 122.47, 114.14, 111.78, 60.86, 56.03, 14.37.

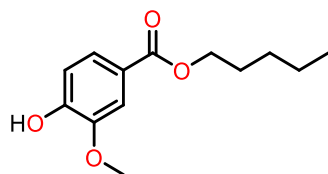


**Butyl 4-hydroxy-3-methoxybenzoate (E<sub>1c</sub>)**. butyl 4-hydroxy-3-methoxybenzoate as colourless liquid (108 mg, 97%) was synthesized according to the general procedure. <sup>1</sup>H NMR (400 MHz, CDCl<sub>3</sub>) δ 7.64 (dd, *J* = 8.3, 1.8 Hz, 1H), 7.56 (d, *J* = 2.0 Hz, 1H), 6.94 (d, *J* = 8.0 Hz, 1H), 6.38 (br, 1H), 4.30 (t, *J* = 6.0 Hz, 2H), 3.91 (s, 3H), 1.75 (m, 2H), 1.47 (m,

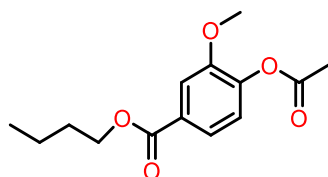
2H), 0.98 (t,  $J = 7.5$  Hz, 3H).  $^{13}\text{C}$  NMR (101 MHz,  $\text{CDCl}_3$ )  $\delta$  166.64, 150.05, 146.27, 124.07, 122.52, 114.13, 111.79, 64.75, 56.03, 30.82, 19.29, 13.78.



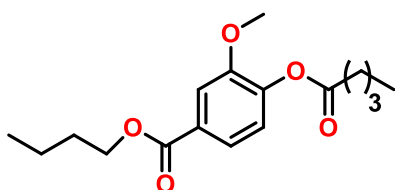
**Hexyl 4-hydroxy-3-methoxybenzoate (E<sub>1d</sub>).** hexyl 4-hydroxy-3-methoxybenzoate as colourless liquid (118 mg, 94%) was synthesized according to the general procedure.  $^1\text{H}$  NMR (400 MHz,  $\text{CDCl}_3$ )  $\delta$  7.65 (dd,  $J = 8.3, 1.8$  Hz, 1H), 7.56 (d,  $J = 1.8$  Hz, 1H), 6.95 (d,  $J = 8.3$  Hz, 1H), 6.31 (br, 1H), 4.30 (t,  $J = 6.7$  Hz, 2H), 3.93 (s, 3H), 1.82 – 1.67 (m, 2H), 1.38 (m, 6H), 0.91 (t,  $J = 7.0$  Hz, 3H).  $^{13}\text{C}$  NMR (101 MHz,  $\text{CDCl}_3$ )  $\delta$  166.61, 150.02, 146.24, 124.07, 122.56, 114.11, 111.77, 65.04, 56.04, 31.48, 28.72, 25.72, 22.56, 14.01.



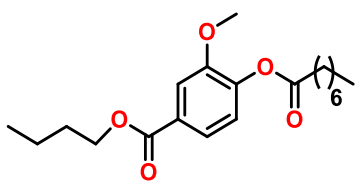
**Pentyl 4-hydroxy-3-methoxybenzoate (E<sub>1e</sub>).** Pentyl 4-hydroxy-3-methoxybenzoate as colourless liquid (117 mg, 99%) was synthesized according to the general procedure.  $^1\text{H}$  NMR (400 MHz,  $\text{CDCl}_3$ )  $\delta$  7.64 (dd,  $J = 8.3, 1.5$  Hz, 1H), 7.56 (d,  $J = 2.0$  Hz, 1H), 6.94 (d,  $J = 8.0$  Hz, 1H), 6.37 (br, 1H), 4.29 (t,  $J = 7.0$  Hz, 2H), 3.91 (s, 3H), 1.83 – 1.71 (m, 2H), 1.46 – 1.32 (m, 4H), 0.93 (t,  $J = 7.0$  Hz, 3H).  $^{13}\text{C}$  NMR (101 MHz,  $\text{CDCl}_3$ )  $\delta$  166.63, 150.05, 146.27, 124.06, 122.53, 114.13, 111.79, 65.03, 56.03, 28.46, 28.21, 22.37, 13.99.



**Butyl 4-acetoxy-3-methoxybenzoate (E<sub>2a</sub>).** butyl 4-acetoxy-3-methoxybenzoate as colourless liquid (126 mg, 95%) was synthesized according to the general procedure. <sup>1</sup>H NMR (400 MHz, CDCl<sub>3</sub>) δ 7.71 – 7.64 (m, 2H), 7.11 (d, *J* = 8.0 Hz, 1H), 4.34 (t, *J* = 6.5 Hz, 2H), 3.90 (s, 3H), 2.34 (s, 3H), 1.84 – 1.68 (m, 2H), 1.48 (dd, *J* = 15.0, 7.5 Hz, 2H), 0.99 (t, *J* = 7.5 Hz, 3H). <sup>13</sup>C NMR (101 MHz, CDCl<sub>3</sub>) δ 168.50, 165.94, 151.03, 143.52, 129.23, 122.72, 122.51, 113.40, 65.06, 56.05, 30.76, 20.63, 19.25, 13.75.

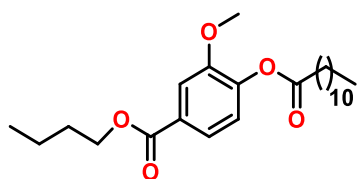


**Butyl 3-methoxy-4-(propionyloxy) benzoate (E<sub>2b</sub>).** butyl 3-methoxy-4-(propionyloxy) benzoate as colourless liquid (151 mg, 98%) was synthesized according to the general procedure. <sup>1</sup>H NMR (400 MHz, CDCl<sub>3</sub>) δ 7.70 – 7.63 (m, 2H), 7.09 (d, *J* = 8.0 Hz, 1H), 4.33 (t, *J* = 6.0 Hz, 2H), 3.88 (s, 3H), 2.60 (t, *J* = 7.0 Hz, 2H), 1.81 – 1.71 (m, 4H), 1.47 (m, 4H), 0.98 (m, 6H). <sup>13</sup>C NMR (101 MHz, CDCl<sub>3</sub>) δ 171.35, 165.97, 151.07, 143.67, 129.07, 122.72, 122.50, 113.35, 65.02, 56.00, 33.69, 30.76, 26.98, 22.15, 19.25, 13.71, 13.74.



**Butyl 3-methoxy-4-(octanoyloxy)- benzoate (E<sub>2c</sub>).** butyl 3-methoxy-4-(octanoyloxy)- benzoate as colourless liquid (173 mg, 99%) was synthesized according to the general procedure. <sup>1</sup>H NMR (400 MHz, CDCl<sub>3</sub>) δ 7.70 – 7.63 (m, 2H), 7.09 (d, *J* = 8.0 Hz, 1H), 4.33 (t, *J* = 6.0 Hz, 2H), 3.88 (s, 3H), 2.59 (t, *J* = 8.0 Hz, 2H), 1.76 (m, 4H), 1.42 – 1.27 (m, 10H), 0.99 (t, *J* = 7.4 Hz, 3H), 0.90 (t, *J* = 6.0 Hz, 3H). <sup>13</sup>C NMR (101 MHz, CDCl<sub>3</sub>) δ 171.35,

165.96, 151.07, 143.68, 129.07, 122.72, 122.50, 113.35, 65.02, 55.98, 33.99, 31.69, 30.76, 28.95, 24.96, 22.60, 19.25, 14.06, 13.74.



**Butyl 4-(dodecanoyloxy)-3-methoxybenzoate(E2a).** Butyl 3-methoxy-4-(octanoyloxy)-benzoate as colourless liquid (197 mg, 97%) was synthesized according to the general procedure.  $^1\text{H}$  NMR (400 MHz,  $\text{CDCl}_3$ )  $\delta$  7.69 – 7.64 (m, 2H), 7.08 (d,  $J = 8.0$  Hz, 1H), 4.33 (t,  $J = 6.0$  Hz, 2H), 3.88 (s, 3H), 2.59 (t,  $J = 7.0$  Hz, 2H), 1.76 (m, 4H), 1.52 – 1.41 (m, 4H), 1.28 (s, 14H), 0.98 (t,  $J = 8.0$  Hz, 3H), 0.90 (t,  $J = 6.0$  Hz, 3H).  $^{13}\text{C}$  NMR (101 MHz,  $\text{CDCl}_3$ )  $\delta$  171.32, 165.94, 151.07, 143.68, 129.06, 122.71, 122.49, 113.34, 65.00, 55.96, 33.99, 31.91, 30.77, 29.72, 28.89, 24.96, 22.69, 19.25, 14.10, 13.74.

## NMR SPECTRA SOME OF COMPOUNDS

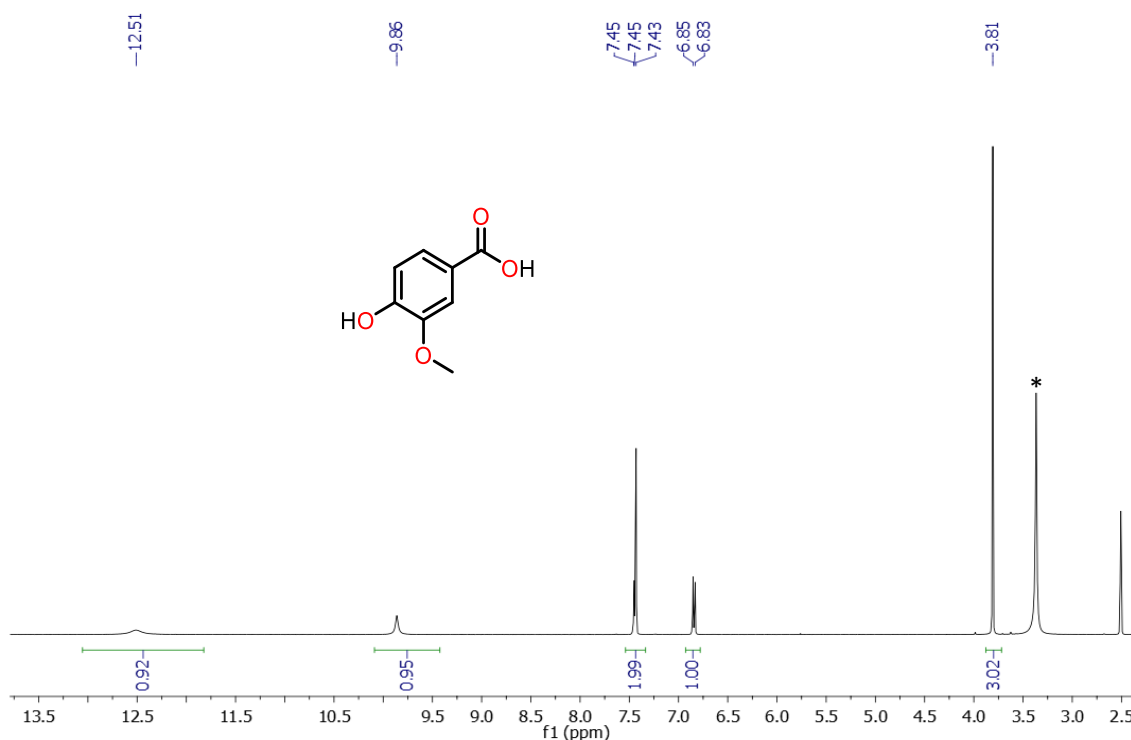


**Figure 4.5.6.**  $^1\text{H}$  NMR (400 MHz) spectrum of **vanillic acid** in  $\text{DMSO-d}_6$  at r.t. (\* marks as water peak)

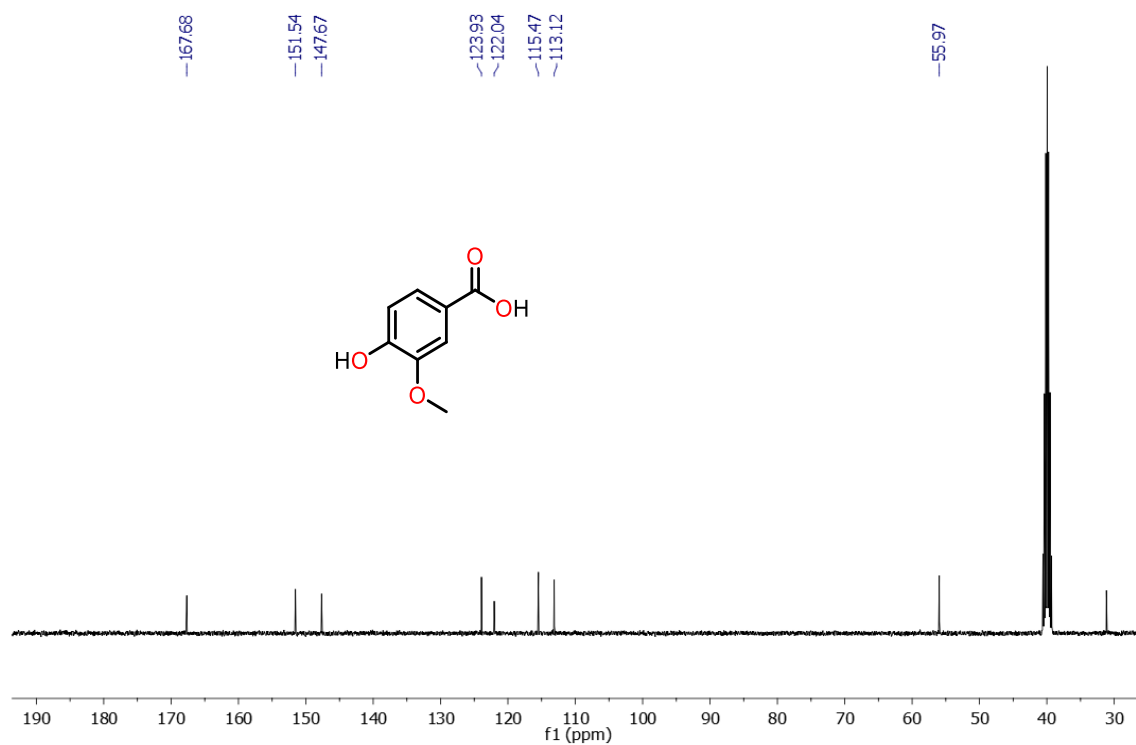


**Figure 4.5.6.**  $^{13}\text{C}$   $\{^1\text{H}\}$  NMR (101 MHz) spectrum of **vanillic acid** in  $\text{DMSO-d}_6$  at r.t.

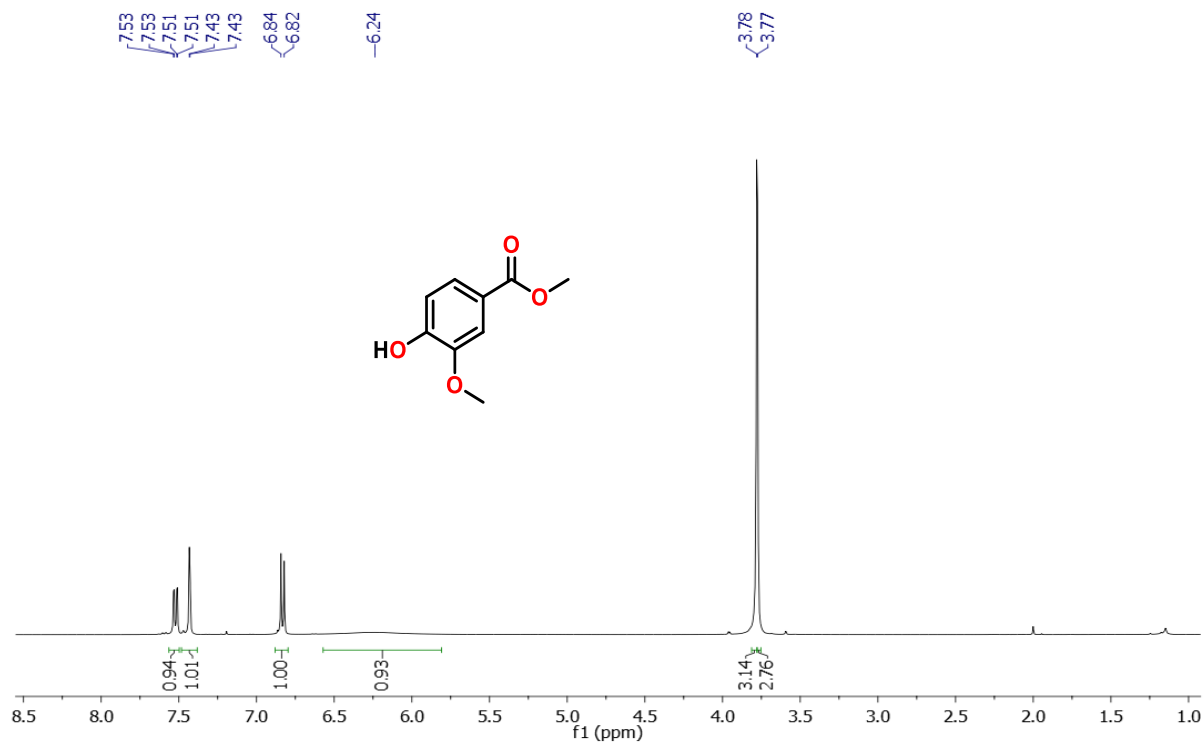


**Figure 4.5.7.**  $^1\text{H}$  NMR (400 MHz) spectrum of **methyl 4-hydroxy-3-methoxybenzoate** in  $\text{CDCl}_3$  at r.t.

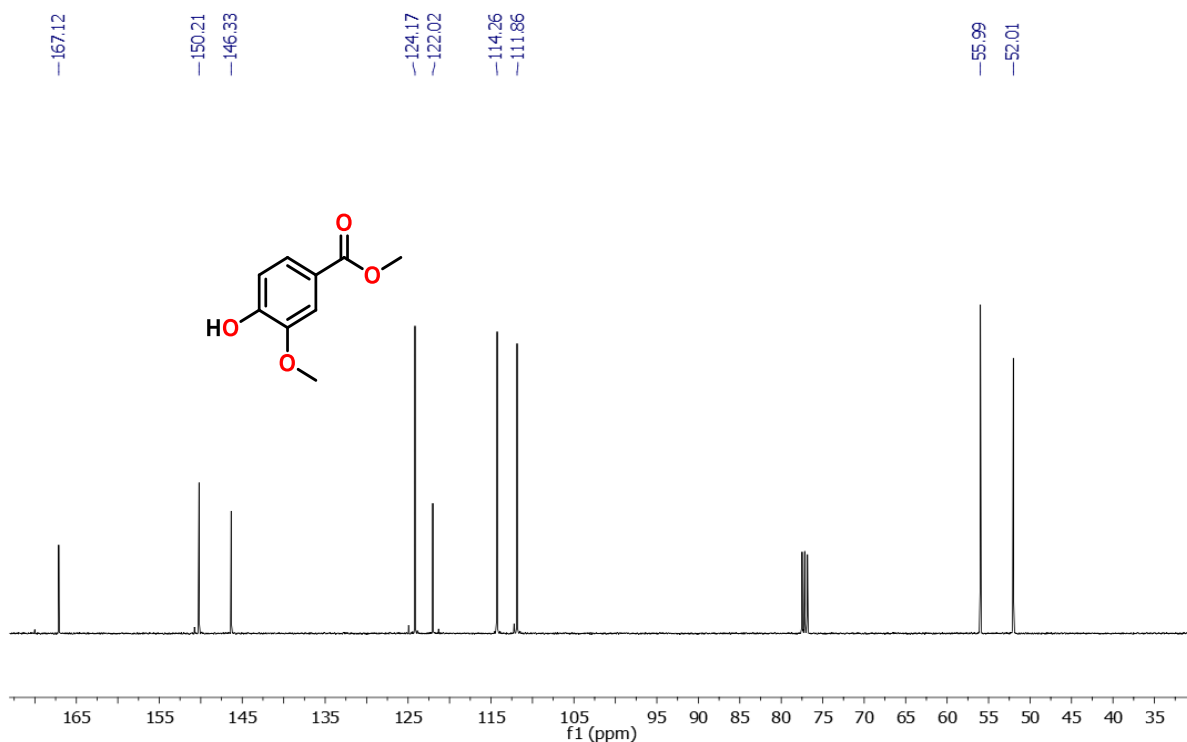


**Figure 4.5.8.**  $^{13}\text{C}\{^1\text{H}\}$  NMR (101MHz) spectrum of methyl 4-hydroxy-3-methoxybenzoate in  $\text{CDCl}_3$  at r.t.

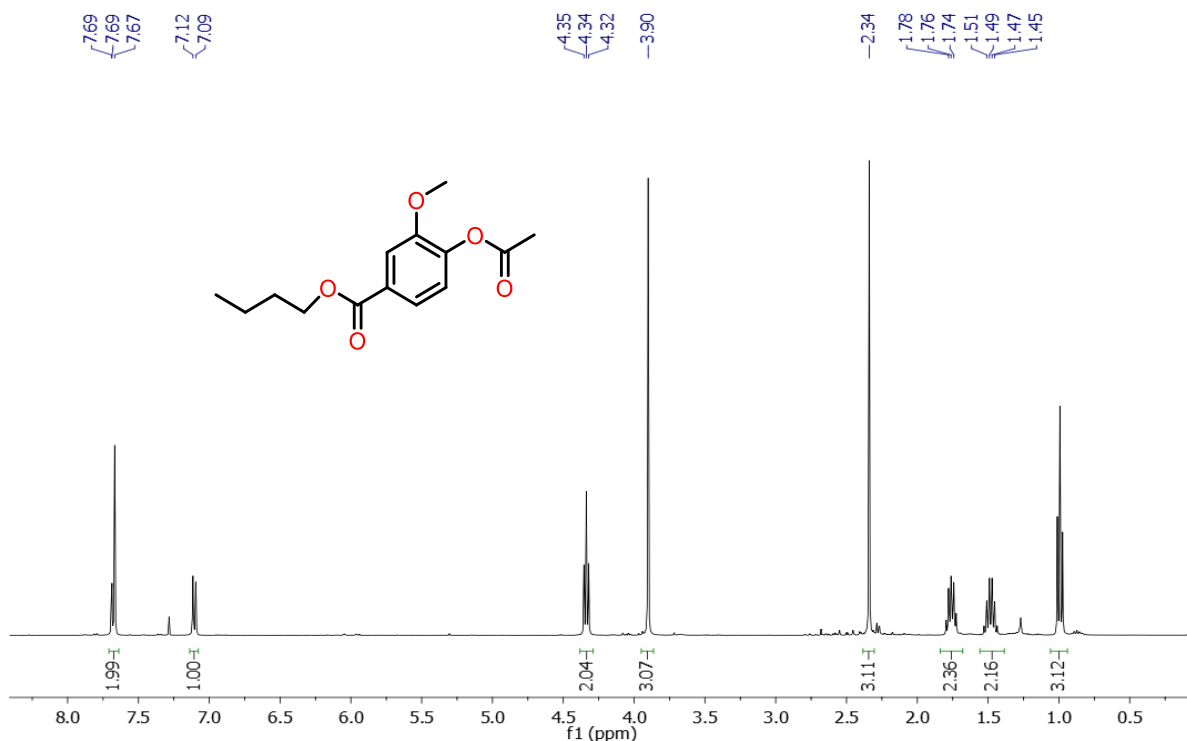


**Figure 4.5.8.**  $^1\text{H}$  NMR (400 MHz) spectrum of butyl 4-acetoxy-3-methoxybenzoate in  $\text{CDCl}_3$  at r.t.

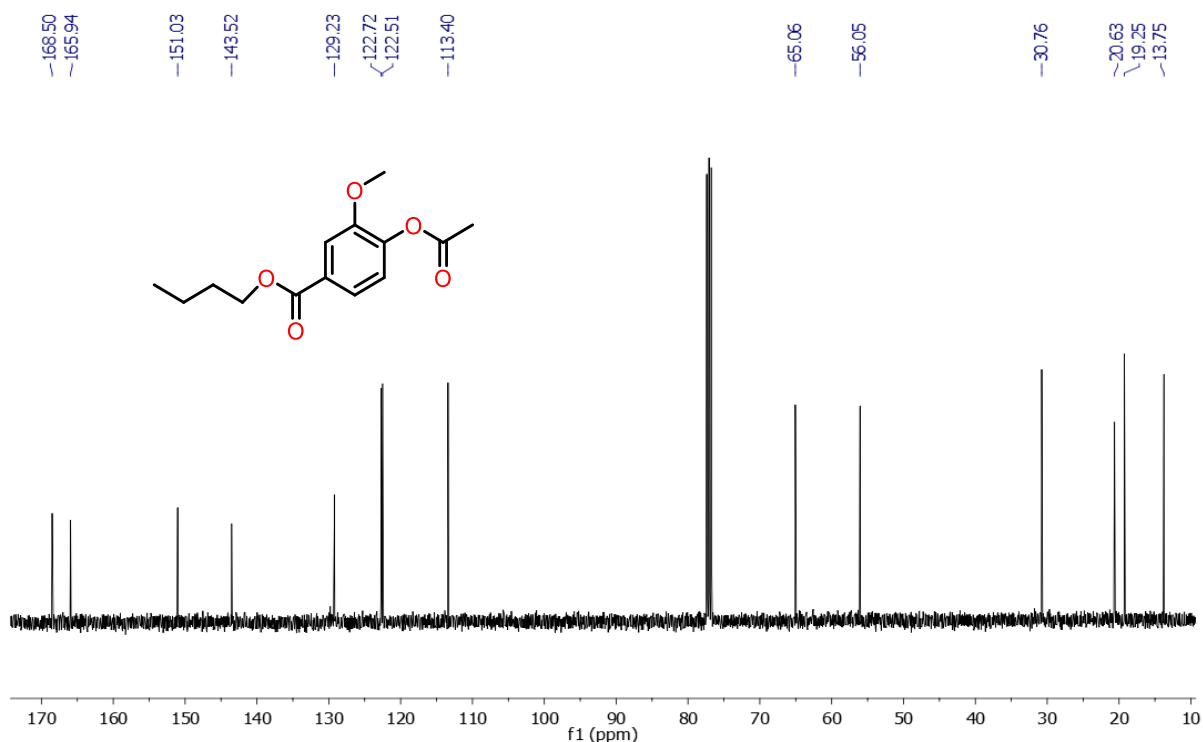


**Figure 4.5.9.** <sup>13</sup>C {<sup>1</sup>H} NMR (101 MHz) spectrum of **butyl 4-acetoxy-3-methoxybenzoate** in CDCl<sub>3</sub> at r.t.

## X-ray structure determination

Crystallographic data and structure determinations details are compiled in Table 4.5.1. The crystals were obtained by slow diffusion of diethyl ether into a solution of **7** in DCM at r.t. The crystals were coated with silicon oil on a glass slide and a suitable single crystal was mounted on a glass fibre. Crystal data were collected with a Rigaku Oxford diffractometer and with an INCOATEC micro source (Mo-K $\alpha$  radiation,  $\lambda = 0.71073$  Å, multilayer optics) at 100 K. The structure was determined using direct methods employed in ShelXT, OleX, and refinement was carried out using least-square minimization implemented in ShelXL. All nonhydrogen atoms were refined with anisotropic displacement parameters. Hydrogen atom positions were fixed geometrically in idealized positions and were refined using a riding model. CCDC 2243929 (for complex **7**) contains the supplementary crystallographic data.

**Table 4.5.1.** Crystallographic Data and Refinement Parameters for complex **7**

Empirical formula	C <sub>16</sub> H <sub>25</sub> FeN <sub>3</sub> O <sub>5</sub>
CCDC	2243929
Formula weight (g mol <sup>-1</sup> )	395.24
Temperature (K)	100.00(10)
Wavelength	0.71073
Crystal system	orthorhombic
Space group	Pna2 <sub>1</sub>
<i>a</i> (Å)	12.6355(3)
<i>b</i> (Å)	12.7504(4)
<i>c</i> (Å)	11.0033(3)
$\alpha$ (deg)	90
$\beta$ (deg)	90
$\gamma$ (deg)	90
volume (Å <sup>3</sup> )	1772.72(8)
Z	4
<i>D</i> <sub>calc</sub> (g cm <sup>-3</sup> )	1.4811
$\mu$ (mm <sup>-1</sup> )	0.882
<i>F</i> (000)	832
Crystal Size	0.2 × 0.2 × 0.1 mm <sup>3</sup>
$\theta$ Range (deg)	7.16 to 63.74
Index Ranges	-16 ≤ <i>h</i> ≤ 18, -18 ≤ <i>k</i> ≤ 18, -15 ≤ <i>l</i> ≤ 15
Reflections collected	18716
Independent reflections ( <i>R</i> <sub>int</sub> )	4611 [ <i>R</i> <sub>int</sub> = 0.0440, <i>R</i> <sub>sigma</sub> = 0.0395]
Completeness to theta = 25.07 <sup>o</sup>	99.60
Refinement method	Full-matrix least-squares on <i>F</i> <sup>2</sup>
Data/Restraints/parameters	4611/1/228
Goodness-of-fit on <i>F</i> <sup>2</sup>	0.761
Final <i>R</i> indices [ <i>I</i> > 2 $\sigma$ ( <i>I</i> )]	<i>R</i> <sub>1</sub> = 0.0315, w <i>R</i> <sub>2</sub> = 0.0913
<i>R</i> indices (all data)	<i>R</i> <sub>1</sub> = 0.0363, w <i>R</i> <sub>2</sub> = 0.0976
Largest diff. peak/hole (e Å <sup>-3</sup> )	1.39/-1.06

#### 4.6 Reference:

1. Kamm, B.; Gruber, P. R.; Kamm, M. *Wiley-VCH*: **2006**; p 964.
2. Clark, J. H.; Luque, R.; Matharu, A. S. *Green Chemistry, Annu. Rev. Chem. Biomol. Eng.* **2012**, *3*, 183–207

3. Belgacem, M.N.; Gandini, A. *Elsevier*, **2011**.
4. Sudarsanam, P.; Zhong, R.; Van den Bosch, S.; Coman, S.M.; Parvulescu, V.I.; Sels, B.F. *Chem. Soc. Rev.*, **2018**, 47, 8349–8402.
5. Deng, W.; Zhang, H.; Wu, X.; Li, R.; Zhang, Q.; Wang, Y. *Green Chem.*, **2015**, 17, 5009–5018.
6. Behling, R.; Valange, S.; & Chatel, G. *Green chemistry*, **2016**, 18, 1839-1854.
7. Fitzgerald, D. J.; Stratford, M.; Narbad, A. *International journal of food microbiology*, **2003**, 86, 113-122.
8. Walton, N. J.; Mayer, M. J.; Narbad, A. Vanillin. *Phytochemistry* **2003**, 63, 505–515.
9. Esposito, L.; Formanek, K.; Kientz, G.; Mauger, F.; Maureaux, V.; Robert, G.; Truchet, F. *Kirk-Othmer Encyclopedia of Chemical Technology*, 4th edn, **1997**, 24, 812-825.
10. Bjørsvik, H.-R.; Minisci, M. *Org. Process Res. Dev.* **1999**, 3, 330–340.
11. Fache, M.; Boutevin, B.; Caillol, S. *ACS sustainable chemistry & engineering*, **2016**, 4, 35-46.
12. Jana, N. C.; Sethi, S.; Saha, R.; Bagh, B. *Green Chemistry*, **2022**, 24, 2542-2556.
13. Tai, A.; Sawano, T.; Ito, H. *Biosci.,Biotechnol.,Biochem.* **2012**, 76, 314– 318.
14. Pang, C.; Zhang, J.; Wu, G.; Wang, Y.; Gao, H.; Ma, J. *Polymer Chemistry*, **2014**, 5, 2843-2853.
15. Zhang, S.; Cheng, Z.; Zeng, S.; Li, G.; Xiong, J.; Ding, L.; Gauthier, M. *J. Appl. Polym. Sci.* **2020**, 137, 49189– 49198.
16. de Haro, J. C.; Allegretti, C.; Smit, A. T.; Turri, S.; D’Arrigo, P.; Griffini, G. *ACS Sustainable Chemistry & Engineering*, **2019**, 7, 11700-11711.

17. Zhu, H.; Yang, J.; Wu, M.; Wu, Q.; Liu, J.; Zhang, J.; *ACS Sustainable Chem. Eng.*, **2021**, *9*, 15322–15330.
18. Elamathi, P.; Kolli, M. K.; Chandrasekar, G. *International Journal of Nanoscience*, **2018**, *17*, 1760010.
19. Zhou, Y.; Xiong, W.; Jin, Y.; Wang, P.; Wei, W.; Ma, J.; Zhang, X. *Green Chemistry*, 2023, *25*, 1179-1190.
20. Kumar, A.; Srivastava, R. *ACS Appl.NanoMater*, **2021**, *4*, 9080–9093.
21. Zheng, M. W.; Lin, K. Y. A.; Lin, C. H. *Waste and Biomass Valorization*, **2020**, *11*, 6917-6928.
22. Sun, W., Lin, P., Tang, Q., Jing, F., Cao, Q., & Fang, W. *Catalysis Science & Technology*, **2021**, *11*, 7268-7277.
23. Zheng, M. W., Lai, H. K., & Lin, K. Y. A. *Waste and Biomass Valorization*, **2018**, *10*, 2933-2942.
24. Yuan, Z., Chen, S., & Liu, B. *Journal of Materials Science*, **2017**, *52*, 164-172.
25. Lin, K.Y.A.; Lai, H.Y.; Chen, Z.Y. *J. Taiwan Inst. Chem. Eng.*, **2017**, *78*, 337–343.
26. Pearl, I.A.; *Organic syntheses,coll*,**1963**, *4*, 972.
27. Rautiainen, S.; Chen, J.; Vehkamäki, M.; Repo, T. *Topics in catalysis*, 2016, *59*, 1138-1142.
28. Kuramoto, S.; Jenness, R.; Coulter, S. T. *Journal of Dairy Science*, 1957, *40*, 187-191.
29. Panoutsopoulos, G. I.; Beedham, C. *Cellular Physiology and Biochemistry*, 2005, **15**, 89–98.
30. Robbins, W. J.; Lathrop, E. C. *Soil Science*, **1919**, *7*, 475-486.
31. Shilpy, M.; Ehsan, M. A.; Ali, T. H.; Abd Hamid, S. B.; Ali, M. E. *RSC advances*, 2015, *5*, 79644-79653.

32. Crestini, C.; Caponi, M. C.; Argyropoulos, D. S.; Saladino, R. *Bioorganic & medicinal chemistry*, **2006**, *14*, 5292-5302.
33. Pan, J.; Fu, J.; Lu, X. *Energy & Fuels*, **2015**, *29*, 4503-4509.
34. Mallat, T.; Baiker, A. *Chemical reviews*, **2004**, *104*, 3037-3058.
35. da Silva, E. B.; Zabkova, M.; Araújo, J. D.; Cateto, C. A.; Barreiro, M. F.; Belgacem, M. N.; Rodrigues, A. E. *chemical engineering research and design*, **2009**, *87*, 1276-1292.
36. Ren, Q. G.; Chen, S. Y.; Zhou, X. T.; Ji, H. B. *Bioorganic & medicinal chemistry*, **2010**, *18*, 8144-8149.
37. Cainelli, G.; Cardillo, G.; Cainelli, G.; Cardillo, G. *Chromium Oxidations in Organic Chemistry*, 1984, 118-216.
38. Tidwell, T. T. *Synthesis*, 1990, *1990*, 857-870.
39. Blackburn, L.; Taylor, R. J. *Organic letters*, **2001**, *3*, 1637-1639.
40. Ünver, H.; Kani, I. *Polyhedron*, **2017**, *134*, 257-262.
41. Ünver, H.; Kani, I. *Journal of Chemical Sciences*, **2018**, *130*, 1-9.
42. Wu, C.; Liu, B.; Geng, X.; Zhang, Z.; Liu, S.; Hu, Q. *Polyhedron*, **2019**, *158*, 334-341.
43. Kulakova, A. N.; Bilyachenko, A. N.; Levitsky, M. M.; Khrustalev, V. N.; Korlyukov, A. A.; Zubavichus, Y. V.; ... & Shul'pin, G. B. *Inorganic chemistry*, **2017**, *56*, 15026-15040.
44. Hazra, S.; Martins, L. M.; da Silva, M. F. C. G.; Pombeiro, A. J. Syntheses and crystal structures. *RSC advances*, **2015**, *5*, 90079-90088.
45. Frija, L. M.; Alegria, E. C.; Sutradhar, M.; Cristiano, M. L. S.; Ismael, A.; Kopylovich, M. N.; Pombeiro, A. J. *Journal of Molecular Catalysis A: Chemical*, **2016**, *425*, 283-290.

46. Sutradhar, M.; Roy Barman, T.; Pombeiro, A. J.; Martins, L. M. *Catalysts*, **2019**, *9*, 1053.
47. Ma, Z.; Wang, Q.; CBA Alegria, E.; C. Guedes da Silva, M. F.; MDRS Martins, L.; Telo, J. P.; ... & JL Pombeiro, A. *Catalysts*, **2019**, *9*, 424.
48. Zavahir, S., Xiao, Q., Sarina, S., Zhao, J., Bottle, S., Wellard, M., ... & Zhu, H. Y. *Acs Catalysis*, **2016**, *6*, 3580-3588.
49. Gao, Q.; Giordano, C.; Antonietti, M. *Angewandte Chemie International Edition*, **2012**, *51*, 11740-11744.
50. Ray, R., Chandra, S., Maiti, D., & Lahiri, G. K. *Chemistry—A European Journal*, **2016**, *22*, 8814-8822.
51. Devari, S.; Deshidi, R.; Kumar, M.; Kumar, A.; Sharma, S.; Rizvi, M.; ... & Shah, B. *A. Tetrahedron Letters*, **2013**, *54*, 6407-6410.
52. Su, H.; Zhang, K. X.; Zhang, B.; Wang, H. H.; Yu, Q. Y.; Li, X. H.; ... & Chen, J. S. *Journal of the American Chemical Society*, **2017**, *139*, 811-818.
53. Wu, Z.; Hull, K. L. *Chemical Science*, **2016**, *7*, 969-975.
54. Weiss, C. J.; Das, P.; Miller, D. L.; Helm, M. L.; Appel, A. M. *Acs Catalysis*, **2014**, *4*, 2951-2958.
55. Jaworski, J. N.; McCann, S. D.; Guzei, I. A.; Stahl, S. S. *Angewandte Chemie*, **2017**, *129*, 3659-3664.
56. Ning, X.; Li, Y.; Yu, H.; Peng, F.; Wang, H.; Yang, Y. *Journal of Catalysis*, **2016**, *335*, 95-104.
57. Li, H.; Qin, F.; Yang, Z.; Cui, X.; Wang, J.; Zhang, L. *Journal of the American Chemical Society*, **2017**, *139*, 3513-3521.
58. Zhu, J.; Zhao, Y.; Tang, D.; Zhao, Z.; Carabineiro, S. A. *Journal of Catalysis*, **2016**, *340*, 41-48.

59. Zhang, G.; Liu, E.; Yang, C.; Li, L.; Golen, J. A.; Rheingold, A. L. *European Journal of Inorganic Chemistry*, **2015**, 2015, 939-947.
60. Mahmoud, A. G.; Guedes da Silva, M. F. C.; Śliwa, E. I.; Smoleński, P.; Kuznetsov, M. L.; Pombeiro, A. J. *Chemistry—An Asian Journal*, **2018**, 13, 2868-2880.
61. Lagerspets, E.; Lagerblom, K.; Heliövaara, E.; Hiltunen, O. M.; Moslova, K.; Nieger, M.; Repo, T. *Molecular catalysis*, **2019**, 468, 75-79.
62. Marais, L.; Burés, J.; Jordaan, J. H.; Mapolie, S.; Swarts, A. J. *Organic & Biomolecular Chemistry*, **2017**, 15, 6926-6933.
63. Ochen, A.; Whitten, R.; Aylott, H. E.; Ruffell, K.; Williams, G. D.; Slater, F.; ... & Sanganee, M. J. *Organometallics*, **2018**, 38, 176-184.
64. Ma, R.; Xu, Y.; & Zhang, X. *ChemSusChem*, **2015**, 8, 24-51.
65. Jha, A.; Patil, K. R.; & Rode, C. V. *ChemPlusChem*, **2013**, 78, 1384-1392.
66. Jha, A.; Rode, C. V. *New Journal of Chemistry*, **2013**, 37, 2669–2674.
67. Zhang, J.; Zhang, F.; Guo, S.; Zhang, J. *New Journal of Chemistry*, **2018**, 42, 11117-11123.
68. Saha, S.; Abd Hamid, S. B. *RSC advances*, **2017**, 7(16), 9914-9925.
69. Reddy, P. N.; Rao, B. G.; Rao, T. V.; Reddy, B. M. *Catalysis Letters*, **2019**, 149, 533-543.
70. Hinde, C. S.; Ansovini, D.; Wells, P. P.; Collins, G.; Aswegen, S. V.; Holmes, J. D.; ... & Raja, R. *ACS Catalysis*, **2015**, 5, 3807-3816.
71. Baguc, I. B.; Celebi, M.; Karakas, K.; Ertas, I. E.; Keles, M. N.; Kaya, M.; Zahmakiran, M. *ChemistrySelect*, 2017, 2, 10191-10198.
72. Ramana, S.; Rao, B. G.; Venkataswamy, P.; Rangaswamy, A.; Reddy, B. M. *Journal of Molecular Catalysis A: Chemical*, **2016**, 415, 113-121.
73. Yang, L.; Ma, R.; Zeng, H.; Rui, Z.; Li, Y. *Catalysis Today*, **2020**, 355, 280-285.

74. Sun, W.; Wu, S.; Lu, Y.; Wang, Y.; Cao, Q.; Fang, W. *ACS Catalysis*, **2020**, *10*(14), 7699-7709.
75. Martín-Perales, A. I.; Rodriguez-Padron, D.; Garcia Coletto, A.; Len, C.; de Miguel, G.; Munoz-Batista, M. J.; Luque, R. *Industrial & Engineering Chemistry Research*, **2020**, *59*, 17085-17093.
76. Bozell, J. J.; Hames, B. R.; Dimmel, D. R. *The Journal of Organic Chemistry*, **1995**, *60*, 2398-2404.
77. Zucca, P.; Sollai, F.; Garau, A.; Rescigno, A.; Sanjust, E. *Journal of Molecular Catalysis A: Chemical*, **2009**, *306*, 89-96.
78. Hu, J.; Hu, Y.; Mao, J.; Yao, J.; Chen, Z.; Li, H. *Green chemistry*, **2012**, *14*, 2894-2898.
79. Zakzeski, J.; Bruijninx, P. C.; Jongerius, A. L.; Weckhuysen, B. M. *Chemical reviews*, **2010**, *110*, 3552-3599.
80. Crestini, C.; Pro, P.; Neri, V.; Saladino, R. *Bioorganic & medicinal chemistry*, **2005**, *13*, 2569-2578.
81. Lange, H.; Decina, S.; Crestini, C. *European polymer journal*, **2013**, *49*, 1151-1173.
82. Lawrence, M. A.; Green, K. A.; Nelson, P. N.; Lorraine, S. C. *Polyhedron*, **2018**, *143*, 11-27.
83. Peris, E.; Crabtree, R. H. *Chemical Society Reviews*, **2018**, *47*, 1959-1968.
84. Jana, A.; Das, K.; Kundu, A.; Thorve, P. R.; Adhikari, D.; Maji, B. *ACS Catalysis*, **2020**, *10*, 2615-2626.
85. Wu, X. J.; Wang, H. J.; Yang, Z. Q.; Tang, X. S.; Yuan, Y.; Su, W.; ... & Verpoort, F. *Organic Chemistry Frontiers*, **2019**, *6*, 563-570.
86. Panda, S.; Saha, R.; Sethi, S.; Ghosh, R.; Bagh, B. *The Journal of Organic Chemistry*, **2020**, *85*, 15610-15621.

87. Ghosh, R.; Behera, R. R.; Panda, S.; Behera, S. K.; Jana, N. C.; Bagh, B.  
*ChemCatChem*, **2023**, *15*, e202201062.
88. Saha, R.; Panda, S.; Nanda, A.; Bagh, B. *The Journal of Organic Chemistry*, **2023**.
89. Koehne, I.; Schmeier, T. J.; Bielinski, E. A.; Pan, C. J.; Lagaditis, P. O.;  
Bernskoetter, W. H.; ... & Schneider, S. *Inorganic chemistry*, **2014**, *53*, 2133-2143.
90. Mao, S.; Budweg, S.; Spannenberg, A.; Wen, X.; Yang, Y.; Li, Y. W.; ... & Beller,  
M. *ChemCatChem*, **2022**, *14*, e202101668.
91. Lagaditis, P. O.; Sues, P. E.; Sonnenberg, J. F.; Wan, K. Y.; Lough, A. J.; Morris, R.  
H. *Journal of the American Chemical Society*, **2014**, *136*, 1367-1380.
92. Driscoll, O. J.; Hafford-Tear, C. H.; McKeown, P.; Stewart, J. A.; Kociok-Köhn, G.;  
Mahon, M. F.; Jones, M. D. *Dalton Transactions*, **2019**, *48*, 15049-15058.
93. Surendhran, R.; D'Arpino, A. A.; Sciscent, B. Y.; Cannella, A. F.; Friedman, A. E.;  
MacMillan, S. N.; ... & Lacy, D. C. *Chemical science*, **2018**, *9*, 5773-5780.
94. Darari, M.; Francés-Monerris, A.; Marekha, B.; Doudouh, A.; Wenger, E.; Monari,  
A.; ... & Gros, P. C. *Molecules*, **2020**, *25*, 5991.
95. Chakraborty, S.; Dai, H.; Bhattacharya, P.; Fairweather, N. T.; Gibson, M. S.;  
Krause, J. A., & Guan, H. *Journal of the American Chemical Society*, **2014**, *136*,  
7869-7872.
96. Curley, J. B.; Smith, N. E.; Bernskoetter, W. H.; Ertem, M. Z.; Hazari, N.; Mercado,  
B. Q.; ... & Wang, X. *ACS Catalysis*, **2021**, *11*, 10631-10646.
97. Chakraborty, S.; Bhattacharya, P.; Dai, H.; & Guan, H. *Accounts of Chemical  
Research*, **2017**, *48*, 1995-2003.
98. Abbott, A. P.; Capper, G.; Davies, D. L.; Rasheed, R. K.; Tambyrajah, V. *Chemical  
communications*, **2003**, 70-71.
99. Smith, E. L.; Abbott, A. P.; Ryder, K. S. *Chemical reviews*, **2014**, *114*, 11060-11082.

100. Nebra, N.; García-Álvarez, J. *Molecules*, **2020**, *25*, 2015.
101. Giofrè, S. V., Tiecco, M., Ferlazzo, A., Romeo, R., Ciancaleoni, G., Germani, R., & Iannazzo, D. *European Journal of Organic Chemistry*, **2021**, *2021*, 4777-4789.
102. Kafle, A., & Handy, S. T. *Tetrahedron*, **2017**, *73*, 7024-7029.
103. McElroy, C. R., Constantinou, A., Jones, L. C., Summerton, L., & Clark, J. H. *Green Chemistry*, **2015**, *17*, 3111-3121.
104. Droesbeke, M. A., & Du Prez, F. E. *ACS Sustainable Chemistry & Engineering*, **2019**, *7*, 11633-11639.
105. Jana, N. C., Sethi, S., Saha, R., & Bagh, B. *Green Chemistry*, **2022**, *24*, 2542-2556.
106. Ghosh, R., Jana, N. C., Panda, S., & Bagh, B. *ACS Sustainable Chemistry & Engineering*, **2021**, *9*, 4903-4914.
107. Sethi, S.; Jana, N.C.; Behera, S.; Behera, R.R.; Bagh B. *ACS Omega*, **2023**, *8*, 868-878.

## Chapter 5

### Iron Catalyzed Oxidation of Primary Alcohols: Reaction Media Induced Chemodivergent Aldehyde and Acid Selectivity

**5.1 ABSTRACT:** Selective catalytic transformations are vital in organic syntheses and chemodivergent synthesis has a special value. Selective oxidations of alcohols to the corresponding carbonyls or complete oxidation to carboxylic acids are among the crucial reactions in organic chemistry. In recent years, catalysis with base metal iron has received a special significance because iron is highly abundant, cheap, non-toxic and sustainable. Therefore, iron catalyzed oxidation of alcohols is an important research topic. We have used a readily synthesized tridentate NNN ligand (**L**<sub>1</sub>) to synthesize an air-stable iron complex (**1**) in almost quantitative yield. Complex **1** proved to be an effective catalyst for the selective peroxidative oxidation of primary alcohols to aldehydes using *tert*-butyl hydroperoxide (TBHP) under solvent-free condition. The same iron complex is highly efficient for the selective oxidation of activated and unactivated primary alcohols to the corresponding carboxylic acids in highly polar solvents such as water and deep eutectic solvent (DES). In DES (choline chloride/glycerol (1:2)), ppm level (1 ppm) catalyst loading was used to give very high TON (10000) and TOF (10000/h) for the selective oxidation of primary alcohol to carboxylic acids. A wide variety of primary alcohols (benzylic, allylic and aliphatic) were selectively converted to the respective carboxylic acids in good to excellent isolated yields. This is excellent example of reaction media induced chemodivergent oxidation of primary alcohols to aldehydes and carboxylic acids. Using green reaction media such as water and type-III DES (or no added solvent) in the present catalytic oxidation of alcohols is no doubt sustainable.

**5.2 INTRODUCTION:** Transition metal complexes have become the essential tools for the efficient and selective organic transformations. Most of the significant industrial chemical processes utilize a wide variety of transition metal catalysts and they are equally important in academia for small lab-scale organic syntheses. A vast majority of those processes are dominated by noble metal catalysts and their rarity on the earth-crust, high cost and toxicity are detrimental for large-scale applications. In contrast, base metals are earth-abundant, cheap and non-toxic (or much less toxic compared to their heavier counterparts) and thus, base metal catalysts are ideal for organic syntheses. Iron is a particularly lucrative arsenal in the toolbox of synthetic chemists as iron is the most abundant transition metal (and third most abundant metal), very inexpensive, non-toxic and ecofriendly. In addition, iron enjoys several stable oxidation states and several coordination geometries are accessible.<sup>1</sup> As a result, iron complexes have found applications in all different fields of homogeneous catalysis.<sup>2</sup> In 2004, Bolm et al. published a comprehensive review article which gave an excellent overview of iron catalyzed reactions in organic transformations and this triggered a serious surge on the developments of iron catalysts.<sup>3</sup> It is not surprising that iron complexes have found serious attentions also in oxidation chemistry which is frequently used in academic laboratory as well as in industry.<sup>4</sup> The oxidations of alcohols to carbonyl compounds or their full oxidation to acids are among the central oxidation reactions in organic chemistry and are of interest for the production of new fine chemicals and energy materials.<sup>5</sup> There is a large pool of stoichiometric oxidants for the selective oxidation of alcohols to aldehydes or ketones, which is an essential reaction in organic syntheses. Effective stoichiometric oxidants include hypervalent iodine reagents,<sup>26</sup> activated dimethyl sulfoxides,<sup>24</sup> and metal-based oxidants such as manganese dioxide<sup>22</sup> and chromium salt.<sup>23</sup> Selective oxidation of alcohols to carboxylic acid, involving cascade oxidation of alcohol to carbonyl to carboxylic acid, is equally important in organic chemistry. Several effective metal-based oxidants such as Jones reagent

(CrO<sub>3</sub>/H<sub>2</sub>SO<sub>4</sub>),<sup>10</sup> Collins reagent (CrO<sub>3</sub>/2 pyridine),<sup>11</sup> pyridinium chlorochromate,<sup>12</sup> pyridinium dichromate,<sup>13</sup> ruthenium tetraoxide,<sup>14</sup> ruthenate and perruthenate ions<sup>15</sup> have been developed for this transformation. Most of these stoichiometric oxidants (particularly chromium-based) are carcinogenic and toxic. In addition, those stoichiometric oxidants produce a huge amount of byproduct waste. Current trend to develop environmental compatible and sustainable oxidation protocols lead to two types of oxidations namely aerobic oxidations and peroxidative oxidations. Air is the most sustainable and green oxidant, however, many synthetic protocols used pressurized oxygen cylinder. Various metal catalysts including iron catalysts have been developed for the aerobic oxidation of alcohols.<sup>16</sup> For the peroxidative oxidations, hydrogen peroxide (H<sub>2</sub>O<sub>2</sub>) and *tert*-butyl hydroperoxide (TBHP) are generally used as green oxidants. Several transition metal catalysts such as iron,<sup>17</sup> cobalt,<sup>18</sup> copper,<sup>19</sup> ruthenium<sup>20</sup> and palladium<sup>21</sup> have been used the alcohol oxidation utilizing ecofriendly peroxide oxidants.

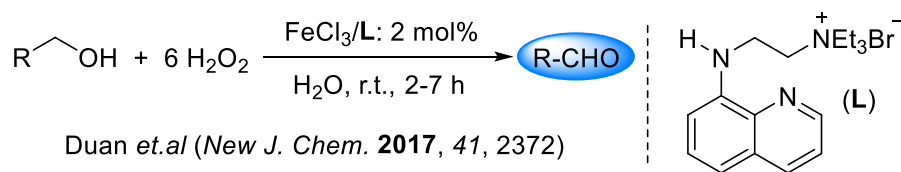
Selective peroxidative oxidation of alcohols to carbonyl compounds or complete oxidation to carboxylic acids is a challenging task. Peroxidative oxidation of secondary alcohols to ketones selectively is considerably easy as further oxidation to acid is pretty difficult task as the oxidation of ketones to acids involves the oxidative cleavage of C-C bond. A few iron catalysts have been reported for the peroxidative oxidation of secondary alcohols to ketones.<sup>22</sup> In contrast, selective peroxidative oxidation of primary alcohol to aldehyde is tough as aldehydes are reactive and cascade oxidation continues to give carboxylic acids. Therefore, product obtained by peroxidative oxidation of primary alcohol often contains a mixture of aldehyde and carboxylic acid and there are a few examples of iron catalyzed protocols.<sup>23</sup> Stefano et al. used imine-based iron complex for the peroxidative oxidation of both primary and secondary alcohols using H<sub>2</sub>O<sub>2</sub>. Moderate conversion of primary alcohols was noted; however, selectivity towards aldehyde was very poor.<sup>23b</sup> Recently, Caselli *et al.*

also reported iron catalyzed (5 mol% catalyst loading) chemoselective peroxidative oxidation (using  $\text{H}_2\text{O}_2$  as oxidant) of primary alcohols to aldehydes.<sup>23a</sup> Various substituted benzyl alcohols were subjected to oxidation and decent to excellent (45-95%) conversions were noted. However, selectivity to aldehyde was not great (70-90%) in most of substrates. Both conversion and selectivity for the allylic alcohols were poor. The reported oxidation protocol was virtually ineffective for unactivated aliphatic primary alcohols. A significant effort has been devoted to develop efficient iron catalysts which can selectively oxidize primary alcohols to aldehydes or selectively oxidize primary alcohols to carboxylic acid. However, the number of reports on selective peroxidative oxidation of primary alcohols using iron catalysts is very limited. Duan *et al.* reported a chemoselective peroxidative oxidation (using  $\text{H}_2\text{O}_2$  as oxidant) of primary alcohols to aldehydes by using a recyclable and water-soluble iron catalyst (2 mol% catalyst loading) (Scheme 5.2.1).<sup>24</sup> Various benzylic and allylic primary alcohols were oxidized to the corresponding aldehydes in good to excellent yields with little formation of carboxylic acids. In addition, a few unactivated aliphatic primary alcohols was also successfully oxidized to the corresponding aldehydes. There is only one example of iron catalyst for the selective peroxidative oxidation of primary alcohol to carboxylic acid. Schachner *et al.* reports air-stable iron catalysts (4 mol% catalyst loading) for the selective oxidation of benzylic alcohols to the corresponding benzoic acids (Scheme 5.3.1).<sup>25</sup> However, the peroxidative oxidation was performed at elevated temperature (70 °C) in presence of a large excess of  $\text{H}_2\text{O}_2$  (6 eq.). An essential goal in synthetic chemistry is the development of highly selective catalytic protocols and chemodivergent reaction is a vital strategy for the efficient syntheses of diverse molecular structures from the common starting materials. Several factors such as metal, ligand, additive, temperature, pressure, pH, time and solvent can switch the chemoselectivity in a catalytic chemical transformation.<sup>26</sup> To the best of our knowledge, there is no example of iron catalyst (or any transition metal catalyst)

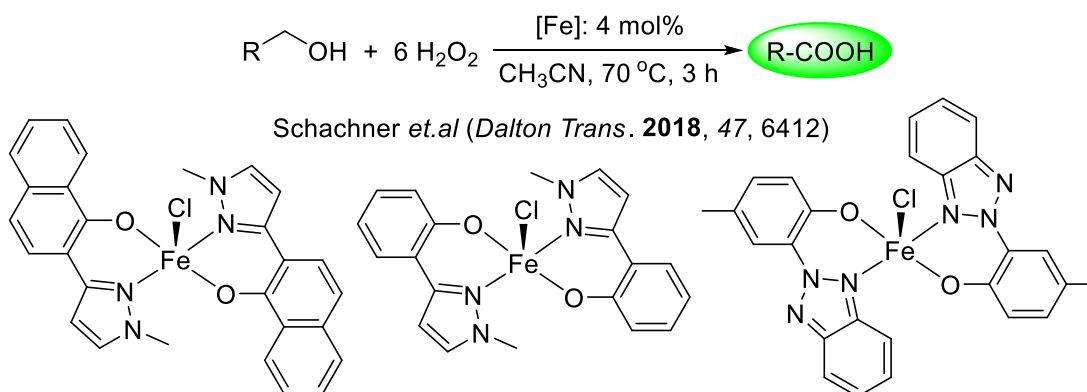
capable of performing chemodivergent oxidation of primary alcohol selectively to aldehyde and selectively to carboxylic acids. Herein, we report a reaction media induced chemodivergent peroxidative oxidation of primary alcohols to aldehydes and acids catalyzed by an iron complex (Scheme 5.2.1). The air-stable iron catalyst is extremely efficient (ppm level catalyst loading) for the selective peroxidative oxidation of primary alcohols to carboxylic acids in highly polar solvents and same iron catalyst is equally effective for the selective peroxidative oxidation of primary alcohols to aldehydes in the absence of any solvent.

**Scheme 5.2.1. Iron catalyzed peroxidative oxidation of primary alcohol**

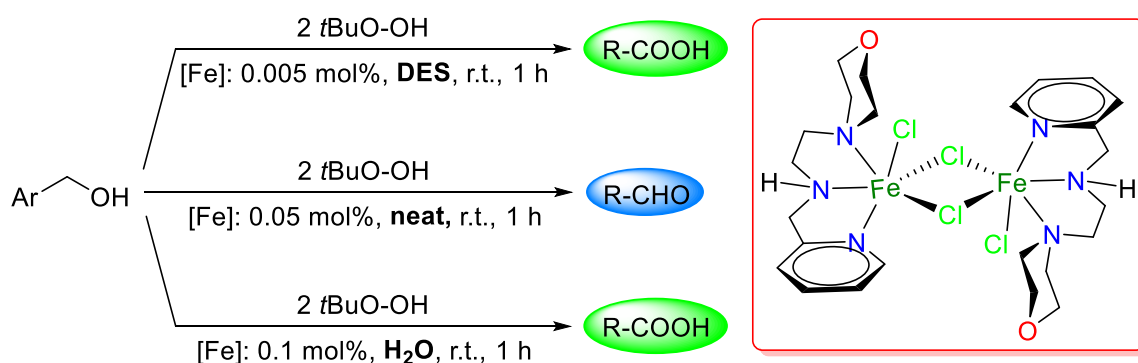
Previous work: Iron catalyzed selective peroxidative oxidation of primary alcohol to **aldehyde**



Previous work: Iron catalyzed selective peroxidative oxidation of primary alcohol to **acid**



**Present work:** Iron catalyzed **chemodivergent** oxidation of primary alcohol to **aldehyde** and **acid**



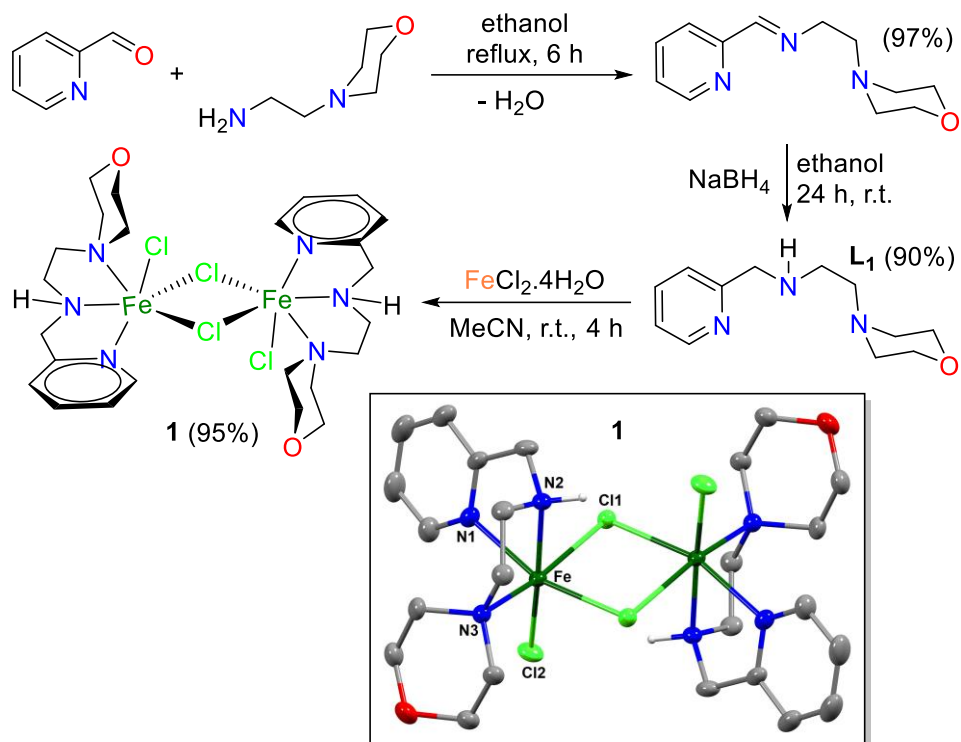
## 5.3 RESULTS AND DISCUSSION

Ligand selection is crucial for the development of effective metal catalysts. The capacity of ligands to alter the steric and electronic properties of the metal core is considered as an important factor in homogeneous catalysis. For example, Duan *et al.* utilized a tridentate NNN ligand for the iron catalyzed peroxidative oxidation of primary alcohol selectively to carboxylic acid. However, iron complex was in situ generated and the true identity of the iron catalyst was unknown. In this regard, we wanted to develop a well-defined iron catalyst with a tridentate NNN ligand which can be readily synthesized from cheap starting materials. The

tridentate NNN coordination might well give good stability of the resultant metal complex. A previously reported tridentate NNN ligand **L**<sub>1</sub> was chosen, which was synthesized by condensation of 2-morpholino ethylamine with 2-pyridinecarboxaldehyde followed by reduction of the Schiff base imine intermediate (Scheme 5.3.1). We selected iron precursor as our goal was to develop sustainable base metal catalyst. Easy coordination of tridentate NNN ligand **L**<sub>1</sub> with cheap iron(II) chloride precursor at r.t. in air yielded complex **8** as a NMR-silent air-stable yellow solid (Scheme 5.3.2). Complex **8** was characterized by mass spectrometry, IR spectroscopy and elemental analysis. In the mass spectrum of complex **8**, a peak was observed at 661.0831 which corresponds to the molecular ion peak [M-Cl]<sup>+</sup>. In the IR spectrum of unbound ligand **L**<sub>1</sub>, a distinctive peak at 3200 cm<sup>-1</sup> was observed which is the characteristic stretching vibration associated with the N–H bond. However, same N–H bond stretching vibration has undergone slight displacement and was observed at 3194 cm<sup>-1</sup> for complex **1**. The IR spectra of complex **1** displayed medium intense bands in the range 3000 to 2800 cm<sup>-1</sup>, which are identified as the symmetric and asymmetric stretching vibrations of aromatic C–H bonds.<sup>27-29</sup> The characteristic stretching vibrations of pyridyl (C=N) and phenyl (C=C) ring was observed in the range 1400–1630 cm<sup>-1</sup> for both the ligand and complex **8**. More importantly, C–O bonds, present in the backbone of both the ligand and complex showed sharp bands within the range of 1260 to 1390 cm<sup>-1</sup>. Furthermore, the crystal structure of the complex **8** was determined using Single crystal X-ray diffraction study. Crystallographic refinement parameters and important bond lengths are given in ESI (Table 4.5.1) while ellipsoid view (30 % probability) of the complex molecule is displayed in Scheme 5.3.2 along with atom numbering. For the sake of clarity in the image, hydrogens are omitted except the hydrogen present in the amine nitrogen atom. Crystal structure reveal that complex **8** crystallizes in the monoclinic system with *P*21/*n* space group. Complex **8** is a centrosymmetric dimer with two bridging chlorides and one terminal chloride atoms around

the metal centers. The asymmetric unit of **8** consists of half of the dimer along with a chloroform molecule, placed in a general position. Each iron center in **8** is coordinated by three nitrogen atoms of the ligand **L1**, two bridging chlorides and one terminal chlorine atom. As evident from the bond angles (74.51(8)–172.71(6)°), the geometry of the metal center can be best described as distorted octahedral. Inside the octahedral geometry, pyridyl nitrogen (N1), amine nitrogen (N2), terminal chloride (Cl3) and one of the bridging chlorides (C11) construct the basal plane while other bridging chloride (C11) and morpholine ring nitrogen (N3) atom are in axial position. It is worth noted that the secondary amine nitrogen arm contains one acidic proton which can easily be deprotonated in presence of an external base to create vacant sites around octahedral geometry (often this geometry is consider as catalytically less favourable due to poor scope of substrate binding). Moreover, bond distances around the metal centers in **8** are in the range 2.203(2)–2.6382(7) Å and the distance between two iron centers is 3.656 Å and all these bond lengths are consistent with previously reported dichloro bridged Fe(II) complexes.<sup>30-35</sup> A strong intramolecular hydrogen bonding between amine proton and terminal chloride and various other intermolecular hydrogen bonding such as C–H···Cl and C–H···O provides the solid state stability in **8**. Additionally, the single proton in solvated chloroform is also involved in hydrogen bonding with bridging chlorides and terminal chlorides as well.

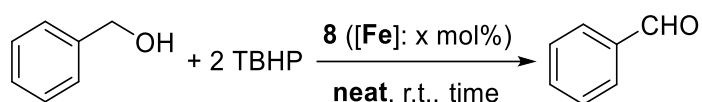
**Scheme 5.3.1. Synthesis of iron complex 8 with the molecular structures, using 50% probability ellipsoids (Hydrogen atoms are omitted for clarity)**



With well-characterized and air-stable iron complex (**1**) in hand, we set out to investigate its catalytic activity for the peroxidative oxidation of primary alcohol using TBHP as green oxidant (Table 5.3.1). The reaction optimization was performed using benzyl alcohol as standard substrate. As solvents produce most of the waste in a chemical transformation, we chose to perform the peroxidative oxidation under solvent-free condition. We started the peroxidative oxidation of benzyl alcohol with 2 eq. of TBHP in presence of 5 mol% catalyst (complex **8**) loading and the reaction was run for 6 h at r.t. (entry 1). Complete conversion of benzyl alcohol to benzaldehyde with almost quantitative isolated yield (96%) of benzaldehyde was obtained. Thereafter, the reaction time was gradually reduced to 1 h and complete oxidation of benzyl alcohol to benzaldehyde was noted (entry 2). Encouraged by the results, we steadily decreased the catalyst loading and complete oxidation of benzyl alcohol to benzaldehyde was obtained in presence of 1 mol% catalyst loading (entry 3). The catalyst loading was further reduced to 0.05 mol% and full oxidation of benzyl alcohol to benzaldehyde with almost quantitative isolated yield was obtained in 1 h at r.t. (entry 5). Further reduction of reaction time to 30 min lead to incomplete oxidation of benzyl alcohol to

benzaldehyde with roughly 20% unreacted benzaldehyde (entry 6). In absence of TBHP (entry 7) and complex **1** (entry 8), very poor conversion (less than 10%) of benzyl alcohol was obtained. So, entry 5 (depicted as bold) was concluded as the optimized reaction condition for the oxidation of benzyl alcohol to benzaldehyde. We also tested iron salt  $\text{FeCl}_2 \cdot 4\text{H}_2\text{O}$  as catalyst under very same reaction condition and very poor oxidation of benzyl alcohol was noted (entry 9). It is worth to mention that present peroxidative oxidation of benzyl alcohol was absolutely selective to aldehyde; formation of benzoic was not observed.

**Table 5.3.1. Catalytic performance of **8** for the peroxidative oxidation of benzyl alcohol to benzaldehyde.<sup>a</sup>**



entry	catalyst (mol%)	TBHP (eq.)	time (h)	conversion <sup>b</sup> (%)	yield <sup>c</sup> (%)
1	<b>8 (5)</b>	2	6	>99	96
2	<b>8 (5)</b>	2	4/2/1	>99	95/96/96
3	<b>8 (4/2/1)</b>	2	1	>99	96/95/96
4	<b>8 (0.1)</b>	2	1	>99	95
<b>5</b>	<b>8 (0.05)</b>	<b>2</b>	<b>1</b>	<b>&gt;99</b>	<b>96</b>
6	<b>8 (0.05)</b>	2	0.5	82	76
7	<b>8 (0.05)</b>	0	1	<10	n.d.
8	<b>8 (0)</b>	2	1	<10	n.d.
9	$\text{FeCl}_2 \cdot 4\text{H}_2\text{O}$ (0.05)	2	1	<15	n.d.

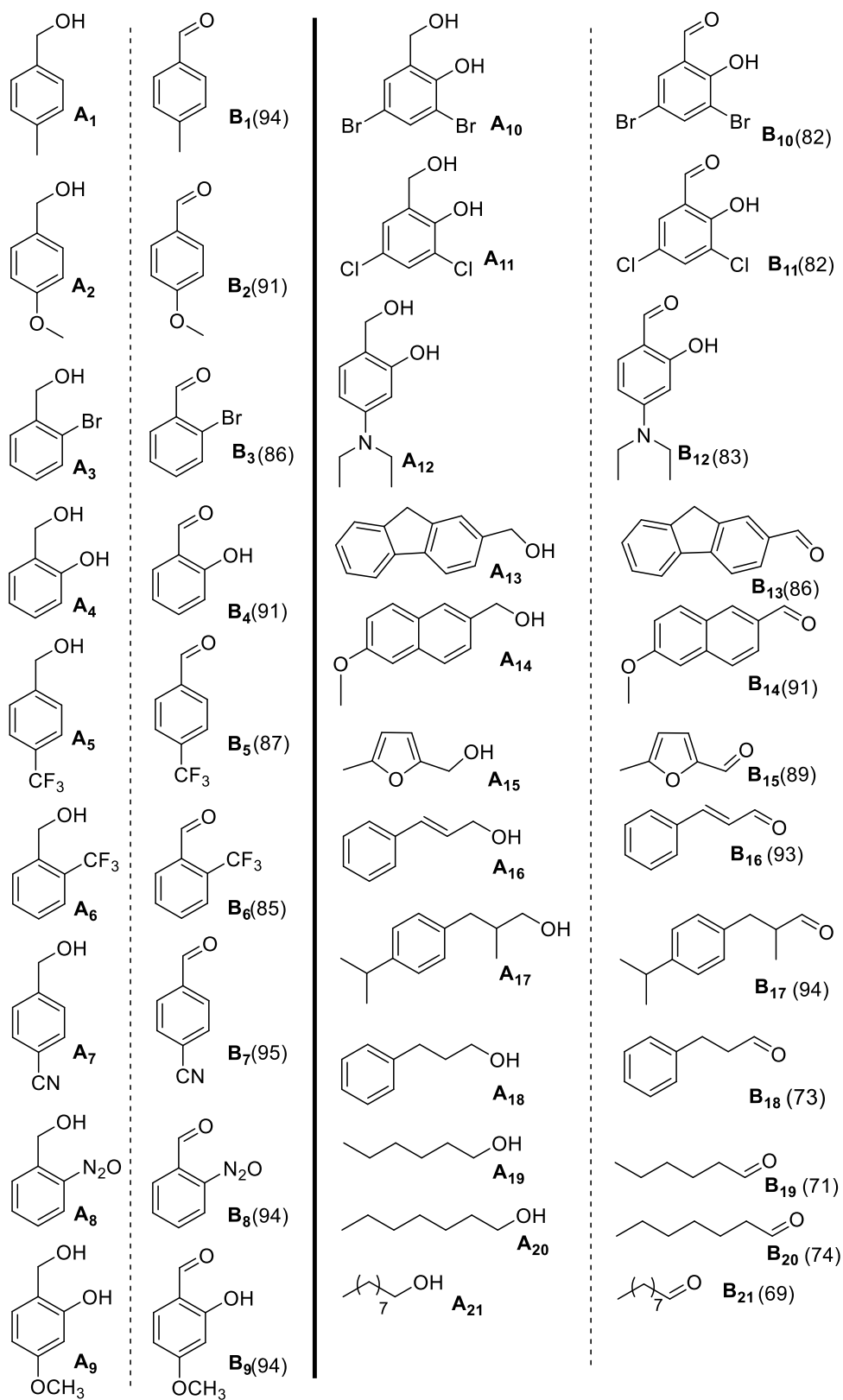
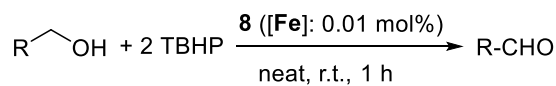
<sup>a</sup>Reactions conducted with 5.0 mmol of benzyl alcohol, 10.0 mmol of TBHP and 5/4/2/1/0.1/0.05 mol% of **8**. <sup>b</sup>Conversions were determined by  $^1\text{H}$  NMR spectroscopy using 1,3,5-trimethoxybenzene as standard. <sup>c</sup>Isolated yields.

Since complex **8** proved to be an efficient catalyst for the peroxidative oxidation of benzyl alcohol to benzaldehyde, the generality of the performance of complex **1** for the oxidation of various primary alcohol was tested. Previously optimized oxidation protocol (Table 1, entry

5: 5 mmol of substrate, 2 eq. TBHP, 0.05 mol% complex **8**, r.t., 1 h) was utilized for oxidation of various benzylic, allylic and aliphatic alcohols to expand the substrate scope (Scheme 5.3.2). We started with substituted benzylic alcohol with electron donating substituents such as methyl, methoxy, bromo and hydroxyl at *ortho*- and *para*-positions and excellent selectivity and yields of the corresponding aldehydes (**B**<sub>1</sub>: 94%, **B**<sub>2</sub>: 91%, **B**<sub>3</sub>: 86% and **B**<sub>4</sub>: 91%) were obtained. Substituted benzylic alcohol with electron withdrawing substituents such as trifluoromethyl, cyano and nitro groups were cleanly oxidized to the corresponding aromatic aldehydes (**B**<sub>5</sub>: 87%, **B**<sub>6</sub>: 85%, **B**<sub>7</sub>: 95% and **B**<sub>8</sub>: 94%). Using present catalytic protocol, substituted benzylic alcohols with multiple electron donating substituents were also smoothly oxidized to the respective aldehydes (**B**<sub>9</sub>: 94%, **B**<sub>10</sub>: 82%, **B**<sub>11</sub>: 82% and **B**<sub>12</sub>: 83%). So, the electronic nature of the substituents has no effect on the outcome of this peroxidative oxidation. We also tested polycyclic and heteroaromatic primary alcohols and excellent selectivity and yields of the corresponding aldehydes (**B**<sub>13</sub>: 86%, **B**<sub>14</sub>: 91% and **B**<sub>15</sub>: 89%) were obtained. In addition to the benzylic alcohol, allyl alcohol as activated primary alcohol was also tested. Representative example was illustrated, where cinnamyl alcohols underwent facile peroxidative oxidation to give cinnamaldehyde selectively (**B**<sub>16</sub>: 93%). In all those peroxidative oxidations, no substrate was oxidized to carboxylic acid. Thereafter, unactivated aliphatic primary alcohols were subjected to the optimized peroxidative oxidation protocol. 3-(4-isopropylphenyl)-2-methylpropanal was selectively oxidized to the respective aldehyde in excellent isolated yield (**B**<sub>17</sub>: 94%). 3-phenyl-1-propanol, *n*-hexanol, *n*-heptanol and *n*-nonanol were oxidized to the corresponding aldehydes in good yields (**B**<sub>18</sub>: 73%, **B**<sub>19</sub>: 71%, **B**<sub>20</sub>: 74% and **B**<sub>21</sub>: 69%). Although decent aldehyde selectivity (roughly 80%) was observed for challenging aliphatic primary alcohols, we also observed the formation of over-oxidation carboxylic acid product (roughly 20%). This catalytic system is applicable to a

wide variety of primary alcohols and noteworthy functional group tolerance was also observed.

**Scheme 5.3.2. Substrate scope for the selective oxidation of primary alcohols to aldehydes<sup>a,b</sup>**

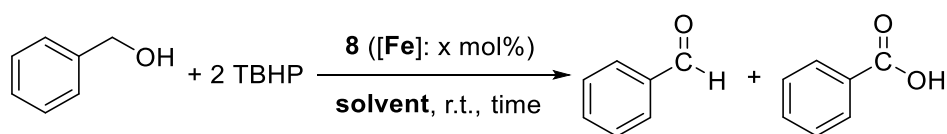


<sup>a</sup>Reactions conducted with 5.0 mmol of primary alcohol, 10.0 mmol of TBHP and 0.05 mol% of **8** at r.t. under neat condition for 1 h. <sup>b</sup>Isolated yields.

Acetonitrile is a heavily used reaction medium for the oxidation of substituted benzyl alcohols.<sup>36-38</sup> Chlorinated solvents (for example DCM) is also frequently used for the same purpose. However, acetonitrile and DCM are considered as hazardous solvents. Solvent selection for sustainable catalytic transformations is a vital consideration. The nature of solvent may directly influence the outcome of a homogeneous catalytic reaction, but the effect of various solvent parameters on a catalytic process is often ignored. Moreover, Jessop *et al.* nicely illustrated how a careful solvent selection can significantly increase the performance of a homogeneous catalyst.<sup>39</sup> Recently, Bagh *et al.* showed the influence of the solvent polarity and coordination ability on the aerobic oxidation of vanillyl alcohol to vanillin.<sup>40</sup> Although nice selectivity to primary alcohol to aldehyde was observed for the present catalytic oxidation protocol under solvent-free condition, we wanted to investigate the effect of solvent on the present peroxidative oxidation of primary alcohols. We selected five solvents DCM, acetone, acetonitrile and water with increasing solvent polarity and tested the catalytic performance of complex **8** in those solvents (Table 5.3.2). At first, peroxidative oxidations of benzaldehyde were performed with 2 eq. of TBHP in presence of 0.1 mol% catalyst loading at r.t. for 30 mins in those five solvents. In the least polar DCM, a small amount of benzaldehyde (16%) was formed and the rest was unreacted benzyl alcohol (entry 1). In acetone with a higher dielectric constant, amount of benzaldehyde increased to 34% (entry 2). However, a large amount of unreacted starting material was present. Thereafter, the peroxidative oxidation was performed in acetonitrile with even higher solvent polarity (entry 3) and interestingly we observed the formation of both benzaldehyde (25%) and benzoic acid (40%). Finally, the peroxidative oxidation was performed in highly polar water (entry 5) and full oxidation of benzyl alcohol was observed with a large amount of benzoic acid (78%) and small amount of aldehyde (22%). Then, the reaction time was increased to 1 h and we were pleased to see the complete and selective oxidation of benzyl alcohol to benzoic acid in water

(entry 6). The optimized reaction condition for the selective peroxidative oxidation of benzyl alcohol to benzoic acid is as follows: 5 mmol of substrate, 2 eq. TBHP, 0.05 mol% complex **8**, r.t., 1 h and water as solvent (entry 6, depicted in bold). Hence, profound effect of solvents on the outcome of benzyl alcohol oxidation was observed and selective oxidation of primary alcohol to carboxylic acid was achieved in green solvent water. We also wanted to check the catalytic performance of complex **8** in other green and sustainable solvents. In the last decade, deep eutectic solvents (DESs) have emerged as an appealing ecofriendly and sustainable reaction media with minor economic and environmental impact.<sup>41-46</sup> In addition, DESs are highly polar. So, we selected a non-toxic metal-free and commonly used type-III DES which is a 1:2 mixture of choline chloride (ChCl) and glycerol and following peroxidative oxidations of benzyl alcohol were carried out in this DES (entry 6-9). We tested the peroxidative oxidation of benzyl alcohol in ChCl/glycerol (1:2) using previously optimized reaction condition and complete oxidation of benzyl alcohol to benzoic acid was observed in 1 h with 0.1 mol% catalyst loading (entry 6). Catalyst loading was further reduced to 0.001 mol% and complete oxidation of benzyl alcohol to benzoic acid was noted again in 1 h (entry 8). If the reaction time was reduced to 30 mins, benzaldehyde was also observed along with benzoic acid (entry 9). Very low catalyst loading was achieved in DES and entry 8 was considered as another optimized reaction conditions. Therefore, complex **8** was proved to be an extremely efficient catalyst in DES for the selective oxidation of benzyl alcohol to benzoic acid.

**Table 5.3.2. Catalytic performance of 1 for the peroxidative oxidation of benzyl alcohol in different solvents.<sup>a</sup>**



entry	catalyst <b>8</b>	time	solvent	dielectric	benzaldehyde <sup>b</sup>	benzoic acid <sup>b</sup>
-------	-------------------	------	---------	------------	---------------------------	---------------------------

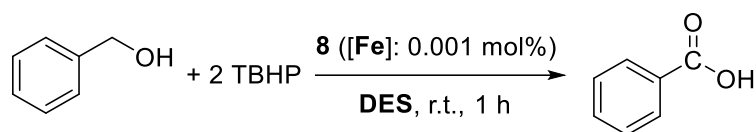
	(mol%)	(h)		constant ( $\epsilon$ )	(%)	(%)
1	0.1	0.5	DCM	8.40	16	0
2	0.1	0.5	acetone	21.01	34	0
3	0.1	0.5	MeCN	36.64	25	40
4	0.1	0.5	water	78.54	22	78
<b>5</b>	<b>0.1</b>	<b>1</b>	<b>water</b>	<b>78.54</b>	<b>0</b>	<b>&gt;99 (95<sup>c</sup>)</b>
6	0.1	1	DES <sup>d</sup>	83.74	0	>99 (95 <sup>c</sup> )
7	0.05/0.01	1	DES <sup>d</sup>	83.74	0	>99 (94 <sup>c</sup> )
<b>8</b>	<b>0.001</b>	<b>1</b>	<b>DES<sup>d</sup></b>	<b>83.74</b>	<b>0</b>	<b>&gt;99 (96<sup>c</sup>)</b>
9	0.001	0.5	DES <sup>d</sup>	83.74	28	72

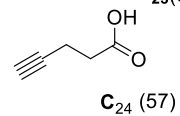
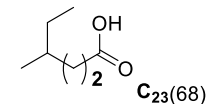
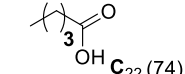
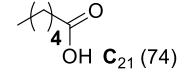
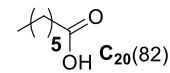
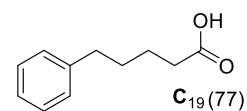
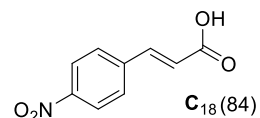
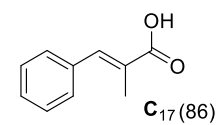
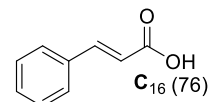
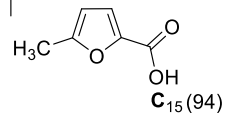
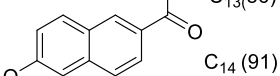
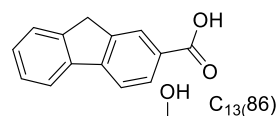
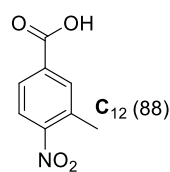
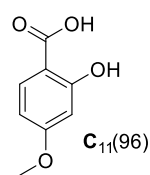
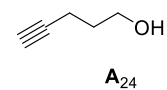
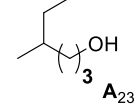
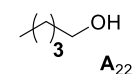
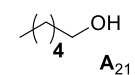
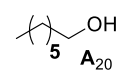
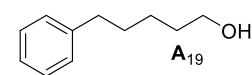
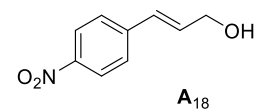
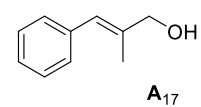
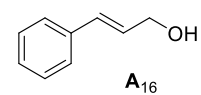
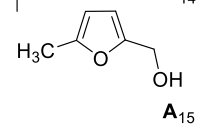
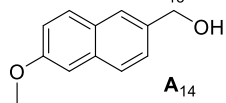
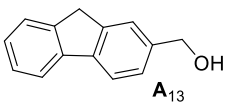
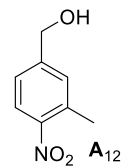
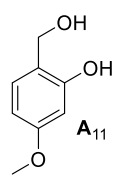
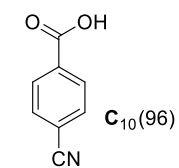
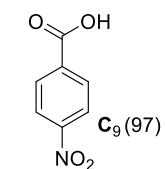
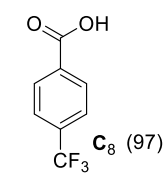
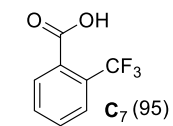
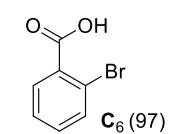
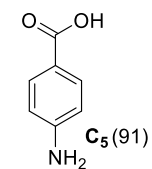
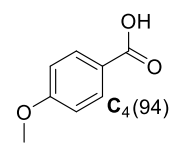
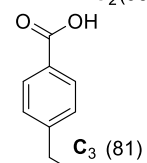
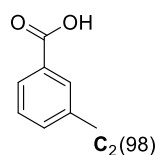
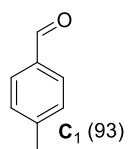
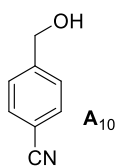
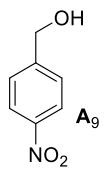
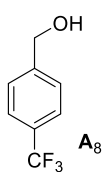
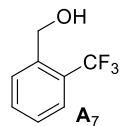
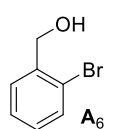
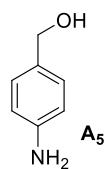
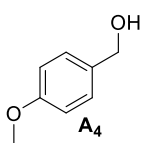
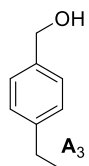
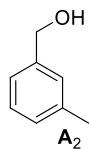
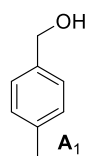
<sup>a</sup>Reactions conducted with 5.0 mmol of benzyl alcohol, 10.0 mmol of TBHP and 0.1/0.05/0.001 mol% of **8** in 2 mL of solvent. <sup>b</sup>Conversions were determined by <sup>1</sup>H NMR spectroscopy using 1,3,5-trimethoxybenzene as standard. <sup>c</sup>Isolated yields. <sup>d</sup>DES stands for ChCl/glycerol (1:2).

Since complex **8** displayed very high efficiency for the catalytic peroxidative oxidation of benzyl alcohol to benzoic acid in highly polar solvents, the generality of the performance of complex **8** for the oxidation of various primary alcohol was tested. Following two optimized oxidation protocols were used for the peroxidative oxidation of various benzylic, allylic and aliphatic alcohols to expand the substrate scope: A. Table 5.3.2, entry 9: 5 mmol of substrate, 2 eq. TBHP, 0.001 mol% complex **8**, 2 mL ChCl/glycerol (1:2), r.t., 1 h and B. Table 5.3.2, entry 6: 5 mmol of substrate, 2 eq. TBHP, 0.1 mol% complex **8**, 2 mL water, r.t., 1 h (Scheme 5.3.3). At first various substituted benzylic alcohols with various electron donating and electron withdrawing groups were subjected to oxidative under above mentioned optimized reaction conditions. All substituted benzylic alcohols were selectively oxidized to the corresponding carboxylic acids with excellent isolated yields (C<sub>1</sub>: 93%, C<sub>2</sub>: 98%, C<sub>3</sub>: 81%, C<sub>4</sub>: 94%, C<sub>5</sub>: 91%, C<sub>6</sub>: 97%, C<sub>7</sub>: 95%, C<sub>8</sub>: 97%, C<sub>9</sub>: 97%, C<sub>10</sub>: 96%, C<sub>11</sub>: 96% and C<sub>12</sub>:

88%). Polycyclic and heteroaromatic primary alcohols were also cleanly oxidized to the corresponding carboxylic acids (**C13**: 86%, **C14**: 91% and **C15**: 94%). Allylic alcohols were also effectively oxidized to the respective carboxylic acids in high isolated yields (**C16**: 76%, **C17**: 86% and **C18**: 84%). Finally, we tested unactivated aliphatic primary alcohols and they were cleanly oxidized to the corresponding carboxylic acids in good isolated yields (**C19**: 76%, **C20**: 76%, **C21**: 76%, **C22**: 86% and **C23**: 84%). Finally, optimized oxidation protocol in water was also tested for a few selective primary alcohols and corresponding carboxylic acids were isolated in good to excellent yields (**C2**: 94%, **C4**: 91%, **C7**: 91%, **C9**: 97%, **C12**: 85%, **C14**: 87%, **C15**: 90%, **C17**: 85%, **C19**: 72% and **C20**: 74%).

**Scheme 5.3.3. Substrate scope for the selective oxidation of primary alcohols to carboxylic acids<sup>a,b</sup>**



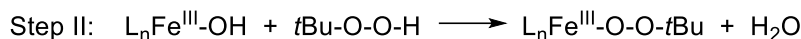
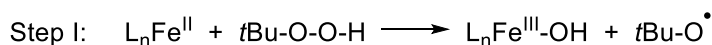


<sup>a</sup>Reactions conducted with 5.0 mmol of primary alcohol, 10.0 mmol of TBHP and 0.001 mol% of **8** in 2 mL of ChCl/glycerol (1:2) at r.t. for 1 h. <sup>b</sup>Reactions conducted with 5.0 mmol of primary alcohol, 10.0 mmol of TBHP and 0.1 mol% of **1** in water (2 mL) at r.t. for 1 h.

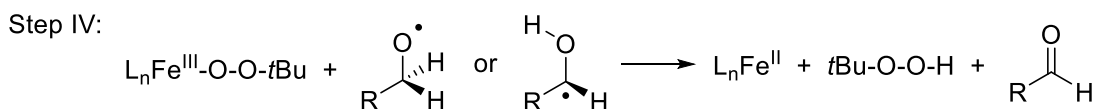
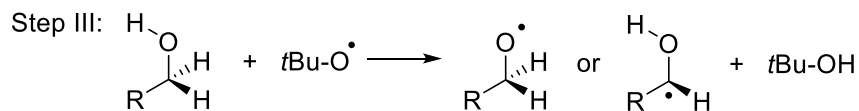
It is important to recycle and reuse a catalyst for sustainable catalytic development. The role of solvent is equally important as solvents in a chemical reaction often produce the most amount of chemical waste. Therefore, recycling the reaction media is even more important than catalyst recycling. Therefore, we set out to explore the possibility of catalyst and reaction media recovery and reuse. After performing the catalytic oxidation of vanillyl alcohol to vanillic acid using standard optimized reaction conditions, we extracted the product vanillic acid with ethyl acetate, another green solvent. After the second set of reactions, the recovered reaction media and catalyst were reused for another four times without any significant change in activity for both methods. Therefore, the solution of the iron catalyst in DES (ChCl/glycerol (1:2)) was effectively recycled five times

Finally, based on past reports, a plausible catalytic path is proposed.<sup>47</sup> First step involves the reaction of TBHP with Fe(II) complex to give oxidized Fe(III)-hydroxy species and *tert*-butoxy radical. Fe(III)-hydroxy species further reacts with TBHP to give Fe(III)-peroxo species. Then there are two possible paths. Path A involves the reaction of alcohol with *tert*-butoxy radical to generate either carbon- or oxygen-center radical which finally reacts with Fe(III)-peroxo species to give aldehyde and regenerate starting Fe(II) species. Path B involves the formation of iron(IV)-oxo species which further reacts with carbon- or oxygen-center radical to give aldehyde and regenerate Fe(II)-hydroxy species.

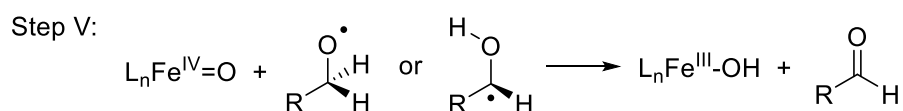
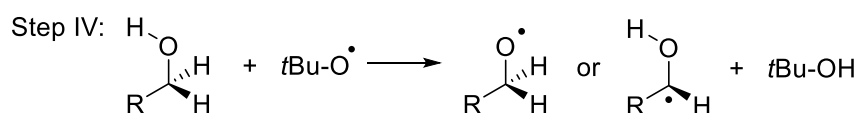
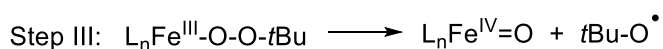
#### **Scheme 5.3.4. Plausible reaction path for complex **8** catalyzed alcohol oxidation**



**Path A:**



**Path B:**



## 5.4 CONCLUSIONS

In conclusion, we have developed an air-stable iron catalyst for the efficient peroxidative oxidation of activated and unactivated primary alcohols at ambient reaction conditions. Using iron as a base metal catalyst is a significant development for selective oxidation of primary alcohols. Under neat condition, the peroxidative oxidation of primary alcohol was highly selective to aldehyde and various activated alcohols such as benzylic and allylic alcohols with different functionalities were effectively oxidized to the corresponding aldehydes. A slight loss of aldehyde selectivity was observed for challenging aliphatic alcohols and small amount of carboxylic acids were formed as over-oxidation product. In highly polar solvents such as water deep eutectic solvent (ChCl/glycerol (1:2)), the catalytic peroxidative oxidation of primary alcohol was selective to carboxylic acid. It is worth to mention that those oxidations were performed in green reaction media such as water and type-III DES. A wide variety of

activated and unactivated alcohols such as benzylic, allylic and aliphatic alcohols with different functional groups were effectively oxidized to the corresponding carboxylic acids. Thus, present catalytic protocol exhibited broad substrate scope and notable functional group tolerance. This is an interesting example of reaction media induced chemodivergent oxidation of primary alcohol. Very low catalyst loading particularly ppm level catalyst loading for the oxidation of primary alcohol to carboxylic acid is realistic for possible industrial use. The catalyst in deep eutectic solvent can be recycled several times. In conclusion, developing base metal catalyzed sustainable catalytic protocols for chemoselective oxidation of primary alcohols is a significant achievement. Further investigation will involve the use of the present iron catalyst for the selective oxidation of secondary alcohols.

## 5.5 experimental section

### Syntheses of ligand and corresponding iron complex

**General experimental.** Syntheses of ligand and iron complex were carried out in air. All solvents (acetonitrile, dichloromethane, diethyl ether, hexanes, ethyl acetate, ethanol, methanol) and chemicals were purchased from commercial suppliers and used without further purification. For recording NMR spectra,  $\text{CDCl}_3$  and  $\text{DMSO-d}_6$  was purchased from Sigma-Aldrich and used without further purification.  $^1\text{H}$  and  $^{13}\text{C}$  NMR spectra were recorded at Bruker AV-400 and JEOL-400 ( $^1\text{H}$  at 400 MHz and  $^{13}\text{C}$  at 101 MHz).  $^1\text{H}$  NMR chemical shifts are referenced in parts per million (ppm) with respect to tetramethylsilane ( $\delta$  0.00 ppm) and  $^{13}\text{C}\{^1\text{H}\}$  NMR chemical shifts are referenced in ppm with respect to  $\text{CDCl}_3$  ( $\delta$  77.16 ppm). The coupling constants ( $J$ ) are reported in hertz (Hz). The following abbreviations are used to describe multiplicity: s = singlet, bs = broad signal, d = doublet, t = triplet, q = quadrate, m = multiplate. High resolution mass spectra were recorded on a Bruker micrOTOF-Q II Spectrometer. Elemental analysis was carried out on a EuroEA Elemental

Analyser. Infrared (IR) spectra were recorded on a Perkin-Elmer FT-IR spectrophotometer. Crystal data were collected with Rigaku Oxford diffractometer and with INCOATEC micro source (Mo-K $\alpha$  radiation,  $\lambda = 0.71073 \text{ \AA}$ , multilayer optics) at 293 K.

**Synthesis of 8.** A mixture of **L1** (0.221 g, 1.00 mmol) and FeCl<sub>2</sub>.4H<sub>2</sub>O (0.198 g, 1.00 mmol) in acetonitrile (15 mL) was stirred at r.t. for 24 h resulting in a pale-yellow precipitate. All volatiles were removed under high vacuum to give a light-yellow solid which was extracted with dichloromethane (15 mL). Then the solvent was removed under high vacuum to give a yellow solid as pure complex **1** (0.330 g, 95%). X-ray quality single crystals were obtained by slow diffusion of diethyl ether into a solution of **1** in dichloromethane. HRMS (ESI-TOF) m/z: [M – Cl]<sup>+</sup> calcd for C<sub>24</sub>Fe<sub>2</sub>H<sub>38</sub>Cl<sub>3</sub>N<sub>6</sub>O<sub>2</sub> 661.0831; found 661.0831. Anal. Calcd for C<sub>24</sub>Fe<sub>2</sub>H<sub>38</sub>Cl<sub>4</sub>N<sub>6</sub>O<sub>2</sub> (694.05): Elemental Analysis: C, 41.38; H, 5.49; Cl, 20.32; Fe, 15.87; N, 11.97; O, 4.58

**General procedure for oxidations (reaction optimization and).** Benzyl alcohol (0.540 g, 5 mmol) and complex **8** (5/ 3/ 2/ 1/ 0.05/0.01/0.005 mol %) and TBHP (0.50 mmol) were taken in deep eutectic solvent and was transferred into a seal tube fitted with a magnetic stir-bar. The reaction mixture was heated at appropriate temperature (r.t./ 50 °C/ 70 °C/ 100 °C) in an oil bath for appropriate time (1 to 12 h). Thereafter, the reaction mixture was cooled down to r.t. (in case of heating) and was extracted using ethyl acetate (3 X 5 mL) and all volatiles were removed under reduced pressure to give white solid as pure product. The product was analysed by <sup>1</sup>H NMR spectroscopy.

**General procedure for the recycling of the reaction medium:** benzyl alcohol (0.540 g, 5 mmol), complex **8** (0.01 mol %) and TBHP (0.50 mmol) were taken in deep eutectic solvent and was transferred into a seal tube fitted with a magnetic stir-bar. The reaction mixture was allowed to run for 2 hours at room temperature. After completion of the reaction the crude

was extracted using ethyl acetate (15 mL) and reimagining DES was placed in seal tube equipped with magnetic stir-bar. Vanillyl alcohol (0.076 g, 0.50 mmol) and complex **1** (2 mol %) were taken and the reaction mixture was allowed to run 2 h at room temperature. The entire process was repeated for four times and no change in catalytic activity was observed. Vanillic acid was isolated almost  $\leq 99\%$  in all reaction run.

## NMR DATA OF SOME SUBSTRATE

**Benzaldehyde (F1)** Benzaldehyde as colourless liquid was synthesized according to the general procedure.  $^1\text{H NMR}$  (700 MHz,  $\text{CDCl}_3$ )  $\delta$  10.02 (s, 1H), 7.88 (d,  $J = 7.3$  Hz, 2H), 7.70 – 7.59 (m, 1H), 7.59 – 7.44 (m, 2H).  $^{13}\text{C NMR}$  (176 MHz,  $\text{CDCl}_3$ )  $\delta$  192.40 (s), 136.41 (s), 134.47 (s), 129.37 (d,  $J = 129.5$  Hz), 129.00 (s).

**4-Methoxybenzaldehyde (F2)** 4-Methoxybenzaldehyde was synthesized according to the general procedure.  $^1\text{H NMR}$  (700 MHz,  $\text{CDCl}_3$ )  $\delta$  9.88 (s, 1H), 7.83 (d,  $J = 8.6$  Hz, 2H), 7.00 (d,  $J = 8.7$  Hz, 2H), 3.87 (d,  $J = 14.3$  Hz, 3H).  $^{13}\text{C NMR}$  (176 MHz,  $\text{CDCl}_3$ )  $\delta$  190.86 (s), 164.63 (s), 131.99 (s), 129.94 (s), 114.32 (s), 55.58 (s).

**2-Hydroxy-4-Methoxybenzaldehyde (F3)** 2-Hydroxy-4-Methoxybenzaldehyde synthesized according to the general procedure  $^1\text{H NMR}$  (700 MHz,  $\text{CDCl}_3$ )  $\delta$  11.47 (s, 1H), 9.72 (s, 1H), 7.38 (t,  $J = 53.9$  Hz, 1H), 6.87 – 6.22 (m, 2H), 3.86 (s, 3H)  $^{13}\text{C NMR}$  (176 MHz,  $\text{CDCl}_3$ )  $\delta$  194.32 (s), 166.86 (s), 164.53 (s), 135.22 (s), 115.23 (s), 108.33 (s), 100.71 (s), 55.66 (s).

**3,5-Dibromo-2-Hydroxybenzaldehyde (F4)** 3,5-Dibromo-2-Hydroxybenzaldehyde was synthesized according to the general procedure  $^1\text{H NMR}$  (400 MHz,  $\text{CDCl}_3$ )  $\delta$  11.53 (s, 1H), 9.83 (s, 1H), 7.92 (d,  $J = 2.3$  Hz, 1H), 7.69 (d,  $J = 2.3$  Hz, 1H).  $^{13}\text{C NMR}$  (101 MHz,  $\text{CDCl}_3$ )  $\delta$  194.92 (s), 157.28 (s), 141.99 (s), 134.93 (s), 123.70 – 119.48 (m), 112.99 – 112.19 (m), 111.88 – 111.13 (m).

**Benzoic acid (D1)** Benzoic acid was synthesized according to the general procedure  $^1\text{H}$  NMR (400 MHz,  $\text{CDCl}_3$ )  $\delta$  10.36 (s, 1H), 8.23 – 8.11 (m, 2H), 7.65 (t,  $J = 7.4$  Hz, 1H), 7.51 (t,  $J = 7.7$  Hz, 2H).  $^{13}\text{C}$  NMR (101 MHz,  $\text{CDCl}_3$ )  $\delta$  172.41 (s), 133.84 (s), 130.24 (s), 129.36 (s), 128.51 (s).

**3-Methylbenzoic acid (D2)** 3-Methylbenzoic acid was synthesized according to the general procedure  $^1\text{H}$  NMR (400 MHz,  $\text{CDCl}_3$ )  $\delta$  7.95 (d,  $J = 8.5$  Hz, 2H), 7.44 (s, 1H), 7.40 (d,  $J = 7.5$  Hz, 1H), 2.45 (s, 3H).  $^{13}\text{C}$  NMR (101 MHz,  $\text{CDCl}_3$ )  $\delta$  175.66 – 164.08 (m), 138.34 (s), 134.59 (s), 130.72 (s), 129.76 – 129.00 (m), 128.41 (s), 127.38 (s), 21.28 (s).

**4-Methylbenzaldehyde (D3)** 4-Methylbenzaldehyde was synthesized according to the general procedure  $^1\text{H}$  NMR (400 MHz,  $\text{CDCl}_3$ )  $\delta$  7.95 (d,  $J = 8.5$  Hz, 2H), 7.44 (s, 1H), 7.40 (d,  $J = 7.5$  Hz, 1H), 2.45 (s, 3H).  $^{13}\text{C}$  NMR (101 MHz,  $\text{CDCl}_3$ )  $\delta$  175.66 – 164.08 (m), 138.34 (s), 134.59 (s), 130.72 (s), 129.76 – 129.00 (m), 128.41 (s), 127.38 (s), 21.28 (s).

**4-Methoxybenzoic acid (D4)** 4-Methoxybenzoic acid was synthesized according to the general procedure according to the general procedure  $^1\text{H}$  NMR (400 MHz,  $\text{CDCl}_3$ )  $\delta$  7.95 (d,  $J = 8.5$  Hz, 2H), 7.44 (s, 1H), 7.40 (d,  $J = 7.5$  Hz, 1H), 2.45 (s, 3H).  $^{13}\text{C}$  NMR (101 MHz,  $\text{CDCl}_3$ )  $\delta$  175.66 – 164.08 (m), 138.34 (s), 134.59 (s), 130.72 (s), 129.76 – 129.00 (m), 128.41 (s), 127.38 (s), 21.28 (s).

**2-Hydroxy-4-Methoxybenzoic acid (D5)** 2-Hydroxy-4-Methoxybenzoic acid was synthesized according to the general procedure according to the general procedure  $^1\text{H}$  NMR (400 MHz,  $\text{CDCl}_3$ )  $\delta$  7.95 (d,  $J = 8.5$  Hz, 2H), 7.44 (s, 1H), 7.40 (d,  $J = 7.5$  Hz, 1H),

2.45 (s, 3H).  $^{13}\text{C}$  NMR (101 MHz,  $\text{CDCl}_3$ )  $\delta$  175.66 – 164.08 (m), 138.34 (s), 134.59 (s), 130.72 (s), 129.76 – 129.00 (m), 128.41 (s), 127.38 (s), 21.28 (s).

## NMR SPECTRA OF SOME SUBSTRATE

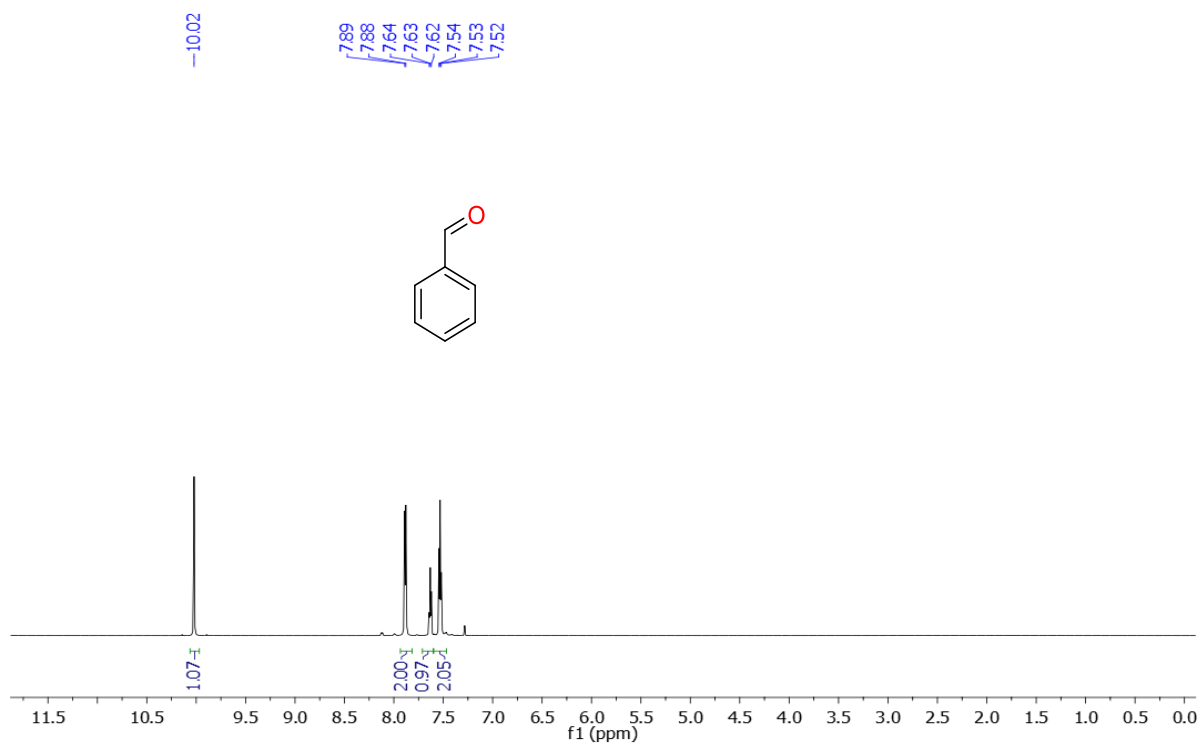


**Figure 5.5.1.**  $^{13}\text{C}$   $\{^1\text{H}\}$  NMR (101 MHz) spectrum of **Benzaldehyde** in  $\text{CDCl}_3$  at r.t.

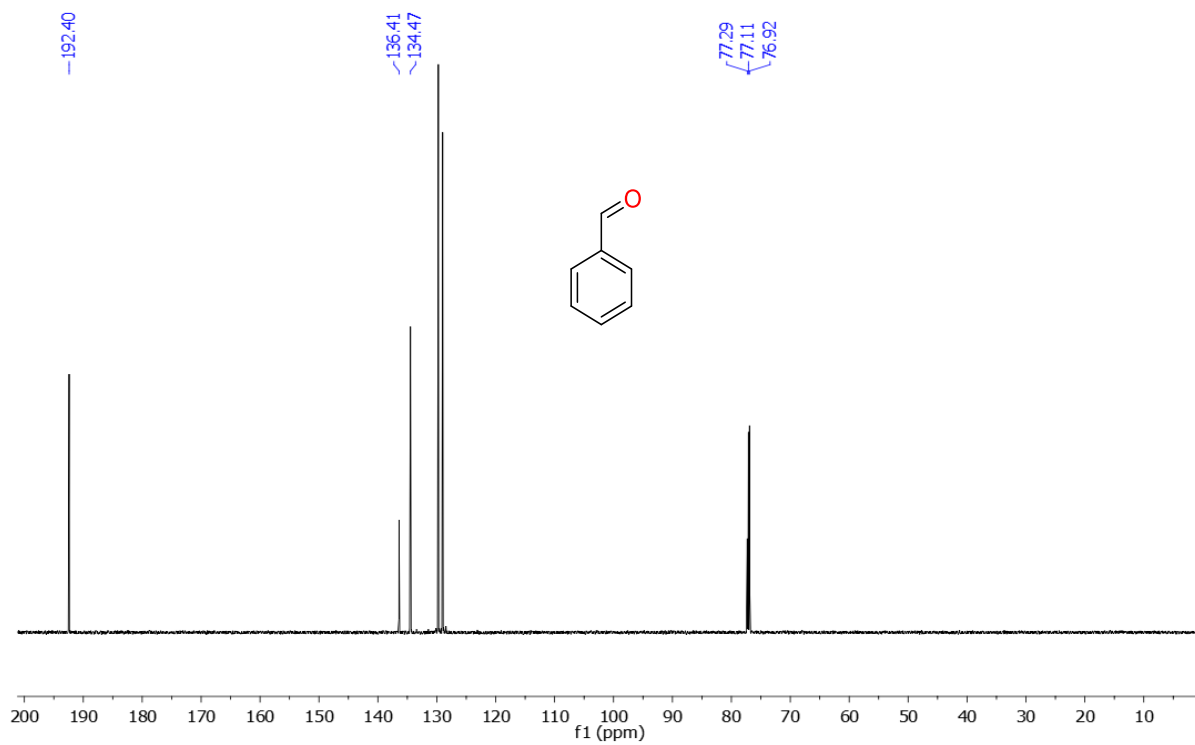


**Figure 5.5.2.**  $^{13}\text{C}$   $\{^1\text{H}\}$  NMR (101 MHz) spectrum of **Benzaldehyde** in  $\text{CDCl}_3$  at r.t.

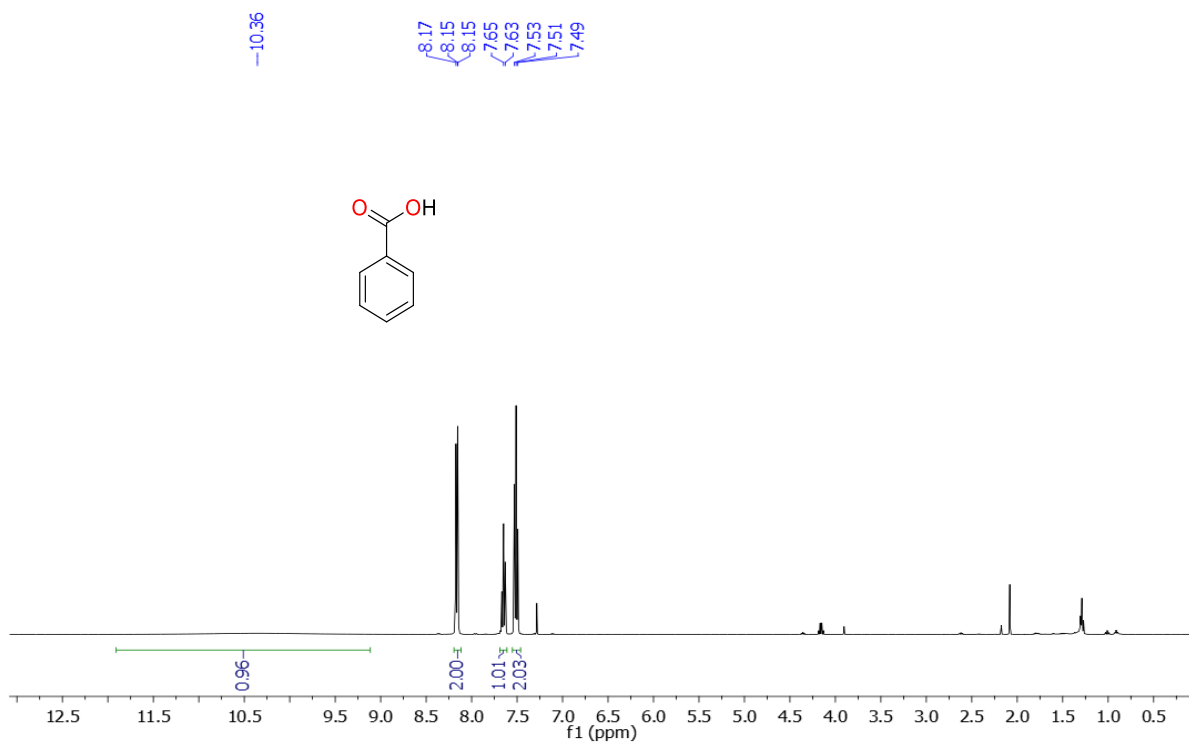


**Figure 5.5.3.** <sup>13</sup>C {<sup>1</sup>H} NMR (101 MHz) spectrum of **Benzoic Acid** in CDCl<sub>3</sub> at r.t.

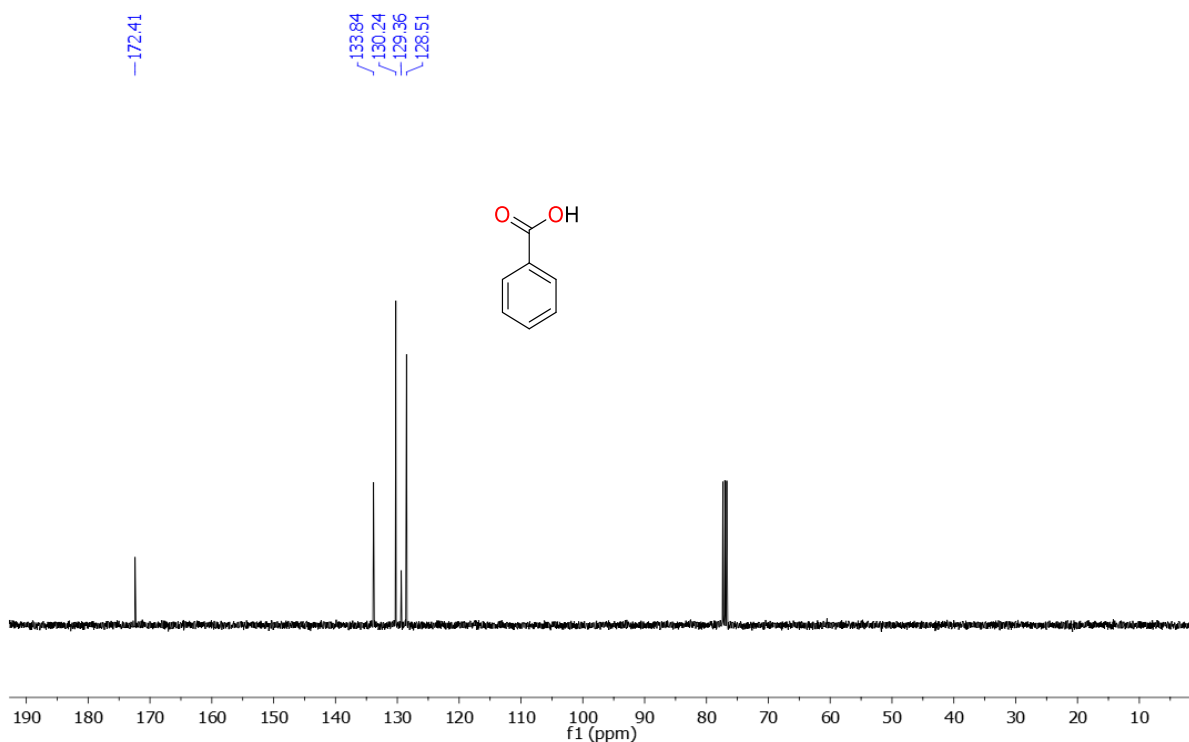


**Figure 5.5.4.** <sup>13</sup>C {<sup>1</sup>H} NMR (101 MHz) spectrum of **Benzoic Acid** in CDCl<sub>3</sub> at r.t.

## X-ray structure determination

Crystallographic data and structure determinations details are compiled in Table S1. The crystals were obtained by slow diffusion of diethyl ether into a solution of **7** in DCM at r.t. The crystals were coated with silicon oil on a glass slide and a suitable single crystal was mounted on a glass fibre. Crystal data were collected with a Rigaku Oxford diffractometer and with an INCOATEC micro source (Mo-K $\alpha$  radiation,  $\lambda = 0.71073 \text{ \AA}$ , multilayer optics) at 100 K. The structure was determined using direct methods employed in ShelXT, OleX, and refinement was carried out using least-square minimization implemented in ShelXL. All nonhydrogen atoms were refined with anisotropic displacement parameters. Hydrogen atom positions were fixed geometrically in idealized positions and were refined using a riding model.

**Table 5.5.1.** Crystallographic Data and Refinement Parameters for complex **7**

Empirical formula	C <sub>13</sub> H <sub>20</sub> Cl <sub>5</sub> FeN <sub>3</sub> O
Formula weight (g mol <sup>-1</sup> )	696.578
Temperature (K)	100.00(10)
Wavelength	0.71073
Crystal system	monoclinic
Space group	P21/n
<i>a</i> (Å)	9.8542(5)
<i>b</i> (Å)	14.7222(8)
<i>c</i> (Å)	14.3741(9)
$\alpha$ (deg)	90.000(5)
$\beta$ (deg)	108.889(6)
$\gamma$ (deg)	90.000(5)
volume (Å <sup>3</sup> )	1973.09(8)
<i>Z</i>	4
<i>D</i> <sub>calc</sub> (g cm <sup>-3</sup> )	1.5477
$\mu$ (mm <sup>-1</sup> )	1.446
<i>F</i> (000)	832
Crystal Size	0.2 × 0.2 × 0.1 mm <sup>3</sup>
$\theta$ Range (deg)	7.16 to 63.74
Index Ranges	-12 ≤ <i>h</i> ≤ 13, -20 ≤ <i>k</i> ≤ 20, -

	$18 \leq l \leq 19$
Reflections collected	18716
Independent reflections ( $R_{\text{int}}$ )	4611 [ $R_{\text{int}} = 0.0440$ , $R_{\text{sigma}} = 0.0395$ ]
Completeness to $\theta = 25.07^\circ$	99.60
Refinement method	Full-matrix least-squares on $F^2$
Data/Restraints/parameters	4611/1/228
Goodness-of-fit on $F^2$	0.761
Final $R$ indices [ $I > 2\sigma(I)$ ]	$R_1 = 0.0315$ , $wR_2 = 0.0913$
$R$ indices (all data)	$R_1 = 0.0427$ , $wR_2 = 0.0983$
Largest diff. peak/hole ( $e \text{ \AA}^{-3}$ )	1.39/-1.06

## 5.6 REFERENCE

1. Fürstner, A. *Angew. Chem. Int. Ed.* **2009**, *48*, 1364–1367.
2. Bauer, I.; Knölker, H.-J. *Chem. Rev.* **2015**, *115*, 3170–3378.
3. Bolm, C.; Legros, J.; Le Paih, J.; Zani, L. *Chem. Rev.* **2004**, *104*, 6217–6254.
4. (a) review on catalytic oxidations. Kopylovich, M. N.; Ribeiro, A. P.; Alegria, E. C.; Martins, N. M.; Martins, L. M.; Pombeiro, A. J. Catalytic oxidation of alcohols: Recent advances. *Adv. Organomet. Chem.*, **2015**, *63*, 91-174 (b) review on catalytic oxidations. Olenin, A. Y.; Mingalev, P. G.; Lisichkin, G. V. Partial catalytic oxidation of alcohols: catalysts based on metals and metal coordination compounds. *Pet. Chem.*, **2018**, *58*, 577-592. (c) Sheldon, R. A.; Arends, I. W.; Ten Brink, G. J.; Dijkstra, A. Green, catalytic oxidations of alcohols. *Acc. Chem. Res.*, **2002**, *35*, 774-781.
5. (a) ten Brink, G.-J.; Arends, I. W. C. E.; Sheldon, R. A. *Science*, **2000**, *287*, 1636–1639. (b) review or good paper on oxidation of alcohol to carbonyls and acid. Wei, Z. Ru, S.; Zhao, Q.; Yu, H.; Zhang, G.; Wei, Y. Highly efficient and practical aerobic oxidation of alcohols by inorganic-ligand supported copper catalysis. *Green Chem.*, **2019**, *21*, 4069-4075 (c) review or good paper on oxidation of alcohol to carbonyls and acid. Nutting, J. E.; Mao, K.; Stahl, S. S. Iron (III) nitrate/TEMPO-catalyzed aerobic

- alcohol oxidation: distinguishing between serial versus integrated redox cooperativity. *J. Am. Chem. Soc.*, **2021**, *143*, 10565-10570.
6. Ren, Q. G.; Chen, S. Y.; Zhou, X. T.; Ji, H. B. Highly efficient controllable oxidation of alcohols to aldehydes and acids with sodium periodate catalyzed by water-soluble metalloporphyrins as biomimetic catalyst. *Bioorg. Med. Chem.*, **2010**, *18*, 8144-8149.
  7. Tidwell, T. T. Oxidation of alcohols by activated dimethyl sulfoxide and related reactions: an update. *Synthesis*, **1990**, 857-870.
  8. Blackburn, L.; Taylor, R. J. In situ oxidation– imine formation– reduction routes from alcohols to amines. *Org. Lett.*, **2001**, *3*, 1637-1639.
  9. Cainelli, G.; Cardillo, G.; Cainelli, G.; Cardillo, G. Oxidation of alcohols. *Chromium Oxidations in Organic Chemistry*, 1984, 118-216.
  10. Tojo, G.; Fernandez, M. I. Oxidation of Alcohols to Aldehydes and Ketones; Springer Science & Business Media, 2006, 1-95.
  11. Thottathil, J. K.; Moniot, J. L.; Mueller, R. H.; Wong, M. K. Y.; Kissick, T. P. J. *Org. Chem.* **1986**, *51*, 3140.
  12. Hunsen, M. Pyridinium chlorochromate catalyzed oxidation of alcohols to aldehydes and ketones with periodic acid. *Tetrahedron Lett.*, **2005**, *46*, 1651-1653.
  13. Czernecki, S., Georgoulis, C., Stevens, C. L., & Vijayakumaran, K. Pyridinium dichromate oxidation. Modifications enhancing its synthetic utility. *Tetrahedron Lett.*, **1985**, *26*, 1699-1702.
  14. Singh, B.; Srivastava, S. Kinetics and mechanism of ruthenium tetroxide catalysed oxidation of cyclic alcohols by bromate in a base. *Transition Met. Chem.*, **1991**, *16*, 466-468.

15. Piccialli, V.; Ruthenium tetroxide and perruthenate chemistry. Recent advances and related transformations mediated by other transition metal oxo-species. *Molecules*, **2014**, *19*, 6534-6582.
16. (a) Hoover, J. M.; Ryland, B. L.; Stahl, S. S. Mechanism of copper (I)/TEMPO-catalyzed aerobic alcohol oxidation. *J. Am. Chem. Soc.*, **2013**, *135*, 2357-2367. (b) Jiang, X.; Zhang, J.; Ma, S. Iron catalysis for room-temperature aerobic oxidation of alcohols to carboxylic acids. *J. Am. Chem. Soc.* **2016**, *138*, 8344-8347.
17. Hosseini-Monfared, H.; Näther, C.; Winkler, H.; Janiak, C. Highly selective and “green” alcohol oxidations in water using aqueous 10% H<sub>2</sub>O<sub>2</sub> and iron-benzenetricarboxylate metal–organic gel. *Inorg. Chim. Acta*, **2012**, *391*, 75-82.
18. Sutradhar, M.; Alegria, E. C.; Mahmudov, K. T.; da Silva, M. F. C. G.; Pombeiro, A. J. Iron (III) and cobalt (III) complexes with both tautomeric (keto and enol) forms of aroylhydrazone ligands: Catalysts for the microwave assisted oxidation of alcohols. *RSC Adv.*, **2016**, *6*, 8079-8088.
19. Figiel, P. J.; Kopylovich, M. N.; Lasri, J.; da Silva, M. F. C. G.; da Silva, J. J. F.; Pombeiro, A. J. Solvent-free microwave-assisted peroxidative oxidation of secondary alcohols to the corresponding ketones catalyzed by copper (II) 2, 4-alkoxy-1, 3, 5-triazapentadienato complexes. *Chemical comm.*, **2010**, *46*, 2766-2768.
20. Sarkar, S. K.; Jana, M. S.; Mondal, T. K.; Sinha, C. Alcohol oxidation reactions catalyzed by ruthenium–carbonyl complexes of thioarylazoimidazoles. *Appl. Organomet. Chem.*, **2014**, *28*, 641-651.
21. Sun, W.; Wu, S.; Lu, Y.; Wang, Y.; Cao, Q.; Fang, W. Effective control of particle size and electron density of Pd/C and Sn-Pd/C nanocatalysts for vanillin production via base-free oxidation. *ACS Catalysis*, **2020**, *10*, 7699-7709.

22. Martins, N. M.; Mahmudov, K. T.; da Silva, M. F. C. G.; Martins, L. M.; Pombeiro, A. J. Copper (II) and iron (III) complexes with arylhydrazone of ethyl 2-cyanoacetate or formazan ligands as catalysts for oxidation of alcohols. *New J. Chem*, **2016**, *40*, 10071-10083.
23. (a) Lenze, M.; Bauer, E. B. Chemoselective, iron (II)-catalyzed oxidation of a variety of secondary alcohols over primary alcohols utilizing H<sub>2</sub>O<sub>2</sub> as the oxidant. *Chem Comm*, **2013**, *49*, 5889-5891. (b) Olivo, G.; Giosia, S.; Barbieri, A.; Lanzalunga, O.; Di Stefano, S. Alcohol oxidation with H<sub>2</sub>O<sub>2</sub> catalyzed by a cheap and promptly available imine-based iron complex. *Org. Biomol. Chem*, **2016**, *14*, 10630-10635. (c) Panza, N.; di Biase, A.; Rizzato, S.; Gallo, E.; Tseberlidis, G.; Caselli, A. Catalytic Selective Oxidation of Primary and Secondary Alcohols Using Nonheme [Iron(III)(Pyridine-Containing Ligand)] Complexes. *European Journal of Organic Chemistry*, **2020**, *2020*, 6635-6644.
24. Yan, Q.; Fang, Y. C.; Jia, Y. X.; Duan, X. H. Chemoselective hydrogen peroxide oxidation of primary alcohols to aldehydes by a water-soluble and reusable iron (III) catalyst in pure water at room temperature. *New J. Chem*, **2017**, *41*, 2372-2377.
25. Stanje, B.; Traar, P.; Schachner, J. A.; Belaj, F.; Mösch-Zanetti, N. C. Iron catalyzed oxidation of benzylic alcohols to benzoic acids. *Dalton Trans*, **2018**, *47*, 6412-6420.
26. (a) Beletskaya, I. P.; Nájera, C.; Yus, M. Chemodivergent reactions. *Chem. Soc. Rev*, **2020**, *49*, 7101-7166. (b) Peng, J. B.; Wu, X. F. Ligand-and Solvent-Controlled Regio-and Chemodivergent Carbonylative Reactions. *Angew. Chem., Int. Ed*, **2018**, *57*, 1152-1160.
27. Lagaditis, P. O.; Sues, P. E.; Sonnenberg, J. F.; Wan, K. Y.; Lough, A. J.; Morris, R. H. Iron (II) complexes containing unsymmetrical P–N–P' pincer ligands for the

- catalytic asymmetric hydrogenation of ketones and imines. *J. Am. Chem. Soc.*, **2014**, *136*, 1367-1380.
28. Mao, S.; Budweg, S.; Spannenberg, A.; Wen, X.; Yang, Y.; Li, Y. W.; Beller, M. Iron-Catalyzed Epoxidation of Linear  $\alpha$ -Olefins with Hydrogen Peroxide. *ChemCatChem*, **2022**, *14*, e202101668.
29. Koehne, I.; Schmeier, T. J.; Bielinski, E. A.; Pan, C. J.; Lagaditis, P. O.; Bernskoetter, W. H.; Schneider, S. Synthesis and structure of six-coordinate iron borohydride complexes supported by PNP ligands. *Inorg. Chem.*, 2014, *53*, 2133-2143.
30. Driscoll, O. J.; Hafford-Tear, C. H.; McKeown, P.; Stewart, J. A.; Kociok-Köhn, G.; Mahon, M. F.; Jones, M. D. (2019). The synthesis, characterisation and application of iron (III)-acetate complexes for cyclic carbonate formation and the polymerisation of lactide. *Dalton Trans.*, 2019, *48*, 15049-15058.
31. Surendhran, R.; D'Arpino, A. A.; Sciscent, B. Y.; Cannella, A. F.; Friedman, A. E.; MacMillan, S. N.; Lacy, D. C. Deciphering the mechanism of O<sub>2</sub> reduction with electronically tunable non-heme iron enzyme model complexes. *Chemical science*, 2018, *9*, 5773-5780.
32. Darari, M.; Francés-Monerris, A.; Marekha, B.; Doudouh, A.; Wenger, E.; Monari, A.; Gros, P. C. Towards Iron (II) Complexes with Octahedral Geometry: Synthesis, Structure and Photophysical Properties. *Molecules*, 2020, *25*, 5991.
33. Chakraborty, S.; Dai, H.; Bhattacharya, P.; Fairweather, N. T.; Gibson, M. S.; Krause, J. A.; Guan, H. Iron-based catalysts for the hydrogenation of esters to alcohols. *J. Am. Chem. Soc.*, **2014**, *136*, 7869-7872.
34. Chakraborty, S.; Dai, H.; Bhattacharya, P.; Fairweather, N. T.; Gibson, M. S.; Krause, J. A.; Guan, H. Iron-based catalysts for the hydrogenation of esters to alcohols. *Journal of the American Chemical Society*, **2014**, *136*(22), 7869-7872.

35. Chakraborty, S.; Bhattacharya, P.; Dai, H.; Guan, H. Nickel and iron pincer complexes as catalysts for the reduction of carbonyl compounds. *Acc. Chem. Res.*, **2015**, *48*(7), 1995-2003.
36. Kang, Z.; Wu, C.; Dong, L.; Liu, W.; Mou, J.; Zhang, J., Xu, C. 3D porous copper skeleton supported zinc anode toward high capacity and long cycle life zinc ion batteries. *ACS Sustain. Chem. Eng.*, **2019**, *7*, 3364-3371.
37. Shah, S. S.; & Singh, N. P. Pseudohalide assisted aerobic oxidation of alcohols in the presence of visible-light. *Tetrahedron Letters*, **2018**, *59*, 247-251.
38. Kongkaew, M.; Sitthisuwannakul, K.; Nakarajouyphon, V.; Pornsuwan, S.; Kongsaree, P.; Sangtrirutnugul, P. Benzimidazole–triazole ligands with pendent triazole functionality: unexpected formation and effects on copper-catalyzed aerobic alcohol oxidation. *Dalton Trans.*, **2016**, *45*, 16810-16819.
39. Dyson, P. J.; Jessop, P. G. Solvent effects in catalysis: rational improvements of catalysts via manipulation of solvent interactions. *Catal. Sci. Technol.*, **2016**, *6*, 3302-3316.
40. Jana, N. C., Sethi, S., Saha, R., & Bagh, B. Aerobic oxidation of vanillyl alcohol to vanillin catalyzed by air-stable and recyclable copper complex and TEMPO under base-free conditions. *Green Chem*, **2022**, *24*, 2542-2556.
41. Nebra, N.; García-Álvarez, J. Recent progress of Cu-catalyzed azide-alkyne cycloaddition reactions (CuAAC) in sustainable solvents: Glycerol, deep eutectic solvents, and aqueous media. *Molecules*, **2020**, *25*, 2015.
42. Giofrè, S. V.; Tiecco, M.; Ferlazzo, A.; Romeo, R.; Ciancaleoni, G.; Germani, R.; Iannazzo, D. Base-Free Copper-Catalyzed Azide-Alkyne Click Cycloadditions (CuAAc) in Natural Deep Eutectic Solvents as Green and Catalytic Reaction Media. *Eur. J. Org. Chem*, **2021**, *2021*, 4777-4789.

43. González-Rivera, J.; Mero, A.; Husanu, E.; Mezzetta, A.; Ferrari, C.; D'Andrea, F.; Bramanti, E.; Pomelli, C.S.; Guazzelli, L. Combining acid-based deep eutectic solvents and microwave irradiation for improved chestnut shell waste valorization. *Green Chem*, **2021**, *23*, 10101-10115.
44. Bjelić, A.; Hočevar, B.; Grilc, M.; Novak, U.; Likozar, B. A review of sustainable lignocellulose biorefining applying (natural) deep eutectic solvents (DESs) for separations, catalysis and enzymatic biotransformation processes. *Rev. Chem. Eng*, **2022**, *38*, 243-272.
45. Ročnik, T.; Likozar, B.; Jasiukaitytė-Grojzdek, E.; & Grilc, M. (2022). Catalytic lignin valorisation by depolymerisation, hydrogenation, demethylation and hydrodeoxygenation: Mechanism, chemical reaction kinetics and transport phenomena. *Chem. Eng. J*, **2022**, 137309.
46. Smith, E. L.; Abbott, A. P.; Ryder, K. S. Deep eutectic solvents (DESs) and their applications. *Chem. Rev.*, **2014**, *114*, 11060-11082.
47. Hazra, S.; Martins, L. M.; da Silva, M. F. C. G.; Pombeiro, A. J. Sulfonated Schiff base copper (II) complexes as efficient and selective catalysts in alcohol oxidation: Syntheses and crystal structures. *RSC adv*, **2015**, *5*(109), 90079-90088.

## Chapter 6

### (Summary of the thesis)

Reduction of different functional groups is one of the key transformations in organic synthesis. To facilitate this, conventionally various hydrogenation methods have been employed. Among them, catalytic transfer hydrogenation has gained widespread acclaim due to its various advantages, such as being a highly atom-economical and efficient catalytic process. This process has been well explored with secondary alcohols such as isopropanol and formic acid. However, only a few reports are available for transfer hydrogenation using challenging primary alcohols such as methanol and ethanol. In my second chapter I have discussed Coordination of 1,4-disubstituted 1,2,3-triazoles ligands and [(p-cymene)RuCl<sub>2</sub>]<sub>2</sub> followed by dehydrochlorination in the presence of a base resulted the formation of half sandwich ruthenium complexes, which are tested for the transfer hydrogenation of aldehydes and ketones in air using ecologically benign and cheap ethanol and methanol as the hydrogen source in the presence of a catalytic amount of a base. A significant research interest has been devoted to develop catalysts for the reduction of cellulose and lignin model compounds furfural and vanillin, respectively. In my third chapter I have demonstrated an iron (II) complex was readily synthesized by facile coordination of NNO pincer ligand with FeCl<sub>2</sub>.4H<sub>2</sub>O, which is efficiently utilized for the catalytic transfer hydrogenation of furfural and vanillin using ethanol as sacrificial hydrogen donor.

Lignin is an alternative major source of monomeric phenolic compounds and the syntheses of fine chemicals by oxidising lignin-based monomeric phenolics are gaining serious attention. In this context, my fourth chapter contains an air stable iron (II) complex employed for selective peroxidative oxidation of biomass derived vanillyl alcohol to vanillic acid in metal free type-III deep eutectic solvent. Vanillic acid has been employed as a new building block for the syntheses of various value-added products. In recent time, chemodivergent

transformation has gain a significance attention in scientific community. The most of the studies for switching the chemoselectivity rely on the catalyst, ligand, additive, solvent, temperature, time, pressure, pH, and even small modifications in the substrate. In my last working chapter, an air stable dimeric iron (II) complex has developed by the facile coordination of NNN pincer ligand and  $\text{FeCl}_2 \cdot 4\text{H}_2\text{O}$ , which is capable in showing chemodivergent transformation of primary alcohol to both aldehyde and acid by switching the solvent condition.